Examination of the regulatory role of the CpxRA two-component system and its relation to virulence in *Legionella pneumophila*

By

Jennifer Rose Tanner

A Thesis submitted to the Faculty of Graduate Studies of

The University of Manitoba

in partial fulfillment of the requirements of the degree of

DOCTOR OF PHILOSOPHY

Department of Microbiology

University of Manitoba

Winnipeg

ABSTRACT

Legionella pneumophila is a natural parasite of aquatic protozoa, and due to similarities in uptake mechanisms, is also an opportunistic intracellular pathogen of human pulmonary macrophages that can lead to pneumonia termed Legionnaires' disease. In protozoa, *L. pneumophila* features a biphasic intracellular lifestyle that alternates between vegetative replicative forms and resilient infectious cyst forms, that when released ensure transmissibility to fresh protozoan hosts. Legionnaires' disease outbreaks are often sourced to anthropogenic water systems that promote generation of cyst-laden aerosols that are inadvertently inhaled by susceptible individuals.

Successful infection of protozoan and macrophage cells is enabled by the presence of a bacterial Dot/Icm Type IV Secretion System that facilitates the delivery of ~300 effector molecules to establish a replicative niche. The CpxRA two-component system has been shown elsewhere to regulate expression of several effector proteins as well as components of the Dot/Icm apparatus; yet inactivation of *cpxRA* via marked deletions did not affect intracellular growth in protozoa or human macrophages.

To investigate this discrepancy, generated Δ*cpxR*, Δ*cpxA*, and Δ*cpxRA* in-frame null mutant strains were assessed for alterations in virulence. Intracellular growth kinetics of Δ*cpxR* and Δ*cpxRA* mutant strains was significantly reduced in the protozoan host *Acanthamoeba castellanii*, but unaffected in human U937-derived macrophages. In corroboration, Δ*cpxR* and Δ*cpxRA* mutant strains demonstrated sodium resistance; a phenotype strongly associated with avirulence. Transcriptome analysis of the *cpxRA* mutant strain revealed a global regulatory impact, with hundreds of genes including those encoding Dot/Icm effector proteins as well as Type II secreted substrates differentially regulated in the two growth phases examined.

Expression of *cpxRA* located within the five-gene (*lpg1441-cpxA*) operon is controlled in a negative manner by the transcription regulator OxyR. Overexpression, but not lack, of OxyR limited the growth of *L. pneumophila* in *A. castellanii* but not in U937-derived macrophages cells or during broth culture. Recombinant CpxR bound a conserved binding site within the *oxyR* promoter region; however, expression control of OxyR remains uncertain, as the promoter activity was unaffected in *cpx* mutant strains. Taken together, this study has conclusively determined that the essentiality of the CpxRA system to *L. pneumophila* virulence is host specific.

ACKNOWLEDEMENTS

Foremost, I would like to express my sincere gratitude to my supervisor Dr. Ann Karen C. Brassinga for seeing potential in me as an honour's student and then encouraging me to continue with graduate studies. Her constant support and guidance as a mentor has been paramount to achieving my goals as a student and developing my confidence as a researcher. She has truly prepared me for what comes ahead in my career as a scientist.

I would like to offer a special thank you to my advisory committee members Drs. Teresa de Kievit, Ivan Oresnik and Dana Schroeder. I appreciate all of the helpful advice and solutions provided over the years that have improved the outcome of this thesis as well as for asking questions that got me thinking from a different perspective.

Also, another huge thank you to the graduate students, undergraduate students, post-docs, lab technicians, professors, prep-room staff, past and present office staff as well as Pranny and Mike for making my time in the Microbiology department such a wonderful experience. I will never forget the help that was given, the conversations had and all the fun times together. In particular, I would like to thank my past lab mates Aniel Moya-Torres, Palak Patel, and Jackie Hellinga for never a dull moment in the lab, Chantalle Pitre for teaching me the workings of the lab and all the fun times we had, as well as my current lab mate Chris Graham for really helping me out and taking on all of the lab responsibilities.

Finally, thank you to my family (Mom (Jody), Dad (David), brothers (Darren and Devin), and Kristyn), my best friends Liz Bracken and Keith Montgomery, and my fiancée Donavan Purdy for your never ending support, I could not have gotten this far without you all.

CONTRIBUTIONS OF AUTHORS

The works presented in Chapters 3 and 4 are the products of collective efforts put forth by multiple authors. My supervisor Dr. Ann Karen Brassinga provided the CpxA protein expression plasmid constructs along with the initial induction conditions that identified the insolubility of the full-length CpxA recombinant protein described in Chapter 3, section 3.2. The microarray procedures including cDNA synthesis, labelling, hybridization, data acquisition, and conversion of raw data to $\log_2$ expression values described in Chapter3, section 3.2 were all conducted in the laboratory of Dr. Sébastien Faucher by Dr. Sébastien Faucher and/or Laam Li (PhD student) at McGill University located in Montreal, Quebec, Canada. Celine Jimenez carried out generation of the Δ*oxyR* in-frame null mutant strain used in the studies of Chapter 4, section 4.3, under the guidance of the procedures described in Chapters 2 and 4, sections 2.6.6 and 4.2, respectively. Electrophoretic mobility shift assays and DNaseI footprinting, along with their respective procedures presented in Chapter 4, sections 4.2 and 4.3, were conducted and/or modified in collaboration with Palak Patel. Dr. Linda Donald carried out the MALDI mass spectrophotometry analysis of the purified recombinant CpxR protein, conducted the analysis of the data obtained, generated Figure 4.4, and supplied the written methodologies presented in Chapter 4 sections 4.2 and 4.3. Jacqueline Hellinga determined all procedures described within section 2.11 of Chapter 2, as well as carried out these procedures for the U937 infection presented in section 4.3 of Chapter 4. She also generated the graphical representation of the U937 infection data displayed in Figure 4.2 panel B.

LIST OF COPYRIGHTED MATERIAL FOR WHICH PERMISSION WAS OBTAINED

Figure 1.1. Environmental Microbiology Reports. 2011 March;3(3):286-96. doi: 10.1111/j.1758-2229.2011.00247.x. Title: *Legionella* spp. outdoors: colonization, communication and persistence (Figure 1). License number: 3875420792484

Figure 1.2. J Bacteriol. 2002 Dec; 184(24):7025-41. Title: Ultrastructural analysis of differentiation in Legionella pneumophila (Figure 2A and 5C). ASM authorizes an advanced degree candidate to republish the requested material in his/her doctoral thesis or dissertation.

Figure 1.6. FEMS Microbiol Lett. 2012 Jan;326(1):12-22. doi: 10.1111/j.1574-6968.2011.02436.x. Title: Signal integration by the Cpx-envelope stress system (Figure 2). License number: 3875410810185

Figure 1.7. FEMS Microbiol Lett. 2012 Jan;326(1):2-11. doi: 10.1111/j.1574-6968.2011.02406.x. Title: Just scratching the surface: an expanding view of the Cpx envelope stress response (Figure 1). License number: 3875410504113

Figure 1.7. Mol Cell. 2016 Feb;61(3):352-63. doi: 10.1016/j.molcel.2015.12.023. Title: A 3' UTR-derive small RNA provides the regulatory noncoding arm of the inner membrane stress response (Figure 7A). License number: 3875410123273

Chapter 3. Mol Microbiol. 2016 Mar; [Epub ahead of print]. doi: 10.1111/mmi.13365. Title: The CpxRA two-component system contributes to *Legionella pneumophila* virulence (Full article). License number: 3876631296770

Appendix 1. Microbiology. 2013 Mar;159(Pt3):475-92. doi: 10.1099/mic.0.062117-0. Title: Regulatory control of temporally expressed integration host factor (IHF) in *Legionella pneumophila* (Figure 9). License number: 3883070544214

TABLE OF CONTENTS

LIST OF TABLES

LIST OF FIGURES

LIST OF ABBREVIATIONS

ACES	N-(2-Acetamido)-2- aminoethanesulfonic acid
ATCC	American Type Culture Collection
ATP	Adenosine triphosphate
bp	Base pair(s)
cDNA	Complimentary Deoxyribonucleic acid
CFU	Colony forming units
Ci	Curie
CPM	Counts per minute
dATP	Deoxyadenosine triphosphate
dCTP	Deoxycytidine triphosphate
dGTP	Deoxyguanosine triphosphate
dNTP	Deoxynucleotide
dTTP	Deoxythymidine triphosphate
DNA	Deoxyribonucleic acid
DTT	Dithiothreitol
EDTA	Ethylenediamine-tetra-acetic acid
g	Gram(s)
x *g*	G-force
GDP	Guanosine diphosphate
GTP	Guanosine triphosphate
kb	Kilobase pairs
L	Litre(s)
M	Molar
mA	milliamps
MALDI	Matrix-assisted laser desorption/ionization
mg	milligram(s)
µg	microgram(s)
mL	millilitre(s)
mM	millimolar
µM	micromolar
MOPS	3-(N-morpholino)propanesulfonic acid
ng	nanogram(s)
PCR	Polymerase chain reaction
PVDF	Polyvinylidene difluoride
RNA	Ribonucleic acid
SDS	Sodium dodecyl sulphate
SDS-PAGE	Sodium dodecyl sulphate polyacrylamide gel electrophoresis
Tm	Temperature
V	Volts
v/v	volume/volume
w/v	weight/volume

Chapter 1. LITERATURE REVIEW

1.1 *Legionella pneumophila* – a well adapted pathogen

1.1.1 *L. pneumophila* and legionellosis

A bacterium, now classified under the genera *Legionella*, garnered worldwide attention during the summer of 1976, when an outbreak of a mysterious pneumonia occurred at the 58th annual convention of the American Legion being held in Philadelphia, Pennsylvania (Fraser *et al.*, 1977). A total of 182 individuals fell ill with 29 succumbing to the infection. The etiological agent was thereafter identified as a Gram-negative bacillus that had no prior implications in human disease and commonly referred to as the "Legionnaires' disease bacterium" (McDade *et al.*, 1977). Eventual DNA analysis and comparisons confirmed the Legionnaires' disease bacterium as a unique species, leading to its taxonomic naming of *Legionella pneumophila*; representing those afflicted as well as the disease outcome (Brenner *et al.*, 1978; Brenner *et al.*, 1979).

Continued research found *L. pneumophila* to not only be responsible for the severe pneumonia Legionnaires' disease but also be responsible for a unique acute illness referred to as Pontiac fever (McDade *et al.*, 1977; Glick *et al.*, 1978). The distinguishing factors for these two diseases are their clinical presentation as well as patient demographics. Symptoms of Legionnaires' disease include chills, fever, dry cough, labored breathing, rales, delirium, abdominal pain and diarrhea (Fraser *et al.*, 1977). This pneumonia is not commonly diagnosed in healthy individuals but rather those with underlying health conditions where risk factors for disease development include; age (> 50 years), sex (male), smoking, chronic pulmonary disease, diabetes and immunosuppression (via disease or drugs) (Fraser *et al.*, 1977; Marston *et al.*, 1994; Fields *et al.*, 2002). Death can result as a consequence of Legionnaires' disease with mortality

rates ranging from 5-25% but reaching as high as 70% in nosocomial infections (Marrie, 2008). Pontiac fever on the other hand, is a self-limiting flu-like illness that has no associated risk factors, no recorded fatalities, and does not develop into pneumonia (Glick *et al.*, 1978). These two illnesses were then termed and are now often referred to as legionellosis, due to the same etiologic agent being responsible for their onset (Fraser and McDade, 1979).

Since this time of *Legionella* discovery, a total of 59 *Legionella* species have been identified and reported within the literature (http://www.bacterio.net). However, over 90% of legionellosis occurrences worldwide have been caused by strains of *L. pneumophila* alone; except in New Zealand and Australia where strains of *L. longbeachae* are responsible for over 30% of legionellosis occurrences (Yu *et al.*, 2002). Legionellosis arises as either sporadic cases throughout the year or as common-source outbreaks, with peak number of incidences occurring during summer and late fall (ECDC, 2015; Hicks *et al.*, 2011). The most recent major outbreaks of *L. pneumophila* derived legionellosis have been reported in New York City, New York in July 2015 with 133 confirmed cases that resulted in 16 deaths (http://www1.nyc.gov/nyc-resources/legionnaires-disease.page), Vila Franca de Xira, Portugal in 2014 with 334 confirmed cases that resulted in 10 deaths (Shivaji *et al.*, 2014), and in Quebec City, Canada in 2012 with 182 confirmed cases that resulted in 13 deaths (Levesque *et al.*, 2014).

Outbreaks of legionellosis are almost exclusively linked to water distribution systems that contain elevated levels of *L. pneumophila* and generate aerosols as a consequence of their mechanics. Examples of these systems that have been identified as the source of outbreaks include air-conditioning cooling towers, whirlpool spas, and decorative fountains (Marrie, 2008). Incidents that diverge from this epidemiological tendency are those caused by *L. longbeachae*, where the source of outbreaks have been linked to potting soil (Steele *et al.*, 1990; Whiley and

Bentham, 2011). Transmission of *L. pneumophila* has been identified to primarily occur through the inhalation of these *Legionella*-laden aerosols into the lungs of susceptible individuals whereby the deposition of the bacterium ultimately leads to the development of legionellosis; more specifically in the case of Legionnaires' disease *L. pneumophila* infects the alveolar macrophages resulting in the manifestation of the described pneumonia (Fraser *et al.*, 1977; McDade *et al.*, 1977; Glick *et al.*, 1978; Horwitz and Silverstein, 1980). Human-to-human transmission however, has not been observed classifying legionellosis as non-communicable. This distinction has led to the idea that humans are not the ideal or targeted replicative niche for *L. pneumophila* but a consequence of its environmental lifestyle and thus an accidental human pathogen (Garduno *et al.*, 2002; Abdelhady and Garduno, 2013).

1.1.2 *L. pneumophila* – an environmental pathogen

It was not long after the realization that the waters of cooling towers were a source of *L. pneumophila* that it became acknowledged that this bacterium is in fact ubiquitous to freshwater environments (Fliermans *et al.*, 1979). *L. pneumophila* has been isolated from streams, rivers and lakes worldwide that exhibit diverse temperature conditions, ranging from 0°C in a polar lake of Antarctica (Carvalho *et al.*, 2008) to greater than 60°C in thermal water bodies of northern Africa (Ghrairi *et al.*, 2013) and southern United States (Fliermans *et al.*, 1981). Aquatic habitats harboring *L. pneumophila* were also found to vary in pH as well as other physiochemical properties revealing this bacterium to be quite robust (Fliermans *et al.*, 1981; Ghrairi *et al.*, 2013).

Fundamental to understanding the ecology of *L. pneumophila* in these natural water systems was the discovery by Rowbotham (1980) that *L. pneumophila* is an intracellular

pathogen of free-living amoeba. *L. pneumophila* is able to resist, in a sophisticated manner, the digestive process carried out by amoebae for nutrient acquisition, where several genera of amoeba have been shown to support the growth of this bacterium and include *Acanthamoeba*, *Hartmannella*, and *Naegleri* [summarized in (Escoll *et al.*, 2013)]. Amoeba-resistance allows *L. pneumophila* to utilize this interaction as a nutritional reservoir, multiplying to high cellular densities and thus expanding their population (Rowbotham, 1980; Holden *et al.*, 1984) (Figure 1.1). Exhausting the protozoan host as a nutritional source leads to release of *L. pneumophila* to the environment where it may encounter a new host cell or integrate into complex biofilm communities (Figure 1.1). Biofilm residency has been demonstrated as means of extracellular replication for *L. pneumophila* but is thought to be a minor contributor to population expansion and more of a means of environmental persistence (Murga *et al.*, 2001). It is the action of free-living amoebae grazing on these *Legionella*-containing biofilm communities and subsequent intracellular replication that is the predominant means of dissemination within the environment (Murga *et al.*, 2001; Kuiper *et al.*, 2004; Declerck *et al.*, 2009) (Figure 1.1).

Another benefit, in addition to a replicative niche, provided by this intracellular interaction is protection from environmental stresses, including chemical disinfectants used to control microbial populations within engineered water systems (Srikanth and Berk, 1993; Srikanth and Berk, 1994). Amoebae have been shown to be less susceptible and even highly resistant to ozone, chlorine, monochloramine, chlorine dioxide, and copper-silver ionization exposure; thus shielding and enabling the survival of internalized *L. pneumophila* from otherwise lethal conditions (Thomas *et al.*, 2004; Critchley and Bentham, 2009).

Exploitation of protozoan hosts has also allowed *L. pneumophila* to acquire the appropriate virulence factors to combat predation by eukaryotic phagocytic cells, including

human macrophages, as the cellular mechanisms for bacterial degradation are quite similar [reviewed in (Molmeret *et al.*, 2005; Escoll *et al.*, 2013)]. However, it is human intervention that has connected this environmental pathogen with its cognate human host cell, the alveolar macrophage. Implementation of engineered water systems that 1) operate at temperatures determined to be optimal for the amoeba - *L. pneumophila* interaction (25-42°C) and thus promote elevated levels of *L. pneumophila* as well as 2) mechanically generate aerosols, formulate the precise conditions needed to encounter human hosts for infection (Figure 1.1) (Fields *et al.*, 2002).

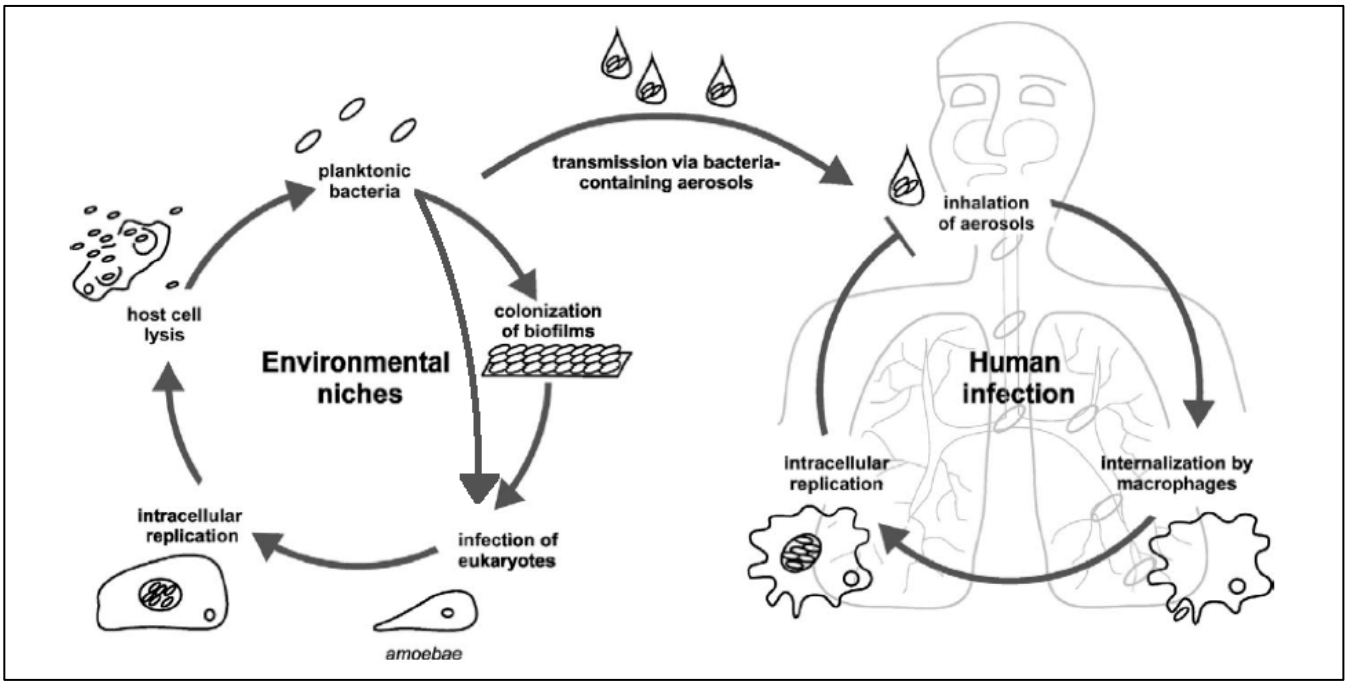

Figure 1.1 Environmental and human interactions of *L. pneumophila*. In natural aquatic habitats, free *L. pneumophila* either infect a new amoebae host cell or integrate into biofilm communities, which then can be grazed upon by amoebae. Once inside amoebae, *L. pneumophila* replicates to maximum cell densities, exhausting its host to point of lysis leading to release into the surrounding environment. In engineered water systems, this same cycle occurs; however, mechanical aerosolization results in air-borne dissemination of *L. pneumophila* and subsequent inhalation by individuals, which can lead to non-communicable legionellosis. Figure has been adapted from (Hilbi *et al.*, 2011).

1.1.3 Intracellular life cycle and morphogenesis

While inhabiting amoebae, *L. pneumophila* undergoes morphological differentiation; transitioning between forms that exhibit varying morphologies as well as physiological and ultrastructural characteristics [reviewed in (Robertson *et al.*, 2014)]. The most well defined forms that provide the foundation for the *L. pneumophila* life cycle are the replicative form (RF) and the cyst form (CF, also referred to as the mature infectious form (MIF) amongst the literature) (Cirillo *et al.*, 1994; Garduno *et al.*, 1998; Garduno *et al.*, 2002; Abdelhady and Garduno, 2013). The RF represent the vegetative state of the bacterium in which metabolism is highly active and cell division readily occurs, supporting population expansion (Garduno *et al.*, 2002). Ultrastructure analysis has revealed RFs to be rod-like in shape and have a characteristic Gram-negative membrane architecture consisting of a readily distinguishable outer membrane, periplasm, and inner membrane as well as a uniform cytoplasmic region (Figure 1.2 A) (Garduno *et al.*, 1998; Faulkner and Garduno, 2002; Garduno *et al.*, 2002). CFs on the other hand, have been identified to be metabolically dormant and possess distinct ultrastructure characteristics of a rounded-irregular shape, altered membrane structures, notably a thickened cell wall with multiple membrane laminations, as well as cytoplasmic poly-β-hydroxybutyrate (PHBA) inclusions (Figure 1.2 B) (Garduno *et al.*, 2002). Furthermore, CFs are observed to be flagellated, display increased resistance to pH alterations, detergent, chlorine and antibiotic exposure as well as enhanced infectivity in cell-based infection models (Abu Kwaik *et al.*, 1997; Garduno *et al.*, 2002). These adaptations of the CF enable *L. pneumophila* to survive extended periods of extracellular residency but still remain primed for infection upon encountering a new host.

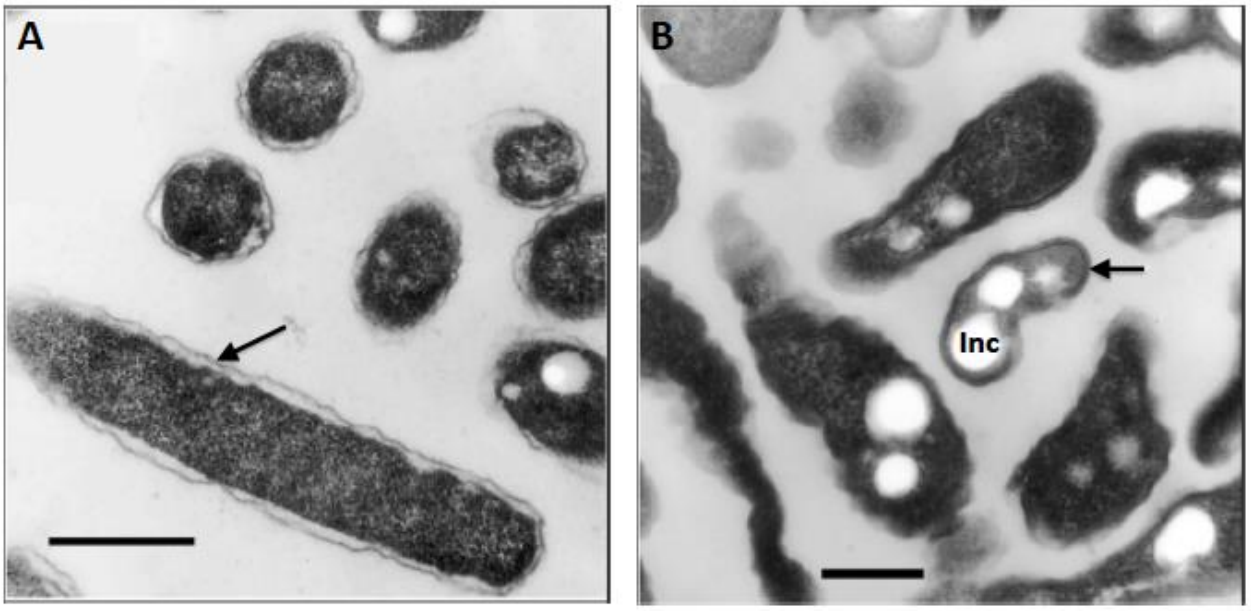

Figure 1.2 Ultrastructural characteristics of replicative (RF) and cyst forms (CF) of *L. pneumophila*. A) RF exhibiting rod-like shape and characteristic Gram-negative membrane structure of a thin outer membrane and easily defined periplasm (arrow). B) CF featuring irregular cell shape, thickened cell wall (arrow), and poly-β-hydroxybutyrate inclusions (Inc) within the cytoplasm. Bars in A) and B) represent 0.5 μm and 0.1 μm, respectively. Figure has been adapted from Faulkner and Garduno (2002).

Partnered with morphological differentiation are a series of intracellular events governed by *L. pneumophila* that together define the life cycle of this bacterium, which is summarized in Figure 1.3. Initiating the cycle is cellular contact and adherence of the CF to the surface of the host cell, which is followed by internalization (Horwitz, 1984; Cirillo *et al.*, 1994; Bozue and Johnson, 1996). Once internalized, *L. pneumophila* resides within a specialized phagosome referred to as the *Legionella*-containing vacuole (LCV). Within this LCV, *L. pneumophila* undertakes two important processes: 1) alters host-cellular trafficking pathways to initially subvert phagosome-lysosome fusion to avoid degradation and subsequently recruits vesicles from the endoplasmic reticulum (ER) as well as transiently associates with host cell mitochondria (Horwitz, 1983; Abu Kwaik, 1996; Swanson and Isberg, 1995; Garduno *et al.*, 1998; Kagan and Roy, 2002; Kagan *et al.*, 2004); 2) Begins transitioning from the CF to the RF via a CF-RF intermediate form in response to changing from an extracellular environment to an intracellular one (Faulkner and Garduno, 2002). *L. pneumophila* continues to orchestrate LCV maturation through interactions with the ER in which ribosomes as well as ER markers are acquired to the LCV membrane (Swanson and Isberg, 1995; Tilney *et al.*, 2001; Kagan and Roy, 2002; Kagan *et al.*, 2004). Establishment of this mature LCV is accompanied by *L. pneumophila* replication that generates a population of RFs (Faulkner and Garduno, 2002). As the infection progresses, the LCV expands to accommodate the increase in bacterial load as well as dissociates from the ER (Faulkner and Garduno, 2002). The nutritional resources of the host cell become limited with the elevated levels of bacteria and a transition to the CF is triggered with the RF transforming into a RF-CF intermediate form (Byrne and Swanson, 1998; Garduno *et al.*, 2002; Faulkner and Garduno, 2002).

Each of these described stages of *L. pneumophila* infection are highly conserved among both amoebae and macrophage host cells; however, in the last stage of infection a critical difference arises. In amoebae, the RF-CF intermediate form fully differentiates to the CF and subsequently is released from the spent amoebae via host cell lysis or is dispelled within vesicles to reinitiate the cycle (Figure 1.3) (Rowbotham, 1986; Berk *et al.*, 1998; Garduno *et al.*, 1998; Bouyer *et al.*, 2007; Abdelhady and Garduno, 2013). Whereas in macrophages, only a small subset of the RF-CF intermediate population has been shown to completely differentiate to the CF, resulting in release of predominately intermediary forms upon host lysis (Figure 1.3) (Garduno *et al.*, 2002; Abdelhady and Garduno, 2013). This incomplete differentiation that occurs in macrophages has been proposed as the rationale for Legionnaires' disease being non-communicable among humans as only the CF is believed and in part be shown to express the full complement of virulence determinants (Cirillo *et al.*, 1994; Garduno *et al.*, 2002; Abdelhady and Garduno, 2013).

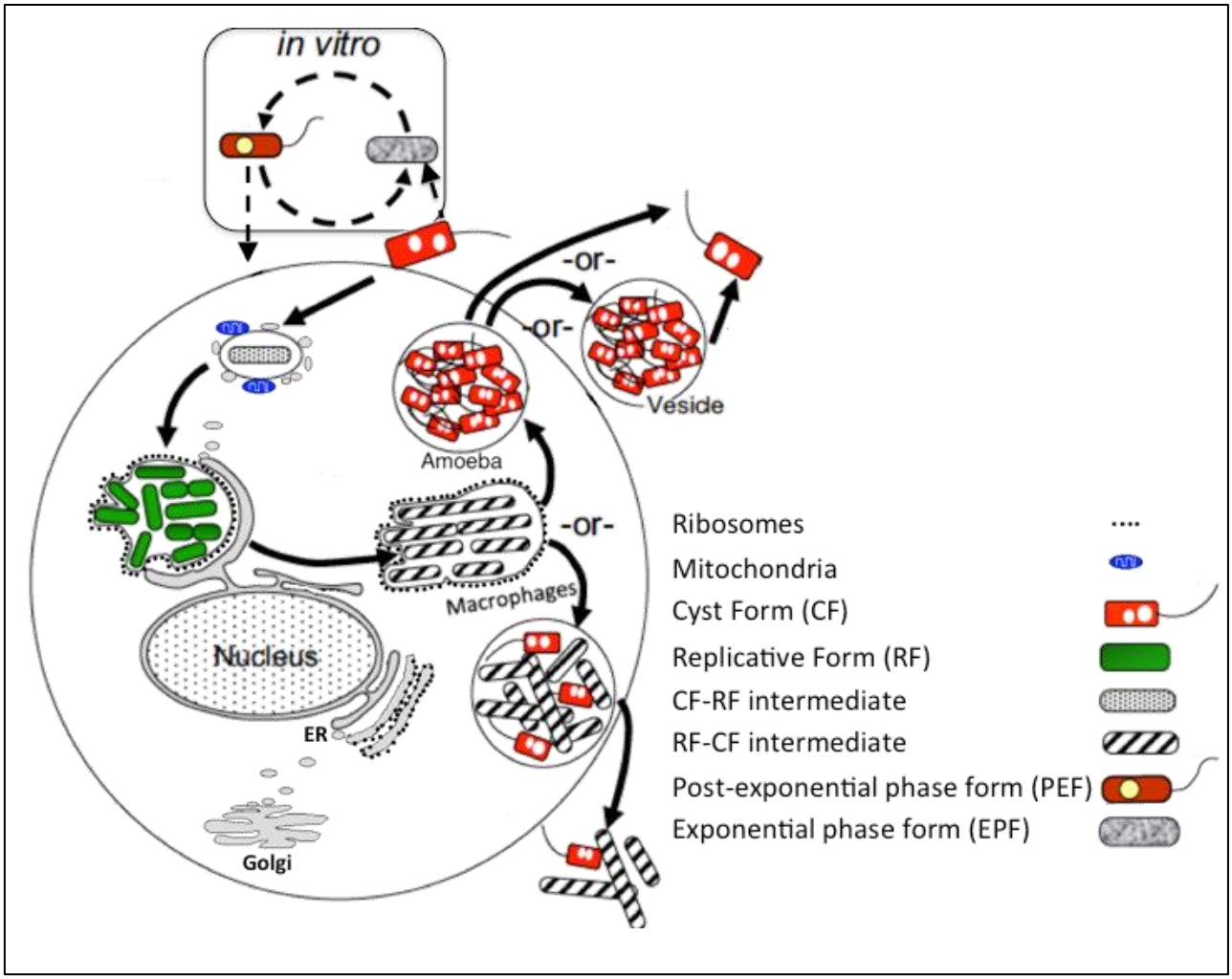

Figure 1.3 Schematic illustrating the intracellular life cycle and *in vitro* growth cycle of *L. pneumophila* with accompanying differential forms. The intracellular life cycle is initiated with a host cell internalizing the hyper-infectious cyst form (CF) and is followed by alterations to host cell cellular trafficking events, including association with mitochondria and the endoplasmic reticulum (ER), in order to establish the *Legionella*-containing vacuole (LCV). Within the ribosome studded LCV, *L. pneumophila* transitions via an intermediary form to the replicative form (RF), to carry out cell division and expand its population. Depending on the host cell, the

RF population may fully differentiate to the CF or remain arrested in the intermediate form and exit the spent host cell as free forms or within vesicles. CFs may be applied to laboratory growth media to initiate the *in vitro* growth cycle. The presence of the nutrient-rich environment triggers the differentiation of the CF to the exponential phase form (EPF), which replicates until nutrients are depleted, establishing the post-exponential phase and prompting developmental changes in *L. pneumophila* to the post-exponential form (PEF). The PEF can cycle back into the EPF when transferred to fresh media or initiate infection of a host cell and carry out the intracellular life cycle as above, exiting as a mature CF in a host cell dependent manner. Figure has been modified from Robertson *et al.* (2014).

1.1.4 *In vitro* growth cycle

In addition to intracellular propagation, *L. pneumophila* can be grown in the laboratory using nutrient rich agar or broth. Under these conditions, *L. pneumophila* experiences a typical bacterial growth cycle of replication during the exponential phase which eventually leads to exhaustion of nutritional resources and the bacteria entering the post-exponential phase (also referred to as the stationary phase), where replication ceases until transfer to fresh media (Figure 1.3) (Byrne and Swanson, 1998). Further characterization of this growth cycle by Byrne and Swanson (1998) revealed *L. pneumophila* undergoes significant developmental changes when transitioning from the exponential to the post-exponential growth phase that resemble the changes that occur during its intracellular life cycle. Post-exponential phase *L. pneumophila*, herein referred to as the post-exponential phase form (PEF), were found to be motile, sodium sensitive, to contain cytoplasmic PHBA inclusions and able to evade phagosome-lysosome fusion, like that of the intracellular CF, and therefore defined as "virulent/transmissive" (Byrne and Swanson, 1998; Garduno *et al.*, 2002). In contrast, exponential phase *L. pneumophila* herein referred to as the exponential phase form (EPF), lacked each of these characteristics and with cell division events occurring at maximum during this phase, EPFs were deemed analogous to intracellular RFs (Byrne and Swanson, 1998; Joshi *et al.*, 2001; Garduno *et al.*, 2002; Garduño, 2008). These similarities in developmental changes that occur during the *in vitro* growth cycle allow for *L. pneumophila* grown in this manner to serve as a model to elucidate the regulatory components and pathways that contribute to morphological differentiation and concomitant expression of virulence traits observed during intracellular growth (Molofsky and Swanson, 2004; Garduño, 2008). However, PEFs do not elicit all the characteristic and morphological changes of CFs and are regarded as stunted in their maturation as when used to initiate

intracellular infections do carry out the intracellular life cycle, including fully differentiating to the CF in the appropriate eukaryotic host cells (Figure 1.3) (Garduno *et al.*, 2002; Garduño, 2008). Thus with the environmentally relevant and Legionnaires' disease associated CFs only observed intracellularly, it is necessary to complement *in vitro* findings with intracellular analysis (Garduño, 2008).

1.2 The Dot/Icm Type IVB secretion system – a major virulence factor

1.2.1 Dot/Icm classification and structural components

Considerable focus among *Legionella* research is and has been dedicated to discerning the virulence determinants that enable the diverse intracellular life style of *L. pneumophila*. Efforts in this regard by two independent research groups during the latter 1990's led to the pivotal finding that alterations in host cellular trafficking events necessary for *L. pneumophila* intracellular growth are largely dependent upon two genetic loci referred to as region I and region II (Berger and Isberg, 1993; Brand *et al.*, 1994; Segal *et al.*, 1998; Vogel *et al.*, 1998). Each study found that when the genes within these regions were mutagenized, *L. pneumophila* exhibited strong reductions in intracellular growth, with many mutants showing a complete absence of growth (Marra *et al.*, 1992; Berger and Isberg, 1993; Sadosky *et al.*, 1993; Berger *et al.*, 1994; Brand *et al.*, 1994; Segal and Shuman, 1997; Segal *et al.*, 1998; Vogel *et al.*, 1998; Purcell and Shuman, 1998; Segal and Shuman, 1999a). In light of these intracellular growth phenotypes, the genes within these regions were termed "*d*efective for *o*rganelle *t*rafficking" (*dot*) and/or "*i*ntrac*e*llular *m*ultiplication" (*icm*), with many having dual annotations due to the simultaneous discovery of these two regions (Marra *et al.*, 1992; Berger and Isberg, 1993).

The protein products (Dot/Icm) encoded by these regions were found to share homology with the components that comprise Type IV secretion systems (T4SS) (Segal *et al.*, 1998; Vogel *et al.*, 1998; Segal and Shuman, 1998). This class of secretion systems encompasses the conventional conjugation machinery as well as adapted systems, evolving to transfer not only DNA but also protein substrates [reviewed in (Christie and Vogel, 2000; Chandran Darbari and Waksman, 2015)]. The Dot/Icm system was shown to function as an adapted system through the identification of the first translocated protein substrate, RalF, as well as to have retained the

ability of conjugal DNA transfer; where each process has been shown to be dependent upon a functional Dot/Icm system (Segal *et al.*, 1998; Vogel *et al.*, 1998; Nagai *et al.*, 2002). Further homology assessments of the Dot/Icm components has found it to be unique among the T4SS family in that it has strong homology to the Tra/Trb conjugation machinery of the IncI plasmids R64 and ColIb-P9, but very limited homology to the components of the more classical T4SS, VirB/VirD4, encoded by the Ti plasmid found within the plant pathogen responsible for crown gall disease, *Agrobacterium tumefaciens* (Segal and Shuman, 1999b; Komano *et al.*, 2000; Christie and Vogel, 2000; Gordon and Christie, 2014). In addition to these homology differences, the Dot/Icm system consists of several novel protein components found only in *Legionella* or closely related bacteria (*Coxiella* and *Rickettsiella*), as well as lacks a contiguous genetic arrangement common to the *virB*/*virD4* T4SS; prompting the sub-classification of the T4SSs to Type IVA encompassing the model VirB/VirD4 system and Type IVB for the more distinct Dot/Icm system (Christie and Vogel, 2000; Nagai and Kubori, 2011).

Through the initial studies of region I and II as well as subsequent mutational analysis, the Dot/Icm secretion apparatus and accessory components have been found to be comprised of 27 proteins, where seven are encoded within region I (Icm –V, –W, –X and Dot –A, –B, –C, –D), 18 within region II (Icm –T, –S, –R, –Q, DotM/IcmP, DotL/IcmO, DotK/IcmN, DotJ/IcmM, DotI/IcmL, DotH/IcmK, DotG/IcmE, DotF/IcmG, DotE/IcmC, DotP/IcmD, DotN/IcmJ, DotO/IcmB, IcmF, and DotU/IcmH), and two encoded downstream of region II (DotV and LvgA) (Marra *et al.*, 1992; Berger and Isberg, 1993; Sadosky *et al.*, 1993; Berger *et al.*, 1994; Brand *et al.*, 1994; Segal and Shuman, 1997; Segal *et al.*, 1998; Vogel *et al.*, 1998; Purcell and Shuman, 1998; Matthews and Roy, 2000; Edelstein *et al.*, 2003; Buscher *et al.*, 2005). Investigations devoted to characterizing the architecture of the Dot/Icm system have unveiled the

core translocation complex to be composed of DotC, DotD, DotH/IcmK, DotG/IcmE, and DotF/IcmG (Vincent *et al.*, 2006b; Kubori *et al.*, 2014). Subcellular localization determined this complex to span both the inner and outer membranes, with DotC, DotD and DotH/IcmK forming a subcomplex localized to the outer membrane and DotG/IcmE as well as DotF/IcmG localizing to the inner membrane but to also associate with the outer membrane in a DotCDH dependent manner (Figure 1.4) (Vincent *et al.*, 2006b). Protein-protein interactions identified DotG/IcmE to self-interact as well as to interact with DotF/IcmG, indicating these proteins likely formed a channel due to their ability to oligomerize and associate with the inner and outer membranes (Figure 1.4) (Vincent *et al.*, 2006b). This overall structure of the core complex was recently supported through visualization of circular complexes on the surface of *L. pneumophila* via transmission electron microscopy that were confirmed through isolation to consist of DotC, DotD, DotH/IcmK, DotG/IcmE, and DotF/IcmG as well as be dependent on the presence of *dotC*, *dotD*, and *dotH/icmK* (Kubori *et al.*, 2014). Further genetic analysis revealed DotG/IcmE to form the central pore within the core complex as *dotG/icmE* mutants resulted in a much larger central pore diameter to occur within the core complex when compared to the pores of the wild-type core complex (Kubori *et al.*, 2014). As well, this analysis found DotF/IcmG to contribute to proper core complex formation as *dotF/icmG* mutants generated complexes with and without DotG/IcmE as the central pore (Kubori *et al.*, 2014). Together, these studies present compelling evidence for the transmembrane core complex of the Dot/Icm system necessary for effector translocation to be composed of DotC, DotD, DotH/IcmK, DotG/IcmE, and DotF/IcmG (see Figure 1.4).

Additional complexes have been elucidated that are also likely to be involved in the overall functioning of the apparatus. The cytoplasmic proteins, IcmS and IcmW, have been

observed to form a heterodimer and together bind a subset of effector proteins to assist in their export (Coers *et al.*, 2000; Ninio *et al.*, 2005; Bardill *et al.*, 2005; Cambronne and Roy, 2007; Ninio *et al.*, 2009). It is believed this interaction is akin to the chaperone-substrate association well characterized for the Type III secretion system as IcmS and IcmW both share the attributes of being small acidic cytoplasmic proteins with cognate binding partners, features common to molecular chaperones, and thus deemed T4SS 'adaptors' (Coers *et al.*, 2000; Parsot *et al.*, 2003; Vincent *et al.*, 2006b). LvgA, a similarly small acidic cytoplasmic protein, has been found to also interact with IcmS and thus proposed to be another adaptor complex; however, no effector targets have been described to date (Vincent and Vogel, 2006). Furthermore, the IcmSW heterodimer associates with the inner-membrane protein, DotL/IcmO, via a specific domain located within the C-terminus of this protein. DotL/IcmO is proposed to function as the Type IV coupling protein (T4CP) for the Dot/Icm system and thus presumed to serve as a receptor for substrates, linking them to the translocation machinery as well as provide energy for substrate secretion via ATP hydrolysis (Buscher *et al.*, 2005; Vincent *et al.*, 2006b; Vincent *et al.*, 2012; Sutherland *et al.*, 2012). DotL/IcmO has also been established to interact with the inner-membrane proteins DotM/IcmP and DotN/ IcmJ via protein stability effects between complex members as well as co- localization and isolation studies (Vincent *et al.*, 2006b; Vincent *et al.*, 2012). Together the, Dot – L, –M, –N subassembly and IcmSW heterodimer are thought to provide the targeting and energetic means necessary for export of adapter dependent substrates, leading to the classification of these associated proteins as the T4CP subcomplex of the Dot/Icm system (see Figure 1.4) (Vincent *et al.*, 2012; Sutherland *et al.*, 2012).

Other complexes with less known in regards to the mechanism by which they contribute to the operation of the Dot/Icm system have too been elucidated. These include IcmR–IcmQ,

DotU/IcmH–IcmF, and DotI/IcmL–DotJ/IcmM (Figure 1.4). Out of these three assemblies, the IcmR-IcmQ interaction itself has been more extensively investigated finding IcmR to function as a chaperone of IcmQ by preventing aggregation of IcmQ as well as blocking IcmQ permeabilization of lipid membranes (Coers *et al.*, 2000; Dumenil and Isberg, 2001; Dumenil *et al.*, 2004; Raychaudhury *et al.*, 2009). However, the role of membrane disruption by IcmQ has in the functioning of the Dot/Icm system remains speculative, with possible roles in assembly or stabilization of the translocon as *icmQ* mutants are unable to replicate intracellularly (Coers *et al.*, 2000; Dumenil and Isberg, 2001; Raychaudhury *et al.*, 2009). Similarly, the inner-membrane DotU/IcmH-IcmF complex is suggested to also stabilize the core complex, except seems to do so by modulating DotH/IcmK levels via unknown mechanisms (Sexton *et al.*, 2004a; VanRheenen *et al.*, 2004). Whereas the DotI/IcmL-DotJ/IcmM heterocomplex, which localizes to the inner-membrane as well, is hypothesized to act as an inner-membrane conduit for effector proteins by transiently associating with the core complex to form a "translocation-active super complex" based on homology models to other T4SS (see Figure 1.4) (Kuroda *et al.*, 2015). Further assessments of these complexes and their individual components are needed to delineate the molecular mechanisms these proteins attribute to the Dot/Icm system.

The remaining Dot/Icm components have not been associated with the described complexes; however, these proteins have been investigated in regards to subcellular localization and in some instances been ascribed functions. The DotB protein has been identified to oligiomerize into a hexameric ring localized to the cytoplasm that has been shown to function as an ATPase and therefore proposed to provide energy to the Dot/Icm system (Figure 1.4) (Sexton *et al.*, 2004b). DotA on the other hand, is an inner-membrane protein with several transmembrane domains that when examined under certain experimental conditions is able to be

exported by the Dot/Icm system and form ring-like structures that are predicted to interact with the host membrane (Figure 1.4) (Nagai and Roy, 2001). Likewise, IcmT is also an integral membrane protein believed to interact with host cell membranes, as it has been connected to pore formation that leads to cell lysis and *L. pneumophila* egress (Figure 1.4) (Molmeret *et al.*, 2002). DotK/IcmN, is another component with membrane association however, it localizes to the outer-membrane and contains the peptidoglycan-binding domain of the OmpA family; a finding that has led to the supposition that DotK/IcmN is responsible for anchoring the Dot/Icm system to the peptidoglycan layer (Figure 1.4) (Morozova *et al.*, 2004; Vincent *et al.*, 2006b; Nagai and Kubori, 2011). For DotO/IcmB, DotE/IcmC, DotV, DotP/IcmD, IcmV and IcmX only subcellular localization has been defined with all but IcmX, which resides in the periplasm, being targeted to the inner-membrane (Figure 1.4) (Matthews and Roy, 2000; Vincent *et al.*, 2006b; Nagai and Kubori, 2011). Given the number of intricate parts, it is clear the Dot/Icm system is a sophisticated and complex secretion machine with equally complex mechanics that require further investigation to fully comprehend the coordination of each component to achieve the successful delivery of the numerous effector proteins harbored by *L. pneumophila*.

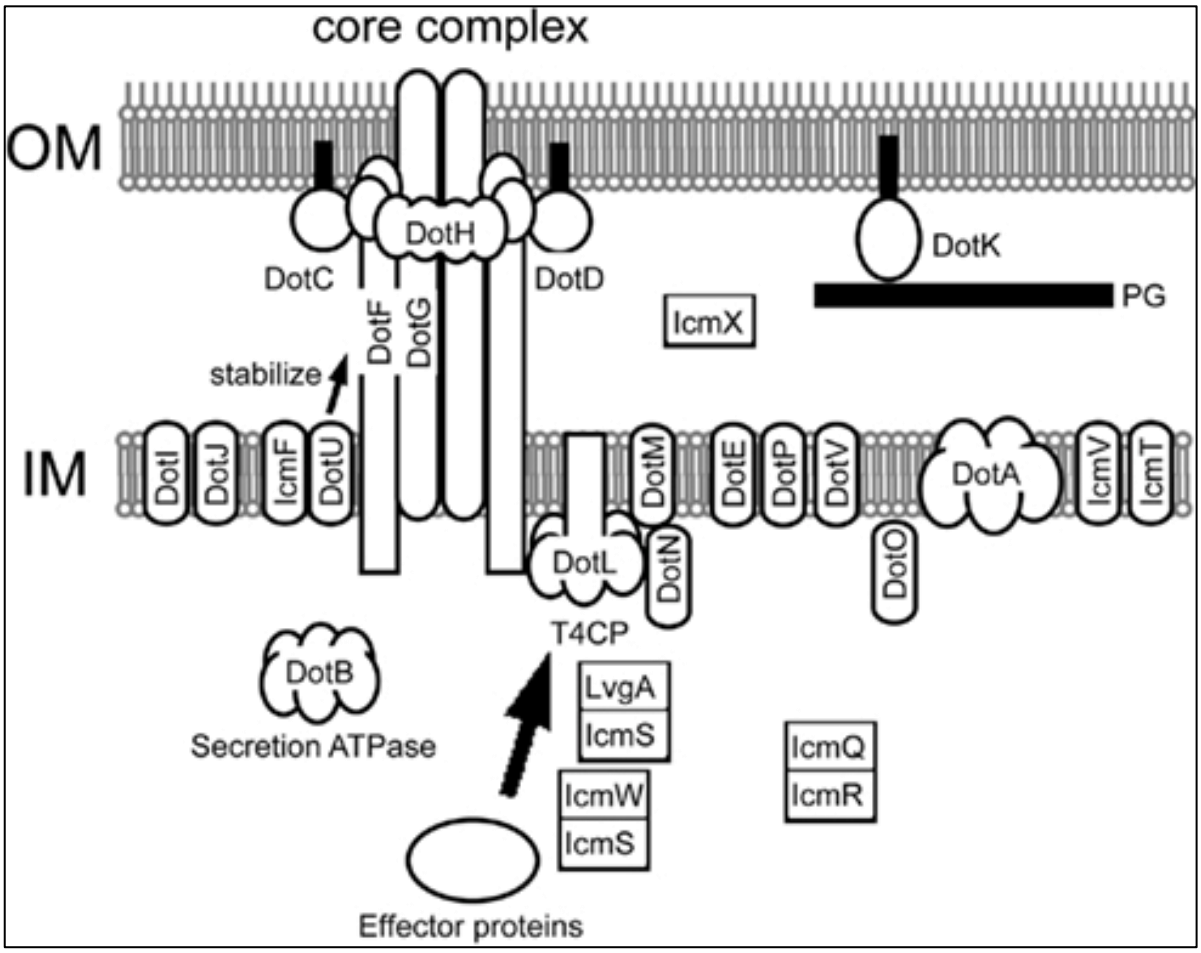

Figure 1.4 Schematic illustrating the *L. pneumophila* Dot/Icm Type IVB secretion system

Subcellular localization of the 27 Dot/Icm components are depicted with the designation of the outer-membrane (OM) and inner-membrane (IM). Highlighted are the core complex (DotC, DotD, DotH/IcmK, DotG/IcmE, DotF/IcmG), Type IV coupling protein complex (T4CP) consisting of DotL/IcmO, DotM/IcmP, DotN/IcmJ in association with the adapter complex IcmSW, translocon stabilizing complex (DotU/IcmH – IcmF), IcmS-LvgA adapter complex, IcmRQ assembly and the DotI/IcmL–DotJ/IcmM heterocomplex. The ATPase, DotB, and potential peptidoglycan (PG) binding protein, DotK/IcmN, are also indicated. Figure has been modified from Nagai and Kubori (2011).

1.2.2 Dot/Icm effector proteins – Discovery and functional roles

Since the recognition of the first Dot/Icm translocated effector protein, RalF, the repertoire of *L. pneumophila* effector proteins has been expanded to ~300. Identification of this vast number of effectors has been mediated by several key factors and sets of analysis. One key observation being, these Dot/Icm translocated substrates are essential to the intracellular survival of *L. pneumophila* as impeded effector secretion (i.e. a non-functional Dot/Icm system) results in the targeting of *L. pneumophila* to the lysosome and consequently to its degradation; a process normally subverted by this bacterium (Berger and Isberg, 1993; Brand *et al.*, 1994; Segal *et al.*, 1998; Vogel *et al.*, 1998). This modulation of host cellular processes by *L. pneumophila* effectors was thought to likely require these proteins to contain elements related to host factors central to eukaryotic vesicle trafficking and signaling pathways. As expected when initial targeted homology assessments of available gene databases were conducted, domains associated with eukaryotic proteins such as the Sec-7 domain and coiled-coil motifs were identified in the *L. pneumophila* effectors RalF and LidA, respectively (Nagai *et al.*, 2002; Conover *et al.*, 2003; Chen *et al.*, 2004). Upon completion of *L. pneumophila* strain genomes, analysis found several other types of eukaryotic protein motifs and domains to be present in encoded protein effectors as well as proteins with no known or minimal prevalence amongst prokaryotic genomes that show levels of similarity to proteins only found in eukaryotes, which were termed "eukaryotic-like" proteins and believed to also be effectors (Chien *et al.*, 2004; Cazalet *et al.*, 2004; de Felipe *et al.*, 2005). At the same time, experimental approaches were being utilized in other studies to identify potential effectors including, Dot/Icm dependent protein translocation screens via interbacterial transfer assays as well as genetic library screens for ORFs that were detrimental to growth and/or vesicular trafficking in the yeast model, *Saccharomyces cerevisiae*; all of which

yielded novel effector proteins (Luo and Isberg, 2004; Shohdy *et al.*, 2005; Campodonico *et al.*, 2005). A mechanism-focused study on how some effectors may be targeted to the Dot/Icm system revealed a C-terminal signal sequence necessary for the translocation of a subset of effectors, supplying another effector property for *in silico* analysis that uncovered additional *L. pneumophila* effectors (Kubori *et al.*, 2008). Taking *in silico* analysis even further, a group devised a sophisticated algorithm for distinguishing effectors within the *L. pneumophila* genome based on several features determined to be common among previously identified effector proteins, that when applied discovered a number of previously undefined effectors (Burstein *et al.*, 2009). Within each of these aforementioned studies and those conducted over the years, proteins ascribed as effectors have been validated as being secreted to the host-cell cytosol in a Dot/Icm dependent manner by the use of several reporter translocation assays; bringing together the findings of a number of works into the effector repertoire recognized today for *L. pneumophila*.

Functional roles have been distinguished for ~50 of the identified effectors revealing several host cellular pathways to be targeted by *L. pneumophila* [reviewed in (Finsel and Hilbi, 2015)]. Communication with the endocytic and secretory pathways has been evident since the initial microscopy observations of the infection process, where the phagosome harboring *L. pneumophila* avoids phagosome-lysosome fusion and instead acquires secretory vesicles to establish the LCV. Avoidance of the endocytic pathway by *L. pneumophila* is not completely understood however, as the LCV has been found to retain the small GTPases Rab5 and Rab7 that function in the endosomal maturation signaling process as markers of the early and late endosomes, respectively (Urwyler *et al.*, 2009; Stenmark, 2009; Jean and Kiger, 2012; Hoffmann *et al.*, 2014). Interestingly, recent studies have identified the effector, VipD, to bind Rab5

localized to host endosomes and hydrolyze phosphatidylinositol-3-phosphate (PtdIns(3)*P*), removing this lipid from the membrane (Ku *et al.*, 2012; Gaspar and Machner, 2014; Lucas *et al.*, 2014). This is significant as phosphoinositide (PI) lipids have predominant subcellular localizations that help to define organelle identity as well as take part in cellular signaling by facilitating the recruitment of enzymes or other factors needed in signaling events (Di Paolo and De Camilli, 2006; Jean and Kiger, 2012). PtdIns(3)*P* predominately localizes to early endosomes and is required to recruit factors needed in endosomal targeting, thus VipD-removal of this lipid from endosomes within the vicinity of the LCV likely contributes to endosomal avoidance by interfering with their ability to interact with the LCV (Di Paolo and De Camilli, 2006; Jean and Kiger, 2012; Gaspar and Machner, 2014). An effector capable of hydrolyzing PtdIns(3)*P in vitro*, SidP, has also been identified supporting lipid modification as a viable means of interference (Toulabi *et al.*, 2013). Equally intriguing, PtdIns(3)*P* lipids localize to the LCV as well, being acquired almost immediately after infection and gradually lost within two hours post-infection (Weber *et al.*, 2014). Effectors LidA, SetA, RidL, and LtpD have been determined to bind PtdIns(3)*P in vitro* indicating a possible anchoring mechanism to the LCV for these effectors, but also another means of interfering with endosomal signaling by potentially excluding the binding of host signaling proteins (Brombacher *et al.*, 2009; Jank *et al.*, 2012; Finsel *et al.*, 2013; Harding *et al.*, 2013). The combined interference by competitive occupancy and removal of PtdIns(3)*P* highlights promising mechanisms utilized by *L. pneumophila* to achieve endosomal avoidance.

In contrast, a number of effectors have been implicated in manipulating the secretory pathway to recruit vesicles to the LCV, with a major target of this pathway being the small GTPase Rab1. Rab GTPases are pivotal organizers of membrane trafficking processes as they

too localize to specific organelles or membrane compartments where they cycle between active GTP bound and inactive GDP bound states to spatiotemporally regulate host membrane trafficking factors (Stenmark, 2009; Jean and Kiger, 2012; Li and Marlin, 2015). Proteins that catalyze these Rab cycling events are Guanine nucleotide exchange factors (GEFs) and GTPase-activating proteins (GAPs), which promote the exchange of GDP for GTP or GTP hydrolysis to GDP by Rab GTPases, respectively. Rab1 is responsible for targeting ER-derived vesicles to the Golgi by specifically localizing to the ER exit sites and the *cis* face of the Golgi apparatus. *L. pneumophila* exploits this functional role to re-route vesicles exiting the ER to the LCV by recruiting Rab1 to the cytoplasmic face of the LCV and modulating its activity with thus far six effector proteins (Derre and Isberg, 2004; Kagan *et al.*, 2004).

Studies have identified the recruitment to the LCV and activation of Rab1 to be dependent upon the multifunctional effector SidM/DrrA (Machner and Isberg, 2006; Murata *et al.*, 2006). The central domain of this protein functions as a highly efficient Rab1 GEF that generates active GTP-Rab1 and couples this exchange activity with displacing the GDP-dissociation inhibitor (GDI) from Rab1 to retain activated Rab1 at the LCV (Ingmundson *et al.*, 2007; Machner and Isberg, 2007; Schoebel *et al.*, 2009; Suh *et al.*, 2010; Zhu *et al.*, 2010). GDIs are responsible for extracting inactive GDP-Rab proteins from membranes and inhibiting spontaneous GDP-GTP exchange that would lead to their inappropriate activation (Stenmark, 2009; Li and Marlin, 2015). To release Rab proteins to specific membrane sites, a GDI displacement factor (GDF) is required; as indicated above SidM/DrrA fulfills this functional role as well, thus acting as both a GEF and GDF. Counteracting Rab1 activation is the effector LepB, which inactivates Rab1 by stimulating GTP hydrolysis that leads to eventual removal of Rab1 from the LCV and thus serves as a Rab1 GAP (Ingmundson *et al.*, 2007). However, Rab1 is

retained and reaches maximal levels on the LCV two hours post-infection that is then followed by a steady decline, even though LepB is continuously secreted by the Dot/Icm system (Ingmundson *et al.*, 2007).

To delay LepB-inactivation of Rab1, it has been determined that *L. pneumophila* covalently modifies GTP-Rab1 through the AMPylation activity exhibited by the N-terminal region of SidM/DrrA, which transfers an adenosine monophosphate (AMP) moiety onto activated Rab1 that effectively inhibits LepB interaction and results in retention of Rab1 on the LCV (Muller *et al.*, 2010; Hardiman and Roy, 2014). This modification is reversible to allow for the timely inactivation of Rab1 by LepB, through the deAMPylase activity of the secreted effector SidD (Neunuebel *et al.*, 2011; Tan and Luo, 2011). The effector, AnkX, also covalently modifies Rab1 through the addition of a phosphocholine moiety that contributes to inhibiting LepB interaction as well, and can be reversed by the Dot/Icm transferred dephosphocholinase Lem3 (Mukherjee *et al.*, 2011; Tan *et al.*, 2011). However, this modification has been shown to be unable to compensate for the AMPylation function in retaining Rab1 on the LCV and thus how phosphocholination fits into the modification processes that contribute to the temporal association of Rab1 with the LCV has yet to be determined (Hardiman and Roy, 2014). The complexity of Rab1 modulation is further enhanced by the identification of a "super effector" LidA that exhibits extremely high binding affinity for Rab1, that when bound can inhibit LepB interaction, AMPylation, deAMPylation, phosphocholination and dephosphocholination (Machner and Isberg, 2006; Schoebel *et al.*, 2011; Neunuebel *et al.*, 2012). Again, the timing of LidA interaction and reasoning for LidA inhibiting Rab1 modification has yet to be determined.

Evidenced by the activities described above, significant advances in determining the functional roles of *L. pneumophila* effectors have been made nonetheless, only a fraction of the

identified effectors have ascribed functions leaving many to be determined. Hindering the progress of these investigations is the high degree of functional redundancy *L. pneumophila* exhibits in its effector repertoire. Simply generating single effector deletion mutant strains often does not result in significant intracellular growth defects or perturbed LCV formation (Luo and Isberg, 2004). This is exemplified by a study that found generating large genetic deletions encompassing clusters of effectors only resulted in growth defects in some amoebae hosts but not in others examined (O'Connor *et al.*, 2011). Furthermore, within this same study deletions encompassing 31% of encoded effectors did not effectively impede the intracellular growth of *L. pneumophila* in murine bone marrow derived macrophages.

It is hypothesized the large number of *L. pneumophila* effectors is the result of horizontal gene transfer that has occurred through the continuous intracellular cycling between varying environmental hosts (Cazalet *et al.*, 2004; Chien *et al.*, 2004; Gomez-Valero *et al.*, 2011; Gomez-Valero and Buchrieser, 2013). Acquiring such a quantity of effectors is presumed to be highly beneficial as it allows *L. pneumophila* to be a "generalist" in host selection (O'Connor *et al.*, 2011; Ensminger *et al.*, 2012; Ensminger, 2016). Each unique protozoan host encounter, requiring a different subset of effectors to meet the new challenges of that host, is likely to provide selective pressure for retention of each effector that benefits *L. pneumophila* survival. Even though the effector(s) maybe non-essential or perform redundant functions in a number of other hosts, the function(s) are needed in a specific host and provide a potential advantage against predation in future host encounters. Evidence supporting this is the relatedness of effectors to eukaryotic host factors in sequence, domain structure or function and by the fact that 20 different species of Amoebae thus far have been shown to support the growth of *L. pneumophila* (Gomez-Valero *et al.*, 2011; Gomez-Valero and Buchrieser, 2013; Tyson *et al.*,

2014). Because of this functional redundancy, continued progress in unraveling effector functions will remain dependent upon the combined revelations of investigating protein-protein interactions, enzymatic activities, crystal structures and regulatory cascades.

1.3 Regulatory cascades associated with virulence and morphogenesis

To coordinate morphological differentiation with the induction of virulence traits necessary for transmission as well as environmental survival, *L. pneumophila* employs dramatic changes in gene expression. This is reflected in the several hundred genes identified in transcriptomic studies to be differentially regulated either during post-exponential phase when grown in broth or during later time points of intracellular growth in amoeba or macrophage host cells (Bruggemann *et al.*, 2006; Faucher *et al.*, 2011). Governing these changes in gene expression are two parallel but interconnected regulatory networks that are activated through the nutritional sensing of *L. pneumophila* that is similar to the stringent response characterized in *Escherichia coli* (summarized in Figure 1.5) (Magnusson *et al.*, 2005).

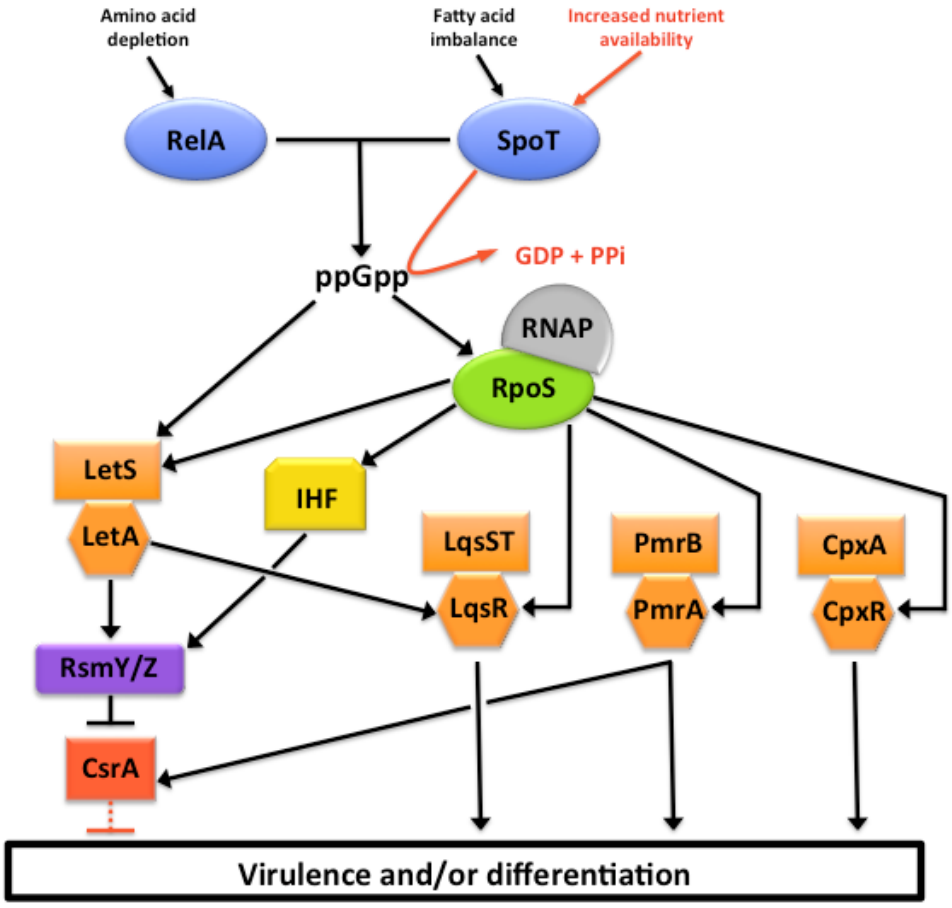

Figure 1.5 Regulatory cascades governing virulence and differentiation in *L. pneumophila*

Under conditions of nutrient stress, the stringent response components RelA and SpoT synthesize the cellular signaling molecule ppGpp, which activates the sensor kinase LetS to initiate the response regulator LetA as an activator of the small non-coding RNAs (ncRNAs), RsmY and RsmZ. The ncRNAs then sequester the RNA binding protein CsrA to relieve its post-transcriptional repression of virulence and/or differentiation. In a parallel cascade, ppGpp induces RpoS expression and increases its competiveness for RNA polymerase (RNAP) that then promotes the increased expression of response regulators LqsR, PmrA, and CpxR. Each of these two-component systems (TCSs) influence a number of virulence related genes including Dot/Icm

system components and effectors, likely coordinating the virulence outputs that occur downstream of RpoS. Cooperative regulatory interactions occur between the two cascades; with RpoS inducing RsmY/Z expression through interactions with LetS and IHF, as well as the contribution of LetA to the induction of LqsR in concert with RpoS. When nutrient conditions are favorable (red), SpoT hydrolyzes ppGpp lowering the cellular levels of the signal such that the regulatory cascades become arrested and this allows for the accumulation of free CsrA. CsrA then binds and represses transcripts of the virulence state to promote replication.

1.3.1 Stringent response signaling

Being most well studied in *Escherichia coli*, the stringent response is triggered by nutrient deprivation that is sensed by two key proteins, RelA and SpoT (Magnusson *et al.*, 2005; Potrykus and Cashel, 2008; Hauryliuk *et al.*, 2015). RelA specifically senses amino acid starvation by monitoring for the presence of uncharged tRNA in the ribosomal acceptor site (A-site) (Wendrich *et al.*, 2002). Upon detecting uncharged tRNA, RelA is able to form stable interactions with both the uncharged tRNA and the 50s ribosomal subunit to adopt a conformation that activates its synthesis capabilities of the crucial stringency messenger, guanosine tetraphosphate (ppGpp) (Agirrezabala *et al.*, 2013). SpoT on the other hand, senses nutritional stresses other than amino acid starvation including depletion of fatty acids, carbon sources and iron (Xiao *et al.*, 1991; Seyfzadeh *et al.*, 1993; Vinella *et al.*, 2005). It too synthesizes ppGpp in response to these nutritional changes, but in a much more reduced capacity in comparison to RelA (Xiao *et al.*, 1991). The mechanisms that lead to the synthesis of ppGpp by SpoT are not as well defined as those for RelA but have been linked to acyl carrier protein (ACP) binding to a specific domain of SpoT that is predicted to relay changes in fatty acid metabolism depending on the form of ACP bound (Battesti and Bouveret, 2006; Angelini *et al.*, 2012). In addition to being a weak synthase of ppGpp, SpoT is also a strong ppGpp hydrolase; a function necessary for balancing cellular ppGpp levels.

The increased pool of ppGpp that results from the combined synthesis activities of RelA and SpoT provokes extensive changes in the transcriptional landscape by binding RNA polymerase (RNAP) and altering RNAP activity at promoter sites (Magnusson *et al.*, 2005; Hauryliuk *et al.*, 2015). Influences on transcription by ppGpp are also facilitated through its impacts on sigma factor competiveness for RNAP, favoring interactions with alternative sigma

factors such as σ^S (RpoS) needed for expression of stress resistance factors (Magnusson *et al.*, 2005; Potrykus and Cashel, 2008; Sharma and Chatterji, 2010). These gene expression changes give rise to pleotropic effects on physiological processes including growth inhibition, reduced synthesis of translation machinery and a shift to amino acid biosynthesis; adjustments required for cellular maintenance and survival.

Homologues of RelA and SpoT have been identified in *L. pneumophila*. Both homologues were found to be required for ppGpp accumulation, with RelA retaining the ability to respond to amino acid starvation as a major synthase and SpoT conserved as a minor synthase when experiencing disruptions in fatty acid biosynthesis (Zusman *et al.*, 2002; Dalebroux *et al.*, 2009). Generation of ppGpp is critical for the transition of *L. pneumophila* to a virulent state and to carry out differentiation as a complete lack of ppGpp due to *relAspoT* combinatorial deletions results in hyperfilamentous *L. pneumophila* that is unable to induce motility, remains sodium resistant and has limited viability when grown to post-exponential phase in broth (Dalebroux *et al.*, 2009). Furthermore, the absence of ppGpp renders *L. pneumophila* susceptible to phagosome-lysosome fusion and incapable of transmission between macrophage host cells (Dalebroux *et al.*, 2009). However, reduction of ppGpp levels was also determined to be essential as it enables the return of *L. pneumophila* to the replicative state upon encountering more favorable nutritional environments, where ppGpp hydrolysis was linked to the presence of SpoT indicating the bifunctional activity of SpoT has been conserved in *L. pneumophila* (Dalebroux *et al.*, 2009).

1.3.2 Transcriptional and post-transcriptional regulation

To orchestrate these cellular changes, ppGpp communicates with downstream regulatory factors important to the *L. pneumophila* transmissive process. This includes a post-transcriptional regulatory cascade that is highly conserved amongst Gammaproteobacteria and consists of the following: A two-component system (TCS) that governs the expression of small non-coding RNAs (ncRNAs) responsible for binding multiple homodimers of a RNA binding protein (RBP), to effectively sequester the RBP from eliciting its post-transcriptional regulation on multiple target transcripts [reviewed in (Vakulskas *et al.*, 2015)]. Well-studied examples of this regulatory cascade include the BarA/UvrY (TCS), CsrB and CsrC (ncRNAs), and CsrA (RBP) of *E. coli* and the GacAS (TCS), RsmY and RsmZ (ncRNAs), and RsmA (RBP) of *Pseudomonas* spp.; each with differing outcomes in regards to changes in metabolism, physiology and virulence (Pessi *et al.*, 2001; Heeb *et al.*, 2002; Suzuki *et al.*, 2002; Brencic *et al.*, 2009; Humair *et al.*, 2010; Vakulskas *et al.*, 2015).

In *L. pneumophila*, this post-transcriptional circuitry is managed by the LetAS TCS, which is homologous to the GacAS TCS and functionally similar to the BvgAS TCS of *Bordetella*. LetAS exhibits rheostat-like controls over the multiple phosphotransfer reactions that occur within the sensor kinase LetS and relayed to the cognate response regulator LetA for its activation (Hammer *et al.*, 2002; Edwards *et al.*, 2010). The signal triggering the phosphorelay of LetS has been deemed to be elevated levels of ppGpp based on the transcriptome changes and phenotypes of *letA* and *letS* mutant strains. Both mutant strains are primarily sodium resistant and display impaired cytotoxicity as well as motility in comparison to the motile, sodium sensitive, and cytotoxic parental *L. pneumophila* during the post-exponential phase (Hammer *et al.*, 2002). No transcriptional changes occurred in the exponential phase of these mutant strains

in comparison to parental *L. pneumophila* but marked changes do occur during the post-exponential phase, where virulence and transmission genes are down regulated and replicative genes are up regulated; indicating these mutants constitutively resemble RF-like mutants unable to generate ppGpp (Sahr *et al.*, 2009). However, these regulatory impacts are considered to be indirect as intensive searches of the *L. pneumophila* genome for promoters containing the probable LetA binding consensus sequence revealed only the two small ncRNAs, *rsmY* and *rsmZ*, to be under the control of LetA (Sahr *et al.*, 2009). These ncRNAs have been determined to be the antagonists of the *L. pneumophila* post-transcriptional regulator CsrA, with the nomenclature of these factors reflecting their homologies to their regulatory counterparts in the *Pseudomonas* and *E. coli* post-transcriptional cascades (Fettes *et al.*, 2001; Kulkarni *et al.*, 2006; Rasis and Segal, 2009; Sahr *et al.*, 2009). CsrA has been identified to be pivotal to the cell cycle changes of *L. pneumophila* as conditional mutants of *csrA* leads to premature motility, cytotoxicity, and differentiation to coccoid bacteria during exponential phase whereas over expression of *csrA* leads to filamentous bacteria that are limited in motility and have impaired cytotoxicity during the post-exponential phase (Fettes *et al.*, 2001; Molofsky and Swanson, 2003). Furthermore, CsrA directly represses the transcripts of several Dot/Icm effector proteins through binding of the motif A(N)GGA located within the leader sequence of RNA, indicating *L. pneumophila* CsrA utilizes the conserved mechanism of occluding the Shine-Delgarno (SD) sequence (rich in GA motifs) from ribosomal binding to achieve translational repression (Rasis and Segal, 2009; Nevo *et al.*, 2014).

In concert with the LetAS-RsmYZ-CsrA cascade, elevated ppGpp levels also influence the alternative sigma factor RpoS. Under conditions of artificially induced ppGpp synthesis, *rpoS* transcripts are increased and during the post-exponential growth phase, when ppGpp levels are

maximal in *L. pneumophila*, elevated RpoS protein levels are observed (Hales and Shuman, 1999; Dalebroux *et al.*, 2010). Thus it is believed that like in *E. coli*, ppGpp alters the competiveness of RpoS for RNAP to achieve global regulatory changes; however, the targeted genes in *L. pneumophila* are those needed to carry out host transmission rather than enacting the general stress resistance associated with the *E. coli* homologue. The bases for this alternative role of RpoS in *L. pneumophila* are the identified phenotypes of an *rpoS* mutant. Studies have found RpoS is not required for survival during the post-exponential phase of broth culture nor is it needed to maintain the osmotic, oxidative or acid resistance developed by *L. pneumophila* during this growth phase (Hales and Shuman, 1999; Bachman and Swanson, 2001). Yet, RpoS is necessary for the on-set of sodium sensitivity and full motility during the post-exponential phase, while also being essential to the intracellular survival of *L. pneumophila* in *Acanthamoeba castellanii* and to promoting efficient replication in primary murine macrophages (Hales and Shuman, 1999; Bachman and Swanson, 2001).

Supporting these phenotypic findings is a large number of RpoS-dependent gene expression changes of which many are associated with virulence. A transcriptomic analysis of an *rpoS* mutant revealed a significant proportion of genes affected by RpoS during the post-exponential phase are classified as serving pathogenic functions, including genes encoding several Dot/Icm effector proteins as well as genes shown to facilitate the enhanced entry (*enh*) of *L. pneumophila* (Hovel-Miner *et al.*, 2009). Moreover, RpoS was found to induce genes encoding the response regulators of the CpxRA and PmrAB TCSs, both of which regulate Dot/Icm system components and effectors (Hovel-Miner *et al.*, 2009). Regulatory impacts were also observed for the ncRNAs RsmY and RsmZ, in which RpoS was determined to induce their expression through an upstream interaction with LetS; revealing a pathway interface with many

downstream alterations in gene expression that likely contribute the phenotypes observed in the absence of *rpoS* (Hovel-Miner *et al.*, 2009). Likewise, Pitre *et al.* (2013) found RpoS to induce RsmY and RsmZ expression via another upstream mechanism, where RpoS activates the expression of integration host factor (IHF), which then acts as a direct positive transcriptional regulator of RsmY and RsmZ expression. Similarly, Tiaden *et al.* (2007) has also determined another response regulator LqsR, belonging to the *L. pneumophila* quorum sensing system and a contributor to virulence regulation, as being positively influenced by RpoS in combination with LetA as well. These findings point to an overall trend of RpoS accomplishing its central role of virulence regulation via targeting other transcriptional and/or regulatory factors in *L. pneumophila*.

Collectively, these works have established *L. pneumophila* employs transcriptional and post-transcriptional regulatory mechanisms to achieve widespread gene expression changes needed for the timely orchestration of virulence and differentiation. Within these cascades are crossroads that allow for cooperative outcomes as well as versatility in pathway selection that enables multiple input points for accommodation of many different cellular signals. These include the TCSs other than the LetAS system (CpxRA, PmrAB, LqsRST) mentioned above that perceive a variety of unknown signals (with the exception of the identified quorum sensing compound of the LqsRST system) through their sensor kinases and respond by enacting gene expression changes that also contribute to virulence and/or differentiation in *L. pneumophila*. To avoid redundancy, a brief summary of the PmrAB and LqsRST functional roles and regulatory targets can be found in Chapter 3, section 3.1. Only the CpxRA TCS will be discussed in further detail below, as it is the focus of this thesis.

1.3.3 The CpxRA two-component system (TCS)

The *L. pneumophila* CpxRA TCS was identified through bioinformatic analysis as being orthologous to the *E. coli* CpxRA TCS (Gal-Mor and Segal, 2003a). This relatedness provides a foundation for investigations into the *L. pneumophila* CpxRA TCS as this system has been most extensively studied in *E. coli*; where mechanisms of signal transduction and regulatory targets identified in *E. coli* serve as models for the *L. pneumophila* CpxRA TCS. Therefore, it is important to elaborate on these findings in *E. coli* in order to have a better understanding of the knowledge being extended to the *L. pneumophila* CpxRA TCS.

1.3.3.1 Discovery and functional modeling in *E. coli*

The CpxRA TCS was first discovered in *E. coli* when searching for chromosomal genes that altered functions of the conjugative F-plasmid (McEwen and Silverman, 1980). Characterization of a chromosomal mutant with dramatically reduced F-pili formation gave rise to the designation of the mutated locus as, *c*onjugative *p*lasmid e*x*pression A (*cpxA*). Continued investigations of this locus and the encoded proteins revealed CpxA to be a transmembrane sensor kinase and the gene encoded immediately upstream to be the cognate response regulator, *cpxR* (*c*onjugative *p*lasmid e*x*pression *r*egulator) (Weber and Silverman, 1988; Dong *et al.*, 1993).

Amino acid sequence evaluations have classified CpxA as a class I sensor kinase based on the domain organization within its cytoplasmic region being similar to the prototypical sensor kinase EnvZ (Dutta *et al.*, 1999; Hunke *et al.*, 2012). The overall architecture of CpxA is composed of an N-terminal sensing domain situated between two transmembrane domains and a C-terminal cytoplasmic region that consists of a linker and a highly conserved transmitter

domain, with each domain carrying out specific functions to facilitate the signal transduction process (Figure 1.6) (Hunke *et al.*, 2012). The sensing domain located in the periplasmic space is responsible for receiving input signals. When an activating signal is perceived, the signal is transduced across the inner-membrane to the HAMP (*h*istidine kinases, *a*denylyl cyclases, *m*ethyl-accepting chemotaxis proteins and *p*hosphatases) domain that then undergoes conformational changes to deliver the signal to the transmitter domain; thus acting as a link for signal transmission between sensor and transmitter domains (Appleman *et al.*, 2003; Szurmant *et al.*, 2007). The transmitter domain harbors both a *d*imerization and *h*istidine *p*hosphotransfer (DHp) domain and a *ca*talytic (CA) domain responsible for signal output (Buelow and Raivio, 2010; Dutta *et al.*, 1999; Hunke *et al.*, 2012). The DHp domain contains a dimerization motif that allows for binding of another CpxA monomer and in this dimeric state each monomer trans-phosphorylates the other at the conserved histidine residue (H248) located within the DHp domain (Raivio and Silhavy, 1997; Gao and Stock, 2009; Buelow and Raivio, 2010; Hunke *et al.*, 2012). This autophosphorylation event is carried out via the CA domain through the use of ATP and Mg^{2+} (Gao and Stock, 2009; Buelow and Raivio, 2010). The transmitter domains can then act as a kinase and transfer the phosphate molecule to CpxR as well as act as a phosphatase and remove the phosphate molecule in order to balance the signaling output (Raivio and Silhavy, 1997).

CpxR has been determined by bioinformatic analysis to be part of the OmpR-family of DNA binding proteins due to high sequence similarity as well as conservancy of residues key to tertiary structures (Dong *et al.*, 1993; Itou and Tanaka, 2001). As an OmpR-family response regulator, CpxR is a cytoplasmic protein comprised of an N-terminal receiver domain that is connected to a C-terminal effector domain via a flexible linker (Figure 1.6) (Kenney, 2002;

Hunke *et al.*, 2012). The receiver domain consists of a conserved aspartic acid residue at position 51 (D51) that is responsible for receiving the phosphate molecule from the transfer domain of CpxA during the phosphotransfer reaction (Raivio and Silhavy, 1997; Hunke *et al.*, 2012). Phosphorylation at this site leads to dimerization of CpxR monomers at the receiver domains, causing further conformational changes that activate the effector domain for DNA binding (De Wulf *et al.*, 2002; Gao and Stock, 2010). Interactions with DNA occur through a winged helix-turn-helix motif that recognizes promoter regions containing the consensus sequence 5'-GTAAA-(N_5)-GTAAA-3', with each monomer binding a pentamer (Pogliano *et al.*, 1997; Martinez-Hackert and Stock, 1997; De Wulf *et al.*, 1999; De Wulf *et al.*, 2002). These promoter interactions then influence the transcription of the associated gene(s) needed to respond to the initial input signal.

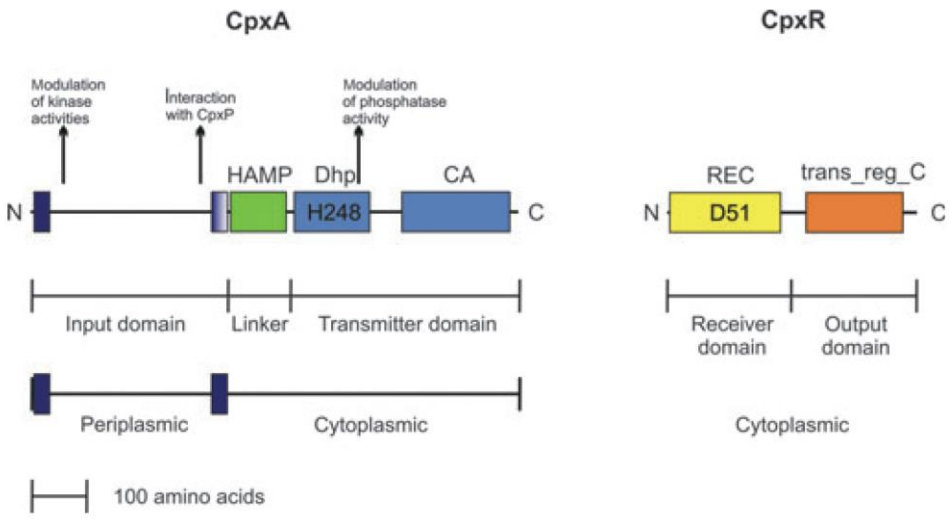

Figure 1.6 Domain architecture of the transmembrane sensor kinase CpxA and the cytoplasmic cognate response regulator CpxR. CpxA consists of two transmembrane domains (navy rectangles) that frame a periplasmic sensing domain (input domain) responsible for sensing and receiving signals. Activation leads to signal transfer across the inner-membrane to the cytoplasmic HAMP domain (green), which delivers the signal to the transmitter domain and initiates dimerization and subsequent autophosphorylation of the conserved histidine residue within the DHp domain (blue rectangle), via the catalytic activities of the CA domain (blue rectangle). CpxR consists of a receiver domain (yellow) that is phosphorylated at a conserved aspartic acid residue, which then results in conformational changes in the effector domain (output domain) (orange) that is connected through a flexible linker to the receiver domain. Within the effector domain is a winged helix-turn-helix motif that enables DNA binding upon activation and is referred to as a Trans_reg_C (Transcriptional regulatory protein, C terminal) domain in some databases. Figure has been sourced from Hunke *et al.* (2012).

1.3.3.2 Accessory factors and signals of the CpxRA TCS in *E. coli* and related bacteria

Since the discovery of this system, investigations have continued in *E. coli* as well as other Gram-negative bacteria, finding this system to be widely spread through out the genera of this group and most highly conserved amongst the *Enterobacteriace* family (De Wulf *et al.*, 2000; Vogt and Raivio, 2012; Raivio, 2014). Within these investigations, expansion of the components that contribute to the sensing and activation of the CpxRA TCS has occurred. These include a periplasmic protein, an outer-membrane lipoprotein, and a small RNA (sRNA) product referred to as CpxP, NlpE, and CpxQ, respectively.

CpxP was discovered during a library screen aimed at identifying other CpxRA regulon members in *E. coli*, where it was found to be divergently transcribed from the *cpxRA* locus and induced by CpxR under conditions established to activate CpxA (Danese and Silhavy, 1998). Evaluations of its protein sequence revealed a signal sequence that indicated transport across the inner-membrane to the periplasm that was then conferred to occur experimentally (Danese and Silhavy, 1998). The function of CpxP was later realized to be a post-translational negative regulator of CpxA based on the following findings: 1) overexpression of *cpxP* leads to the down regulation of Cpx-mediated genes; and 2) addition of CpxP to an *in vitro* reconstituted CpxRA system results in decreased autophosphorylation rates of CpxA (Raivio *et al.*, 1999; Fleischer *et al.*, 2007). It is hypothesized CpxP carries out this repression through direct protein-protein interactions with CpxA. This has been recently supported by elucidation of the CpxP crystal structure, where it was found to form a crescent shaped cap that contains positively charged residues on its concave face that would interact with the negative residues of the CpxA periplasmic region (Zhou *et al.*, 2011). As well, direct but dynamic interactions between CpxP and CpxA have been observed *in vitro* and *in vivo* in *E. coli* using bacterial two-hybrid assays

and membrane-Strep-tagged protein interaction experiments (mSPINE), respectively, further reinforcing this model (Tschauner *et al.*, 2014). However, this direct interaction is somewhat contested within the literature, as experiments using CpxA and CpxP derived from *Vibrio parahemolyticus* as well as an independent study in *E. coli* conducted by Raivio and colleagues, could not detect direct interactions (Kwon *et al.*, 2012; Raivio, 2014). Therefore, the mechanism of inhibition remains to be completely defined.

Under conditions of stress where CpxRA needs to be activated, repression by CpxP must be relieved. It has been shown that this occurs through the means of titration and subsequent degradation, where CpxP binds to misfolded proteins that accumulate in the periplasm, removing it from the periplasmic region of CpxA and then presents the misfolded proteins to the periplasmic protease, DegP (Figure 1.7) (Buelow and Raivio, 2005; Isaac *et al.*, 2005). DegP then degrades the misfolded proteins and CpxP as a consequence of being bound to the misfolded protein (Buelow and Raivio, 2005; Isaac *et al.*, 2005). It is believed that the activated state of the CpxRA system is then shutdown when the stress is alleviated and misfolded proteins no longer accumulate, as this would allow for free CpxP to accumulate due its expression being induced under the CpxRA activating conditions (Figure 1.7) (Buelow and Raivio, 2005; Isaac *et al.*, 2005).

NlpE (*n*ew *l*ipoprotein *E*) was discovered during a library screen of *E. coli* chromosomal regions, whose encoded products were present in multiple copies as a consequence of the plasmid copy number, alleviated extracytoplasmic toxicities elicited by a hybrid reporter protein (Snyder *et al.*, 1995). When trying to understand how the elevated levels of NlpE were alleviating the reporter toxicity, it was found that a gene dependent on CpxR for activation was up regulated under these conditions of elevated NlpE (Snyder *et al.*, 1995). Further investigation

of this connection found that the up regulation of the CpxR-regulated gene as well as the alleviation of toxicity by elevated NlpE required the presence of CpxA and CpxR (Danese *et al.*, 1995). Bioinformatic analysis combined with cellular localization studies found NlpE to reside in the outer-membrane and with the experimental designation as a lipoprotein, it was predicted to be positioned on the periplasmic face of the outer-membrane; however, no other predictions or designations could be made about its potential functions leaving its connection to the CpxRA system unknown (Snyder *et al.*, 1995; Otto and Silhavy, 2002). This mystery was solved in part when the CpxRA system was found to be required for the abiotic surface adhesion of *E. coli*, where the outer-membrane localization of NlpE led the researcher to examine the adhesion and CpxRA response in an *nlpE* mutant (Otto and Silhavy, 2002). In the absence of *nlpE*, adhesion was reduced and the induction of *cpxR* that was found to occur during adhesion was completely abolished, indicating NlpE activated the CpxRA response to adhesion (Otto and Silhavy, 2002). With the localization to the periplasmic side of the outer-membrane, it was thought that NlpE would be in proximity to interact with the CpxA periplasmic sensing domain to relay the changes exhibited during adhesion (Otto and Silhavy, 2002). The crystallographic structure of NlpE supports a potential interaction with CpxA as it was determined to contain an unstable N-terminal β-barrel that anchors to the outer-membrane that could unfold during adhesion stress in order to lengthen itself and contact CpxA (Figure 1.7) (Hirano *et al.*, 2007). Again, the model requires further experimental analysis to confirm these structural changes and potential protein-protein interactions.

CpxQ is the most recent addition to the CpxRA TCS accessory repertoire and is the first sRNA to be identified as being specific to the CpxRA regulon (Chao and Vogel, 2016). Considerations that prompted the researchers to look for this sRNA include the fact that the Cpx

system is activated in the absence of RNA binding protein Hfq and that transcriptomic analyses have shown multiple genes to be differentially regulated by CpxR but do not themselves contain the CpxR binding motif within their promoters, indicating indirect interactions through sRNA (Raivio *et al.*, 2013; Vogt and Raivio, 2014; Chao and Vogel, 2016). Initial searches of a dataset consisting of the Hfq-associated sRNAs of *Salmonella* for the occurrence of the CpxR conserved binding motif within in their promoter regions did not identify any potential prospects; however, many Hfq bound sRNAs were found in *Salmonella enterica* serovar Typhimurium to be produced from within mRNA through processing and would therefore not possess a promoter (Chao *et al.*, 2012; Chao and Vogel, 2016). Re-examination of the Hfq-bound RNA for fragments derived from CpxR regulon members identified a 3' untranslated region (UTR) that corresponded to the *cpxP* transcript, providing an initiation point for the study (Chao and Vogel, 2016). Mutational analysis and *in vitro* assays revealed CpxQ to be generated through the RNaseE cleavage of the *cpxP* transcript and this was shown to likely incorporate Hfq as a stabilization factor (Figure 1.7) (Chao and Vogel, 2016). Functional analysis and regulatory assessments revealed CpxQ to be produced under conditions that disrupt the proton motive force and in response to this down regulates the transcripts of a sodium proton anti-porter to reduce its presence in the inner-membrane, resulting in reduced proton intake that allows for recovery of the proton motive force (Chao and Vogel, 2016).

Another target of CpxQ identified in a separate study conducted in *E. coli*, was the down regulation of the periplasmic chaperone Skp that if left unchecked inserts outer membrane proteins into the inner membrane that leads to disruptions in the proton motive force as well (Figure 1.7) (Grabowicz *et al.*, 2016). Together, these studies reveal a post-transcriptional

mechanism utilized by the CpxRA system to alleviate stress, thus far specifically stresses that occur during disruptions of the proton motive force.

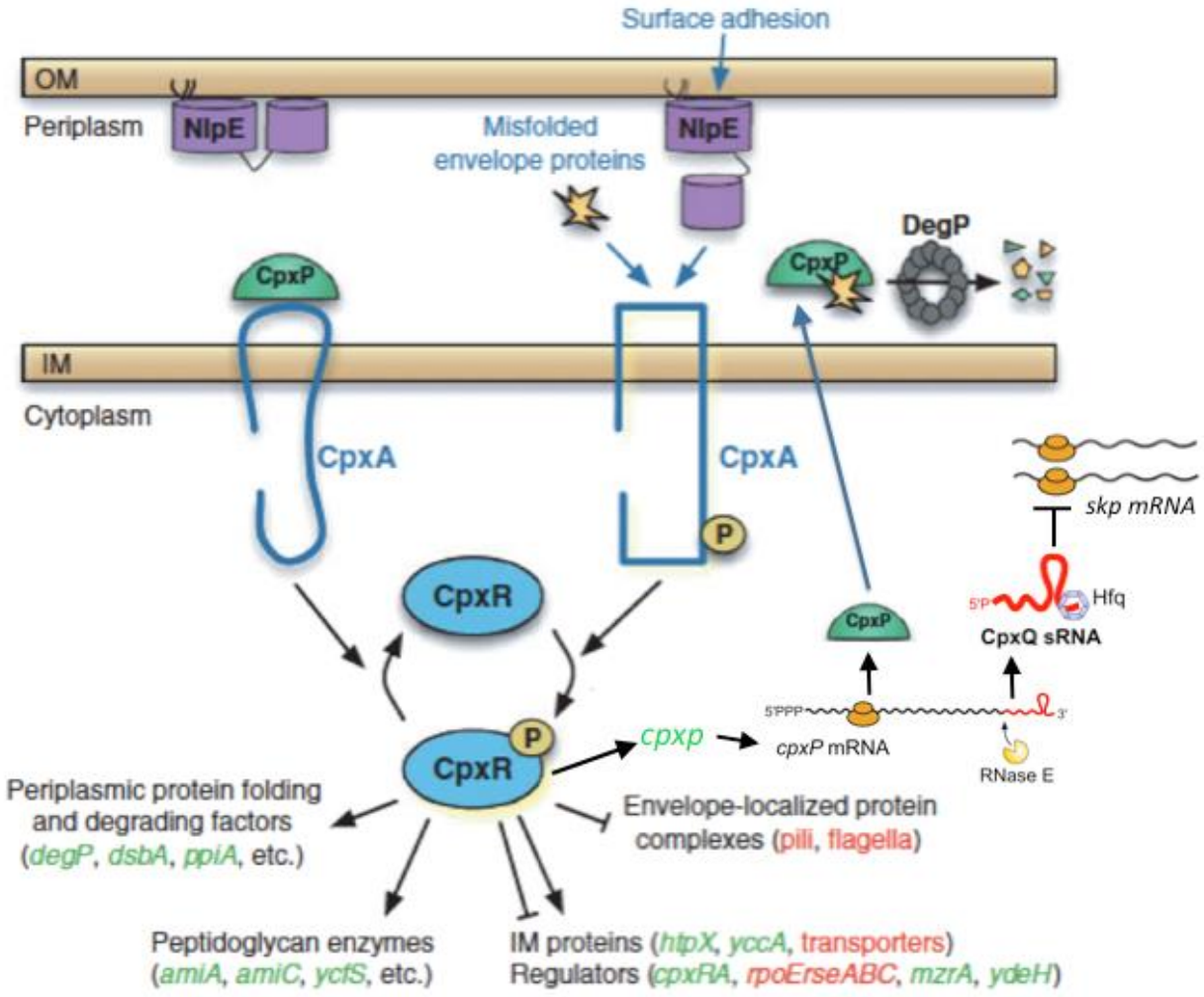

Figure 1.7 Summary of the *E. coli* CpxRA TCS signal transduction, accessory factors and regulon members. The periplasmic protein CpxP inhibits the activity of CpxA by blocking its sensor domain during times of non-stress. When conditions occur that induce cell envelope stress, input signals such as the accumulation of misfolded proteins and/or surface adhesion sensed by NlpE, CpxP is titrated away through binding of misfolded proteins and subsequently degraded by the periplasmic protease, DegP. The unbound periplasmic sensing domain of CpxA is now free to receive activating signals, which includes a potential protein interaction with

NlpE. Activated CpxA carries out autophosphorylation and acts as a kinase to phosphorylate CpxR to enable it as a transcriptional regulator to induce (green font) or repress (red font) the expression of several target genes part of different cellular processes. The CpxR-induced transcription of *cpxP* generates *cpxP* mRNA that is both translated to produce CpxP protein targeted to the periplasm, and further processed by RnasE to produce the sRNA CpxQ; which post-transcriptionally inhibits Skp synthesis to alleviate stress associated with disruptions to the proton motive force. When the envelope stress has been removed, CpxA acts as a phosphatase to remove the phosphate molecule from CpxR and bring the system back to a resting state. Figure has been modified from Vogt and Raivio (2012) and adapted to include components from Chao and Vogel (2016).

1.3.3.3 The CpxRA regulatory targets and implications in virulence of *E. coli* and other bacteria

The signal transduction carried out by CpxA through the key phosphotransfer reactions of autophosphorylation as well as its kinase and phosphatase activities, serve to elicit the appropriate cellular response to extracellular stresses through modulating the activity of CpxR that ultimately implements the required changes in gene expression. Identifying the regulatory targets of CpxR has been readily undertaken since the initial discovery of this system and has been instrumental in understanding the physiological role of this system in Gram-negative bacteria.

The initial targets of CpxR were found to be periplasmic protein and degradation factors that included *degP*, *dsbA*, and *ppiA*, which encode a periplasmic protease, a disulphide bond oxidoreductase, and a peptidyl-prolyl isomerase, respectively (Figure 1.7) (Danese *et al.*, 1995; Pogliano *et al.*, 1997). Each of these targets play major roles in alleviating cell envelope stress by either degrading misfolded proteins that accumulate in the periplasm or catalyzing changes in the protein structure to help proteins properly re-fold. Their determination as direct regulatory targets of CpxR classified the CpxRA system as a major facilitator of the envelope stress response.

Elucidation of these direct regulatory targets provided a consensus binding motif for CpxR that enabled the discovery of other regulon members which included itself and the inhibitory divergently transcribed *cpxP* (Pogliano *et al.*, 1997; Raivio *et al.*, 1999). Regulatory assessments found that activation of the CpxRA system increased the expression of the *cpxRA* operon, which allows this system to bolster its response to the stress input (Figure 1.7). At the same time, CpxR also induces the expression of the inhibitory protein CpxP, which assists in the

response by binding misfolded proteins and presenting them to DegP but also helps return the system to inactivation by blocking further input signals from reaching CpxA (Figure 1.7). Therefore, it was deemed the CpxRA system amplifies its own expression through positive autoregulation but employs a negative feedback loop through the induction of the CpxP inhibitor (Raivio *et al.*, 1999). It has been presumed that bacterial species that maintain this genetic organization with the respective CpxR binding motifs elicit the same mechanism of direct positive autoregulation and indirect negative autoregulation, with examples found in *Yersinia pseudotuberculosis* and *Vibrio cholerae* CpxRA investigations (Liu *et al.*, 2011; Slamti and Waldor, 2009).

As a consequence of being a cleavage product of the *cpxP* mRNA, CpxQ is also induced by CpxR (Figure 1.7). The production of CpxQ in turn enhances the regulatory response of the CpxRA TCS through the post-transcriptional repression of *trans*-encoded mRNAs (Figure 1.7). Investigations in *S. enterica* and *E. coli* have found the cellular targets of CpxQ to include the sodium-proton antiporter, NhaB and the periplasmic chaperone, Skp, respectively (Chao and Vogel, 2016; Grabowicz *et al.*, 2016). Repression of these targets by CpxQ and ultimately CpxR has been linked to alleviating disruptions to the proton motive force; drawing a stronger association of the CpxRA TCS in having a physiological role in detecting and alleviating reductions in membrane potential as part of its envelope stress response (Chao and Vogel, 2016; Grabowicz *et al.*, 2016).

Besides regulating components required for the envelope stress response (including itself), CpxR has been found to also regulate membrane appendages including curli fimbriae and components of the flagellar motor in *E. coli* (Figure 1.7). CpxR was determined to negatively regulate the production of curli fimbriae through the direct interaction with the promoter of its

structural components *csgBA* as well as negatively regulates the expression of *csgD*, which encodes the transcriptional activator for curli expression, thus further inhibiting *csgBA* via an indirect manner (Jubelin *et al.*, 2005; Ogasawara *et al.*, 2010). CpxR also negatively regulates the genes encoding parts of the flagellar motor, *motABcheAW*, by occluding the -35 site within the promoter region, as well as negatively regulating the flagellar master regulatory complex *flhDC* responsible for activating a class of flagellar genes (De Wulf *et al.*, 1999; Raivio *et al.*, 2013).

The CpxRA system has also been linked to pathogenesis in a variety of bacteria with regulatory implications in secretion systems and virulence regulators required for adherence and infection of host cells. In *Y. pseudotuberculosis*, CpxR was shown to directly down regulate the expression of the global regulator *rovA* that has many downstream targets involved in virulence including the Type III secretion system and expression of invasin (Liu *et al.*, 2011). Correlating with CpxR being a negative regulator of virulence, a *cpxR* mutant showed increased internalization when examined in mammalian cells indicating the absence of CpxR increased the invasiveness of *Y. pseudotuberculosis* (Carlsson *et al.*, 2007). Conversely in *Shigella sonnei*, CpxR activates the expression of the major virulence regulator encoded by *virF* and seems to be an essential regulator of *virF* as a *cpxR* mutant abolishes expression of *virF* completely (Nakayama and Watanabe, 1995; Nakayama and Watanabe, 1998). CpxR also negatively regulates virulence in the more distantly related Gram-negative bacterium (relative to the *Enterobacteriace* family described thus far) *Haemophilus ducreyi* (Raivio, 2014). In *H. ducreyi*, CpxR was identified to directly inhibit the expression of two genes, *lspB* and *lpsA2*, that encode parts of a secretion system that is important for avoiding phagocytosis by macrophage host cells as well as are required for full virulence in human and animals models (Vakevainen *et al.*, 2003;

Labandeira-Rey *et al.*, 2009). The impact of CpxRA on *H. ducreyi* was further exemplified by studies that found a *cpxA* mutant strain, likely to produce constitutively phosphorylated CpxR due to the absence of the CpxA phosphatase activity, was found to be impaired for virulence in human volunteers while a *cpxR* mutant strain was found to retain virulence when examined in human volunteers (Spinola *et al.*, 2010; Labandeira-Rey *et al.*, 2011).

These regulatory targets indicate bacteria have adopted the CpxRA system to protect the cell envelope in multiple ways including repressing virulence determinants that reside within the cell envelope. This perhaps is a survival measure that prevents expression of virulence determinants in environments that are not conducive to infection or may help balance the expression of the determinants to avoid overwhelming the host and subsequent predation. On the other hand, the system is also used to enhance virulence in some bacteria and thus it seems the membrane sensing capabilities can be used for both inhibiting and promoting virulence. Continued investigations of the CpxRA system within the model *E. coli* as well as pathogenic bacteria will likely reveal a continued evolution of the processes, including virulence strategies that incorporate the functionalities of this system.

1.4 Thesis Rationale

The focus of studies for the CpxRA TCS of *L. pneumophila* has been regulation as this system was initially discovered in *L. pneumophila* as a direct regulator of the Dot/Icm system component, *icmR* (Gal-Mor and Segal, 2003a). With a connection to the major virulence determinant of *Legionella,* it became a priority to identify other regulon members, as it was likely they too would be related to virulence. Targeted sequence searches of the promoter regions of Dot/Icm system components as well as DNA pattern searches of the whole genome for the presence of the CpxR binding motif did reveal additional regulatory targets of the CpxRA system that were also virulence associated (Altman and Segal, 2008). These included three more Dot/Icm system components (*icmV, icmW,* and *lvgA*) all of which are activated by CpxR, and 11 Dot/Icm effector proteins that are either activated or repressed by CpxR (Altman and Segal, 2008).

A clear connection to virulence regulation was identified for the *L. pneumophila* CpxRA system, indicating this system has retained a similar role in *L. pneumophila* as other pathogenic Gram-negative bacteria in which the CpxRA TCS has been examined. However, when *cpxR* and *cpxA* insertion mutant strains (i.e. coding sequences were disrupted by an antibiotic cassette) were examined in *A. castellanii* and HL-60 macrophage host cells, intracellular growth defects were not detected (Gal-Mor and Segal, 2003a). Likewise, a *cpxR* insertion mutant strain generated via transposon mutagenesis, showed only a limited growth defect and was still able to efficiently replicate when examined in murine bone marrow derived macrophages (Vincent *et al.*, 2006a). These intracellular growth phenotypes left the role of CpxRA system in *L. pneumophila* virulence ambiguous, as virulence regulation is quite evident yet no intracellular manifestations occur to indicate the CpxRA regulatory impacts have a physiological role.

No further research has been conducted to resolve this puzzling connection to virulence nor have efforts been made to identify other regulatory targets of the CpxRA system in *L. pneumophila*. To begin filling this void, the following aims were undertaken in order to gain a better understanding of the regulatory and virulence implications of the CpxRA system in *L. pneumophila*:

1) Expand the CpxRA TCS regulon members in *L. pneumophila* on a global scale and identify those associated with virulence. As part of the regulon expansion, autoregulation so often associated with the CpxRA TCS was also investigated.
2) Re-examine the contribution of the CpxRA TCS to virulence in *L. pneumophila* by conducting intracellular growth assays with unmarked in-frame deletions of the *cpx* system in both *A. castellanii* and U937-derived macrophage host cells.
3) Investigate a gene of interest, *oxyR*, as a potential regulatory target of CpxR in *L. pneumophila*. As well as to explore the role of OxyR in *L. pneumophila* virulence and whether a regulatory relationship occurs between OxyR and the CpxRA TCS.

During the preparation of this thesis, a study conducted by Feldheim *et al.* (2015) was published that also had the goal of expanding the regulon of the CpxRA TCS and re-assessing the role of this system in *L. pneumophila* virulence. Many of their findings supported those discussed in this thesis, with specific similarities and differences between our findings and theirs discussed within Chapter 3, sections 3.3 and 3.4.

Chapter 2. MATERIALS AND METHODS

2.1 Bacterial strains and plasmids

Bacterial strains and plasmids pertinent to studies conducted in Chapter 3 and Chapter 4 are listed in Table 3.1 and Table 4.1, respectively. In all studies conducted, a thymidine auxotroph derivative of *L. pneumophila* Philadelphia-1, referred to as Lp02, was used as the parental strain (Berger and Isberg, 1993). *E. coli* host strains DH5α, DH5αλpir and BL-21(DE3) CodonPlus™RIL were used in all studies for cloning, allelic exchange strategies, and recombinant protein expression, respectively.

Plasmids common to both Chapter 3 and Chapter 4 are as follows: pBH6119 utilized as a transcriptional reporter, in which a promoter region of interest is directionally cloned to drive the expression of a promoter-less green fluorescent protein (GFP) gene; pSR47s suicide plasmid was employed for allelic exchange mutagenesis studies; and the pJB908 plasmid was used for complementation purposes.

2.2 Media and growth conditions

All media and chemical reagents were procured from Sigma Aldrich (St. Louis, MO, USA), Fisher Scientific (Ottawa, ON, Canada) and VWR (Mississauga, ON, Canada).

2.2.1 *E. coli* culture conditions

All *E. coli* strains were cultured on Luria-Bertani (LB) agar (10 g/L tryptone, 5 g/L yeast extract, 5 g/L NaCl, and 15g/L molecular biology grade agar) or in LB broth (same composition as LB agar except agar is not included). Appropriate antibiotics were added to LB media (agar or broth) at the following final concentrations: kanamycin (40 μg/mL), ampicillin (100 μg/mL), and

chloramphenicol (20 μg/mL). Strains grown on agar were incubated overnight at 37°C and those grown in broth were incubated overnight at 37°C with aeration, no longer than 18 hours for both LB media types. For recombinant protein induction Isopropyl-β-D-galactosidase (IPTG) was added to LB broth at a final concentration of 1mM, where indicated, unless specific modifications are stated.

2.2.2 *L. pneumophila* culture conditions

All *L. pneumophila* strains were grown on Buffered Charcoal Yeast Extract (BCYE) agar (10g/L Bacto yeast extract, 1g/L α-Ketoglutaric acid, 1 g/L ACES, 1.5g/L activated charcoal and 15g/L molecular biology grade agar) or in Buffered Yeast Extract (BYE) broth (same composition as BCYE agar except activated charcoal and agar are excluded). Prior to autoclaving, both media types were brought to a pH of 6.6 - 6.7 with 6 M KOH. Subsequent to autoclaving, the media was cooled to 55°C and 4 mL of a 0.1% (w/v) L-Cysteine stock solution (prepared fresh each time and filter sterilized) as well as 1 mL of a 25% Fe-pyrophosphate stock solution (filter sterilized and stored at 4°C) were added per one litre of media.

To prepare a 0.1% (w/v) L-Cysteine stock solution, 0.8 g of L-Cysteine powder is added to 5 mL Milli-Q double-distilled water (ddH_2O), dissolved, adjusted to a pH of 6.6-6.7 with 6 M KOH, and brought to a final volume of 8 mL with Milli-Q ddH_2O. The solution is then filter sterilized via a 0.2 μm syringe filter. To prepare a 25% (w/v) Fe-pyrophosphate stock solution, 10 g of Fe-pyrophosphate crystals are added to 25 mL Milli-Q ddH_2O, dissolved (protected from light), and brought to a final volume of 40 mL with Milli-Q ddH_2O. The solution is then filter sterilized via a 0.2 μm syringe filter and stored at 4°C wrapped in aluminum foil for protection from light.

When required, media was supplemented with a final concentration of thymidine (100 μg/mL), kanamycin (25 μg/mL) and/or sucrose (5% w/v) for growth and selection purposes. Strains grown on agar media were incubated ~3 – 4 days in a humidified incubator at 37°C + 5% CO_2 and strains grown in broth media were incubated up to 24 hours at 37°C with aeration.

2.3 *L. pneumophila* genomic DNA isolation

Legionella strains were grown on BCYE agar containing thymidine for 24 – 48 hours at 37°C + 5% CO_2. One to two loopfuls of cells were harvested from the agar plate and deposited into a microcentrifuge tube containing 440 μL of sterile 1x Tris-EDTA (TE) buffer pH 8.0 and vortexed to re-suspend the cells. To the suspension, 62.5 μL of a 20 mg/ml Proteinase K stock (New England Biolabs) was added and mixed gently by flicking, then 10 μL of a 10% (w/v) SDS stock solution was added and again mixed gently by flicking. The mixture within the microcentrifuge tube was then incubated at 37°C with shaking (~150 rpm) for ~2 hours (or until the suspension has cleared) to fully lyse the cells. After incubation was complete, 50 μL of a 10 M ammonium acetate stock was added and lysate was mixed gently by flicking. For extraction, a volume of phenol/chloroform/isoamyl alcohol (25:24:1) equal to the lysate volume was added to the microcentrifuge tube and shaken by hand vigorously for 15 seconds then immediately centrifuged at 17, 500 x *g* for 10 minutes at room temperature. The aqueous layer was then removed and transferred to a clean microcentrifuge tube and extracted as above two more times. To precipitate genomic DNA from the final aqueous layer, two volumes of ice-cold 100% ethanol was added, mixed gently by flicking and stored at -20°C for at least 1 hour then centrifuged at 17, 500 x *g* for 30 minutes at 4°C. The supernatant was carefully removed from the pellet and the pellet then washed in 100 μL ice-cold 70% ethanol, followed by centrifugation

at 17,500 x *g* for 5 minutes at 4°C. Wash was carefully removed, ensuring not to disturb the pellet, and pellet dried at room temperature. The pellet was re-suspended in 100 µL 1x TE buffer containing a final concentration of 100 µg/µL RNase A, incubated at 37°C for 30 minutes to digest contaminating RNA, and stored overnight at 4°C. Genome was then diluted 1/100 in purified nuclease-free molecular biology grade water (Hyclone™, GE Healthcare) to achieve a working stock concentration of ~40 ng/µL. For long-term storage, genome was placed at -20°C and thawed on ice when needed.

2.4 Preparation of competent cells

2.4.1 Rubidium chloride competent *E. coli* DH5α

E. coli DH5α was grown on LB agar media and a single colony transferred to 5 mL LB broth for growth overnight at 37°C with aeration. The 5 mL overnight culture was then subcultured into 500 mL LB broth pre-warmed to 37°C and incubated at 37°C with shaking until culture reached an optical density at 600 nm (OD_{600}) of 0.45 – 0.55. Once at the appropriate cell density, the culture was placed on ice for five minutes and transferred evenly to two sterile centrifuge bottles (250 mL/centrifuge tube). Cells were pelleted at 3000 x *g* for 20 minutes at 4°C. Supernatant was removed and cells were re-suspended in 100 mL cold (4°C), filter sterilized TFB I buffer (30 mM potassium acetate, 100 mM RbCl, 10 mM $CaCl_2 \bullet 2H_2O$, 50 mM $MgCl_2 \bullet 4H_2O$, and 15 % (v/v) glycerol, adjusted to pH 5.2 with 0.2 M acetic acid) per centrifuge bottle and pelleted at 3000 x *g* for 15 minutes at 4°C. Supernatant was removed and pellets were re-suspended in 10 mL cold (4°C), filter sterilized TFB II buffer (10 mM MOPS, 75 mM $CaCl_2 \bullet 2H_2O$, 10 mM RbCl, and 15% (v/v) glycerol, adjusted to pH 6.5 with 1 M KOH) per

centrifuge tube, then incubated on ice for 15 minutes. The competent cells were then transferred to cold microcentrifuge tubes in 200 µL aliquots, flash frozen in ethanol, and stored at -80°C.

2.4.2 Calcium chloride competent *E. coli* DH5αλpir

E. coli DH5αλpir was grown on LB agar and a single colony transferred to 3 mL LB broth for culturing overnight at 37°C with aeration . Then 0.5 mL of the overnight culture was subcultured to 49.5 mL LB broth and incubated at 37°C with shaking until culture reached an optical density at 600 nm (OD_{600}) of 0.5 – 0.6. Once at the appropriate cell density, the culture was placed on ice for 10 minutes and transferred to a sterile 50 mL conical tube. Cells were pelleted at 3300 x *g* for 10 minutes at 4°C. Supernatant was removed and cells were gently re-suspended in 50 mL cold (4°C) sterile 100 mM $CaCl_2$, then pelleted at 3300 x *g* for 10 minutes at 4°C. Supernatant was removed and pellet re-suspended in 2 mL cold sterile 100 mM $CaCl_2$. Competent cell suspension was stored at 4°C for up to 2 weeks, with 100 µL aliquots used in transformations.

2.4.3 Electrocompetent *L. pneumophila*

L. pneumophila strains were grown as a lawn on BCYE media containing the appropriate supplements for 48 hours at 37°C + 5% CO_2. The entire plate of bacterial cells was scraped using sterile disposable loops (approximately 3 – 4 loopfuls) and re-suspended in 40 mL sterile ice-cold Milli-Q ddH_2O. Cells were pelleted by centrifugation at 3000 x *g* for 15 minutes at 4°C and supernatant removed. Cells were washed two more times by re-suspending the pellet in 40 mL sterile ice-cold Milli-Q ddH_2O and repeating the centrifugation step as described above. Once

washes were complete the pellet was re-suspended in 2 mL of sterile ice-cold 15% (v/v) glycerol, flash frozen in ethanol, and 100 μL aliquots stored at -80°C.

2.5 Bacterial transformations

2.5.1 Transformation of chemically competent *E. coli* strains using heat-shock

100 μL aliquots of chemically competent *E. coli* strains were thawed on ice if stored at -80°C or put on ice to keep cool and cells were then added to the completed 10 μL ligation reaction or ≤1 μg of plasmid. The mixture was incubated on ice for one hour, then shocked at 37°C for 90 seconds and recovered in 500 μL LB broth for one hour at 37°C with shaking. To concentrate the transformed cell suspension, cells were pelleted at 17, 500 x *g* for one minute at room temperature, then 400 μL of the supernatant was removed and cells re-suspended in the remaining ~200 μL of supernatant. The cells were then applied to LB agar containing the appropriate antibiotics in 100 μL and 50 μL aliquots using the spread plate technique and subsequently incubated overnight at 37°C for transformant selection.

2.5.2 Transformation of *L. pneumophila* by electroporation

Electrocompetent *L. pneumophila* strains were thawed on ice and mixed with plasmid DNA (≤ 1 μg) and allowed to incubate on ice for five minutes. Approximately 95 μL of the DNA-cell mixture was transferred to a pre-chilled 1mm-gap BioRad™ electroporation cuvette and electroporated at 2.1 kV for four to five milliseconds using a BioRad MicroPulser™ Electroporator. For recovery, the pulsed cells were then transferred to 1 mL pre-warmed BYE broth and incubated at 37°C with rotation for two hours. The cells were then applied to the

appropriate BCYE agar media using the spread plate technique and grown at 37°C + 5% CO_2 for three to five days (unless otherwise stated) to select for transformants.

2.6 Molecular cloning techniques

Oligonucleotides pertinent to studies conducted in Chapter 3 and Chapter 4 are listed in Table 3.2 and Table 4.2, respectively, and were synthesized by Invitrogen (Life technologies, Grand Island, NY, USA). Oligonucleotides were re-suspended to a concentration of 1 μg/μL using purified nuclease-free molecular biology grade water (Hyclone™, GE Healthcare) and subsequently diluted 1/10 in Hyclone™ water to achieve a working concentration of 100 ng/μL. All restriction and modifying enzymes, dNTPs, Taq polymerase, and Q5® High Fidelity Polymerase were purchased from New England Biolabs (Whitby, ON, Canada).

2.6.1 PCR reactions and conditions

For gradient PCRs, colony PCRs and verification of plasmid inserts, Taq polymerase reactions were employed. Reactions consisted of: 1 μL 1/100 diluted *L. pneumophila* genomic DNA (approximately 40 ng), 1 μL cellular lysate supernatant for colony PCR, or 1/50 diluted isolated plasmid constructs as template, 2.5 μL of 10x ThermoPol® reaction buffer, 0.5 μL of 10 mM dNTP mixture, 2.0 μL of forward primer working stock, 2.0 μL reverse primer working stock, 0.125 μL Taq polymerase, and 16.875 μL of Hyclone™ water to bring reaction volume to 25 μL. A PCR thermocycler was programmed with the following cycling conditions: A one time enzyme initiation at 94°C for 3 minutes, then template denaturation at 94°C for 30 seconds, annealing at temperatures listed in Tables 3.2 and 4.2 for 30 seconds, extension at 72°C for times corresponding to the amplicon size (Tables 3.2 and 4.2) based on the manufacturers guidelines of

1 Kb being synthesized in one minute (amplicons ≤ 250 bp = 15 seconds, >250 bp but ≤ 500 bp = 30 seconds, >500 bp but ≤ 750 bp = 45 seconds, >750 bp but ≤ 1 Kb = 1 minute, and those greater than 1 Kb are one minute plus the appropriate addition of time depending on fragment size) for 25 cycles if gradient PCR and 35 cycles if colony or verification PCR, followed by a final extension at 72°C for 5 minutes. Gradient PCR was used to determine annealing temperatures for all primer sets as the following range of temperatures were tested: 50°C, 51.5°C, 53.9°C, 57.5°C, 62.2°C, 66°C, 68.5°C, and 70°C.

For amplicons used in cloning and/or Sanger sequencing Q5 High-Fidelity polymerase reactions were employed. Reactions consisted of: 1 μL 1/100 diluted *L. pneumophila* genomic DNA (approximately 40 ng) as template, 10 μL of 5x Q5® reaction buffer, 1 μL of 10 mM dNTP mixture, 2.5 μL of forward primer working stock, 2.5 μL reverse primer working stock, 0.5 μL Taq polymerase, and 32.5 μL of Hyclone™ water to bring reaction volume to 50 μL. A PCR thermocycler was programmed with the following cycling conditions: A one time enzyme initiation at 98°C for 30 seconds, then template denaturation at 98°C for 10 seconds, annealing at temperatures listed in Tables 3.2 and 4.2 for 30 seconds, extension at 72°C for times corresponding to the amplicon size (Tables 3.2 and 4.2) based on the manufacturers guidelines of 1Kb being synthesized in 30 seconds (amplicons ≤ 250 bp = 10 seconds, >250 bp but ≤ 500 bp = 15 seconds, >500 bp but ≤ 750 bp = 20 seconds, >750 bp but ≤ 1 Kb = 30 seconds, and those greater than 1 Kb are 30 seconds plus the appropriate addition of time depending on fragment size) for 35 cycles, followed by a final extension at 72°C for 2 minutes.

2.6.2 Agarose gel electrophoresis

Agarose gel electrophoresis was used to verify the presence and size of PCR amplicons, digested amplicons and plasmids, isolated plasmids, and gel-extracted amplicons. Agarose was dissolved in 1x Tris-Acetate-EDTA (TAE) buffer [40 mM Tris, 20 mM acetic acid, and 1 mM EDTA (pH 8.0)] to achieve 1% (w/v) agarose gels for amplicons and plasmids ≥ 1Kb, 1.5% (w/v) agarose gels for amplicons ≥ 300 bp but < 1 Kb, and 2% (w/v) agarose gels for amplicons < 300 bp. Melted agarose gels were cooled to ~55°C then casted with the addition of 10 µL or 20 µL of 0.5 mg/mL ethidum bromide for small or large gels, respectively, in order to visualize DNA. Samples were run alongside either 5 µL of 100 bp or 1 Kb DNA ladders to determine sizing. Agarose gels were electrophoresed in 1x TAE at 100 volts for ~30 minutes and visualized using an Alphaimager™ system.

2.6.3 Generation of plasmid constructs

Amplicons were generated using the appropriate primer sets (see Tables 3.2 and 4.2) in Q5® High-Fidelity polymerase reactions and subsequently purified via gel-extraction as per Qiagen Gel Extraction kit protocol (Qiagen, Toronto, ON, Canada). Following gel-extraction, amplicons were ethanol precipitated to remove contaminating salts by adding 1/10 volume of 10 M ammonium acetate and 2 volumes of ice-cold 100% ethanol, mixed gently and allowed to precipitate overnight at -20°C. DNA was pelleted via centrifugation at 17, 500 x *g* for 15 minutes at 4°C, supernatant removed, then pellet washed in 100 µL ice-cold 70% ethanol and immediately centrifuged at 17, 500 x *g* for 5 minutes at 4°C. Supernatant was removed and pellet dried at room temperature. Pellets were re-suspended in ~30 µL Qiagen elution buffer (EB) and monitored for salt contamination as well as concentration via a NanoDrop™ 2000c

spectrophotometer (Thermo Scientific). Purified amplicons were then subjected to double digestion with the appropriate restriction enzymes (see specific experimental procedures of Chapters 3 and 4 as well as Tables 3.2 and 4.2) using the following reaction: 10 – 15 μL of purified amplicon, 5 μL 10x Bovine Serum albumin (BSA), 5 μL of the appropriate 10x NEB restriction enzyme buffer, 2 μL of each restriction enzyme, and Hyclone™ water such that the reaction volume is brought to 50 μL. Digestion reactions were incubated at 37°C for 2 – 3 hours and subsequently purified as per the Qiagen protocol for DNA cleanup from enzymatic reactions.

The corresponding vector to harbor the amplicon was digested in a similar manner to that of the amplicon except after 2 hours of digestion, 5 μL calf intestinal alkaline phosphatase (CIP) was added to the digestion reaction and incubated for another 1 hour at 37°C. Digested vector was then purified as per the Qiagen protocol for DNA cleanup from enzymatic reactions.

Digested vector and amplicon were ligated using the following 10 μL reaction: 7 μL of digested amplicon, 1 μL of digested vector, 1 μL of 10x T4 DNA ligase reaction buffer, and 1 μL of T4 DNA ligase. Ligations were incubated at 25°C for 2 hours or overnight at 16°C and subsequently mixed with rubidium chloride competent *E. coli* DH5α for transformation; with the exception of gene knock-out plasmids consisting of the pSR47s backbone, which were mixed with calcium chloride competent DH5αλpir cells for transformation.

2.6.4 Colony PCR of transformants to identify *E. coli* clones

Transformants were first subjected to a multi-colony PCR to narrow down potential positive clones. For this, an average of 40 individual colonies were picked with sterile toothpicks, grid plated onto LB agar containing the appropriate antibiotic for selection and the toothpick subsequently deposited into a PCR tube containing 100 μL Hyclone™ water. A total of

5 colonies were deposited per PCR tube. The LB agar grid plate was incubated overnight at 37°C. Mixed colony suspensions were then lysed at 95°C for 10 minutes and subsequently centrifuged at 17, 500 x *g* for 1 minute at room temperature to pellet cell debris. Supernatants (DNA lysates) were then used in Taq polymerase reactions as described. PCR reactions were electrophoresed on agarose gels and samples containing desired bands were subjected to a single colony PCR to define the positive clones.

For single colony PCR, the 5 colonies identified as potentially positive clones were assessed individually. A portion of the colony that grew on the LB agar grid plate was picked with a sterile toothpick and deposited into a PCR tube containing 100 μL Hyclone™ water and lysed as described. Cell debris was pelleted by centrifugation at 17, 500 x *g* for 1 minute at room temperature. Each individual colony lysate was then used as template for an individual Taq polymerase reaction. PCR samples were electrophoresed on agarose gels and the colony whose lysate produced the desired band was re-streaked from the LB agar grid plate onto fresh LB agar containing the appropriate antibiotics for single colonies. A single colony was then used to inoculate two 3 mL LB broth cultures containing the appropriate antibiotics, and incubated overnight at 37°C with rotation. One overnight culture was used for cryopreservation of the positive *E. coli* clone, where 900 μL of overnight culture was mixed with 100 μL 100% sterile DMSO in a cryogenic tube and stored at -80°C. The other overnight culture was used in plasmid isolation conducted via QIAprep Spin Miniprep kit as per the manufacturer's instructions (Qiagen, Toronto, ON, Canada). Plasmids were first verified for the presence of inserts via Taq polymerase PCR reactions and subsequently verified at the DNA sequence level through Sanger sequencing.

2.6.5 Sanger sequencing sample preparation

DNA amplicons to be sent for Sanger sequencing were purified by gel-extraction using the Qiagen Gel Extraction kit as per the manufacturer's instructions. Gel-extracted amplicons were ethanol precipitated to remove contaminating salts by adding 1/10 volume of 10 M ammonium acetate and 2 volumes of ice-cold 100% ethanol, mixed gently and allowed to precipitate overnight at -20°C. DNA was pelleted via centrifugation at 17, 500 x *g* for 15 minutes at 4°C, supernatant removed, then pellet washed in 100 µL ice-cold 70% ethanol and immediately centrifuged at 17, 500 x *g* for 5 minutes at 4°C. Supernatant was removed and pellet dried at room temperature. Pellets were re-suspended in ~30 µL Hyclone™ water and monitored for salt contamination as well as concentration via a NanoDrop™ 2000c spectrophotometer (Thermoscientific). Plasmid constructs to be sent for Sanger sequencing were isolated using QIAprep Spin Miniprep kit as per the manufacturer's instructions except plasmids were eluted using ~30 µL Hyclone™ water and concentration evaluated via a NanoDrop™ 2000c spectrophotometer. DNA amplicons or plasmid constructs were combined with a selected "seq" primer (see Tables 3.2 and 4.2) at the appropriate concentrations and volumes specified by The Centre for Applied Genomics (TCAG) at the Hospital for Sick Children (Toronto, ON, Canada) and reactions subsequently sent for processing.

2.6.6 Homologous recombination to generate *L. pneumophila* unmarked in-frame deletion mutants

Gene knockout constructs consisting of the pSR47s suicide vector backbone (see specific experimental procedures of Chapters 3 and 4 for construction details) were mixed in 1 µg amounts with 100 µL of electrocompotent Lp02 cells and transformed via electroporation. To

select for the first crossover event, cells were plated on BCYE supplemented with thymidine and kanamycin and incubated for four to five days. Transformants were then patched onto BCYE supplemented with thymidine and sucrose to select for the second crossover event. Colonies that grew in the presence of sucrose were then replica plated onto BCYE supplemented with thymidine and BCYE supplemented with thymidine and kanamycin. Only colonies that were kanamycin sensitive were then screened by PCR using "int" primer sets (Tables 3.2 and 4.2) and assessed by agarose gel electrophoresis to identify colonies containing deletions in the genes of interest. Positive mutant strains were subjected to DNA sequencing using the appropriate "KO seq" primers (Tables 3.2 and 4.2) to verify gene deletion regions.

2.7 *In vitro* growth analysis

L. pneumophila strains were grown ~3 days at 37°C on BCYE agar plates. A half loopful of cells were harvested from the plates and re-suspended into 3 mL room temperature BYE broth. Optical density at 600 nm (OD_{600}) was measured using a SmartSpec plus spectrophotometer (BioRad) for the bacterial re-suspensions and used to inoculate BYE broth at a normalized starting OD_{600} of 0.2. Approximately, 150 µl of the normalized bacterial suspensions were loaded in triplicate into 96-well plates (Greiner Bio-One) and allowed to grow for 24 hours with constant shaking at 37°C in a BioTek Synergy 4 hybrid automated microplate reader. OD_{600} readings were taken hourly and converted to cfu/mL using the conversion factor OD_{600} of 1.0 = $5x10^8$ cfu/mL. Values were plotted and statistical analysis performed with GraphPad Prism 6 (GraphPad Software, La Jolla, CA, USA).

2.8 GFP reporter assays

L. pneumophila strains harboring GFP-transcriptional fusion plasmids or the promoter-less GFP reporter plasmid, pBH6119 as a vector control (see specific experimental procedures in Chapters 3 and 4 for construction details), were struck onto BCYE agar plates and incubated for ~3 days at 37°C + 5% CO_2. A half loopful of bacterial cells was scraped from the BCYE agar plates and deposited into 3 mL room temperature BYE broth and re-suspended via vortexing. Optical density at 600 nm (OD_{600}) was determined for the bacterial cell suspensions using a SmartSpec plus spectrophotometer (BioRad) and calculated amounts of the bacterial cell suspensions were transferred to 10 mL room temperature BYE broth to obtain a normalized starting OD_{600} of 0.2. Approximately, 150 µl of the normalized bacterial suspensions were loaded in triplicate into 96-well plates (Greiner Bio-One) with black walls and clear round bottoms. The plate was incubated at 37°C with fast continuous shaking and OD_{600} as well as fluorescence readings (GFP excitation at 488 nm and emission at 510 nm) taken hourly, for a 24 hour period in a BioTek Synergy 4 hybrid automated microplate reader. Normalized units of expression were obtained by dividing the relative fluorescence values (RFU) by the corresponding OD_{600} values and subtracting the normalized values obtained for the vector control strains. Normalized values were plotted and statistical analysis performed with GraphPad Prism 6 (GraphPad Software, La Jolla, CA, USA).

2.7 Purification of recombinant proteins

2.7.1 Protein induction

E. coli BL-21(DE3) CodonPlus™RIL harboring pET16b or pET29b expression vectors were struck onto LB agar containing either ampicillin (100 µg/mL) and chloramphenicol (20

μg/mL) or kanamycin (40 μg/mL) and chloramphenicol (20 μg/mL), respectively, and grown overnight at 37°C. Three to four single colonies were scraped from the LB agar plates and deposited into a beveled flask containing 30 mL LB broth with the appropriate antibiotics added and incubated overnight at 37°C with shaking (~150 rpm). The entire overnight culture was then used to inoculate 970 mL LB broth (total volume 1 L) containing either ampicillin (100 μg/mL) or kanamycin (40 μg/mL) for expression vector maintenance and incubated at 37°C with shaking until culture reached an OD_{600} of 0.5 – 0.6. Chloramphenicol was not included as it retards protein production. Upon reaching this density, cultures were induced with 1 mM IPTG for 2 to 2.5 hours at 37°C and culture subsequently divided evenly into sterile centrifuge bottles for centrifugation at 4200 x *g* for 45 minutes at 4°C to pellet cells. Supernatant was poured off and each pellet was re-suspended in 10 mL cold wash buffer (50 mM Tris-HCl pH 7.5), pooled into one 50 mL conical tube and brought to a final volume of 50 mL with cold wash buffer (50 mM Tris-HCl pH 7.5). Cells were pelleted via centrifugation at 3300 x *g*, supernatant removed and pellet stored at -80°C.

2.7.2 Ni-NTA agarose bead preparation

The bottle of Ni-NTA agarose beads (Qiagen) was vigorously mixed and 2.5 mL of beads were immediately transferred to a sterile 15 mL conical tube and allowed to settle out of the preservation buffer for about one hour at 4°C. The supernatant was carefully removed and beads were washed by re-suspension in 10 mL sterile Milli-Q ddH_2O. Beads were allowed to settle out of the Milli-Q ddH_2O for two hours at 4°C. The supernatant was removed carefully and beads were re-suspended in 10 mL binding buffer (20 mM Tris-HCl pH 8.0, 0.5 M NaCl, and 5 mM imidazole), then stored overnight at 4°C. Just prior to use the supernatant was removed and the

beads were re-suspended in 5 mL cold binding buffer (20 mM Tris-HCl pH 8.0, 0.5 M NaCl, and 5 mM imidazole).

2.7.3 Lysis via French Press

Pelleted cells from section 2.7.1 were removed from -80°C and immediately put on ice. Just prior to French Pressing, the pellet was re-suspended in 20 mL ice-cold binding buffer (20 mM Tris-HCl pH 8.0, 0.5 M NaCl, and 5 mM imidazole) via vortexing and 200 μL of 100x Halt™ Protease Cocktail (Thermo Scientific) as well as 200 μL of 0.5M EDTA were added, followed by gentle inversion for mixing. Cell suspension was lysed using a French Press (20K cell, American Instrument Company, Silver Spring, Md.), where clearing of the suspension was achieved by ~6 cycles through the 20K cell. The lysate was centrifuged at 17, 100 x *g* for 30 minutes to pellet the cellular debris and supernatant mixed with the 5 mL Ni-NTA bead preparation to generate a "slurry". The slurry was incubated at 4°C with gentle rocking on a Orbitron Rotator II (Mandel Scientific, Guelph, Ontario) for one hour to allow binding of the His-tagged recombinant protein to the Ni-NTA agarose beads.

2.7.4 Gravity column, fraction selection, and dialysis

The slurry was then applied to a Pierce® Centrifuge Column fitted with a column extender (Thermo Scientific) and flow-through discarded. Wash buffers (20 mM Tris-HCl pH 8.0 and 0.5 M NaCl) were then applied to the column that contained increasing concentrations of imidazole (0 mM, 10 mM, and 25 mM), where each wash buffer had a total volume of 25 mL. After washes were complete, the His-tagged recombinant protein was eluted from the column by

applying 10 mL elution buffer (0.1 M Tris-HCl pH 8.0, 0.5M NaCl, 0.5 M imidazole, and 0.14 M HCl) and collected in 1.5 mL fractions.

To identify fractions containing the protein of interest, samples of the fractions were subjected to SDS-PAGE. Samples were prepared by combining 25 μL of each fraction with 22.5 μL 2x Laemmli loading buffer and 2.5 μL beta-mercaptoethanol, then heated for 5 minutes at 95°C. Samples were run on denaturing polyacrylamide gels consisting of a 5% stacking gel and 12% separating gel. The gel-electrophoresis was conducted in 1x running buffer (25 mM Tris, 0.19 M glycine, and 0.1% (w/v) SDS) at 200 V for 10 minutes then at 120 V for one hour. Gels were stained with Coomassie Brilliant Blue R-250 staining solution (BioRad) for 30 minutes at room temperature with rotation. Gels were first destained with destain solution I (50%(v/v) ethanol and 10% (v/v) acetic acid) for one hour then destain solution II (5% (v/v) ethanol and 7% (v/v) acetic acid) for two hours. After two hours, destain solution was discarded and fresh destain solution II was applied and left overnight with rotation at room temperature. Results of the SDS-PAGE were correlated with qualitative Bradford assay results also conducted with the fractions. For the qualitative Bradford assay, 20 μL of each fraction were mixed with 80 μL Hyclone™ water and 20 μLBradford reagent (BioRad) and the intensity of color development visually assessed, where bright royal blue indicates higher protein content and mixed blues (hints of brown/red) indicating lower protein content. Fractions containing higher concentrations of the protein of interest based on protein bandwidth in SDS-PAGE and coloring of the Bradford assay were pooled, transferred to dialysis tubing and dialyzed. Dialysis was conducted in 1 L of dialysis buffer (20 mM Tris-HCl pH 8.0, 200 mM KCl, 0.5 mM DTT, 0.2 mM EDTA pH 8.0 and 10% (v/v) glycerol) for four hours at 4°C, then dialysis tube containing pooled fractions was transferred to fresh 1 L dialysis buffer and dialyzed for ~12 hours at 4°C.

2.7.5 Secondary purification via HiTrap Heparin HP column and protein concentration

The 1 mL HiTrap Heparin HP column (GE HealthCare) was first washed with 10 mL Buffer A (see specific experimental procedures of Chapters 3 and 4 for composition details) to remove preservations buffers from the column. Dialyzed protein sample was applied to column and flow-through collected. Column was then washed with 5 mL Buffer A containing 0.5 mM DTT and flow-through also collected. Then column washes corresponding to the volume of dialyzed protein applied to the column were applied and flow-through collected for each wash, where each wash buffer contained increasing concentrations of KCl (see specific experimental procedures of Chapters 3 and 4 for composition details). SDS-PAGE analysis was employed as described in section 2.7.4 to identify which of the collected flow-throughs contained the highest amount of recombinant protein with the least amount of contaminating proteins.

The selected flow-throughs were pooled and applied to Amicon® Ultra 10K Centrifugal filter units (Millipore) and centrifuged at 7200 x *g* for 10 minutes at 4°C to reduce sample volume. Then a total of 10 mL ice-cold protein storage buffer (20 mM Tris-HCl pH 8.0, 200 mM KCl, 0.2 mM EDTA pH 8.0, 0.5 mM DTT, and 30% (v/v) glycerol) was applied in a step-wise manner after volume of sample had been reduced by centrifugation at 7200 x *g* for 10 minutes at 4°C. Once all protein storage buffer had been applied the sample volume was reduced via centrifugation at 7200 x *g* for 10 minutes at 4°C until small amounts of protein precipitation was observed (final volumes usually ranged between 750 μL and 1 mL). Concentrated protein was stored at -20°C.

2.7.6 Determination of protein concentration

Protein concentrations of purified recombinant proteins were determined using a quantitative Bradford assay. A standard curve was generated using Pierce™ Bovine Gamma Globulin (BGG) in which 200 µL of Bradford reagent (BioRad) was combined with 0 µL, 50 µL, 100 µL, 200 µL, and 400 µL of 50 µg /mL BGG and brought to 1 mL with Hyclone™ water to achieve the following protein concentrations on the standard curve: 0 µg /mL, 2.5 µg /mL, 5.0 µg /mL, 10.0 µg /mL, and 20 µg /mL, respectively. A 100 µL 1/10 dilution of concentrated protein was prepared using Hyclone™ water and then further diluted to 1/500 using Hyclone™ water in a total volume of 800 µL. To the 1/500 diluted protein, 200 µL of Bradford reagent (BioRad) was added and reaction mixed. The standard curve samples and protein samples were inserted into a Biochrom Ultraspec pro 500 spectrophotometer set to Bradford assay, with absorbance readings at 595 nm and protein concentration outputs in µg /mL based on the standard curve values.

2.8 Antibody generation and Dot-blot analysis

Custom polyclonal antibodies against purified recombinant proteins (containing their purification tags) were generated in New Zealand White rabbits by a fee-based service (CedarLane laboratory, Burlington, ON, Canada) and were not affinity purified prior to use.

Dot-blot analysis was used to determine antibody dilutions for use in immunoblotting. Purified recombinant protein (used to generate the corresponding antibody) was diluted to 1100 µg/mL in protein dilution buffer (20 mM Tris-HCl pH 8.0, 10 mM $MgCl_2$, 100 mM KCl, 0.05 mg/mL BSA, and 10% (v/v) glycerol) and serially diluted 10-fold to a final dilution of 1/100 in protein dilution buffer. Approximately 5 µL of each dilution was spotted onto strips of nitrocellulose membrane (BioRad) such that each spot contained 5.5 µg, 0.55 µg, and 55 ng of

protein. Strips of membrane were incubated for one hour in blocking buffer (1x Tris-NaCl pH 7.5 containing 0.5% (v/v) Tween-20 and 2% (w/v) non-fat dry milk powder) at room temperature with rocking, washed briefly in wash buffer [1x Tris-HCl pH 7.5 containing 0.5% (v/v) Tween-20], and immunoblotted with varying dilutions of antibody (1:10,000, 1:20,000, 1:40,000, 1:80,000 and 1:160,000) prepared in blocking buffer for one hour at room temperature with rocking. After, the strips of membrane were washed at room temperature three times in wash buffer for 10 minutes each time with rocking, then incubated with goat anti-rabbit conjugated to alkaline phosphatase diluted 1:30,000 in blocking buffer for one hour at room temperature with rocking. Antibody solution was discarded and the strips of membrane were washed at room temperature three times in wash buffer for 10 minutes each time with rocking and then equilibrated in AP buffer (0.1 M Tris-HCl pH 9.5, 0.1 M NaCl, 0.05M $MgCl_2 \bullet 6H_2O$) for 10 minutes at room temperature with rocking. Membranes were developed using 1-Step™ NBT/BCIP solution (Thermo Scientific). Dilution of antibody able to detect the lowest amount of protein applied to the membrane was selected.

2.9 Immunoblotting and densitometry

L. pneumophila cells were grown to early exponential (OD_{600} ~ 0.8), exponential (OD_{600} ~ 1.5), or post-exponential (OD_{600} ~ 3.0) phase in BYE broth. Growth phase samples were centrifuged at 17,500 x *g* for 1 min, washed twice in 1x phosphate buffered saline (PBS), re-suspended to a calculated OD_{600} value of 8.0 (except complementation and/or overexpression strains were re-suspended to OD_{600} value of 2.0, therefore 4-fold diluted), and boiled in Laemmli loading buffer with 1% beta-mercaptoethanol for 5 minutes at 95°C. Samples were run on NuPAGE 4-12% Bis-Tris pre-cast gels (Life technologies) and transferred to PVDF membrane

(Bio-Rad). Membranes were incubated for one hour at room temperature in blocking buffer (1x Tris-NaCl containing 0.5% (v/v) Tween - 20 and 5% (w/v) non-fat dry milk), washed briefly in wash buffer [1x Tris-NaCl containing 0.5% (v/v) Tween – 20], and immunoblotted for 1 h at room temperature with antibodies specific to the protein of interest as well as isocitrate dehydrogenase (ICDH) [a gift from A. Sonenshein (Tufts University)] that were diluted 1:10,000 in blocking buffer. After, membranes were washed at room temperature three times in wash buffer for 10 minutes each time, and goat anti-rabbit conjugated to horseradish peroxidase (Jackson ImmunoResearch Laboratories) diluted 1:200,000 in blocking buffer was applied and incubated at room temperature for 45 minutes. Antibody solution was discarded and the membrane was washed at room temperature three times in wash buffer for 10 minutes each time and developed with Amersham™ ECL™ prime western blotting detection reagent (GE Healthcare). The blots were then exposed to CL-exposure film (Thermo Scientific) for varying time-periods, developed using SRX-101 medical film processor (Konica) and the resulting image scanned with CanoScan LiDE 210 Flatbed scanner (Canon).

For densitometric quantification, scanned images were converted to 8-bit grayscale and analyzed with AlphaView software for AlphaImager systems. Values were then plotted as a ratio of protein of interest band intensity to ICDH band intensity, incorporating any dilution factors when necessary. Statistical analysis was performed using GraphPad Prism 6 (GraphPad Software, La Jolla, CA, USA).

2.10 Radiolabelled electrophoretic mobility shift assay (EMSA)

Radiolabelled probes were prepared in 50 µl PCR labelling reactions: 60-80 ng of template DNA, 5 µl 10x Taq polymerase buffer, 8 µL dNTPs (1.25 mM dATP, 1.25 mM dGTP,

1.25 mM dTTP and 0.3125 mM dCTP), 1 μM of each the forward and reverse primers (see specific experimental procedures of Chapters 3 and 4 as well as Tables 3.2 and 4.2), 0.5 μl Taq polymerase and 5 μl α-^{32}P dCTP (3000 Ci/mmol 10 mCi/mL). Increasing concentrations of recombinant CpxR (0 - 24.6 μM) were combined with labeled probes (~1000 cpm) in binding buffer [10 mM Tris-HCl pH 7.5, 50 mM KCl, 5 mM MgCl2, 0.1 mM EDTA pH 8.0, 0.1 mM DTT, 0.1 mg/mL BSA, 10 ng/mL sonicated salmon sperm DNA, 1 μg/mL poly(dI-dC) and 5% (v/v) glycerol]; binding buffer composition was adapted from Altman and Segal (2008). Binding reactions had a final volume of 20 uL and were allowed to occur for 30 minutes at room temperature. Reactions were halted by adding 2 uL of 10x loading buffer (0.45 M Tris, 0.45 M Boric acid, 10 mM EDTA, and 0.2% (w/v) bromophenol blue) and subsequently run on a 5% non-denaturing polyacrylamide gel in 0.5x Tris-boric acid- EDTA (TBE) buffer (44 mM Tris, 44 mM boric acid and 10 mM EDTA pH 8.0) for three hours at 20 mA, then dried and exposed to Carestream® Kodak® BioMax® MS film (Sigma Aldrich, St. Louis, MO, USA) for 36 hours at -80 °C. Films were developed using SRX-101 medical film processor (Konica). Alternatively, dried gels were exposed to a Kodak phosphor screen overnight and scanned using a Molecular Imager PharosFx™ Plus System (BioRad).

2.11 Culturing U937-derived macrophages

U937-derived macrophages were maintained in 1x RPMI® – 1640 medium (HyClone®, Thermo Scientific) containing 10% Heat inactivated fetal bovine serum (HIFBS) (GIBCO®) in all studies.

2.11.1 Reviving U937 cells from frozen stock vial

A 1 mL cryovial containing U937 cells at passage 8 was thawed at 37°C in a dry bath. Cells were then immediately transferred to 3 mL RPMI + 10% HIFBS pre-warmed to 37°C and centrifuged at 207 x g for five minutes at room temperature to pellet the cells so that supernatant containing DMSO can be removed. Pellet was re-suspended gently in 1 mL pre-warmed RPMI + 10% HIFBS and transferred to a T25 culture flask (Sarstedt) containing 5 mL pre-warmed RPMI + 10% HIFBS. The flask was incubated in a humidified incubator at 37°C + 5% CO_2 and once media contained a heavy suspension of cells the cells were passed to T75 flasks.

2.11.2 Passaging U937 cells

Once a heavy suspension of U937 cells were observed, 1 mL, 2.5 mL or 5 mL of cells (depending on dilution desired 1/25, 1/10 or 1/5, respectively) were removed from the flask and transferred to a sterile 15 mL conical tube and centrifuged at 207 x g for five minutes at room temperature to pellet the cells. Supernatant was discarded and pellet immediately re-suspended in 2.5 mL pre-warmed RPMI + 10% HIFBS, volume of suspension measured, and appropriate volume of pre-warmed RPMI + 10% HIFBS was added to bring the final volume to 5 mL. The 5 mL cell suspension was then transferred to a T75 flask containing 20 mL pre-warmed RPMI + 10% HIFBS. A media control consisting of 5 mL RPMI + 10% HIFBS in a T25 flask was also prepared. All flasks were incubated at 37°C + 5% CO_2 for two, three, or four days if diluted 1/5, 1/10 or 1/25, respectively.

2.11.3 Activation of U937 cells

Contents of four T75 flasks containing heavy cell suspension were transferred to four 50 mL conical tubes and centrifuged at 207 x g for five minutes at room temperature to pellet the cells. Supernatants were discarded and each pellet was re-suspended in 5 mL pre-warmed RPMI + 10% HIFBS, then all suspensions pooled into one 50 mL conical tube. The volume of the pooled suspension was measured and brought to a final volume of 40 mL with pre-warmed RPMI + 10% HIFBS. To this suspension of cells, 80 μL of 100 μg/mL phorbol 12-myristate 13-acetate (PMA) was added, gently mixed by inversion and 5 mL aliquots transferred to eight T75 flasks, each containing 15 mL pre-warmed RPMI + 10% HIFBS. Flasks were incubated at 37°C + 5% CO_2 for 24 hours to allow cells to adhere.

2.12 Intracellular growth kinetic assays using activated U937 cells

2.12.1 Transferring activated cells to infection plates

Monolayers of activated U937 cells were washed three times with pre-warmed RPMI + 10% HIFBS and a final volume of 7.5 mL pre-warmed RPMI + 10% HIFBS was added to each T75 flask. Monolayers of cells were detached from the T75 flasks using a cell scraper (Thermo Scientific Nunc Cell Scraper PE Blade PS Handle Sterile 32 cm^2) and cell suspension pooled into one T75 flask. A 1 mL sample of the pooled suspension was transferred to a sterile microcentrifuge tube and used for counting via a hemocytometer. The samples to be counted were prepared by combining 10 μL of the pooled cell suspension sample with 10 μL of trypan blue, then mixed gently and let stand for one minute. 10 μL of this stained suspension was applied to the hemocytometer and the U937 cells that excluded the trypan blue dye (alive) were counted. An average of the cell counts was calculated and the concentration of cells was

determined using the average cell count multiplied by two (dilution factor) and then multiplied by 10^4 to incorporate the volume of the hemocytometer. Only cell concentrations of ~1 x 10^6 cells/mL were used for transferring in which 1mL of the pooled cell suspension was transferred to each well of a 24-well cell culture microplate (Corning® Costar®) in order to achieve a monolayer consisting of 1x10^6 cells per well. Microplates were incubated at 37°C + 5% CO_2 for 20 – 24 hours to allow the cells to adhere.

2.12.2 Infection of activated U937 cells

Media was removed from the monolayers of U937 cells within the 24-well cell culture microplate and immediately washed three times with pre-warmed RPMI + 10% HIFBS, ensuring the monolayer was left undisturbed. Prior to day of infection procedure, bacterial strains (see specific experimental procedures of Chapters 3 and 4 as well as Tables 3.1 and 4.1) were struck onto BCYE agar containing the appropriate supplements, incubated at 37°C + 5% CO_2 for three days then three single colonies were scraped and deposited into 3 mL BYE broth. Bacterial cultures were grown overnight at 37°C for 21 hours with rotation and 300 µL of overnight culture transferred to a sterile microcentrifuge tube and pelleted via centrifugation at 17, 500 x g for one minute at room temperature. Supernatant was discarded and pellet re-suspended in 1 mL RPMI + 10% HIFBS (1/3 dilution) and optical density at 600 nm was measured. Using the conversion factor of OD_{600} of 1.0 = 1 x10^9 cells/mL, the concentration of the bacterial suspension was determined and a calculated volume of the bacterial suspension was transferred to 10 mL pre-warmed RPMI + 10% HIFBS such that a multiplicity of infection (MOI) of 2 would be achieved when 1 mL of the diluted bacterial suspension was applied to the monolayer. Media was removed from all wells prior to applying the 1 mL bacterial suspension. After the

bacterial suspensions were applied, where each strain was assessed in duplicate, the microplate was centrifuged at 207 x g for five minutes at room temperature to synchronize the infection and incubated at 37°C + 5% CO_2 for one hour. Once the incubation period was completed the media was removed from the monolayers and wells immediately washed three times with pre-warmed RPMI + 10% HIFBS. Monolayers were then treated with 1 mL pre-warmed RPMI + 10% HIFBS containing 100 μg/mL gentamycin for one hour at 37°C + 5% CO_2, with microplate being centrifuged at 207 x g for five minutes at room temperature prior to incubation. Media containing gentamycin was then removed from the wells and the monolayers immediately washed three times in pre-warmed RPMI + 10% HIFBS. Following the final wash, 1 mL of RPMI + 10% HIFBS or 1 mL RPMI + 10% HIFBS containing 100 μg/mL thymidine was applied to each well depending on the growth requirements of the bacterial strain used for infection, and was considered to be time zero. Infections were allowed to proceed at 37°C + 5% CO_2 for 24, 48, and 72 hours.

2.12.3 Lysis of infected U937 cells and serial dilution plating

At times 0, 24, 48 and 72 hours post-infection, the media was removed from the wells corresponding to each time-point and 1 mL of cold (4°C) Hyclone™ water was applied to each well to lyse the U937 cells. Lysis was assisted through repeated pipetting and scraping of the well bottoms until monolayer was no longer visually detected. 100 μL of the lysate was transferred to a 96-well plate and 10-fold serial dilutions carried out to 10^{-5} in Hyclone™ water. Depending on the bacterial strain, serial dilutions were plated onto BCYE agar or BCYE agar containing 100 μg/mL thymidine in 10 μL aliquots and incubated at 37°C + 5% CO_2 for three

days. Colonies were counted using a stereomicroscope and cfu/mL determined. Values obtained were plotted using GraphPad Prism 6 (GraphPad Software, La Jolla, CA, USA).

2.13 Culturing *Acanthamoeba castellanii*

A. castellanii ATCC 30324 were maintained in proteose peptone - yeast extract - glucose (PYG) medium (2% (w/v) proteose peptone, 0.1% (w/v) yeast extract, 4 mM $MgSO_4 \cdot 7H_2O$, 0.4 mM $CaCl_2$, 0.05 mM $Fe(NH_4)_2(SO_4)_2 \cdot 6H_2O$, 2.5 mM $Na_2HPO_4 \cdot 7H_2O$, 2.5 mM KH_2PO_4, 0.1 M glucose and 3.4 mM sodium citrate$\cdot 2H_2O$) prepared as per the specifications outlined by the ATCC. For infections, *A. castellanii* were maintained in AC buffer (same composition as PYG except proteose peptone, yeast extract and glucose are excluded) as this buffer does not support the extracellular growth of *L. pneumophila* as defined by Moffat and Tompkins (1992).

2.13.1 Reviving *A. castellanii* from frozen stock vial

A 1 mL cryovial containing *A. castellanii* at passage 2 was thawed in a 35°C water bath for 2 -3 minutes, then immediately transferred to 5 mL room temperature PYG and centrifuged at 207 x g for five minutes at room temperature to pellet the cells so that supernatant containing DMSO can be removed. Pellet was re-suspended gently in 5 mL room temperature PYG and transferred to a T25 culture flask (Sarstedt). The flask was incubated in a humidified incubator at 25°C and when confluency was reached cells were passaged to a T75 flask.

If *A. castellanii* cells do not adhere and/or do not replicate, a media change was performed. Entire contents of the T25 flask were transferred to a sterile 15 mL conical tube and *A. castellanii* pelleted via centrifugation at 207 x g for five minutes at room temperature. Supernatant was removed, pellet re-suspended in 5 mL fresh room temperature PYG, and

transferred to a new T25 flask. The flask was incubated at 25°C until confluency was reached (usually within 3 to 4 days) and subsequently passaged to a T75 flask using a 1/20 dilution.

2.13.2 Passaging *A. castellanii*

Once *A. castellanii* were confluent, spent PYG media was poured off in a manner avoiding the monolayer of adhered cells and 10 mL of room temperature PYG was added to the T75 flask (if cells were in a T25 flask added only 5 mL PYG). Flask was rotated gently to wash the monolayer and wash then poured off. Immediately following, 10 mL PYG was added to the T75 flask (2.5 mL PYG added if in a T25 flask) and flask tapped firmly to re-suspend the monolayer. Then 0.25 mL, 0.3 mL or 0.5 mL of the re-suspended cells (depending on dilution desired 1/80, 1/60 or 1/40, respectively) were removed from the T75 flask and transferred to a new T75 flask containing 19.75 mL, 19.7 mL or 19.6 mL PYG, respectively. Flasks were incubated at 25°C for two, three, or four days if diluted 1/40, 1/60 or 1/80, respectively, to reach confluency. When passaging from a T25 flask to a T75 flask, 1 mL of the re-suspended cells were transferred to a T75 flask containing 19 mL PYG (1/20 dilution) and incubated at 25°C for 2 two days to reach confluency. A media control was always prepared in which 5 mL PYG was transferred to a T25 flask and incubated at 25°C.

For infection, 10 T75 flasks of passaged *A. castellanii* were generated, where eight flasks are required for infection, one flask for *A. castellanii* maintenance and one flask as an extra in case more cells are required for the infection.

2.13.3 Infection of *A. castellanii*

Spent PYG media was removed from eight T75 flasks containing confluent *A. castellanii* and monolayers washed two times in 10 mL room temperature AC buffer, with each wash discarded. After the second, wash 10 mL AC buffer was added to each flask and monolayer re-suspended by firm tapping. Re-suspended cells were pooled into one T75 flask and a 1 mL sample was transferred to a sterile microcentrifuge tube for counting via a hemocytometer. The samples to be counted were prepared by combining 10 μL of the pooled cell suspension sample with 10 μL of trypan blue, then mixed gently and let stand for one minute. 10 μL of this stained suspension was applied to the hemocytometer and *A. castellanii* that excluded the trypan blue dye (alive) were counted. An average of the cell counts was calculated and the concentration of cells was determined using the average cell count multiplied by two (dilution factor) and then multiplied by 10^4 to incorporate the volume of the hemocytometer. Only cell concentrations of ~1 x 10^5 - 1 x 10^6 cells/mL were used for transferring in which 1mL of the pooled cell suspension was transferred to each well of a 24-well cell culture microplate (Corning® Costar®) in order to achieve a monolayer consisting of ~1 x 10^5 - 1x10^6 cells per well. The microplate was then incubated at 25°C for at least one hour to allow the cells to adhere.

Prior to day of infection procedure, bacterial strains (see specific experimental procedures of Chapters 3 and 4 as well as Tables 3.1 and 4.1) were struck onto BCYE agar, incubated at 37°C + 5% CO_2 for four days, then 1/8 to 1/4 loopful of bacterial cells were scraped from the initial streak area of the agar plate. Bacteria were deposited into 3 mL AC buffer, re-suspended by gentle flicking (do not vortex) and optical density at 600 nm was measured. Using the conversion factor of OD_{600} of 1.0 = 5 x10^8 cells/mL, concentration of the bacterial suspension was determined and a calculated volume of the bacterial suspension was transferred to 15 mL

AC buffer such that a MOI of 0.01 would be achieved when 1 mL of the diluted bacterial suspension was applied to the monolayer. AC buffer was removed from all wells containing the adhered monolayer of *A. castellanii* prior to applying the 1 mL bacterial suspension. After the bacterial suspensions were applied, where each strain was assessed in duplicate, the microplate was incubated at 25°C for one hour to allow the infection to occur. Once the incubation period was completed, the AC buffer was removed from the monolayers and wells immediately washed two times with AC buffer. Following the final wash, AC buffer was removed from the wells and 1mL of AC buffer was applied to each well; this was considered to be time zero. Infections were allowed to proceed at 25°C for 168 hours, with lysis performed at 0, 72, 96, 120, 144 and 168 hours.

2.13.4 Lysis of infected *A. castellanii* and serial dilution plating

At time-points indicated above, the AC buffer within the wells was pipetted up and down followed by scraping of the well bottom with the pipette tip to re-suspend the monolayer of infected *A. castellanii*. A 300 µL sample of the suspension was transferred to a sterile microcentrifuge tube, vortexed vigorously for 30 seconds and then centrifuged at 17, 500 x *g* for 8 minutes at room-temperature to lyse the amoeba. Sample (lysate) was vortexed briefly to re-suspend the bacteria contained within the pellet of *A. castellanii* cell debris. 100 µL of the lysate was transferred to a 96-well plate and 10-fold serial dilutions carried out to 10^{-6} in AC buffer. Serial dilutions were plated onto BCYE agar in 10 µL aliquots and incubated at 37°C + 5% CO_2 for three days. Colonies were counted using a stereomicroscope and cfu/mL determined. Values obtained were plotted using GraphPad Prism 6 (GraphPad Software, La Jolla, CA, USA)

Chapter 3. THE CPXRA TWO-COMPONENT SYSTEM CONTRIBUTES TO *Legionella pneumophila* VIRULENCE

This chapter was published in *Molecular Microbiology*, 2016: Jennifer R. Tanner, Laam Li, Sébastien P. Faucher, and Ann Karen C. Brassinga. (2016). The CpxRA two-component system contributes to *Legionella pneumophila* virulence. Molecular Microbiology. [In press]. doi: 10.1111/mmi.13365. Note: this chapter has been modified from the original publication such that the majority of the materials and methods section is described in Chapter 2.

3.1 INTRODUCTION

Legionella pneumophila is a Gram-negative bacterium ubiquitously found in fresh water environments that include natural as well as anthropogenic systems (van Heijnsbergen *et al.*, 2015). *L. pneumophila* persists within these environments through association with complex biofilm communities and as a parasite of multiple protozoan species (Abdel-Nour *et al.*, 2013). Inhalation of aerosolized *Legionella*-laden water droplets by susceptible individuals leads to establishment of bacterial replicative vacuoles by the bacterium in alveolar macrophages within the lungs, resulting in the severe pneumonia Legionnaires' disease (Horwitz and Silverstein, 1980; Swanson and Hammer, 2000; Fields *et al.*, 2002). Formation of a *Legionella*-containing vacuole (LCV) is key to *L. pneumophila* survival within both of these eukaryotic host cells and is dependent upon a functional Dot/Icm type IV secretion system (T4SS) (Segal *et al.*, 1998; Vogel *et al.*, 1998; Isberg *et al.*, 2009; Richards *et al.*, 2013). This system transfers more than 300 effector proteins into the host cell to modulate cellular trafficking pathways in order to prevent

the fusion of the vacuole with the lysosome, and to recruit vesicles from the endoplasmic reticulum (ER) for vacuole maturation (Hubber and Roy, 2010; Rolando and Buchrieser, 2014).

To cope with the stresses of traversing extracellular and intracellular environments, *L. pneumophila* has adopted a developmental network featuring multiple morphological forms each with defining characteristics (Robertson *et al.*, 2014). In general, transmissive *L. pneumophila* forms [i.e. mature intracellular forms (MIFs) or cyst forms] upon egress from the spent host cell feature motility, reduced metabolism, multiple membrane laminations and poly-β-hydroxybutyrate inclusion bodies facilitating survival in low-nutrient environments, and virulence factors to enable infection of suitable host cells (Pruckler *et al.*, 1995; Faulkner and Garduno, 2002; Bruggemann *et al.*, 2006). Conversely, intracellular replicative bacteria, featuring morphology typical of vegetative cells, are metabolically active using amino acids as carbon and energy sources and thereby the expression of transmissive traits is repressed (Byrne and Swanson, 1998; Faulkner and Garduno, 2002; Molofsky and Swanson, 2004; Bruggemann *et al.*, 2006). Full development of multiphasic intracellular cycle has been demonstrated in protozoa and in the HeLa epithelial cell-line, but not in lymphoid cell-lines including U937 and THP-1 (Abdelhady and Garduno, 2013).

The multiphasic developmental cycle is governed by a complex regulatory cascade that includes several two-component systems (LetAS, LqsRS, PmrAB and CpxRA) [see (Segal, 2013; Robertson *et al.*, 2014) for reviews]. LetAS plays a key role in the transition from replicative to transmissive form initiated by amino acid starvation and perturbations to fatty acid biosynthesis that occur when entering stationary phase *in vitro* or upon exhausting host cellular resources during intracellular replication. Briefly, RelA and SpoT synthesize the alarmone guanosine 3’-diphosphate-5’-diphosphate (ppGpp) which in turn activates LetAS to positively

regulate expression of non-coding RNAs RsmY and RsmZ that bind and sequester CsrA, derepressing expression of transcripts encoding transmissive phase factors (Hammer and Swanson, 1999; Zusman *et al.*, 2002; Dalebroux *et al.*, 2009; Rasis and Segal, 2009; Sahr *et al.*, 2009; Dalebroux *et al.*, 2010). The Lqs system contributes to the transmissive regulatory network by inducing the expression of virulence and transmission factors that include Dot/Icm effectors, enhanced entry proteins (Enh) as well as eukaryotic-like proteins (Tiaden *et al.*, 2008; Tiaden *et al.*, 2010; Kessler *et al.*, 2013; Schell *et al.*, 2015). PmrAB influences virulence factor expression also, by directly regulating a significant number of Dot/Icm effector proteins, as well as induces the transcription of *csrA* during replicative and stationary phases of growth implying a role in differentiation (Zusman *et al.*, 2007; Al-Khodor *et al.*, 2009; Rasis and Segal, 2009).

CpxRA is involved in the regulation of Dot/Icm system components and effectors. CpxR has been shown to directly activate the expression of four Dot/Icm system components *icmR*, *icmV*, *icmW*, and *lvgA* as well as effect varying degrees of activation and repression of 11 translocated effector proteins (Gal-Mor and Segal, 2003a; Altman and Segal, 2008). Decreased levels of DotA, a component key to the functioning of the Dot/Icm system, have been observed in a *cpxR* mutant strain (Vincent *et al.*, 2006a) and interestingly, secretion activity of the Dot/Icm system was shown to be impaired when *cpxR* was inactivated (Murata *et al.*, 2006). Surprisingly, a *cpxR* insertion mutant strain did not display intracellular growth defects within *Acanthamoeba castellanii* or HL-60-derived macrophages (Gal-Mor and Segal, 2003a). Similarly, a *cpxR* insertion mutant strain was able to grow in mouse bone marrow-derived macrophages but with a one log reduction in bacterial counts in comparison to the parental strain (Vincent *et al.*, 2006a). Thus, despite the evidence that the CpxRA system regulates expression of several components of

the Dot/Icm system and effectors, the role of the CpxRA system in virulence and intracellular growth was unclear.

We undertook this study to further clarify the contributing role of the CpxRA system to the intracellular lifestyle of *L. pneumophila*. After ascertaining that *cpxRA* is genetically organized within a multi-gene operon along with *lpg1439-1441*, we generated unmarked in-frame single and combinatorial *cpxRA* gene deletion strains. Expression of *cpxRA* is autoregulated with elevated levels of CpxR in the post-exponential growth phase. Comparative microarray transcriptome analyses of the parental Lp02 and *ΔcpxRA* isogenic mutant strains revealed that the CpxRA system regulates an expanded list of Dot/Icm effectors as well as other key virulence factors that include Type II secreted substrates. Interestingly, we report that strains lacking CpxR, but not CpxA, demonstrate sodium resistance which reverts to the parental phenotype of sodium sensitivity when complemented *in trans*. Furthermore, we also report severe intracellular growth defects of *cpxR* and *cpxRA* mutant strains in *A. castellanii*, but not in U937-derived macrophages. Taken together, this study demonstrates that the CpxRA system is essential for survival of *L. pneumophila* in protozoa corroborating findings of a simultaneous study recently published elsewhere (Feldheim *et al.*, 2015).

3.2 SPECIFIC EXPERIMENTAL PROCEDURES AND MODIFICATIONS

3.2.1 Bacterial strains and plasmids

Bacterial strains and plasmids as well as oligionucleotides used in the studies described in this chapter are listed in Table 3.1 and Table 3.2, respectively.

3.2.2 Construction of Δ*cpxR,* Δ*cpxA,* and Δ*cpxRA* mutant strains

To generate the unmarked in-frame deletions of *cpxR, cpxA,* and *cpxRA, cpxR* and/or *cpxA* 5' and 3' primer sets (Table 3.2) were used to amplify the 5' and 3' flanking regions of *cpxR, cpxA,* or *cpxRA*. 5' and 3' prime fragments were then subsequently cloned into SalI and SacI sites of pSR47S, respectively, creating knockout plasmids pJT378, pJT493, and pJT501 which were confirmed by sequencing using pSR47S seq primers (Tables 3.1 and 3.2). Homologous recombination strategy was employed as described in Chapter 2, section 2.6.6.

3.2.3 Complementation

Complementation of Δ*cpxR,* Δ*cpxA,* and Δ*cpxRA* mutant strains *in trans* was achieved by using pJB908 and complementation fragments generated via overlap extension PCR (OEP). The *lpg1441* prom/OEP *cpxR* and *lpg1441* prom/OEP *cpxA* primer sets (Table 3.2) were used to generate a 291bp promoter fragment upstream of *lpg1441,* the first gene of the five gene operon which includes *cxpR* and *cpxA,* with an 18bp overhang corresponding to the first 18 nucleotides of the *cpxR* or *cpxA* coding sequences at the 3' end of the promoter fragment. The OEP *cpxR*/*cpxR* comp, OEP *cpxA*/*cpxA* comp, and OEP *cpxR*/*cpxA* comp primer sets (Table 3.2) were used to amplify the *cpxR, cpxA,* and *cpxRA* coding sequences with a 21bp overhang corresponding to the last 21 nucleotides of the *lpg1441* promoter fragment, at the 5' end of each

of the coding amplicons. The appropriate *lpg1441* promoter fragment and *cpx* coding amplicon were then combined in equal ng amounts with either *lpg1441* prom/*cpxR* comp or *lpg1441*/*cpxA* comp primer sets in a single PCR reaction to generate $P_{lpg1441}$-*cpxR*, $P_{lpg1441}$-*cpxA*, and $P_{lpg1441}$-*cpxRA* complementation fragments. Complementation fragments were gel isolated and subsequently cloned into SacI and XbaI sites of pJB908 creating complementation constructs pJT731, pJT734, and pJT732 (Table 3.1). Complementation constructs were verified by DNA sequencing using pJB908 seq, *cpxR* seq and *cpxA* seq primers (Table 3.2).

3.2.4 Total RNA isolation and cDNA synthesis

L. pneumophila Lp02 (parental) and Δ*cpxRA* strains were grown at 37°C to exponential phase [E phase (OD_{600} ~1.5)] and post-exponential phase [PE phase (OD_{600} ~3.0)] in BYE supplemented with thymidine. Approximately $1x10^9$ bacterial cells from the overnight cultures were pelleted via centrifugation at 10, 000 x *g* for one minute at room temperature and most of the supernatant removed, approximately ~80 μL - 90 μL of the supernatant was left behind. Bacterial pellets were re-suspended in 1 mL TRIzol® Reagent, mixed, and subsequently incubated at 37°C in a dry bath to lyse the cells. The lysate was transferred to a Phase-lock Heavy gel 2 mL tube (Eppendorf), 200 μL chloroform added, tubes shaken vigorously for 15 seconds and incubated at room temperature for three minutes. Samples were centrifuged at 12, 000 x *g* for 15 minutes at room temperature, the aqueous phase transferred to a new microcentrifuge tube and volume of aqueous phase measured. An equal volume of ice-cold isopropanol was added to the aqueous phase, mixed by gentle flicking, and incubated at room temperature for 10 minutes to precipitate the RNA. Precipitated RNA was pelleted via centrifugation at 17, 500 x *g* for 10 minutes at 4 °C, supernatant removed, pellet washed in 1 mL

ice-cold 75% ethanol and centrifuged at 17, 500 x g for five minutes at 4 °C. Supernatant was removed and wash repeated once more as describe above. Pellets were dried by placing tube on top of dry bath set to 60 °C and monitored to prevent over drying of the pellet. Dried pellets were then re-suspended in 40 µL Hyclone™ water pre-heated to 60 °C and samples incubated in a 60°C dry bath for 10 minutes to fully dissolve the pellet. Concentration and purity of the samples based on the 260/280 and 260/230 ratios were determined by a NanoDrop™ 2000c spectrophotometer. Total RNA samples were then adjusted to the concentration of 200 ng/µL using Hyclone™ water and treated twice with TURBO DNase using a "rigorous digestion" protocol outlined by the manufacturer (Ambion) in a total volume of 150 µL, where digestion was allowed to occur for one hour at 37°C. Inactivation of DNase was carried out as per TURBO DNA-free™ kit instructions (Ambion). DNase digested samples were adjusted to a volume of 500 µL with Hyclone™ water and a sodium acetate – ethanol precipitation of the RNA was then performed to remove salts using the following conditions: 1/10 volume of 3 M RNase free sodium acetate pH 5.5 (Ambion), 1 µL RNAse free glycogen (Ambion), and 2 volumes of 100% ethanol. RNA was precipitated overnight for 16 hours at -20°C, pelleted by centrifugation at 17, 500 x g for 10 minutes at 4 °C, pellet washed two times in 1 mL ice-cold 75% ethanol and dried as described above. Dried pellet was re-suspended in 25 µL Hyclone™ water pre-heated to 60 °C and samples incubated in a 60°C dry bath for 10 minutes to fully dissolve the pellet. Purity and quantity of RNA was determined using a NanoDrop™ 2000c spectrophotometer and by agarose gel electrophoresis. RNA was either stored at -80°C until use for microarray analyses or immediately converted to cDNA for qPCR or Junction PCR analysis with SuperScript® VILO™ cDNA synthesis kit as per manufacturer's instructions (Invitrogen); using the maximum amount of RNA template recommended for 20 µL reactions.

Table 3.1. List of bacterial strains and plasmids used in this study

Strain	Description	Reference or Source
E. coli		
DH5α	F' *endA1 hsdR17(r_k- m_k-) supE44 thi-1 recA1 gyrA (Nal^r) relA1 Δ(lacZYA-argF)U169 deoR*(ϕ80lacΔ(lacZ)M15)	New England Biolabs
DH5αλpir	K-12 F- φ80*lacZ*ΔM15 *endA recAhsdR17 (rm-mK+)supE44 thi-1 gyrA96 relA1 Δ(lacZYA-argF)* U169 *λpir*	M. Swanson (Bryan *et al.*, 2013)
BL21 (DE3) CodonPlus^{TM} RIL	B F$^-$ *ompT hsdS*(r_B^- m_B^-) *dcm*$^+$ Tet^r *gal* λ(DE3) *endA* Hte [*argU ileY leuW* Cam^r]	Stratagene
KB178	BL21 (DE3) CodonPlus^{TM} RIL pKB74	This study
KB578	BL21 (DE3) CodonPlus^{TM} RIL pKB153	This study
L. pneumophila		
Lp02	Str^r, Thy$^-$, HsdR$^-$ derivative of Philadelphia-1 strain; parental strain	M. Swanson (Berger and Isberg, 1993)
Lp03	Lp02 *dotA* mutant	R. Isberg (Berger and Isberg, 1993)
JT382	Lp02 with in-frame deletion of *cpxR* (Δ*cpxR*)	This study
JT523	Lp02 with in-frame deletion of *cpxA* (Δ*cpxA*)	This study
JT532	Lp02 with in-frame deletion of *cpxRA* (Δ*cpxRA*)	This study
CJP126	Lp02 pBH6119	(Pitre *et al.*, 2013)

JT708	Lp03 pBH6119	This study
JT390	Lp02 Δ*cpxR* pBH6119	This study
JT531	Lp02 Δ*cpxA* pBH6119	This study
JT547	Lp02 Δ*cpxRA* pBH6119	This study
JT737	Lp02 Δ*cpxR* pJT731 (*cpxR* complementation)	This study
JT756	Lp02 Δ*cpxA* pJT734 (*cpxA* complementation)	This study
JT738	Lp02 Δ*cpxRA* pJT732 (*cpxRA* complementation)	This study
JT393	Lp02 Δ*cpxR* pJB908	This study
JT736	Lp02 Δ*cpxRA* pJB908	This study
JT739	Lp02 pJT730	This study
JT740	Lp02 Δ*cpxR* pJT730	This study
JT741	Lp02 Δ*cpxA* pJT730	This study
JT742	Lp02 Δ*cpxRA* pJT730	This study

Plasmids

pET16b	N-terminal 10-histidine-tagged fusion protein expression vector; Amp^r	Novagen
pMAL-c2X	N-terminal maltose-binding protein (MBP) fusion protein expression vector; Amp^r	Novagen
pBH6119	Promoter-less GFP vector; Amp^r, Thy^+	M. Swanson (Hammer *et al.*, 2002)
pSR47S	oriTRP4 oriR6K, *Kan^r, sacB*	J. Vogel (Merriam *et*

		al., 1997)
pJB908	RSF1010 cloning vector, Amp^r, Thy^+	J. Vogel (Sexton *et al.*, 2004b)
pJT378	pSR47s with *cpxR* flanking regions	This study
pJT493	pSR47s with *cpxA* flanking regions	This study
pJT501	pSR47s with *cpxR* - *cpxA* flanking regions	This study
pKB74	pET16b::*cpxR*	This study
pKB128	pMAL-c2X::*cpxA*	This study
pKB153	pMAL-c2X::'*cpxA* – truncated version of *cpxA* (1-520 bp are deleted); Amp^r	This study
pJT731	pJB908:: $P_{lpg1441}$-*cpxR*	This study
pJT734	pJB908:: $P_{lpg1441}$-*cpxA*	This study
pJT732	pJB908:: $P_{lpg1441}$-*cpxRA*	This study
pJT730	pBH6119::$P_{lpg1441\text{-}cpxA}$	This study

Table 3.2. Oligonucleotides used in this study.

Primer name and function	Sequence (5' – 3')[a]	Amplicon size (bp)	Annealing Tm (°C)
Cloning			
PF cpxR 5'null	GCGATAgtcgacGATGAAGTGGTTGGCATTTTGCA	588	62.2
PR cpxR 5'null	GCGATAggatccTCCAGTACAGACTACGCATTA		
PF cpxR 3'null	GCGATAggatccTAATGCGTAGTCTGTACTGGA	577	62.2
PR cpxR 3'null	GCGATAgagctcGCTGCCATGCCTAATGAGCGT		
PF cpxR int	GTAGTATGTGTGCATGATGGA	180	62.2
PR cpxR int	GCGATCGATATCATCACCACG		
PF cpxA 5'null	GCGATAgtcgacGATGATGACACAGAACTAACAGA	675	62.2
PR cpxA 5'null	GCGATAggatccTACAGACTACGCATTAAACAT		
PF cpxA 3'null	GCGATAggatccACCTGCTGATGTTAAATAGGAT	685	62.2
PR cpxA 3'null	GCGATAgagctcTGAGACTGCCGTAATGAATCC		
PF cpxA int	TGATGAACTCCCAAGTGATG	240	57.5
PR cpxA int	ATGCCTAATGAGCGTAAAGG		
PF lpg1441prom	GCGATAgagctcGAAGATCGATCATAAATTGC	325	57.5
PR lpg1441prom_gfp	GCGATAtctagaCACTGTTTAATGTACTACTC		
PF lpg1441prom	GCGATAgagctcGAAGATCGATCATAAATTGC	315	51.5
PR OEP cpxR	GAGAATAGAGCTGCTCATAGTTTTTATTAAAGATTAATG		
PF OEP cpxR	CATTAATCTTTAATAAAAACTATGAGCAGCTCTATTCTC	708	62.2
PR cpxR comp	GCGATAtctagaCTACGCATTAAACATGTAC		
PF lpg1441prom	GCGATAgagctcGAAGATCGATCATAAATTGC	315	51.5
PR OEP cpxA	CCAGTACAGACTACGCATAGTTTTTATTAAAGATTAATG		
PF OEP cpxA	CATTAATCTTTAATAAAAACTATGCGTAGTCTGTACTGG	1395	57.5
PR cpxA comp	GCGATAtctagaCTATTTAACATCAGCAGGTA		
PF OEP cpxR	CATTAATCTTTAATAAAAACTATGAGCAGCTCTATTCTC	2068	57.5
PR cpxA comp	GCGATAtctagaCTATTTAACATCAGCAGGTA		
PF cpxR exp	GCGATAcatatgAGCAGCTCTATTCTC	687	53.9
PR cpxR exp	GCGATAggatccATGCGTAGTCTGTACTG		
PF cpxA exp	GCGATAggatccATGCGTAGTCTGTACTG	1374	53.9
PR cpxA exp	GCGATActgcagCTATTTAACATCAGCAGG		
PF icmRprom_DP	GCGATAggatccTATGACGGATGTTATG	283	57.5
PR icmRprom_DP	GCGATAGgaattcAGTTACATCAGGTTCA		
Sequencing			
PF pSR47s seq	CTGTTGCATGGGCATAAAGTTG	-	-

PR pSR47s seq	CACAGGAAACAGCTATGACC	-	-
PF EXT_RAKO seq	ATTCAGAGACCCTCGCAATG	-	-
PF cpxRKO seq	GTTCTTAATGCCGATTCGAG	-	-
PR cpxRKO seq	CTGGTAACCCATGCCGTAG	-	-
PF EXT2_RKO seq	GGGTTACCAGCCAAATCGCAC	-	-
PR EXT2_RKO seq	CTGTGCGCCAATGATTTCGCC	-	-
PF EXT_AKO seq	TGCCGATTCGAGAAGAATAAA	-	-
PF cpxAKO seq	TGCTTATGACCGCAGTATCG	-	-
PR EXT_RAKO seq	AGGCTGAGAGTCGCCAAAT	-	-
PR cpxRAKO seq	TGTATCATTGCTCACAAAATGG	-	-
PR GFP seq**	GTAAGTAGCATCACCTTCA	-	-
PF pJB908 seq	CTCCGTGATGGAATGACAAC	-	-
PR pJB908 seq	GACCGCTTCTGCGTTCTGA	-	-
PF cpxR seq	GTAGTATGTGTGCATGATGGA	-	-
PR cpxR seq	GCGATCGATATCATCACCACG	-	-
PF cpxA seq	TGATGAACTCCCAAGTGATG	-	-
PR cpxA seq	ATGCCTAATGAGCGTAAAGG	-	-

RT-PCR

PF up_RT PR lpg1441_RT	CAGTAAGAGATAGGCATTC CGAGTTCCCTGGTATTA	445	53.9
PF lpg1441_RT PR lpg1440_RT	CACCACTATCATGCAAAT GTAGTGAGCAAGGAAATG	465	53.9
PF lpg1440_RT PR lpg1439_RT	CATTTCCTTGCTCACTAC GGATAGCTCCCTCAATC	430	53.9
PF lpg1439_RT PR cpxR_RT	TCATCAAAGCCCATACT TCCAAATGCTCTCTTATTG	473	53.9
PF cpxR_RT PR cpxA_RT	GAGGAACTCACCGAATA GTGCTGGTTAGTAAATACA	402	53.9
PF motC_RT* PR motB_RT*	CTCGCTGATCCCAGTCAATTAG TGCCGACTTCATTCCTTCAG	403	53.9

PF mip-sda_RT*	TAGCGTCTTGCATGCCTTTAG	465	53.9
PR mip-sda_RT*	CCTACTGTGTGTGAGCTTGATG		
qRT-PCR			
PF gyrB RT-PCR**	CAAGGTATCAGGCGGTCTAC	151	-
PR gyrB RT-PCR**	CTTCTCCAGTTTCAGCAATAGG		
PF ihf α RT-PCR**	GCAAAGCAATAATGGCAGAA	117	-
PR ihf α RT-PCR**	GCTGACCATTTTCAAGAGCA		
PF ihf β RT-PCR**	CGAACTCATTGAACACATCG	162	-
PR ihf β RT-PCR**	GGTGGTCGGTAATGAAGAGA		
PF rsmY RT-PCR+	ATGGATATGTCTGACAGGAAGTC	84	-
PR rsmY RT-PCR+	ATTAGAGAATAAGTGCTGCATCC		
PF rsmZ RT-PCR+	TGGATATGAGTCGTGCAAATGG	110	-
PR rsmZ RT-PCR+	GACTCAGCCCTGGCTTTTC		
PF icmR RT-PCR	CGTGTTAAAGAGATAGGTG	145	-
PR icmR RT-PCR	CATCCGTGTTATCTTTCC		
PF oxyR RT-PCR	TGGAAGAAGAATTAGGTGTTGTG	199	-
PR oxyR RT-PCR	ATGTAAGGCGATACGGTAGG		
PF rpoS RT-PCR	GAAGAGGAATGGTCTGAGCCAGATGATG	188	-
PR rpoS RT-PCR	TCACCCAAGTAAAGTTGAGTCGCATCTA		
PF htpA RT-PCR	TCGTCGTATGGAAGAAGAGC	140	-
PR htpA RT-PCR	CTGCTAAAGCACGAACATCA		

[a]Restriction sites are lowercase font and underlined

*Primer sequences retrieved from Fonseca *et al.* (2014)

** Primer sequences retrieved from Pitre *et al.* (2013)

+ Primer sequences retrieved from Edwards *et al.* (2010)

3.2.5 Junction reverse transcriptase PCR (RT-PCR)

To assess the extent of the transcript for the region of interest, cDNA generated from exponential (E) and post-exponential (PE) phase RNA samples from Lp02 were used as templates in Taq polymerase PCR reactions with gene-specific RT-PCR primer sets (Table 3.2) that amplify regions across putative gene junctions. Also included as template were the RNA samples used in generating the cDNA and genomic DNA as controls for genomic contamination and positive amplification, respectively. All samples were then assessed via agarose gel electrophoresis. Note that figure content and positioning in panel A and B of figure 3.1 was influenced by a figure layout from Fonseca *et al.* (2014).

3.2.6 Microarray analysis and quantitative real-time PCR (qRT-PCR)

Total RNA isolated from *L. pneumophila* Lp02 and Δ*cpxRA* strains at exponential and post-exponential growth phases were subjected to microarray analysis. The microarray platform utilized has been described previously [(Li *et al.*, 2015) GEO accession number GPL19458]. Microarray procedures including cDNA synthesis, labeling, hybridization and data acquisition were performed as outlined in Faucher and Shuman (2013). Statistical analysis between Δ*cpxRA* and the parental strain at each phase was performed using a paired Student's t-test. Genes were considered differentially expressed if they demonstrated an expression ratio value of ±2-fold change with a *p*-value <0.02. qRT-PCR of selected genes using primers listed in Table 3.2 was performed as outlined in Pitre *et al.* (2013), with the exception that Bio-Rad CFX Connect 96-well RT-PCR system and SsoAdvanced SYBR green supermix were used.

3.2.7 GFP reporter constructs for GFP assays

A 291 bp promoter fragment upstream of *lpg1441* ($P_{lpg1441\text{-}cpxA}$) was generated by PCR amplification using the primer set *lpg1441* prom/*lpg1441* prom_gfp (Table 3.2) and directionally cloned into SacI and XbaI sites of promoter-less GFP reporter pBH6119 plasmid creating pJT730 GFP-transcriptional fusion plasmid. The construct, pJT730, was verified by Sanger sequencing using the GFP seq primer (Table 3.2) and subsequently electroporated into Lp02 (parental), Δ*cpxR*, Δ*cpxA*, and Δ*cpxRA* to generate the reporter strains JT739, JT740, JT741, and JT742 (Table 3.1). GFP reporter assays were conducted as described in Chapter 2, section 2.8.

3.2.8 CpxR recombinant protein expression and purification

The CpxR coding sequence was PCR amplified using the *cpxR* exp primer set in a Q5 high fidelity polymerase reaction (Table 3.2) and directionally cloned into NdeI and XhoI restriction sites of his-tagged fusion protein expression vector, pET16b (Novagen) creating the construct pKB74 (Table 3.1). The expression construct was then transformed into *E. coli* BL21 (DE3) CodonPlus™ RIL for over expression and purification.

The compositions of Buffer A and Buffer B used in the HiTrap Heparin HP column purification were as follows: Buffer A (20 mM Tris-HCl pH 8.0 and 25 mM KCl) and Buffer B (20 mM Tris-HCl pH 8.0 and 225 mM KCl). Buffer A and Buffer B were combined to achieve the following increasing concentrations of KCl for application to the column: 25 mM, 50 mM KCl, and 75 mM KCl. These buffers also contained a final concentration of 0.5 mM DTT added just prior to buffer being applied to the column.

3.2.9 CpxA recombinant protein expression and purification

The CpxA coding sequence was PCR amplified using the *cpxA* exp primer set (Table 3.2) and directionally cloned into BamHI and PstI restriction sites of maltose-binding protein fusion vector pMAL-c2X (New England BioLabs (NEB)) creating the construct pKB128. The expression construct was then transformed into *E. coli* BL21 (DE3) CodonPlus™ RIL for over expression and purification.

E. coli BL-21(DE3) CodonPlus™RIL harboring pMAL-c2X::*cpxA* was utilized in an initial test purification where CpxA was determined to be insoluble. Therefore the construct pKB128 was digested with EcoRI and the two sites (one within the multiple cloning site and the other within the gene) were re-ligated to remove the periplasmic and transmembrane domains creating the construct pKB153 that expresses a truncated version of CpxA' with increased solubility. pKB153 was transformed into *E. coli* BL-21(DE3) CodonPlus™RIL to generate the expression strain KB578 (Table 3.1). The expression strain KB578 was struck onto LB agar media containing ampicillin (100 μg/mL) and chloramphenicol (20 μg/mL) and grown overnight at 37°C. Three to four single colonies were scraped from the LB agar plate and deposited into a beveled flask containing 20 mL LB broth with the appropriate antibiotics added and incubated overnight at 37°C with shaking (~150 rpm). Then 10 mL of the overnight culture was then used to inoculate 990 mL LB broth (total volume 1 L) containing 0.2% (w/v) glucose and ampicillin (100 μg/mL) for both expression vector maintenance and repression of maltose genes on the chromosome of the *E. coli* strain as described by the manufacturer (NEB). The 1L culture was incubated at 37°C with shaking until culture reached an OD_{600} of 0.5 (using a conversion factor of OD_{600} 1.0 = $4x10^8$ cells/mL as outlined in the NEB protocol) then induced with 0.3 mM IPTG for two hours at 37°C with shaking. Induced bacterial cells were pelleted and stored at -80°C as

described in Chapter 2, section 2.7.1, except pellet was washed in chilled filter sterilized column buffer (20 mM Tris-HCl pH 7.5, 0.2 M NaCl, and 1 mM EDTA pH 8.0).

Bead preparation was conducted with 3.5 mL amylose resin and column buffer as described in Chapter 2, section 2.7.2. Lysis of the bacterial cells via French Press was conducted as described in Chapter 2, section 2.7.3, except pellet was re-suspended in 20 mL cold column buffer, EDTA was not added as is present in column buffer already and the prepared amylose resin was used for the slurry. Gravity column, fraction selection and dialysis were conducted as described in Chapter 2, section 2.7.4, except column was washed with 12 column volumes of cold column buffer, the protein was eluted using 10 mL column buffer containing 10 mM maltose and dialyzed in dialysis buffer containing 200 mM NaCl rather than KCl. Secondary purification via HiTrap Heparin HP column and protein concentration were performed as described in Chapter 2, section 2.7.5, except Buffer A contained 200 mM NaCl, Buffer B contained 1. 5 M NaCl, Buffer A and Buffer B were combined to achieve the increasing concentrations of 200 mM, 300 mM and 400 mM NaCl, protein was concentrated using an Amicon® Ultra 50K Centrifugal filter units (Millipore) that can only be centrifuged at 5000 xg for four minutes, and the protein storage buffer had the composition of: 20 mM Tris-HCl pH 7.4, 200 mM NaCl, 0.5 mM DTT, and 30% (v/v) glycerol. Protein concentration was determined as described in Chapter 2, section 2.7.6.

3.2.10 Radiolabelled probes for electrophoretic mobility shift assay (EMSA)

Forward and reverse primers (PF *lpg1441*prom/PR *lpg1441*prom_gfp or PF *icmR*prom_DP/PR *icmR*prom_DP) (Table 3.2) were used in labeling reactions described in Chapter 2, section 2.10 to generate $P_{lpg1441\text{-}cpxA}$ or P_{icmR} labeled probes, respectively. Binding

reactions and subsequent gel electrophoresis was conducted as described in Chapter 2, section 2.10.

3.2.11 Sodium sensitivity

L. pneumophila strains were grown in BYE broth at 37°C until post-exponential phase (OD_{600} ~3.0) and diluted 10-fold in sterile water to dilution factor 10^{-6} with 10 µl of each of the dilution factors plated on BCYE with and without 100 mM NaCl. Plates were incubated three days at 37°C and the percentage of bacteria that were sodium resistant was calculated using the following formula as per Byrne and Swanson (1998): [(cfu ml^{-1} on BCYE + cfu/mL on 100 mM NaCl BCYE) / (cfu/mL on BCYE)] x 100. Values were plotted and statistical analysis performed with GraphPad Prism 6 (GraphPad Software, La Jolla, CA, USA).

3.2.12 Intracellular growth kinetic assays in U937- derived macrophages

Differentiated U937 cells were infected with Lp02 (parental), Δ*cpxR*, Δ*cpxA*, Δ*cpxRA*, and Δ*dotA* strains as described in Chapter 2, section 2.12.2.

3.2.13 Intracellular growth kinetic assays in *Acanthamoeba castellanii*

L. pneumophila Lp02 (parental) and isogenic mutant strains harbored pBH6119 to complement the thymidine auxotrophy of the Lp02 eliminating the need for exogenous thymidine supplementation. *A. castellanii* were infected with the following strains as described in Chapter 2, section 2.12.3: Lp02 (parental) (CP126), Δ*cpxR* (JT390), Δ*cpxA* (JT531), Δ*cpxRA* (JT547), and Δ*dotA* (JT708) as well Δ*cpxR* and Δ*cpxRA* complementation strains JT737 and JT738, respectively, as described in Chapter 2, section 2.12.3 (Table 3.1).

3.3 RESULTS

3.3.1 The CpxRA two-component system is co-transcribed in a five-gene operon

Analysis of the genetic region encoding the CpxRA two-component system in *L. pneumophila* Lp02 revealed three genes upstream of *cpxRA* (Figure 3.1A). The three genes, *lpg1441*, *lpg1440*, and *lpg1439*, are encoded in tandem with *lpg1441* positioned as the first open-reading frame with its coding sequence overlapping the start of the *lpg1440* coding sequence by four base pairs (4 bp). Adjoining, *lpg1440* and *lpg1439* coding sequences have an overlap of 41bp with the *cpxR* coding sequence following immediately downstream of *lpg1439*, separated by only a 7 bp intergenic region. At the end of this region of interest is the *cpxA* open-reading frame which overlaps with the *cpxR* coding sequence by 8 bp, as previously determined by Gal-Mor and Segal (2003a). With multiple coding sequence overlaps along with a small intergenic region between *lpg1439* and *cpxR*, it is most likely that these five genes are co-transcribed as a single transcript.

To ascertain that the *lpg1441-cpxA* region is encoded as a polycistronic transcript, junction PCR was employed with cDNA synthesized from total RNA extracted from Lp02 cultured in broth to exponential (E) or post-exponential (PE) growth phases (Figure 3.1A) (Table 3.2). Also included were primers to define the start (up-*lpg1441*) and end (*cpxA*-down) of the transcript as well as primers to amplify the junction regions of *motC-motB* and *sda2-mip* to serve as positive and negative controls of operon structure, respectively (Figure 3.1A, Table 3.2) (Fonseca *et al.*, 2014). PCR products were generated for the *lpg1441-lpg1440*, *lpg1440-lpg1439*, *lpg1439-cpxR*, and *cpxR-cpxA* gene junctions in both E and PE phases (Figure 3.1B). Likewise, PCR products were observed in both E and PE growth phases for the co-transcribed *motC-motB* junction region; however, junction PCR of the divergently transcribed *sda2* and *mip* genes did

not result in a PCR product in either of the growth phases (Figure 3.1B). In addition, PCR products were not generated with the upstream and downstream primer sets in either growth phase defining *lpg1441* and *cpxA* as the first and last gene, respectively, in the transcript (Figure 3.1B). Taken together, *lpg1441-lpg1440-lpg1439-cpxR-cpxA* are genetically organized in an operon structure and transcribed as a polycistronic transcript in both E and PE growth phases matching results recently determined in *L. pneumophila* JR32 (Feldheim *et al.*, 2015).

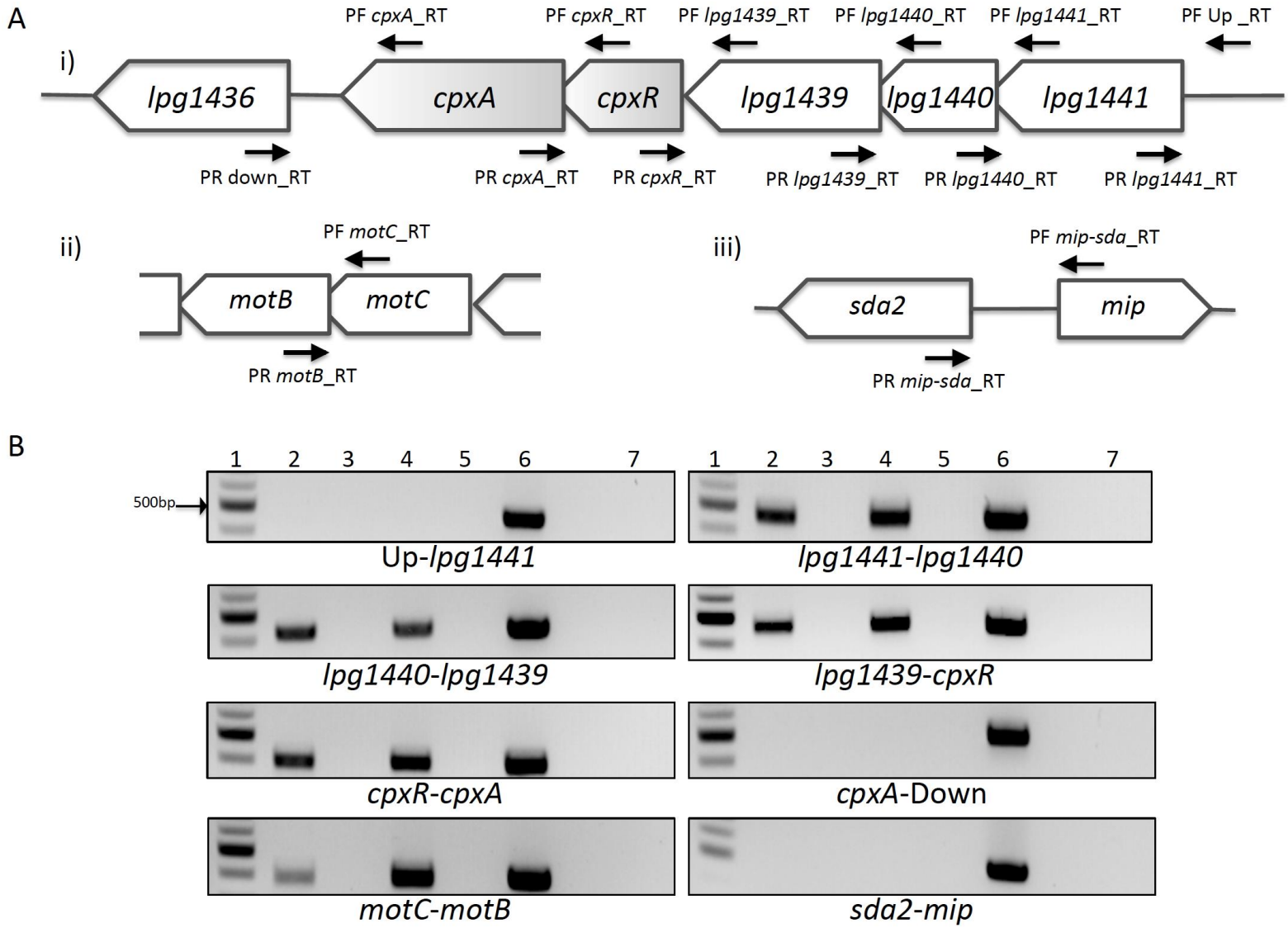
A
i)
PF cpxA_RT
PF cpxR_RT
PF lpg1439_RT
PF lpg1440_RT
PF lpg1441_RT
PF Up _RT
lpg1436
cpxA
cpxR
lpg1439
lpg1440
lpg1441
PR down_RT
PR cpxA_RT
PR cpxR_RT
PR lpg1439_RT
PR lpg1440_RT
PR lpg1441_RT
ii)
PF motC_RT
motB
motC
PR motB_RT
iii)
PF mip-sda_RT
sda2
mip
PR mip-sda_RT
B
1 2 3 4 5 6 7
500bp
Up-lpg1441
lpg1441-lpg1440
lpg1440-lpg1439
lpg1439-cpxR
cpxR-cpxA
cpxA-Down
motC-motB
sda2-mip

Figure 3.1 The CpxRA two-component system is encoded in a multi-gene operon structure. A) Schematic diagrams of the genetic organization of i) region of interest *lpg1441 – cpxA*, ii) operon encoded *motC-motB* (positive control) and iii) divergent genes *sda2-mip* (negative control). The arrows represent the positioning of the primers (listed in Table 3.2) utilized in RT-PCR to assess the indicated junction regions to determine polycistronic transcription events. B) Gel electrophoresis of PCR products of each junction region obtained from reactions using cDNA or total RNA as template from exponential phase (E) and post-exponential phase (PE) growth phase samples. Lanes denote the following: 100bp DNA ladder (1), cDNA PE growth phase (2), total RNA PE growth phase (3), cDNA E growth phase (4), total RNA E growth phase (5), genomic DNA (6) and no template control (7). Data is representative of one of three independent experiments.

3.3.2 In-frame null mutation and complementation strategies

In studies elsewhere, *cpxR* mutants have been generated in *L. pneumophila* using either kanamycin cassette or mini-Tn10 insertion strategies (Gal-Mor and Segal, 2003a; Vincent *et al.*, 2006a). These strategies not only disrupted *cpxR*, but may have also disrupted expression of *cpxA* due to polar effects (Danese *et al.*, 1995). Therefore, to circumvent this difficulty posed by *cpxR* insertion mutants, we employed an in-frame gene deletion strategy to generate Δ*cpxR* (JT382), Δ*cpxA* (JT523), and Δ*cpxRA* (JT532) mutant strains (Table 3.1). Each mutant strain was verified for the in-frame genetic deletion(s) by sequencing (data not shown) as well as appropriate presence and/or absence of CpxR and CpxA proteins by immunoblotting cellular extracts (Figure 3.2).

Complementation of each of the Δ*cpxR*, Δ*cpxA*, and Δ*cpxRA* mutant strains was achieved by *in trans* expression of pJB908-based constructs. To avoid induced gene expression that can result in inappropriate cellular protein levels, which may interfere with the temporal progression of the cell developmental program, the native promoter was employed to direct expression of the complementing gene(s). The native promoter, encompassing a 291bp region upstream of *lpg1441*, was identified based on the operon structure characterized in Figure 3.1 and supporting RNAseq data published elsewhere which detected the presence of a single promoter for the *lpg1441-cpxA* region ($P_{lpg1441\text{-}cpxA}$) (Sahr *et al.*, 2012). Overlap extension PCR was employed to clone the $P_{lpg1441\text{-}cpxA}$ region directly upstream of either *cpxR*, *cpxA* or *cpxRA* into pJB908 creating complement constructs pJT731, pJT734, and pJT732, respectively, for electroporation into the appropriate mutant strain and assessed for presence of CpxR and/or CpxA by immunoblotting (Table 3.1, Figure 3.2). CpxR was detected in cellular extracts of both the Δ*cpxR* and Δ*cpxRA* complemented strains (JT737 and JT738), and CpxA in cellular extracts of

Δ*cpxA* and Δ*cpxRA* complemented strains (JT756 and JT738) (Figure 3.2 and Table 3.1). As pJB908 carries *thyA* (encoding thymidylate synthase) rescuing the auxotrophic thymidine phenotype of Lp02, parental and isogenic mutant strains containing the empty vector pBH6119 (a derivative of pJB908) were used to ensure consistency of results with respect to plasmid-borne *thyA*. In summary, these results indicate that the $P_{lpg1441\text{-}cpxA}$ region effectively drives expression of the *cpxR* and/or *cpxA,* allowing for complementation without induced gene expression.

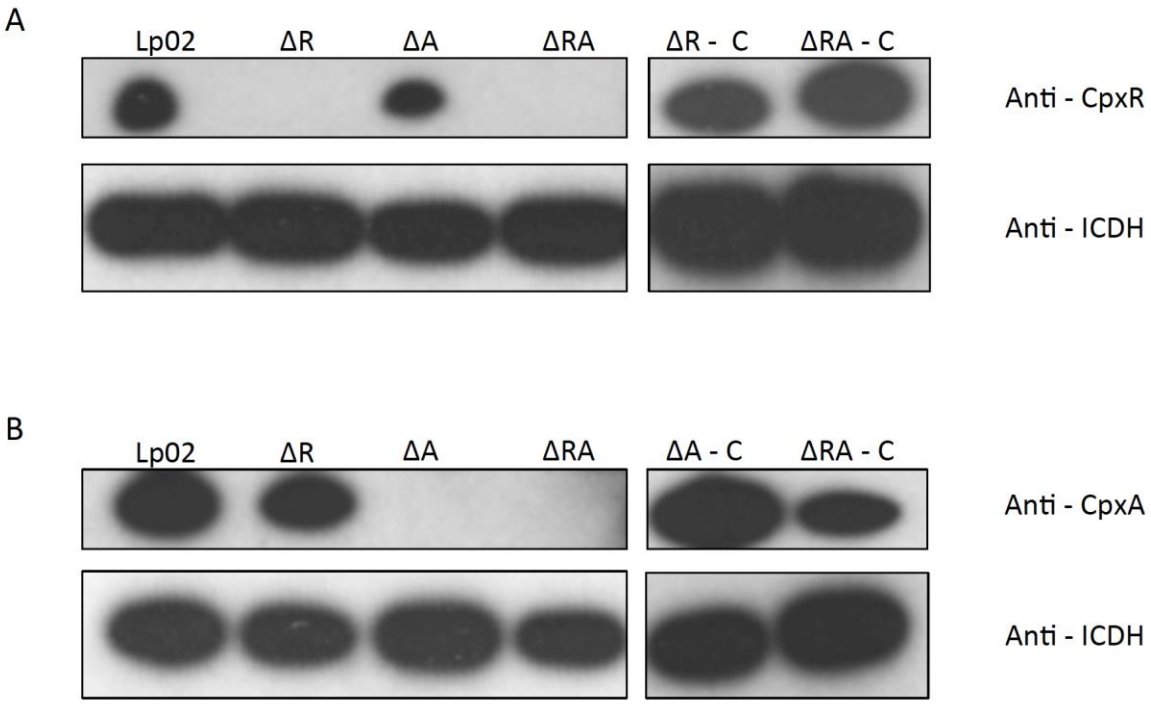

Figure 3.2 Immmunoblots confirm absence of CpxR and/or CpxA in isogenic mutant strains. Immunoblots of A) CpxR and B) CpxA proteins in *L. pneumophila* parental Lp02 (CP126) and isogenic mutant Δ*cpxR* (ΔR) (JT390), Δ*cpxA* (ΔA) (JT531), Δ*cpxRA* (ΔRA) (JT547) strains harboring pBH6119 along with *in-trans* complemented Δ*cpxR* (ΔR - C) (JT737), Δ*cpxA* (ΔA - C) (JT756), and Δ*cpxRA* (ΔRA - C) (JT738) strains. Detection of cellular isocitrate dehydrogenase (ICDH) acted as an internal loading control. Data is representative of one of two independent experiments.

3.3.3 CpxRA exhibits positive and negative autoregulatory control with CpxR directly interacting with the $P_{lpg1441\text{-}cpxA}$ region

The CpxRA system has been shown to positively and negatively autoregulate its expression via feedback mechanisms in *E. coli*, and appears to do so in other pathogens such as *Yersinia pseudotuberculosis* and *Vibrio cholerae* (Raivio *et al.*, 1999; Liu *et al.*, 2012; Slamti and Waldor, 2009). To determine if CpxRA autoregulation occurs in *L. pneumophila*, the $P_{lpg1441\text{-}cpxA}$ region was cloned into the promoter-less GFP reporter plasmid pBH6119 creating pJT730 that was then electroporated into parental Lp02 and Δ*cpxR*, Δ*cpxA*, and Δ*cpxRA* isogenic mutant strains generating JT739, JT740, JT741 and JT742 (Figure 3.3A and Table 3.1). In the parental (JT739) background, the promoter activity remains constant for 10 hours at ~460 RFU/OD_{600} units, and then begins to gradually increase reaching a maximum value of ~1100 RFU/OD_{600} units between 20 and 24 hours (Figure 3.3B). Interestingly, the activities of $P_{lpg1441\text{-}cpxA}$ in Δ*cpxR* (JT740), Δ*cpxA* (JT741), and Δ*cpxRA* (JT742) mutant strain backgrounds were significantly altered in comparison to the $P_{lpg1441\text{-}cpxA}$ activity levels in the Lp02 background (Figure 3.3B). Initially, slightly elevated levels of $P_{lpg1441\text{-}cpxA}$ activity were observed in all mutant strain backgrounds, which decreased over time to reach a value similar to that observed in Lp02 (JT739) by seven hours (Figure 3.3B). Similarly to what was observed in the Lp02 (JT739) background, at 10 hours the $P_{lpg1441\text{-}cpxA}$ activity increased in all mutant strains; however, the rate was much more accelerated and reached maximal levels of ~1800, 2300, and 2500 RFU/OD_{600} units in the Δ*cpxA* (JT740), Δ*cpxR* (JT741), and Δ*cpxRA* (JT742) mutant strain backgrounds, respectively (Figure 3B). In regard to the Δ*cpxA* strain (JT741), the elevated $P_{lpg1441\text{-}cpxA}$ activity in the absence of the sensor kinase CpxA suggests that CpxR acts as a positive autoregulator. Studies elsewhere have shown that lack of functional CpxA promotes CpxR to be in a

continuously active (i.e. phosphorylated) state due to the lack of phosphatase activity normally performed by CpxA (Danese *et al.*, 1995; Raivio and Silhavy, 1997; Wolfe *et al.*, 2008; Spinola *et al.*, 2010). CpxR also appears to act as a negative autoregulator as significantly elevated $P_{lpg1441\text{-}cpxA}$ activities were observed in the Δ*cpxR* (JT741) and Δ*cpxRA* (JT742) mutant strain backgrounds (Figure 3.3B).

CpxR autoregulation of *cpxRA* expression has been shown to be direct in *E. coli* and *V. cholerae* due to the presence of a CpxR consensus binding site sequence (GTAAA-N_5-GTAAA) within the promoter region upstream *cpxRA* (Raivio *et al.*, 1999; Slamti and Waldor, 2009). In this view, analysis of the $P_{lpg1441\text{-}cpxA}$ region revealed a sequence that closely matched that of the reported *L. pneumophila* CpxR binding site (GTAAA-N_6-GWAAA), suggesting that direct autoregulation of *cpxRA* expression is likely in *L. pneumophila* as well (Altman and Segal, 2008; Segal, 2013). The putative binding site sequence, AGAAA-N_6-GTAAA contains two mismatches and is located 107 bp upstream of the *lpg1441* coding sequence and 81 bp upstream of the transcriptional start site previously determined for the $P_{lpg1441\text{-}cpxA}$ region by Sahr *et al.* (2012) (Figure 3.3A).

Recently, the *L. pneumophila* CpxR consensus sequence has been revised to TGTAAA-N_5-TGWAAA, which modifies the putative binding site within the $P_{lpg1441\text{-}cpxA}$ region to contain four mismatches (Feldheim *et al.*, 2015) (Figure 3.3A). To examine whether CpxR is able to interact with a binding motif containing an increased number of mismatches, electrophoretic mobility shift assays (EMSAs) were conducted with purified recombinant CpxR and radiolabeled $P_{lpg1441\text{-}cpxA}$ region. Progressive band migration was observed with increasing CpxR concentrations, where maximal migration occurred at 24.6 μM, indicating CpxR directly interacts with the $P_{lpg1441\text{-}cpxA}$ region (Figure 3.3C).

For comparison of binding affinities, EMSA studies were also conducted with radiolabeled P_{icmR} as this region has been shown in previous studies elsewhere to contain the CpxR binding motif with two mismatches (TGTAAA-N_5-AGAAAG) and to be directly bound by CpxR (Gal-Mor and Segal, 2003a). Similar to what was observed for the $P_{lpg1441\text{-}cpxA}$ region, band migration gradually increased and reached a maximum with 24.6 μM CpxR (Figure 3.4). This suggests that CpxR is able to bind with similar affinity to a motif with four mismatches as a region with two mismatches. Taken together, the *lpg1441-cpxA* operon appears to be autoregulated by CpxRA through the direct interaction of CpxR with the $P_{lpg1441\text{-}cpxA}$ regulatory region.

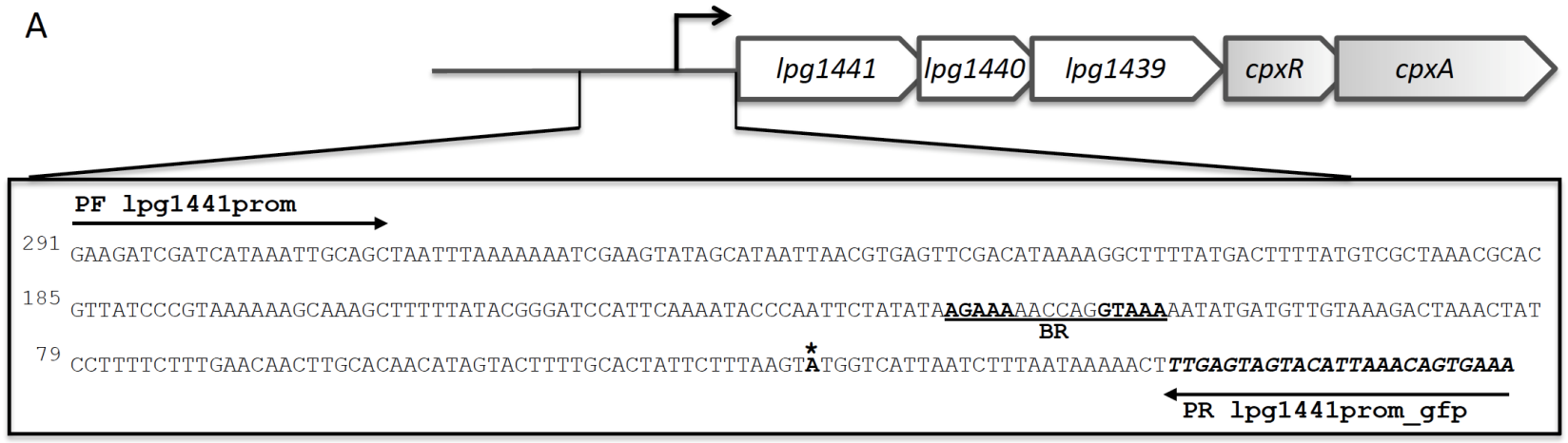
A
lpg1441
lpg1440
lpg1439
cpxR
cpxA
PF lpg1441prom
291 GAAGATCGATCATAAATTGCAGCTAATTTAAAAAAATCGAAGTATAGCATAATTAACGTGAGTTCGACATAAAAGGCTTTTATGACTTTTATGTCGCTAAACGCAC
185 GTTATCCCGTAAAAAAGCAAAGCTTTTTATACGGGATCCATTCAAAATACCCAATTCTATATAAGAAAAACCAGGTAAAAATATGATGTTGTAAAGACTAAACTAT
BR
79 CCTTTTCTTTGAACAACTTGCACAACATAGTACTTTTGCACTATTCTTTAAGTATGGTCATTAATCTTTAATAAAAACTTTGAGTAGTACATTAAACAGTGAAA
PR lpg1441prom_gfp

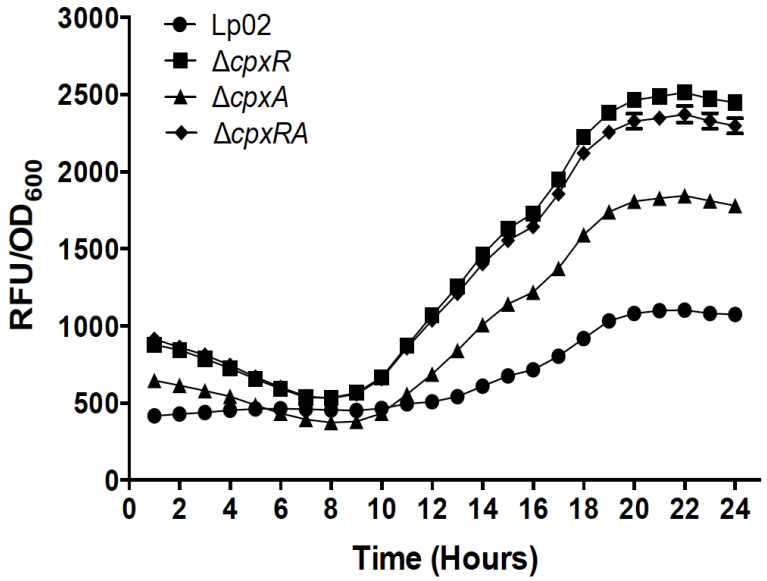
B
Lp02
ΔcpxR
ΔcpxA
ΔcpxRA
RFU/OD600
3000
2500
2000
1500
1000
500
0
0 2 4 6 8 10 12 14 16 18 20 22 24
Time (Hours)

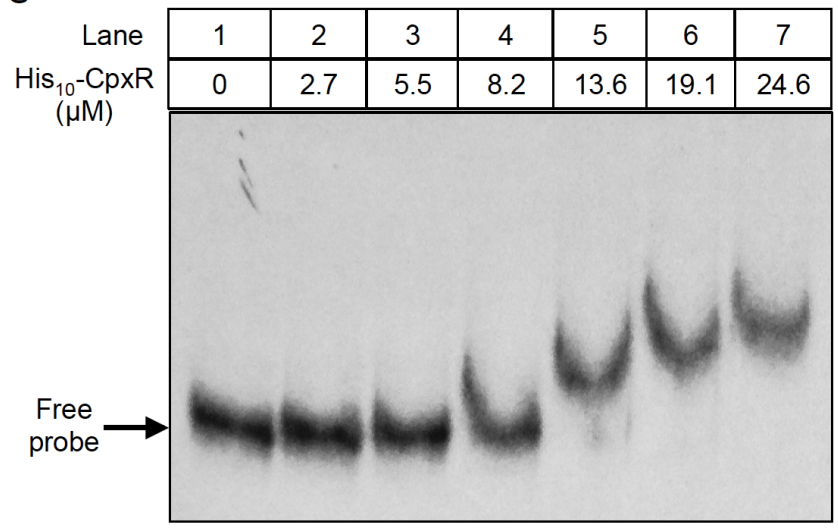
C
Lane 1 2 3 4 5 6 7
His10-CpxR (μM) 0 2.7 5.5 8.2 13.6 19.1 24.6
Free probe

Figure 3.3 CpxRA two-component system exhibits both positive and negative autoregulatory control, with CpxR directly interacting with the $P_{lpg1441\text{-}cpxA}$ region A) Schematic diagram depicting the promoter region driving expression of the *lpg1441-cpxA* operon. Identified are the transcriptional start site (asterisk and boldface font) determined by Sahr *et al.* (2012), a potential CpxR binding region (BR) underlined with binding motif in boldface font and the *lpg1441* coding sequence in italicized boldface font. Nucleotide numbering corresponds to the distance from the translational start site. Arrows represent the primers utilized in generating the promoter region fragment ($P_{lpg1441\text{-}cpxA}$). B) Normalized fluorescence values of *L. pneumophila* Lp02 (JT739) (solid circle), Δ*cpxR* (JT740) (solid square), Δ*cpxA* (JT741) (solid triangle), and Δ*cpxRA* (JT742) (solid diamond) mutant strains harboring GFP reporter construct pBH6119::$P_{lpg1441\text{-}cpxA}$ (pJT730). Data is representative of one of three independent experiments conducted in triplicate. Error bars represent ± standard errors of the means (SEM) of three technical replicates. C) EMSA performed with purified recombinant CpxR and radiolabeled $P_{lpg1441\text{-}cpxA}$ region. Amount of His_{10}-CpxR included in each binding reaction is indicated above each lane.

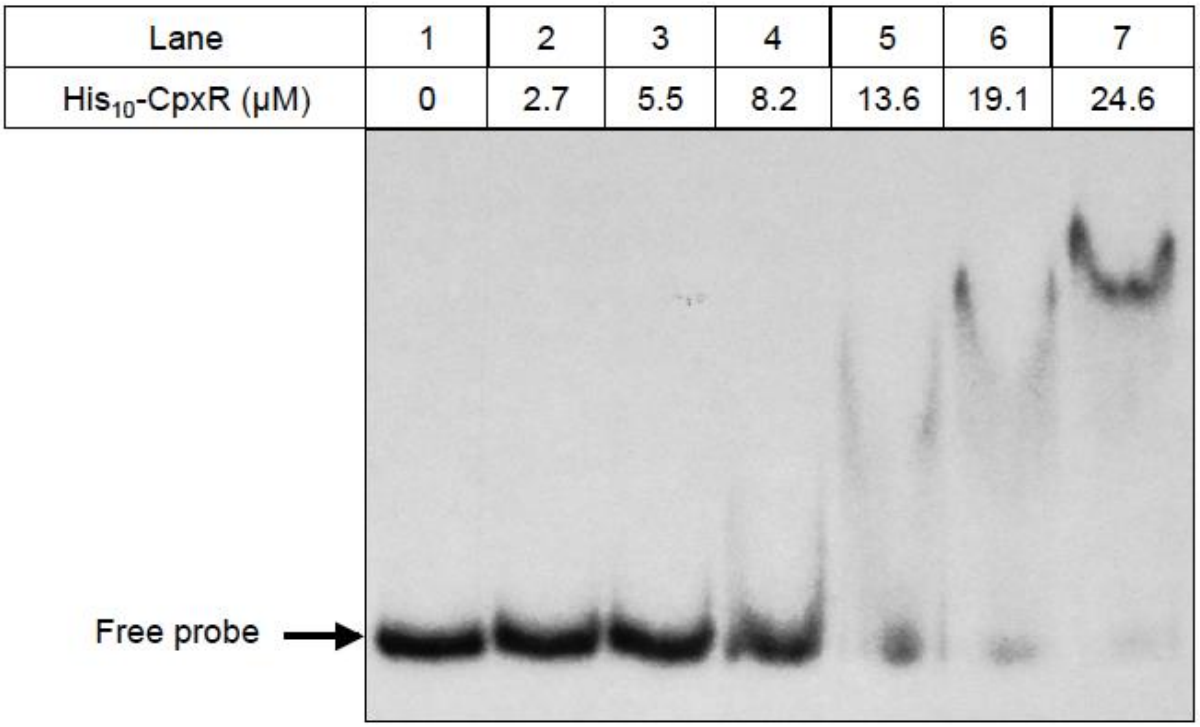

Figure 3.4 CpxR directly binds the *icmR* promoter region containing a CpxR binding site. EMSA conducted with purified recombinant CpxR and radiolabeled P_{icmR} region. Amount of His_{10}-CpxR included in each binding reaction is indicated above each lane.

3.3.4 Elevated CpxR levels occur in post-exponential growth phase

To correlate $P_{lpg1441\text{-}cpxA}$ activities with protein levels, immunoblot assays were performed with normalized parental Lp02 cellular protein extracts from early exponential (EE), exponential (E), and post-exponential (PE) growth phases (Figure 3.5). CpxR is detected throughout the progressive growth phases and appears to reach maximal protein levels in the post-exponential phase (Figure 3.5A). Densitometry analyses of the CpxR immunoblot bands, when normalized to isocitrate dehydrogenase (ICDH) immunoblots, quantified CpxR to be 5.5-fold more in the PE growth phase than the EE growth phase (Figure 3.5B). Thus, these results indicate that a maximal level of CpxR is achieved during PE growth phase, corroborating $P_{lpg1441\text{-}cpxA}$ activity levels observed with GFP reporter assays (Figure 3.3B).

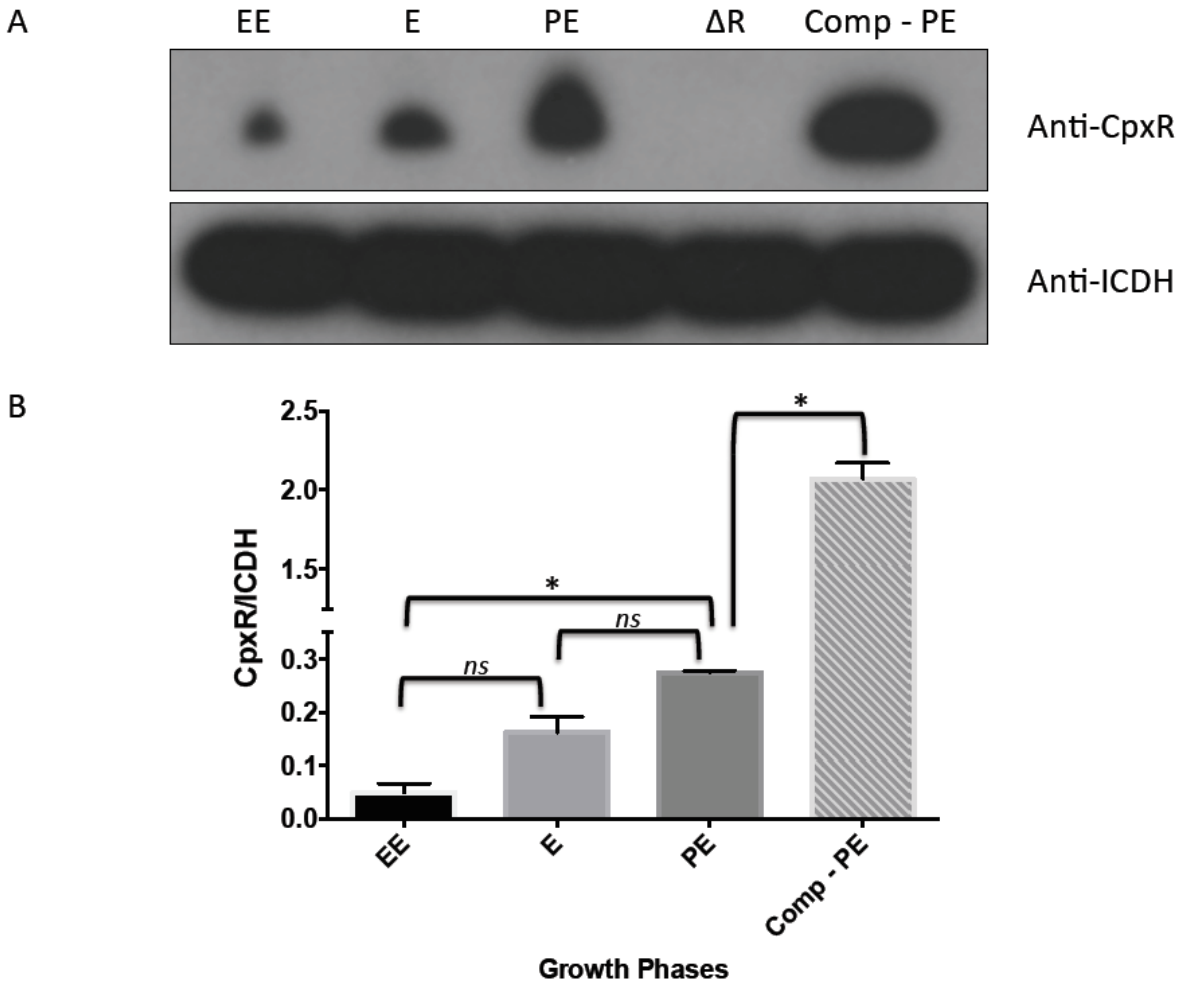

Figure 3.5 CpxR is maximally expressed in the post-exponential growth phase.

A) Immunoblot detection of CpxR in early exponential (EE), exponential (E) and post-exponential (PE) growth phases of *L. pneumophila* Lp02 harboring pBH6119 (CP126). The Δ*cpxR* mutant (ΔR) (JT390) harboring pBH6119 is included as a negative control. The Δ*cpxR* mutant strain harboring pJT731 demonstrates *in trans* complementation of CpxR in post-exponential growth phase (Comp-PE) (JT737). Detection of isocitrate dehydrogenase (ICDH) was included as an internal loading control. Data is representative of one of two independent experiments. B) Quantitative densitometry of CpxR protein levels seen in panel A. Plotted are the means of CpxR/ICDH ratios obtained for each growth phase with error bars representing ±

standard errors of the means (SEM) of two independent experiments. A 4-fold dilution of the Comp-PE sample was incorporated when plotting the densitometric value. Asterisk indicates statistical difference ($P < 0.05$) of CpxR protein levels by Student's *t*-test with Welch's correction. *ns*, no significance.

3.3.5 The CpxRA regulon

CpxR has been previously identified to regulate four Dot/Icm system components (*icmR*, *icmV*, *imcW*, and *lvgA*) as well as 11 effector proteins; however, the global regulatory role of the CpxRA system has not been examined (Gal-Mor and Segal, 2003a; Altman and Segal, 2008). To address this, DNA microarray analysis was employed to identify genome-wide direct and indirect regulatory targets of the CpxRA system using cDNA generated from total RNA isolated from Δ*cpxRA* and parental Lp02 grown to E or PE phases in broth. When compared to Lp02 transcriptome levels, 458 and 360 genes were determined to be differentially regulated in the Δ*cpxRA* mutant strain during E and PE growth phases, respectively. To validate the microarray analysis, gene expression profiles of eight selected genes during E and PE phases were assessed by qRT-PCR analysis and correlated to the transcriptome data producing a correlation coefficient of 0.88 (Figure 3.6).

In both E and PE growth phases, a large number of genes were found to be downregulated. In the E growth phase, 421 genes and nine small regulatory RNAs (sRNAs) were downregulated whereas 335 genes and seven sRNAs were downregulated in the PE growth phase [Table S1, available in the on-line version of (Tanner *et al.*, 2016)]. Conversely, only a small number of genes were upregulated with 27 genes in E growth phase and 17 genes in the PE growth phase along with one sRNA were found to be upregulated in each growth phase [Table S1, available in the on-line version of (Tanner *et al.*, 2016)]. Thus, these results indicate that the CpxRA system appears to have an overall positive regulatory effect on global gene expression.

Differentially regulated genes included genes encoding products involved in amino acid, carbohydrate, lipid and energy metabolism, as well as transport functions and protein secretion [Table S1, available in the on-line version of (Tanner *et al.*, 2016)]. Additionally, several genes

related to virulence along with genes encoding effector proteins were also identified [Table S1, available in the on-line version of (Tanner *et al.*, 2016)]. Some of these genes have been previously characterized as members of the CpxR regulon, such as *icmR*, *icmV*, *icmW*, *lvgA*, l*egA10*, *legA11*, *cegC4*, *sidM/drrA*, *ceg18*, and *cegC3* (Table 3.3). Each of these regulon members demonstrated similar up or downregulation in the absence of CpxRA as previously described except for *ceg18* and *cegC3* which displayed strong down and upregulation, respectively (Table 3.3) (Gal-Mor and Segal, 2003a; Altman and Segal, 2008). Furthermore, *dotA* expression was found to be downregulated in E growth phase which is in agreement with the findings of Vincent *et al.* (2006a) in that DotA protein levels were reduced more so during E growth phase in a *cpxR* mutant strain. A group of 23 genes encoding effectors were identified to be differentially regulated during the E and PE growth phases, which have not been previously characterized to be regulated by the CpxRA system (Table 3.3). Of the 23 genes, 8 were determined to be upregulated in the Δ*cpxRA* mutant strain correlating with previous findings that CpxR is an activator as well as a repressor of effector expression (Altman and Segal, 2008).

Interestingly, a gene encoding the chitinase *chiA*, was found to be severely downregulated in both the E (-50-fold) and PE (-100-fold) growth phases in the Δ*cpxRA* strain [Table S1, available in the on-line version of (Tanner *et al.*, 2016) and Table 3.4]. ChiA has been shown to be an excreted substrate of the Type II secretion system (DebRoy *et al.*, 2006) prompting further investigation and identification of other substrates found to be dependent on the Type II secretion system. Of the 26 genes encoding substrates identified elsewhere to be translocated by the Type II secretion system, the expression of 14 genes were found to be downregulated in either the E and/or PE growth phases in the Δ*cpxRA* mutant strain (Table 3.4) (DebRoy *et al.*, 2006; Gomez-Valero *et al.*, 2011; Cianciotto, 2013). Taken together, these

results suggest that the CpxRA system is a major transcriptional regulator of genes encoding substrates that are transported by the Type IV and Type II secretion systems.

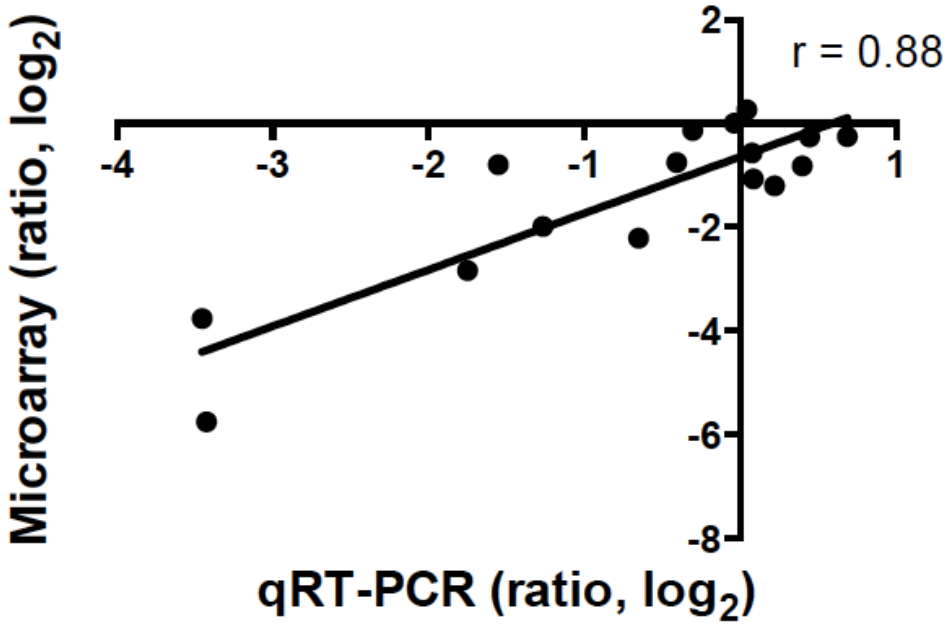

Figure 3.6 Microarray transcriptome analyses of parental Lp02 and isogenic Δ*cpxRA* correlates with qPCR of select genes. Validation of the microarray data was performed by qPCR using eight selected genes (*ihf α*, *ihf β*, *rsmY*, *rsmZ*, *icmR*, *oxyR*, *rpoS*, and *htpA*). Microarray data was plotted against qRT-PCR data and Pearson correlation coefficient ("r") calculated.

Table 3.3. Virulence associated genes with significant expression (>2-fold) changes in the Δ*cpxRA* mutant strain in comparison to the parental Lp02 strain.

Gene[a]	Fold Change (E)	Fold Change (PE)	Gene Product; Comments
lpg0038	2.1	-	LegA10; Dot/Icm effector
lpg0045	-3.7	-8.9	Putative Dot/Icm effector
lpg0120	-2.8	-8.1	IcmL homologue; Transport and binding, Toxin production / other pathogen functions, Protein fate / hydrolases / secretion
lpg0191	-3.9	-	Ceg5; Dot/Icm effector
lpg0294	-13.8	-16.6	Putative Dot/Icm effector
lpg0436	2.2	-	LegA11; Dot/Icm effector
lpg0443	-	-7.1	IcmR; Component of Dot/Icm secretion system
lpg0525	-6.9	-26.8	LvgA; Component of Dot/Icm secretion system
lpg0537	-4.8	-17.9	LetE (transmission trait enhancer); Toxin production / other pathogen functions,
lpg0693	-3.0	-	LigA (*L. pneumophila* infectivity gene A); Toxin production / other pathogen
lpg0708	-2.2	-	IcmL homologue; Toxin production / other pathogen functions, Protein fate /
lpg0898	-5.4	-22.1	Ceg18; Dot/Icm effector
lpg1101	-3.0	-	Lem4; Dot/Icm effector
lpg1144	287.7	159.9	CegC3; Dot/Icm effector
lpg1145	-	-5.1	Lem7; Dot/Icm effector
lpg1273	-3.1	-	Putative Dot/Icm effector
lpg1336	4.8	-	EnhA (enhanced entry protein A); Toxin production/other pathogen functions
lpg1517	-4.7	-	LssD (Component of Type I secretion system); Toxin production / other pathogen functions, Protein fate / hydrolases / secretion
lpg1851	-2.8	-3.5	Lem14; Dot/Icm effector
lpg1872	-2.2	-3.3	LepA; Dot/Icm effector

lpg1884	-9.7	-11.2	LegC2/YlfB; Dot/Icm effector
lpg1947	21.7	-	Lem16; Dot/Icm effector
lpg1958	-	2.1	LegL5; Putative Dot/Icm effector
lpg1962	-2.8	-2.6	LirB; Dot/Icm effector
lpg1969	11.4	3.4	PieE/Lem18; Putative Dot/Icm effector
lpg1972	2.0	-	PieF; Putative Dot/Icm effector
lpg2155	-	2.3	SidJ; Dot/Icm effector
lpg2200	-3.7	-	CegC4; Dot/Icm effector
lpg2298	-3.0	-	LegC7/YlfA; Dot/Icm effector
lpg2322	3.7	-	LegA5; Dot/Icm effector
lpg2327	14.2	22.1	Putative Dot/Icm effector
lpg2328	-4.8	-6.7	Lem22; Dot/Icm effector
lpg2464	-	-21.8	SidM/DrrA; Dot/Icm effector
lpg2529	8.7	4.3	Lem27; Putative Dot/Icm effector
lpg2639	-	-4.7	EnhC (Enhanced entry protein); Toxin production/other pathogen functions
lpg2640	-	-5.1	EnhB (Enhanced entry protein); Toxin production/other pathogen functions
lpg2686	-12.3	-	DotA; Component of Dot/Icm secretion system
lpg2687	-3.3	-5.4	IcmW; Component of Dot/Icm secretion system
lpg2688	-2.3	-	IcmV; Component of Dot/Icm secretion system
lpg2689	-2.4	-5.8	IcmX; Component of Dot/Icm secretion system
lpg2718	-2.3	-	WipA; Dot/Icm effector
lpg2826	-3.0	-	Ceg34; Dot/Icm effector
lpg2999	-7.3	-	LegP; Dot/Icm effector

[a]Boldface font indicates genes encoding Dot/Icm effectors not previously identified to be regulated by CpxR

Table 3.4. Protein substrates dependent on Type II secretion with significant expression changes in the CpxRA mutant strain.

Gene	Fold Change (E)	Fold Change (PE)	Gene Product; Comments
lpg0189	-14.4	-	Unknown
lpg0422	-20.7	-	GamA; Glucoamylase
lpg0467	-2.4	-	ProA; Zinc metalloprotease
lpg0956	-3.5	-4.9	Unknown
lpg1116	-50.0	-100.2	ChiA; Chitinase
lpg1385	-	-9.5	NttA; Unknown function
lpg1962*	-2.8	-2.6	LirB; putative peptidyl-prolyl cis-trans isomerase
lpg2622	-	-8.0	NttB; Unknown function
lpg2644	-3.6	-	Unknown function; Contains collagen helix repeat
lpg2689*	-2.4	-5.8	IcmX; Unknown function, Component of Dot/Icm secretion system
lpg2814	-2.2	-	LapA; Leucine, phenylalanine, and tyrosine aminopeptidase
lpg2837	-	-7.4	PlaC; Glycerophospholipid:cholesterol acyltransferase
lpg2848	-2.9	-	SrnA; Type 2 ribonuclease
lpg2999*	-7.3	-	LegP; Predicted astacin-like zinc endopeptidase

*Also found to be substrates and/or component of the Dot/Icm Type IV secretion system [IcmX; (Matthews and Roy, 2000), LegP; (Cazalet *et al.*, 2004; de Felipe *et al.*, 2005), LirB; (Zusman *et al.*, 2008)]

3.3.6 Sodium sensitivity and intracellular growth are affected by the CpxRA system

Sodium sensitivity is considered to be a hallmark feature of virulence (Sadosky *et al.*, 1993; Vogel *et al.*, 1996; Byrne and Swanson, 1998). Therefore, gain of sodium resistance often results in loss of virulence. To determine whether deletion of *cpxR* and/or *cpxA* altered sodium sensitivity, parental Lp02 (CP126) and Δ*cpxR* (JT390), Δ*cpxA* (JT531), Δ*cpxRA* (JT547) mutant strains were grown to post-exponential phase, serial diluted, and spotted onto BCYE media containing or lacking 100mM NaCl. The avirulent and sodium resistant Δ*dotA* (JT708) mutant strain was also included as a positive control (Berger and Isberg, 1993; Sadosky *et al.*, 1993; Vogel *et al.*, 1996). In comparison to the parental strain (CP126), the Δ*cpxR* (JT390), Δ*cpxRA* (JT547) and Δ*dotA* (JT708) mutant strains exhibited significant increases in sodium resistance whereas the sodium sensitivity of the Δ*cpxA* (JT531) mutant strain was unchanged (Figure 3.7A). Sodium sensitivity was fully and partially restored to parental levels when *cpxR* (JT737) and *cpxRA* (JT738) were supplied *in trans* under the control of the native $P_{lpg1441\text{-}cpxA}$, respectively (Figure 3.7B). It should be noted that for the sodium resistance assays, the empty vector pBH6119 was electroporated into parental Lp02 and mutant strains to rescue the auxotrophic thymidine phenotype of Lp02 with the intent to correlate results with those of the *in trans* complemented strains containing pJB908-based constructs. Sodium resistance levels of Δ*cpxR* (JT393) and Δ*cpxRA* (JT736) mutant strains harboring the empty vector pJB908 were similar to those of Δ*cpxR* and Δ*cpxRA* mutant strains harboring pBH6119, thereby alleviating any concerns regarding vector-specific bias in sodium resistance (Figure 3.7B). Taken together, these results suggest that the presence of CpxR contributes to the sodium sensitivity in *L. pneumophila*

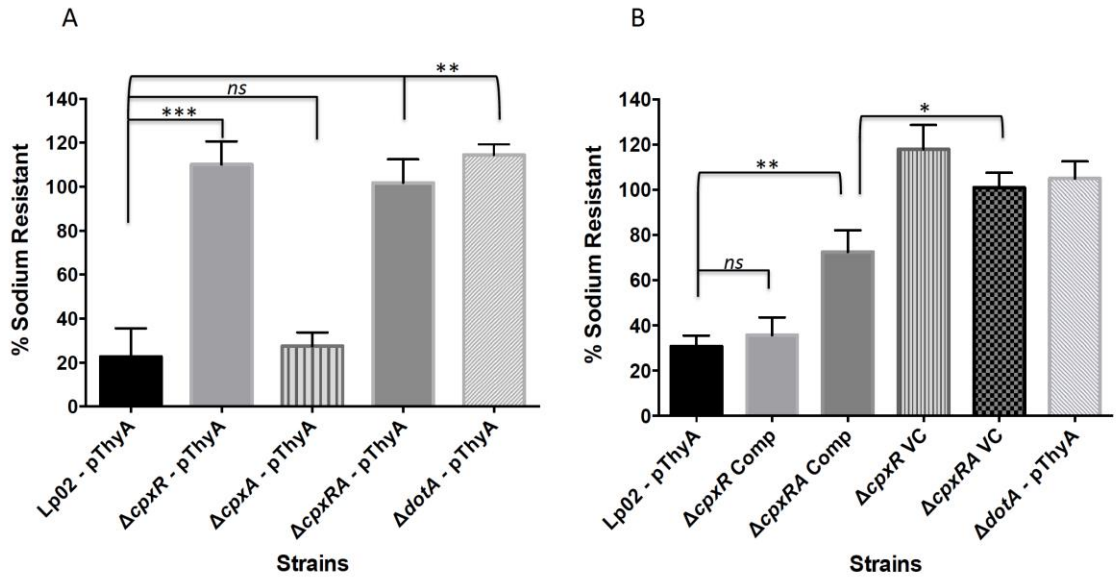

Figure 3.7 Lack of CpxR, but not CpxA, contributes to increased sodium resistance. Sodium resistance (%) of *L. pneumophila* Lp02 (Lp02-pThyA) (CP126), as well as Δ*cpxR* (Δ*cpxR*-pThyA) (JT390), Δ*cpxA* (Δ*cpxA*-pThyA) (JT531), Δ*cpxRA* (Δ*cpxRA*-pThyA) (JT547), and Δ*dotA* (Δ*dotA*-pThyA) (JT708) mutant strains harboring pBH6119 (pThyA) and B) Lp02-pThyA (CP126), Δ*dotA*-pThyA (JT708), and complementation strains Δ*cpxR* (Δ*cpx*R Comp) (JT737), Δ*cpxRA* (Δ*cpxRA* Comp) (JT738) expressing pJT731 and pJT732, respectively, as well as Δ*cpxR* (Δ*cpx*R VC) (JT393) and Δ*cpxRA* (Δ*cpxRA* VC) (JT738) harboring empty vector, pJB908, to serve as a vector control (VC). Data displayed in panels A and B represent means ± standard deviations of three independent experiments conducted in triplicate. Asterisks indicate statistical difference ($p \leq 0.001$ for ***, $p < 0.01$ for **, and $p < 0.05$ for *) of sodium resistance levels by Student's *t*-test with Welch's correction. *ns*, no significance.

To assess whether the sodium resistance/sensitivity phenotypes of the Δ*cpx* mutants also affected virulence, intracellular growth kinetics of the mutant strains were assessed in the U937 human monocytic cell-line and *Acanthamoeba castellanii* protozoa infection models. Similar to parental Lp02, the Δ*cpxR* (JT382), Δ*cpxA* (JT523) and Δ*cpxRA* (JT532) mutant strains replicated successfully in differentiated U937-derived macrophages with a steady increase in bacterial counts over 72 hours, whereas the avirulent Δ*dotA* (Lp03) mutant strain, used as a negative control, was defective for intracellular growth (Figure 3.8A). Surprisingly, the Δ*cpxR* (JT390) and Δ*cpxRA* (JT547) mutant strains were defective for intracellular growth in *A. castellanii* similar in profile to the Δ*dotA* (JT708) mutant strain Figure 3.8B). The parental and mutant strains used in the *A. castellanii* infection assays contained empty vector pBH6119 to rescue the thymidine auxotrophic phenotype of Lp02 in order to circumvent the apparent inability of protozoa importing exogenously supplemented thymidine; a situation not encountered with U937-derived macrophage infection assays (personal communication with Alex Ensminger). It should also be noted that centrifugation was employed to force bacteria-cell contact in the infection protocol with U937-derived macrophages, but not with *A. castellanii* cells. However, inclusion of the centrifugation step in additional infection experiments with *A. castellanii* did not alter the trends of the intracellular growth kinetic data of the Δ*cpx* mutant strains despite the differences in starting MOIs, thereby discounting any experimental bias with respect to forced cell contact (Figures 3.8B and 3.8C).

Intracellular growth kinetics of Δ*cpxR* (JT737) and Δ*cpxRA* (JT738) mutant strains were restored when complemented *in trans* reaching bacterial counts ~10-fold greater than the parental strain (CP126) (Figure 3.8D). This increase in bacterial load is most likely due to the higher protein levels of CpxR, and possibly CpxA, as a consequence of plasmid copy number.

Densitometric analysis of the complemented Δ*cpxR* mutant (JT737) strain supports this hypothesis as protein levels of CpxR was approximately 7.5-fold higher when compared to levels in parental Lp02 in PE growth phase (Figure 3.5B). Additionally, similar growth rates to that of parental Lp02 were observed when *cpx* mutant and complementation strains were grown in BYE broth, demonstrating that the intracellular growth phenotypes presented by Δ*cpxR* (JT390) and Δ*cpxRA* (JT547) strains is specific to protozoan intracellular environments as they do not occur *in vitro* (Figure 3.9). Collectively, these results indicate that CpxR is essential for intracellular growth in *A. castellanii*, but dispensable for growth in U937-derived macrophages.

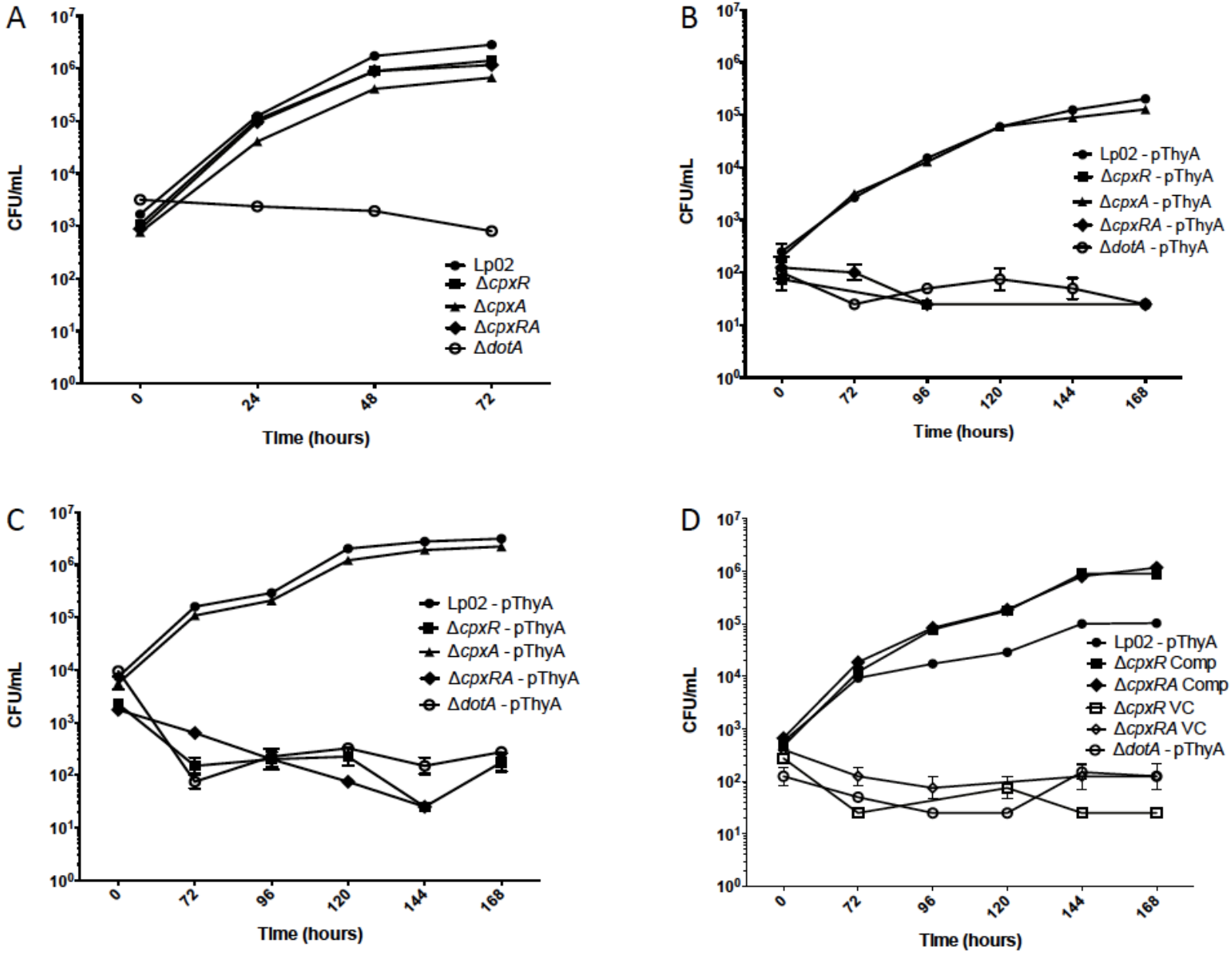
A
CFU/mL
Time (hours)
Lp02
ΔcpxR
ΔcpxA
ΔcpxRA
ΔdotA
B
Lp02 - pThyA
ΔcpxR - pThyA
ΔcpxA - pThyA
ΔcpxRA - pThyA
ΔdotA - pThyA
C
Lp02 - pThyA
ΔcpxR - pThyA
ΔcpxA - pThyA
ΔcpxRA - pThyA
ΔdotA - pThyA
D
Lp02 - pThyA
ΔcpxR Comp
ΔcpxRA Comp
ΔcpxR VC
ΔcpxRA VC
ΔdotA - pThyA

Figure 3.8 CpxRA two-component system is required for *L. pneumophila* intracellular growth in *Acanthamoeba castellanii*, but not in differentiated human U937 macrophages. A) Intracellular growth kinetics of *L. pneumophila* Lp02, Δ*cpxR* (JT382), Δ*cpxA* (JT523), Δ*cpxRA* (JT532) and Δ*dotA* (Lp03) in differentiated U937 cells at 37°C. Intracellular growth kinetics of *L. pneumophila* Lp02 (Lp02-pThyA) (CP126) as well as Δ*cpxR* (Δ*cpxR* - pThyA) (JT390), Δ*cpxA* (Δ*cpxA* - pThyA) (JT531), Δ*cpxRA* (Δ*cpxRA* - pThyA) (JT547), and Δ*dotA* (Δ*dotA*-pThyA) (JT708) mutant strains harboring pBH6119 (pThyA) in B) *A. castellanii* at 25°C and C) *A. castellanii* at 25°C with forced cell contact via a centrifugation step. D) Intracellular growth kinetics of *L. pneumophila* complementation strains Δ*cpxR* (Δ*cpxR* Comp) (JT737) and Δ*cpxRA* (Δ*cpxRA* Comp) (JT738) harboring pJT731 and pJT732, respectively, as well as Δ*cpxR* (Δ*cpxR* VC) (JT393), and Δ*cpxRA* (Δ*cpxRA* VC) (JT736) strains containing empty vector pJB908. Lp02-pThyA and Δ*dotA*-pThyA strains are included as positive and negative control, respectively. Data in panels A, B, C, and D represent means of duplicate infections plated in triplicate and is representative of one of three independent experiments. Errors bars represent ± standard errors of the means (SEM).

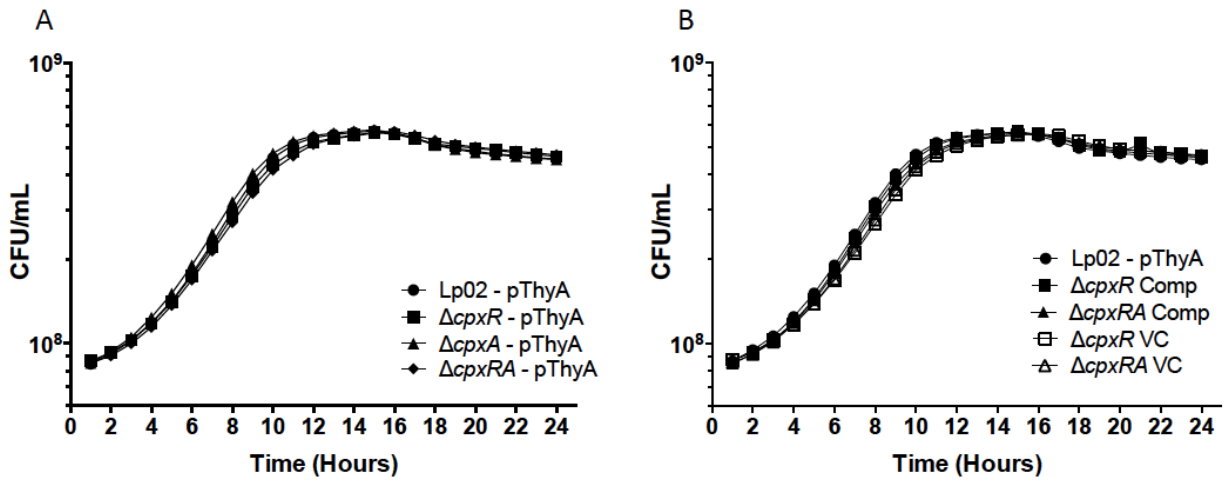

Figure 3.9 Growth of *cpx* in-frame null mutants and complementation strains is not altered when grown in BYE broth. A) *L. pneumophila* Lp02 (Lp02– pThyA) and Δ*cpxR* (Δ*cpxR*-pThyA), Δ*cpxA* (Δ*cpxA* - pThyA), Δ*cpxRA* (Δ*cpxRA* - pThyA) mutant strains harboring pBH6119 (pThyA) grown at 37°C in a 96-well plate over 24 hours. B) *L. pneumophila* complementation strains Δ*cpxR* (Δ*cpxR* Comp), Δ*cpxA* (Δ*cpxA* Comp), Δ*cpxRA* (*Δcpx*RA Comp) harboring pJT731, pJT734, pJT732, respectively, and Δ*cpxR* and Δ*cpxRA* mutant strains harboring pJB908 (Δ*cpxR* VC and Δ*cpxRA* VC) as well as Lp02-pThyA, grown at 37°C in a 96-well plate over 24 hours. Data in panels A and B are representative of three independent experiments conducted in triplicate. Error bars represent ± standard errors of the means (SEM) of three technical replicates.

3.4 DISCUSSION

L. pneumophila traverses extra- and intracellular environments using cellular differentiation as an adaptive mechanism to counter the stresses imparted by varied surroundings. Governing these cellular changes is a global regulatory network that allows for concomitant expression of virulence factors and morphological traits that is coordinated at the genetic level. Contributing to virulence factor expression is the CpxRA two-component system, which has been found to regulate several Dot/Icm components and effectors (Gal-Mor and Segal, 2003a; Vincent *et al.*, 2006a; Altman and Segal, 2008); however, further characterization of this system and its regulon has not been undertaken.

Through examination of the chromosomal arrangement of the genes surrounding *cpxRA* (Figure 3.1A), analysis of the mRNA junctions (Figure 3.1B), and consultation of RNA-seq data procured from the *L. pneumophila* Paris strain (Sahr *et al.*, 2012), we were able to determine that the *cpxRA* system is encoded within a five-gene operon in *L. pneumophila* Lp02 as recently reported for *L. pneumophila* JR32 (Feldheim *et al.*, 2015). This arrangement is quite unique as only one other Gammaproteobacterium, *Haemophilus ducreyi*, shares a similar multi-gene operon arrangement (Labandeira-Rey *et al.*, 2009). All other Gammaproteobacteria examined to date, many of which belong to the *Enterobacteriace* family, have *cpxRA* encoded as an independent two-gene operon with its negative regulatory factor, *cpxP*, divergently transcribed (see Figure 3.10) (Raivio, 2014). The lack of conservation exhibited by the genetic arrangement of *cpxRA* within the *L. pneumophila* genome implies *L. pneumophila* has acquired this system and modified it to satisfy particular regulatory needs (see Figure 3.10).

Chromosomal gene arrangement of *the cpx* locus

L. pneumophila

Philadelphia*

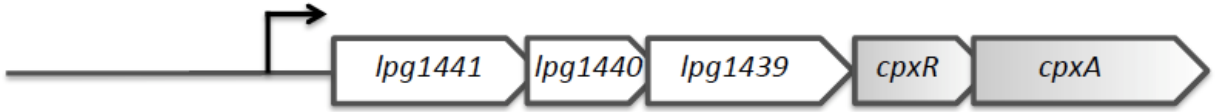

Paris*

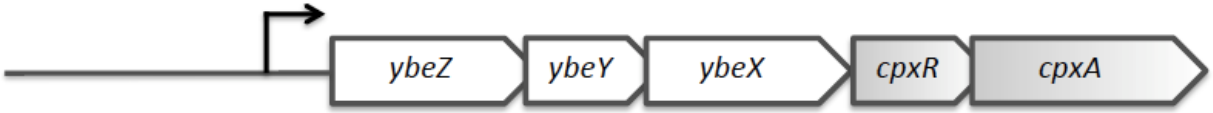

Lens

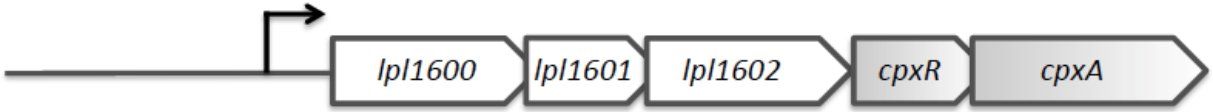

Corby*

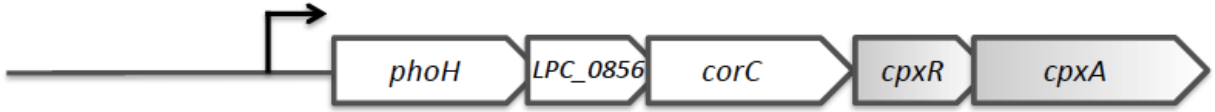

Gammaproteobacteria

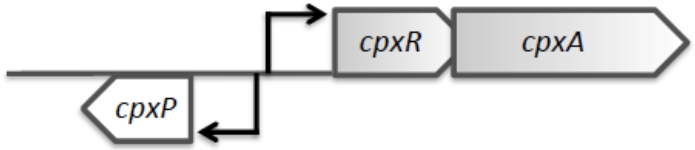

Figure 3.10 Schematic illustrating the unique arrangement of the genetic region that encodes the CpxRA system in *L. pneumophila*. Included are the chromosomal regions of strains Philadelphia, Paris, Lens, and Corby as annotated in the LegioList database (http://genolist.pasteur.fr/LegioList). These are to be compared to the arrangement identified and/or predicted for other Gammaproteobacteria, with the exception of *H. ducreyi* (Labandeira-Rey *et al.*, 2009), and include the following bacteria that have been investigated experimentally; *E. coli* (De Wulf *et al.*, 1999), *Salmonella enterica* serovar Typhimurium (Nakayama *et al.*, 2003), *Shigella sonnei* (Nakayama and Watanabe, 1998), *Yersinia pseudotuberculosis* (Carlsson *et al.*, 2007), *Y. enterolitica* (Heusipp *et al.*, 2004), *Vibrio cholerae* (Slamti and Waldor, 2009), and *Xenorhabdus nematophila* (Herbert *et al.*, 2007). Asterisks (*****) denote arrangements that occur on the negative strand however for simplicity have been drawn in the positive orientation.

A regulatory function that the CpxRA system may satisfy in *L. pneumophila*, in addition to regulating virulence associated genes, is sensing and combating cellular stress. The three genes encoded upstream of *cpxRA*, *lpg1441*/*1440*/*1439*, each have been annotated to be homologous to proteins either connected to or with putative (and to some extent experimentally verified) functional roles related to stress conditions. The *lpg1441* gene encodes a protein product related to the *E. coli* YbeZ, which by bioinformatic analysis has been determined to be a PhoH-like protein (Kazakov *et al.,* 2003). YbeZ contains a putative ATPase domain as well as shows homology to the N-terminal region of superfamily I helicase and is thus predicted to be a metal-dependent RNA helicase (Koonin and Rudd, 1996; Kazakov *et al.*, 2003; Rasouly *et al.*, 2009). The downstream gene *lpg1440* encodes a protein homologous to YbeY of *E. coli*, which has been identified as a RNA endonuclease involved in 16s rRNA maturation as well as translation efficiency and accuracy by degrading defective 70S ribosomes (Jacob *et al.*, 2013). The presence of YbeY has been shown to be essential for the growth of *Vibrio cholerae*, and necessary for thermo-tolerance in *E. coli* and *Yersinia enterolitica* as well as play a key role in an "extreme" SOS response recently elucidated in *E. coli* (Rasouly *et al.*, 2009; Erental *et al.*, 2014; Vercruysse *et al.*, 2014; Leskinen *et al.*, 2015). In addition, interaction network studies have found YbeY and YbeZ to interact indicating they may function together as each have links to RNA modification (Butland *et al.*, 2005; Rasouly *et al.*, 2009). The third gene of this cluster, *lpg1439* (*ybeX*), is predicted to encode a homologue of CorC, which in *Salmonella* Typhimurium has been shown to be involved in the efflux of magnesium as well as cobalt and thus presumed to function during times of metal stress (Gibson *et al.*, 1991). Therefore, based on each of these functional roles as a whole this gene cluster is potentially a stress response operon with the

CpxRA system likely sensing the stress signal as this is a conserved function for this system among other bacteria [reviewed in (Vogt and Raivio, 2012)]

Affirmation of *cpxRA* operon structure provided the rationale to adopt an in-frame null mutant strategy as well as the utilization of overlap extension PCR technique for complementation that allowed for the appropriate presence and/or absence of CpxR and CpxA proteins, as confirmed by immunoblot analysis (Figure 3.2). Moreover, it identified the promoter region driving the expression of the *cpxRA* system and allowed for investigation of autoregulatory control often associated with this system in other organisms. In *E. coli*, it has been well defined that CpxA is bifunctional and acts as a kinase as well as a phosphatase of CpxR, where phosphorylated CpxR (CpxR~P) is considered the active regulatory form (Raivio and Silhavy, 1997). Investigations to identify CpxRA regulon members in *E. coli* identified CpxR~P as a direct activator of the *cpxRA* operon; a scenario presumed to occur in other *Enterobacteriaceae* due to the presence of a consensus CpxR binding site motif in the promoter region upstream of *cpxRA* (De Wulf *et al.*, 1999; Raivio *et al.*, 1999; De Wulf *et al.*, 2000; Slamti and Waldor, 2009). Based on the results of this study we favor a similar model of direct positive autoregulation to also occur in *L. pneumophila* Lp02 for the following reasons. Firstly, the $P_{lpg1441\text{-}cpxA}$ activity increased in the absence of CpxA (Figure 3.3B), which presumably would leave CpxR in a constitutively phosphorylated state due to the lack of CpxA phosphatase activity. This presumption is based on the fact that *L. pneumophila* CpxA contains the key motif, H-E/D-x-x-T/N, identified elsewhere to be necessary for phosphatase activity within the HisKA subfamily of histidine kinases; which includes *E. coli* CpxA, the prototypical EnvZ as well as many other sensor kinases (Figure 3.11) (Dutta *et al.*, 2000; Mascher *et al.*, 2006; Huynh *et al.*, 2010; Willett and Kirby, 2012). A substitution is noted within this critical motif, T245S;

however, mutational analysis of EnvZ elsewhere indicated that full phosphatase activity is retained when the threonine residue is replaced by serine (Figure 3.11) (Dutta *et al.*, 2000). Secondly, CpxR was observed to directly bind to the $P_{lpg1441\text{-}cpxA}$ region that contains a putative CpxR binding motif, albeit with four mismatches to the newly defined consensus, in a similar affinity to that of the well-established regulon member, *icmR* (Figures 3.3A, 3.3C, and 3.4) (Gal-Mor and Segal, 2003a; Feldheim *et al.*, 2015). Lastly, we are inclined to surmise the negative autoregulation of the $P_{lpg1441\text{-}cpxA}$ region observed in the absence of *cpxR* or *cpxRA* is indirect and propose CpxR indirectly regulates *cpxRA* by activating an unidentified negative regulator. This scenario is similar to that in *E. coli* where CpxR activates the expression of the accessory protein CpxP, which in turn negatively regulates *cpxRA* expression in a feedback inhibition mechanism (Raivio *et al.*, 1999). However, this scenario requires further investigation in *L. pneumophila* given that no functional orthologue of CpxP has been identified and the fact that *cpxRA* is uniquely located within a multi-gene operon structure.

Figure 3.11 The phosphatase function of *L. pneumophila* CpxA is orthologously conserved. Alignment of the CpxA protein sequences from *L. pneumophila* Philadelphia -1 (Lpn_CpxA) and *E. coli* (Ecoli_CpxA) was performed using Clustal Omega. Highlighted in gray is the HiskA domain with the phosphatase motif, H-E-x-x-T, bolded and the T245S residue change that occurs in the *L. pneumophila* CpxA is indicated by a black triangle.

Transcriptomic analysis considerably expanded the CpxRA regulon in *L. pneumophila*. Identified regulon members include genes whose products fall within several functional categories; however, in alignment with the goals of this study, those encoding virulence-associated factors were of interest [Table S1, available in the on-line version of (Tanner *et al.*, 2016)]. Genes encoding Dot/Icm effectors, additional to those observed previously to be regulated by CpxR, were ascertained as CpxRA regulon members (Gal-Mor and Segal, 2003a; Altman and Segal, 2008)(Table 3.3). Our data shows that CpxRA regulates these effectors, some in a positive manner and others in a negative manner, in both exponential and post-exponential growth phases (Table 3.3). A minority of these CpxRA regulated effectors have designated roles in the infection process due to functional redundancy. The effectors SidM/DrrA (Machner and Isberg, 2006; Murata *et al.*, 2006), PieE (Mousnier *et al.*, 2014), LegC2 (de Felipe *et al.*, 2008), and LegC7 (de Felipe *et al.*, 2008; O'Brien *et al.*, 2015) have been attributed to modulating host vesicular trafficking whereas SidJ has been determined to be a 'metaeffector' that modulates the activity of another effector (Jeong *et al.*, 2015). Correlating the functional roles identified for some of the CpxRA regulated effectors with the positive and negative regulation elicited by CpxRA on the genes encoding these effectors, reveals *L. pneumophila* likely requires the CpxRA system to achieve timely expression of Dot/Icm effectors necessary for interactions with host cells.

L. pneumophila strains featuring a dysfunctional T2SS are defective for growth in protozoa and survival in tap water, particularly at low temperatures of 25, 17, and 12^{o}C, indicating the importance of the type II secretion system (T2SS) in the planktonic persistence of *L. pneumophila* in aquatic environments (Soderberg *et al.*, 2004; Soderberg *et al.*, 2008; Cianciotto, 2013). The survival of *L. pneumophila* in water appears to be promoted by T2SS-

dependent substrates, which are hyperexpressed at low temperatures (Hindre *et al.*, 2008). Conversely, T2SS mutants are impaired for growth in THP-1- and U937-derived macrophages as well as murine and human primary macrophages (Rossier *et al.*, 2004; McCoy-Simandle *et al.*, 2011; Cianciotto, 2013). The discovery of several Type II secreted substrates as members of the CpxRA regulon strengthens the contributory role of CpxRA to *L. pneumophila* virulence. Type II secretion-dependent substrates PlaC, ProA, SrnA, and NttA have been previously characterized to be required for survival of *L. pneumophila* within amoeba (Rossier *et al.*, 2009; Tyson *et al.*, 2013) whereas ChiA is required for *L. pneumophila* persistence within the lung of the A/J mouse model (DebRoy *et al.*, 2006) (Table 3.4). Albeit the individual effects of these Type II secreted proteins on intracellular survival are modest, there is support that their effects are additive as a double mutant of ProA and SrnA exhibits a greater reduction in survival than the individual mutations alone (Rossier *et al.*, 2009). With CpxRA regulating a multitude of Type II secreted substrates concurrently, its contribution to the survival of *L. pneumophila* in amoeba is more significant than previously thought.

Supporting the view that the CpxRA system has a contributing role in the virulence of *L. pneumophila* are the phenotypes we identified for strains lacking CpxR. The sensitivity to sodium is a characteristic strongly linked with the virulence of *L. pneumophila* (Sadosky *et al.*, 1993; Vogel *et al.*, 1996; Byrne and Swanson, 1998). Absence of CpxR resulted in a gain of sodium resistance and in turn a loss of virulence in *A. castellanii*, but not in human U937 differentiated macrophages (Figures 3.7A, 3.8A, and 3.8B). The loss of virulence was fully rescued in *A. castellanii*, but sodium sensitivity was only partially achieved, by *in trans* complementation of *cpxR* (Figures 3.7 and 3.8D). The partial complementation may be due to the effects of higher levels of sodium encountered *in vitro* in comparison to the *in vivo* assays.

This finding contrasts in part to previous studies on CpxR. While our findings matched those reported elsewhere (Gal-Mor and Segal, 2003a; Vincent *et al.*, 2006a) regarding no significant growth defect for single and combinatorial *cpxRA* strains in HL-60-derived and A/J mouse bone marrow-derived macrophages, our findings differs with respect to the mutant strains assayed in *A. castellanii* in comparison to those reported by Gal-Mor and Segal (2003a). This discrepancy may be due to genotypic differences between the parental *L. pneumophila* strains JR32 utilized by Gal-Mor and Segal (2003a) and Lp02 used in this study. *L. pneumophila* JR32 has recently been characterized to contain a nonsynonymous mutation within the cytoplasmic dimerization and phosphotransfer domain of the sensor kinase PmrB (Rao *et al.*, 2013). A similar mutation occurring within this domain of the orthologue *Pseudomonas aeruginosa* PmrB has been shown to result in a more constitutively active state as the mutation likely disrupts phosphatase activity required to deactivate the response regulator PmrA (Moskowitz *et al.*, 2012). If PmrAB is indeed in a more active state in *L. pneumophila* JR32, then the underlying regulatory effects of its target genes, which also include Dot/Icm effectors and some Type II secreted substrates, could be masking the phenotypes elicited by the lack of functional CpxR (Zusman *et al.*, 2007; Al-Khodor *et al.*, 2009). Alternatively, the lower temperature of 25°C used during *A. castellanii* infection in our study compared to the 37°C used by Gal-Mor and Segal (2003a) may also be contributing to the differences in growth phenotypes. However, modification of the protozoa infection protocol to include competition assays has led the Segal laboratory to report that CpxR, and to a much lesser extent CpxA, was required for intracellular growth in *A. castellanii* protozoa (Feldheim *et al.*, 2015) matching our findings.

The dispensability of *cpxR* for intracellular growth in stabilized macrophage cell-lines, in our study U937-derived macrophages, but necessity for growth in *A. castellanii* is a phenotype

that has been reported in studies elsewhere concerning regulatory factor mutants of *L. pneumophila*. For instance, the Δ*rpoS* mutant strain was able to replicate in HL-60-, THP-1- and U937-derived macrophages, but not in *A. castellanii* and *A. polyphaga* protozoa (Abu-Zant *et al.*, 2006; Bachman and Swanson, 2001; Hales and Shuman, 1999; Hovel-Miner *et al.*, 2009). RpoS, a stationary phase sigma factor, is involved in the regulation of pathways associated with intracellular replication and differentiation into transmissive forms (Bachman and Swanson, 2004; Hovel-Miner *et al.*, 2009; Morash *et al.*, 2009; Pitre *et al.*, 2013). However, lack of RpoS impaired intracellular replication during early stage of infection in murine and human primary macrophages. Likewise for the response regulator LetA; Δ*letA* mutant strain is unable to replicate in *A. castellanii*, but replicate efficiently in HL-60 and inefficiently in murine primary macrophages (Hammer *et al.*, 2002; Lynch *et al.*, 2003; Gal-Mor and Segal, 2003b). A possible explanation for these observations is that these transcription regulators impact the expression of genes that encode products necessary for survival in protozoan hosts and to some extent murine primary macrophages, but dispensable for growth in stabilized macrophage cell-lines; highlighting a potential permissiveness of these cell lines to *L. pneumophila* strains.

In summary, the CpxRA system is required for *L. pneumophila* intracellular survival in protozoa and although dispensable for growth in U937-derived macrophages, it remains to be seen whether this two-component regulatory system is required for successful infection of primary human macrophages. Nevertheless, this study highlights the instrumental role of CpxRA system in the survival of *L. pneumophila* in protozoa.

3.5 ACKNOWLEDGMENTS

We thank M. Swanson (University of Michigan) for her kind gift of pBH6119 and parental Lp02, J. Vogel (Washington University) for his kind gift of pSR47s and pJB908, R. R. Isberg (Tufts University) for his kind gift of Lp03, and A. Sonenshein (Tufts University) for his kind gift of ICDH antibody. This work was supported by University of Manitoba Start-Up funds, Natural Sciences and Engineering Research Council (NSERC) Discovery Grant funds, and Canadian Foundation for Innovation (CFI) Grant funds awarded to A.K.C.B as well as a Natural Sciences and Engineering Research Council (NSERC) Discovery Grant 418289–2012 and John R. Evans Leaders Fund – Funding for research infrastructure from the Canadian Foundation for Innovation awarded to S.F.P. J.R.T was supported a University of Manitoba Faculty of Science Graduate Fellowship and a Manitoba Graduate Scholarship.

Chapter 4. *Legionella pneumophila* OXYR IS A REDUNDANT TRANSCRIPTIONAL REGULATOR THAT CONTRIBUTES TO EXPRESSION CONTROL OF THE TWO-COMPONENT CPXRA SYSTEM

4.1 INTRODUCTION

Legionella pneumophila is a Gram-negative water-borne bacterium that exhibits a complex ecology (Fraser *et al.*, 1977; McDade *et al.*, 1977). It has been isolated from natural waterways that range from lakes and rivers to more extreme environments such as Antarctic freshwater lakes and thermal spring waters (Skaliy and McEachern, 1979; Martinelli *et al.*, 2001; Carvalho *et al.*, 2008; Ghrairi *et al.*, 2013). Fundamental to *L. pneumophila* survival in these aquatic environments is interactions with protozoan species that provide an intracellular replicative niche for the bacterium (Rowbotham, 1980; Fields, 1996). Outside host cells, *L. pneumophila* persists for extended periods of time in either a planktonic state or as a member of complex biofilm communities until a preferred host is encountered (Mampel *et al.*, 2006; Declerck *et al.*, 2007; Stewart *et al.*, 2012; Abdel-Nour *et al.*, 2013). As a consequence of being a resident of freshwater systems, *L. pneumophila* also colonizes man-made water systems many of which are heated providing ideal conditions for *L. pneumophila* proliferation (van Heijnsbergen *et al.*, 2015). Aerosolization of *Legionella*-contaminated water sources allows for airborne distribution of *L. pneumophila* that can lead to infection of immunocompromised individuals that have inadvertently inhaled the bacterium (Fields *et al.*, 2002). Within the human lung, resident alveolar macrophages provide an intracellular replicative niche for *L. pneumophila* with an established infection leading to either the mild flu-like Pontiac fever or a more serious pneumonia Legionnaires' disease (Glick *et al.*, 1978; Horwitz and Silverstein, 1980).

To navigate these harsh and changing environments, *L. pneumophila* possesses a genetic arsenal that encodes factors necessary for its survival as well as regulatory elements needed to regulate these factors. These factors include a group of >300 effector molecules delivered into the host cell cytoplasm by a Dot/Icm Type IVB secretion system that enable *L. pneumophila* to evade the phagosome-lysosome fusion pathway and subsequently establish a replicative niche (Segal *et al.*, 1998; Vogel *et al.*, 1998; Rolando and Buchrieser, 2014). Expression of the Dot/Icm system and associated effectors is under the control of several regulatory factors that include LetAS, PmrAB, CpxRA, and LqsRS two-component systems as well as the stationary phase sigma factor RpoS; each able to positively as well as negatively impact the expression of this virulence system (Gal-Mor and Segal, 2003a; Gal-Mor and Segal, 2003b; Altman and Segal, 2008; Al-Khodor *et al.*, 2009; Hovel-Miner *et al.*, 2009; Zusman *et al.*, 2007; Tanner *et al.*, 2016).

Equally vital to *L. pneumophila* inhabiting extra- and intracellular environments is cellular differentiation [reviewed by (Robertson *et al.*, 2014)]. Upon exhausting a protozoan host, replicating *L. pneumophila* sense a decline in nutrient availability and transition to a hyper infectious and highly resilient mature intracellular form (MIF) henceforth referred to as cyst forms (Garduno *et al.*, 1998; Garduno *et al.*, 2002; Molofsky and Swanson, 2004). Differentiation to cyst forms prepare *L. pneumophila* for release to the nutritionally limited aquatic environment and enables the transmission of the bacterium to a new host cell by expressing factors for motility, virulence and stress resistance, as well as exhibiting ultrastructural changes that include multiple membrane laminations and poly-β-hydroxybutyrate inclusions (Pruckler *et al.*, 1995; Faulkner and Garduno, 2002; Garduno *et al.*, 2002). Regulatory factors shown to be required for *L. pneumophila* differentiation to cyst forms are RpoS, the

LetAS system and the global regulator Integration Host Factor (IHF) (Faulkner *et al.*, 2008; Morash *et al.*, 2009).

Central to coordinating post-exponential *L. pneumophila* differentiation with virulence factor expression is a regulatory cascade that resembles that of the stringent response in *Escherichia coli* (Magnusson *et al.*, 2005). Nutritional gauging by *L. pneumophila* triggers the production of the alarmone, guanosine tetraphosphate (ppGpp), in response to diminished amino acid and fatty acid levels (Hammer and Swanson, 1999; Zusman *et al.*, 2002; Dalebroux *et al.*, 2009). The LetAS system senses the accumulation of ppGpp and activates the expression of the two small regulatory RNAs, RsmY and RsmZ, to in turn relieve the post-transcriptional repression elicited by the carbon storage regulator, CsrA (Hammer *et al.*, 2002; Rasis and Segal, 2009; Sahr *et al.*, 2009). Sequestration of CsrA allows for the production of motility and virulence determinants associated with cyst differentiation. The additional regulatory influences that elicit control over differentiation (RpoS, IHF, LetAS) and virulence expression (LetAS, PmrAB, CpxRA, LetAS systems and RpoS) as mentioned above, are integrated into this nutritional sensing cascade to achieve a sophisticated level of transcriptional modulation necessary for environmental adaptation.

Evidently *L. pneumophila* utilizes dynamic changes in gene expression to cope with alterations in its aquatic and/or intracellular niche. Nonetheless, the *L. pneumophila* genome encodes over 100 additional transcriptional regulator orthologues, which likely contribute to tolerating the stresses inherent to its lifestyle requiring further functional and mechanistic analyses (Chien *et al.*, 2004). LeBlanc and colleagues (LeBlanc *et al.*, 2008) undertook an initial study on a *L. pneumophila* transcriptional regulator designated OxyR ($OxyR_{Lp}$) encoded by *lpg1815* and orthologous to other well characterized OxyR regulators identified in several Gram

negative bacteria. Efforts by LeBlanc *et al.* (2008) to delete the *oxyR*$_{Lp}$ coding sequence were unsuccessful, leading to the hypothesis that OxyR$_{Lp}$ is essential and consequently limited investigations to *in vitro* and *in silico* analysis. DNA binding interactions as well ectopic transcription assays conducted in *E. coli* identified OxyR$_{Lp}$ to negatively regulate the expression of *ahpC2D*, encoding the peroxide-scavenging enzymes alkylhydroperoxidase C and D, respectively (LeBlanc *et al.*, 2008). Interestingly, exposure of OxyR$_{Lp}$ to hydrogen peroxide stress (H_2O_2), did not incur changes in promoter binding or transcriptional control indicating a fundamental difference between the OxyR$_{Lp}$ and the well-studied *E. coli* OxyR (OxyR$_{Ec}$). In *E. coli*, conformational changes occur in OxyR in response to oxidative stress. Under oxidizing conditions, a reversible disulfide bond is formed between two conserved cysteine residues locking OxyR$_{Ec}$ in a conformation that alters its interaction with target promoters to elicit transcriptional changes (Toledano *et al.*, 1994; Lee *et al.*, 2004). Alignment of OxyR$_{Lp}$ and OxyR$_{Ec}$ amino acid sequences revealed that OxyR$_{Lp}$ contains amino acid substitutions that have been experimentally proven with OxyR$_{Ec}$ elsewhere to result in a loss of redox mediated structural changes (Choi *et al.*, 2001; LeBlanc *et al.*, 2008); Thus, it was concluded that OxyR$_{Lp}$ has not retained the ability to respond accordingly to oxidative changes; however, OxyR$_{Lp}$ could still influence the expression of genes associated with post-exponential traits including those related to the oxidative stress response.

In this study, we undertook a multi-faceted approach to explore the contributions of OxyR$_{Lp}$ to *L. pneumophila* survival and to provide new insights into the regulatory interactions of OxyR$_{Lp}$. We firstly established *oxyR*$_{Lp}$ as a non-essential gene through the successful generation of an in-frame null mutant of *oxyR*$_{Lp}$ in *L. pneumophila*, as well as determined OxyR$_{Lp}$ protein levels remain stable throughout the progressive growth phases indicating

constitutive expression rather than cell cycle dependency. Growth of the Δ*oxyR*$_{Lp}$ mutant strain was unaffected *in vitro* and *in vivo* when examined in the hosts *Acanthamoeba castellanii* and U937-derived macrophages. Interestingly, overexpression of OxyR$_{Lp}$ reduced intracellular growth in *A. castellanii,* but not in culture or U937 cells. Regulatory investigations revealed the CpxRA system to potentially regulate *oxyR*$_{Lp}$ expression as CpxR directly bound a region of the *oxyR*$_{Lp}$ promoter however; *oxyR*$_{Lp}$ promoter activity was unaffected in *cpx* mutant strain backgrounds. Unexpectedly, we identified OxyR$_{Lp}$ to negatively regulate the expression of the *cpxRA* system and consequently effect the expression of CpxR regulated genes, revealing a potential complex regulatory loop between OxyR and the CpxRA system. Collectively, our findings confirm *oxyR* as a transcriptional regulator in *L. pneumophila* but found this role to be non-essential to the intracellular survival of *L. pneumophila,* indicating *oxyR* maybe functionally redundant.

4.2 SPECIFIC EXPERIMENTAL PROCEDURES AND MODIFICATIONS

4.2.1 Bacterial strains and plasmids

Bacterial strains and plasmids as well as oligionucleotides used in the studies described in this chapter are listed in Table 4.1 and Table 4.2, respectively.

4.2.2 Construction of in-frame null mutant strains

An unmarked in-frame deletion of *oxyR*$_{Lp}$ (*lpg1815*) was generated using the homologous recombination strategy described in Chapter 2, section 2.6.6. To construct the *oxyR*$_{Lp}$ knockout plasmid, pCJ405, *oxyR*$_{Lp}$ 5' and 3' flanking regions were amplified using the *oxyR*$_{Lp}$ 5' and 3' primer sets (Table 4.1 and Table 4.2), and the resulting fragments cloned into SalI and SacI sites of pSR47s. Construction of pCJ405 was confirmed by sequencing using pSR47s seq primers (Table 4.2) and subsequently electroporated into Lp02 cells.

Combinatorial Δ*cpxR* Δ*oxyR*$_{Lp}$, Δ*cpxA* Δ*oxyR*$_{Lp}$, and Δ*cpxRA* Δ*oxyR*$_{Lp}$ mutant strains were generated using the homologous recombination strategy described in Chapter 2, section 2.6.6 as above. The *oxyR*$_{Lp}$ knockout plasmid, pCJ405, was electroporated into Lp02 Δ*cpxR*, Δ*cpxA*, and Δ*cpxRA* mutant strain backgrounds and subsequent selection, counter-selection, PCR screening procedures as well as DNA sequencing of positive mutant strains using pSR47s seq primers (Table 4.2) were conducted as outlined in Chapter 2, section 2.6.6. An additional Taq polymerase PCR screen of selected mutant strains with *cpxR* and/or *cpxA* int primer sets was conducted to confirm the combinatorial mutants retained the appropriate *cpx* mutant backgrounds (Table 4.2).

Table 4.1. List of bacterial strains and plasmids used in this study.

Strain	Description	Reference or Source
E. coli		
DH5α	F' *endA1 hsdR17(r_k- m_k-) supE44 thi-1 recA1 gyrA (Nal^r) relA1 Δ(lacZYA-argF)U169 deoR*(ϕ80lacΔ(lacZ)M15)	New England Biolabs
DH5αλpir	K-12 F- φ80*lacZ*ΔM15 *endA recAhsdR17 (rm- mK+)supE44 thi-1 gyrA96 relA1 Δ(lacZYA-argF)* U169 *λpir*	M. Swanson (Bryan *et al.*, 2013)
BL21 (DE3)	B F$^-$ *ompT hsdS*(r_B^- m_B^-) *dcm*$^+$ Tet^r *gal* λ(DE3) *endA* Hte [*argU ileY leuW* Cam^r]	Stratagene
CodonPlus^{TM} RIL		
KB178	BL21 (DE3) CodonPlus^{TM} RIL pKB74	(Tanner *et al.*, 2016)
KB302	BL21 (DE3) CodonPlus^{TM} RIL pETLpo*xyR*	(LeBlanc *et al.*, 2008)
L. pneumophila		
Lp02	Str^r, Thy$^-$, HsdR$^-$ derivative of Philadelphia-1 strain; parental strain	M. Swanson (Berger and Isberg, 1993)
Lp03	Lp02 *dotA* mutant	R. Isberg (Berger and Isberg, 1993)
CJ413	Lp02 with in-frame deletion of *oxyR* (Δ*oxyR)*	This study
JT382	Lp02 with in-frame deletion of *cpxR (*Δ*cpxR*)	(Tanner *et al.*, 2016)
JT523	Lp02 with in-frame deletion of *cpxA (*Δ*cpxA*)	(Tanner *et al.*, 2016)
JT532	Lp02 with in-frame deletion of *cpxRA (*Δ*cpxRA*)	(Tanner *et al.*, 2016)
JT709	JT382 with in-frame deletion of $oxyR_{Lp}$ (Δ*cpxR* Δ$oxyR_{Lp}$)	This study
JT710	JT523 with in-frame deletion of $oxyR_{Lp}$ (Δ*cpxA* Δ$oxyR_{Lp}$)	This study
JT711	JT532 with in-frame deletion of $oxyR_{Lp}$ (Δ*cpxRA* Δ$oxyR_{Lp}$)	This study
CJP126	Lp02 pBH6119	(Pitre *et al.*, 2013)
JT708	Lp03 pBH6119	(Tanner *et al.*, 2016)

JT550	Lp02 Δ*oxyR*$_{Lp}$ pBH6119	This study
JT390	Lp02 Δ*cpxR* pBH6119	(Tanner *et al.*, 2016)
JT531	Lp02 Δ*cpxA* pBH6119	(Tanner *et al.*, 2016)
JT547	Lp02 Δ*cpxRA* pBH6119	(Tanner *et al.*, 2016)
JT713	Lp02 Δ*cpxR* Δ*oxyR*$_{Lp}$ pBH6119	This study
JT715	Lp02 Δ*cpxA* Δ*oxyR*$_{Lp}$ pBH6119	This study
JT717	Lp02 Δ*cpxRA* Δ*oxyR*$_{Lp}$ pBH6119	This study
CJ481	Lp02 Δ*oxyR*$_{Lp}$ pJT396 (*oxyR*$_{Lp}$ complementation)	This study
JT397	Lp02 pJT396 (overexpressing OxyR$_{Lp}$)	This study
CJ571	Lp02 Δ*oxyR*$_{Lp}$ pJB908	This study
JT094	Lp02 pJB908	This study
Reporter strains		
JT294	Lp02 pJT277	This study
JT549	Lp02 Δ*oxyR*$_{Lp}$ pJT277	This study
JT387	Lp02 Δ*cpxR* pJT277	This study
JT530	Lp02 Δ*cpxA* pJT277	This study
JT546	Lp02 Δ*cpxRA* pJT277	This study
JT712	Lp02 Δ*cpxR* Δ*oxyR*$_{Lp}$ pJT277	This study
JT714	Lp02 Δ*cpxA* Δ*oxyR*$_{Lp}$ pJT277	This study
JT716	Lp02 Δ*cpxRA* Δ*oxyR*$_{Lp}$ pJT277	This study
JT510	Lp02 pJT502	This study
JT511	Lp02 Δ*cpxR* pJT502	This study
JT529	Lp02 Δ*cpxA* pJT502	This study
JT545	Lp02 Δ*cpxRA* pJT502	This study
JT548	Lp02 Δ*oxyR*$_{Lp}$ pJT502	This study
JT739	Lp02 pJT730	(Tanner *et al.*, 2016)

JT741	Lp02 Δ*cpxA* pJT730	(Tanner *et al.*, 2016)
JT743	Lp02 Δ$oxyR_{Lp}$ pJT730	This study
Plasmids		
pKB74	pET16b::*cpxR*, N-teriminal 10-histidine-tagged CpxR fustion protein expression vector, Amp^r	(Tanner *et al.*, 2016)
pETLpo*xyR*	pET29b::$oxyR_{Lp}$, C-terminal 6-histidine-tagged $OyxR_{Lp}$ fusion protein expression vector, Kan^r	(LeBlanc *et al.*, 2008)
pBH6119	Promoter-less GFP vector; Amp^r, Thy^+	M. Swanson (Hammer *et al.*, 2002)
pSR47s	oriTRP4 oriR6K, Kan^r, *sacB*	J. Vogel (Merriam *et al.*, 1997)
pJB908	RSF1010 cloning vector, Amp^r, Thy^+	J. Vogel (Sexton *et al.*, 2004b)
pCJ405	pSR47s with $oxyR_{Lp}$ flanking regions	This study
pJT396	pJB908:: P_{oxyR}-$oxyR_{Lp}$	This study
pJT277	pBH6119::P_{oxyR}	This study
pJT502	pBH6119::P_{icmR}	This study
pJT730	pBH6119::$P_{lpg1441\text{-}cpxA}$	(Tanner *et al.*, 2016)

Table 4.2. Oligonucleotides used in this study.

Primer name and function	Sequence (5' – 3')[a]	Amplicon size (bp)	Annealing Tm (°C)
Cloning			
PF oxyR 5'null	GCGATAgtcgacCTGGCGATCAGGAATCCAATGA	785	51.5
PR oxyR 5'null	GCGATAggatccTCTCTTAAATTCATAATTTCTC		
PF oxyR 3'null	GCGATAggatccATTAGCATAGAAATTATTATA	793	51.5
PR oxyR 3'null	GCGATAgagctcAGCAAGAAACCCATAAACTAT		
PF oxyR SCRN	CTGCAGATTTGTAATTTATGTCAC	996 (WT)	62.2
PR oxyR SCRN	CTTCATGAAAGCTCATCCAGC	135 ($\Delta oxyR_{Lp}$)	
PF oxyR int	GCTCGTCAGTCGGAAGATCTA	197	66.0
PR oxyR int	GCCATGATAGCAACATCCAGT		
PF oxyRflnk up_seq	GCACCCAGTAAGACCATTGA	2091	66.0
PR oxyRflnk dn_seq	GATGCCCAAAAGGCAATAAC		
PF cpxR int*	GTAGTATGTGTGCATGATGGA	180	62.2
PR cpxR int*	GCGATCGATATCATCACCACG		
PF cpxA int*	TGATGAACTCCCAAGTGATG	240	57.5
PR cpxA int*	ATGCCTAATGAGCGTAAAGG		
PF oxyRprom	GCGATAggatccGCCGATAAATTGTTCAAAGTAG	1134	57.5
PR oxyR comp	GCGATAtctagaCTATGCTAATTTGGATTGAAC		
Promoter amplicons			
PF oxyRprom	GCGATAggatccGCCGATAAATTGTTCAAAGTAG	291	62.2
PR oxyRprom_gfp	GCGATAtctagaCTTTACATCTGCCAGGATGAC		
PF icmRprom	GCGATAggatccGTGTTCCTTGTGTTTGGGTTA	339	62.2
PR icmRprom_gfp	GCGATAtctagaCGTGCACTGTCATCAGTAT		
PF icmRprom_DP	GCGATAggatccTATGACGGATGTTATG	283	57.5
PR icmRprom_DP	GCGATAGgaattcAGTTACATCAGGTTCA		
PF magA int	CTCTATCGCTAACGCACAAG	302	62.2
PR magA int	CAGACGATTTTCCTGAGAGG		
Sequencing			
PF pSR47s seq*	CTGTTGCATGGGCATAAAGTTG	-	-
PR pSR47s seq*	CACAGGAAACAGCTATGACC	-	-
PF EXToxyKOseq	CAAAAAGGCCATTAAACCAG	-	-
PR EXToxyKOseq	ACGTAGACATTGCGATGAGG	-	-

PF oxyRKOseq	TTTGCTATTACATTGGAATCAA	-	-
PR oxyRKOseq	CAACGCTTAAAAGGAAGCAC	-	-
PR GFP seq[**]	GTAAGTAGCATCACCTTCA	-	-
PF pJB908 seq[*]	CTCCGTGATGGAATGACAAC	-	-
PR pJB908 seq[*]	GACCGCTTCTGCGTTCTGA	-	-
PF oxyR seq	GCTCGTCAGTCGGAAGATCTA	-	-
PR oxyR seq	GCCATGATAGCAACATCCAGT	-	-

[a]Restriction sites are lowercase font and underlined

[*]Primer sequences retrieved from Tanner *et al.* (2016)

[**] Primer sequences retrieved from (Pitre *et al.*, 2013)

4.2.3 Complementation and overexpression of $OxyR_{Lp}$

Construction of the complementation vector, pJT396, was achieved by amplifying $oxyR_{Lp}$ with its upstream promoter region using the PF *oxyR*prom/PR *oxyR* comp primer set (Table 4.1 and Table 4.2) and cloning the complementation fragment into BamHI and XbaI sites of pJB908. DNA sequencing with pJB908 seq and *oxyR* seq primers (Table 4.2) confirmed the correct assembly of pJT396. For complementation *in trans*, pJT396 was electroporated into Lp02 Δ$oxyR_{Lp}$ cells and for overexpression (OE) of $OxyR_{Lp}$ pJT396 was electroporated parental Lp02 cells, generating CJ481 and JT397 strains, respectively (Table 4.1).

4.2.4 GFP reporter constructs for GFP assays

$oxyR_{Lp}$ (P_{oxyR}) and *icmR* (P_{icmR}) promoter fragments were generated by Q5 High-Fidelity polymerase PCR amplification using the primer sets PF *oxyR*prom/PR *oxyR*prom_gfp and PF *icmR*prom/PR *icmR*prom_gfp respectively (Table 4.2). Promoter fragments for *oxyR* and *icmR* were then directionally cloned into BamHI and XbaI sites of pBH6119 generating pJT277 and pJT502 *gfp*-transcriptional fusion plasmid constructs, respectively (Table 4.1). DNA sequencing with the *gfp* seq primer was used to verify the correct insertion of the promoter fragments (Table 4.2). The P_{oxyR} (pJT277), P_{icmR} (pJT502), and $P_{lpg1441\text{-}cpxA}$ (pJT730) GFP reporter plasmids were electroporated into the appropriate strain backgrounds to generate the reporter strains listed in Table 4.1. GFP reporter assays were conducted as described in Chapter 2, section 2.8.

4.2.4 $OxyR_{Lp}$ recombinant protein expression and purification

E. coli expression strain KB302 (harboring pET29b::$oxyR_{Lp}$) was induced and purified as described in Chapter 2, section 2.7. The compositions of Buffer A and Buffer B used in the

HiTrap Heparin HP column purification were as follows: Buffer A (20 mM Tris-HCl pH 8.0 and 200 mM KCl) and Buffer B (20 mM Tris-HCl pH 8.0 and 1.5 M KCl). Buffer A and Buffer B were combined to achieve the following increasing concentrations of KCl for application to the column: 200 mM, 300 mM KCl, 400 mM KCl and 500 mM KCl. These buffers also contained a final concentration of 0.5 mM DTT added just prior to buffer being applied to the column.

4.2.5 CpxR recombinant protein expression and purification

CpxR recombinant protein was induced and purified as described Chapter 2, section 2.7, with the details described in Chapter 3 section 3.2.8.

4.2.6 Mass Spectrometry

For mass spectrometry analysis, purified His_{10}-CpxR was diluted to 1 mg/mL in 0.1 M NH_4HCO_3, then treated with 10 mM DTT for 45 min at 60°C. The sample was cooled to room temperature, and incubated for 30 min in the dark with 55 mM iodoacetamide (Shevchenko *et al.*, 1996). After extensive dialysis into 0.1 M NH_4HCO_3 (Orr *et al.*, 1995), protein was digested overnight at 37°C with TPCK-treated trypsin. Equal aliquots of protein and DHB matrix (saturated 2,5-dihydroxybenzoic acid in 50% water, 2% formic acid) were loaded onto a metal target for analysis by MALDI time-of-flight mass spectrometry on a prototype instrument built in the department of Physics and Astronomy at the University of Manitoba (Loboda *et al.*, 2000). Spectra were analyzed using in-house software developed with the instrument. Swiss-Prot (Bairoch *et al.*, 2004) and NCBI databases (Coordinators, 2015) were accessed to check for contaminants using MASCOT (Perkins *et al.*, 1999).

4.2.7 Radiolabelled probes for electrophoretic mobility shift assay (EMSA)

Forward and reverse primers primers (PF *oxyR*prom/PR *oxyR*prom_gfp or PF *icmR*prom_DP/PR *icmR*prom_DP) (Table 4.2) were used in labeling reactions described in Chapter 2, section 2.10 to generate P_{oxyR} or P_{icmR} labeled probes, respectivley. Binding reactions and subsequent gel electrophoresis was conducted as described in Chapter 2, section 2.10.

4.2.8 DNaseI footprinting

The P_{oxyR} and P_{icmR} regions were amplified using PF *oxyR*prom/PR *oxyR*prom_gfp and PF *icmR*prom_DP/PR *icmR*prom_DP primer sets (Table 4.2), respectively. Probe labelling, DNaseI footprinting and corresponding DNA sequence ladder reactions as well as sample processing was performed as described in LeBlanc *et al.* (2008) with the following modifications. The sense strand (BamHI site) was labelled and binding reactions were performed with 60,000 cpm of labelled probe with 6.25 μM (P_{icmR}) and 12.45 μM (P_{oxyR}) of His_{10}-CpxR recombinant protein. The sequencing ladder was prepared using the Sequenase™ Quick Denature Plasmid Sequencing Kit (Affymetrix, Santa Clara, CA). The Glycol/heat denaturation protocol was followed as described by the manufacturer with 1:20 dilution of labelling mix. Footprinting reactions and sequencing ladders were run on 8% sequencing gels at 1500 volts for ~ 2 hours. Gels were then dried and exposed to either a Kodak phosphor screen overnight or Carestream® Kodak® BioMax® MS and MR films (Sigma Aldrich, St. Louis, MO, USA) for 24 hours at -80 °C, depending on resolution observed. Kodak phosphor screen was scanned using Molecular Imager PharosFX™ Plus System (BioRad) and films were developed using SRX-101 medical film processor (Konica).

4.2.9 Intracellular growth kinetic assays in U937- derived macrophages

Differentiated U937 cells were infected with Lp02 (parental), Δ*oxyR*$_{Lp}$, Δ*oxyR*$_{Lp}$ harboring *oxyR*$_{Lp}$ complementation plasmid pJT396 (CJ481), Lp02 (parental) harboring *oxyR*$_{Lp}$ complementation plasmid pJT396 (JT397), Δ*oxyR*$_{Lp}$ containing pJB908 (CJ571) and Δ*dotA* strains as described in Chapter 2, section 2.12.2 (Table 4.1).

4.2.10 Intracellular growth kinetic assays in *Acanthamoeba castellanii*

L. pneumophila Lp02 (parental) and isogenic mutant strains harbored pBH6119 to complement the thymidine auxotrophy of the Lp02 eliminating the need for exogenous thymidine supplementation. *A. castellanii* were infected with the following strains as described in Chapter 2, section 2.12.3: Lp02 (parental) (CP126), Δ*oxyR*$_{Lp}$ (JT550), Δ*oxyR*$_{Lp}$ harboring *oxyR*$_{Lp}$ complementation plasmid pJT396 (CJ481), Lp02 (parental) harboring *oxyR*$_{Lp}$ complementation plasmid pJT396 (JT397), Δ*oxyR*$_{Lp}$ containing pJB908 (CJ571), and Δ*dotA* (JT708) as described in Chapter 2, section 2.12.3 (Table 4.1).

4.3 RESULTS

4.3.1 Cellular levels of $OxyR_{Lp}$ are constant throughout growth phases

In a previous study by LeBlanc *et al.* (2008), efforts to genetically delete $oxyR_{Lp}$ were unsuccessful leading to the conclusion that $oxyR_{Lp}$ is an essential gene in *L. pneumophila*. The mutagenesis strategy utilized by LeBlanc *et al.* (2008) involved allelic replacement with an antibiotic cassette via a counterselectable vector employing nitroreductase (*rdxA*). Several mutants have been successfully generated in previous studies using this method (LeBlanc *et al.*, 2006; Morash *et al.*, 2009); however, the success rate is fairly low and thus, use of a suicide vector may be more effective. To test this, an in-frame null mutant strategy that has efficiently generated single and multi-gene deletion mutants recently in our laboratory as well as in previous studies elsewhere was selected (Vincent and Vogel, 2006; Vincent *et al.*, 2006b; Tanner *et al.*, 2016). This approach employs generating an in-frame knockout fragment via specific primer design and the suicide vector pSR47s, which has *sacB* as the counterselectable marker (Chapter 2, section 2.6.6 for details) (Table 4.1) (Merriam *et al.*, 1997). When applied to the $oxyR_{Lp}$ genetic region within *L. pneumophila* Lp02 (parental), this strategy yielded an isogenic $oxyR_{Lp}$ in-frame null mutant ($\Delta oxyR_{Lp}$) that was confirmed by DNA sequencing as well as immunoblot analysis, where $OxyR_{Lp}$ was not detected in the cellular extracts of the $\Delta oxyR_{Lp}$ (CJ413) strain (Figure 4.1A). Thus, contrary to previous findings $oxyR_{Lp}$ is not essential for *L. pneumophila* survival *in vitro* and is readily mutagenized.

Expression of $oxyR_{Lp}$ has been investigated previously through a GFP transcriptional reporter assay that found the $oxyR_{Lp}$ promoter region (P_{oxyR}) activity was maximal during the post-exponential growth phase, indicating $oxyR_{Lp}$ expression is growth phase dependent *in vitro* (LeBlanc *et al.*, 2008). This finding is further corroborated by two separate transcriptome studies

that compared the gene expression profile of *L. pneumophila* during exponential and post-exponential growth phases when grown in BYE broth, where in both instances *oxyR*$_{Lp}$ was found to be upregulated ~3-fold during the post-exponential growth phase (Bruggemann *et al.*, 2006; Weissenmayer *et al.*, 2011). However, OxyR$_{Lp}$ seems to exhibit regulatory control over two small non-coding RNAs (sRNAs), LprA and LprB, during the exponential growth phase indicating there is a role for OxyR$_{Lp}$ during this growth phase as well (Faucher *et al.*, 2010). Thus, it was of interest to investigate whether the transcriptional changes observed for *oxyR*$_{Lp}$ translate to differing OxyR$_{Lp}$ levels between the growth phases in *L. pneumophila*. To accomplish this, cellular extracts of *L. pneumophila* Lp02 during early exponential (EE), exponential (E), and post-exponential (PE) growth phases were subjected to immunoblot analysis. OxyR$_{Lp}$ was detected throughout each growth phase (Figure 4.1A). Quantification via densitometric analysis showed a slightly higher amount of OxyR$_{Lp}$ in the post-exponential phase however this difference was not statistically significant, and likely not biologically relevant (Figure 4.1B). Taken together, OxyR$_{Lp}$ does not exhibit growth phase dependent changes in cellular levels that coincide with transcriptional changes observed for *oxyR*$_{Lp}$ *in vitro*.

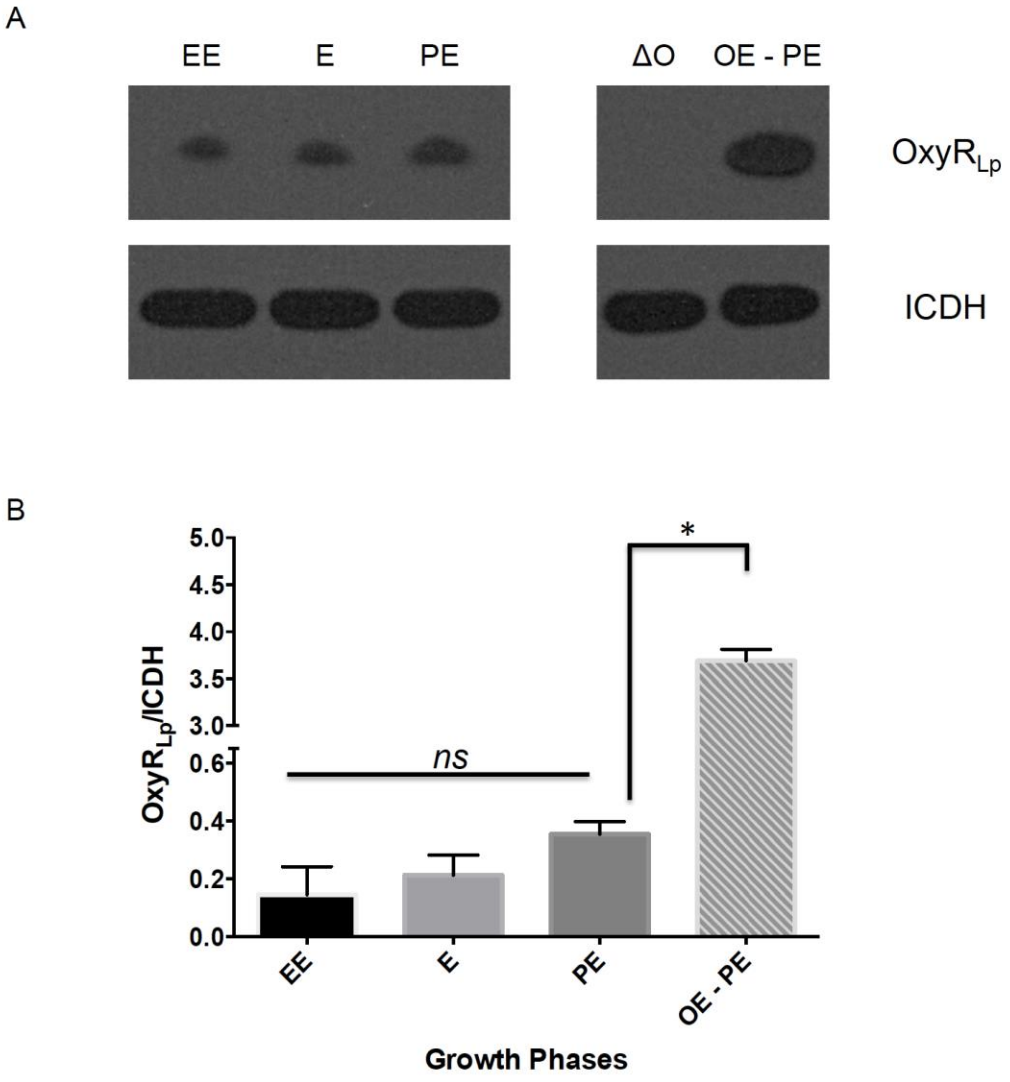

Figure 4.1 OxyR$_{Lp}$ does not exhibit growth phase dependent changes in cellular levels. Immunoblot A) and quantitative densitometry B) of OxyR$_{Lp}$ and isocitrate dehydrogenase (ICDH) in early exponential (EE), exponential (E), and post-exponential (PE) growth phases in *L. pneumophila* Lp02. In panel A) Lp02 harboring the *oxyR$_{Lp}$* complementation construct, pJT396, during post-exponential phase (overexpressing, OE-PE) and Δ*oxyR$_{Lp}$* mutant strain grown to post-exponential phase (ΔO) were also included. Plotted in panel B) are the means of OxyR$_{Lp}$/ICDH ratios obtained for each growth phase. For the OxyR$_{Lp}$ OE strain, the 4-fold

dilution factor of the sample was incorporated into the densitometric value and the $OxyR_{Lp}$/ICDH ratio subsequently determined and plotted. Single asterisk (*) indicates a statistical difference of $p < 0.05$ while *ns* indicates no significant differences in $OxyR_{Lp}$ protein levels by Student's *t*-test with Welch's correction. Error bars represent ± standard errors of the means (SEM) of two independent experiments. Results shown in panel A) represent one of two independent experiments.

4.3.2 $OxyR_{Lp}$ is dispensable for the intracellular growth of *L. pneumophila* in protozoan or macrophage host cells

In response to oxidative stress, $OxyR_{Ec}$ activates genes to counter damage that may occur in the presence of reactive oxygen species (Chiang and Schellhorn, 2012). While $OxyR_{Lp}$ appears to be functionally divergent from the orthologous role as an oxidative stress response regulator, it is possible that $OxyR_{Lp}$ may be required to combat the oxidative burst encountered during the process of infecting host cells (LeBlanc *et al.*, 2006; LeBlanc *et al.*, 2008). Thus, to determine whether $oxyR_{Lp}$ contributes to the intracellular survival of *L. pneumophila*, the intracellular growth kinetics of the Δ$oxyR_{Lp}$ mutant strain were examined in the protozoan infection model *Acanthamoeba castellanii* as well as the U937 human monocytic cell-line. For both parental Lp02 and the Δ$oxyR_{Lp}$ mutant strain, a continuous increase in bacterial counts were observed over the 168 hour infection period in *A. castellanii*, whereas the avirulent Δ*dotA* mutant strain included as a negative control (Segal and Shuman, 1999a), did not exhibit replication (Figure 4.2A). When the Δ$oxyR_{Lp}$ mutant strain was complemented *in trans* with $oxyR_{Lp}$ under the control of its native promoter (Δ$oxyR_{Lp}$ Comp), an increase of ~4.5-fold in bacterial counts was observed in comparison to parental Lp02 (Figure 4.2A). However, Δ$oxyR_{Lp}$ harboring the empty vector (Δ$oxyR_{Lp}$ VC) exhibits a similar increase in counts indicating the elevated counts of the Δ$oxyR_{Lp}$ Comp strain maybe an artifact of the vector backbone used in complementation (Figure 4.2A). Interestingly, when $OxyR_{Lp}$ is overexpressed via parental Lp02 harboring the complementation construct (Lp02 OE), a significant decrease in bacterial counts is observed throughout the infection in comparison to parental Lp02, with Lp02 OE counts being ~ 40-fold less by then end of the infection period (Figure 4.2A). This decrease in bacterial load is likely due to the ~10-fold increase in $OxyR_{Lp}$ levels detected in the cellular extracts of the Lp02 OE

strain when $OxyR_{Lp}$ band intensity was assessed by densitometric analysis (Figure 4.1A and 4.1B). However, this significant growth defect is not observed when the Lp02 OE strain is grown in BYE broth, indicating the impeded growth phenotype is specific to an *in vivo* environment (Figure 4.3).

The growth profiles of Δ$oxyR_{Lp}$, Δ$oxyR_{Lp}$ Comp, and Lp02 OE strains in U937-derived macrophages demonstrated similar increasing bacterial counts over the 72 hour period to that of parental Lp02 (Figure 4.2B). The avirulent Δ*dotA* mutant strain did not exhibit replication as expected and reported elsewhere (Berger and Isberg, 1993). Taken together, these results indicate $oxyR_{Lp}$ is not required for intracellular replication in both U937-derived macrophages and *A. castellanii* protozoa, although elevated $OxyR_{Lp}$ levels appear to impede intracellular replication of *L. pneumophila* in *A. castellanii* protozoa inferring a host-specific role.

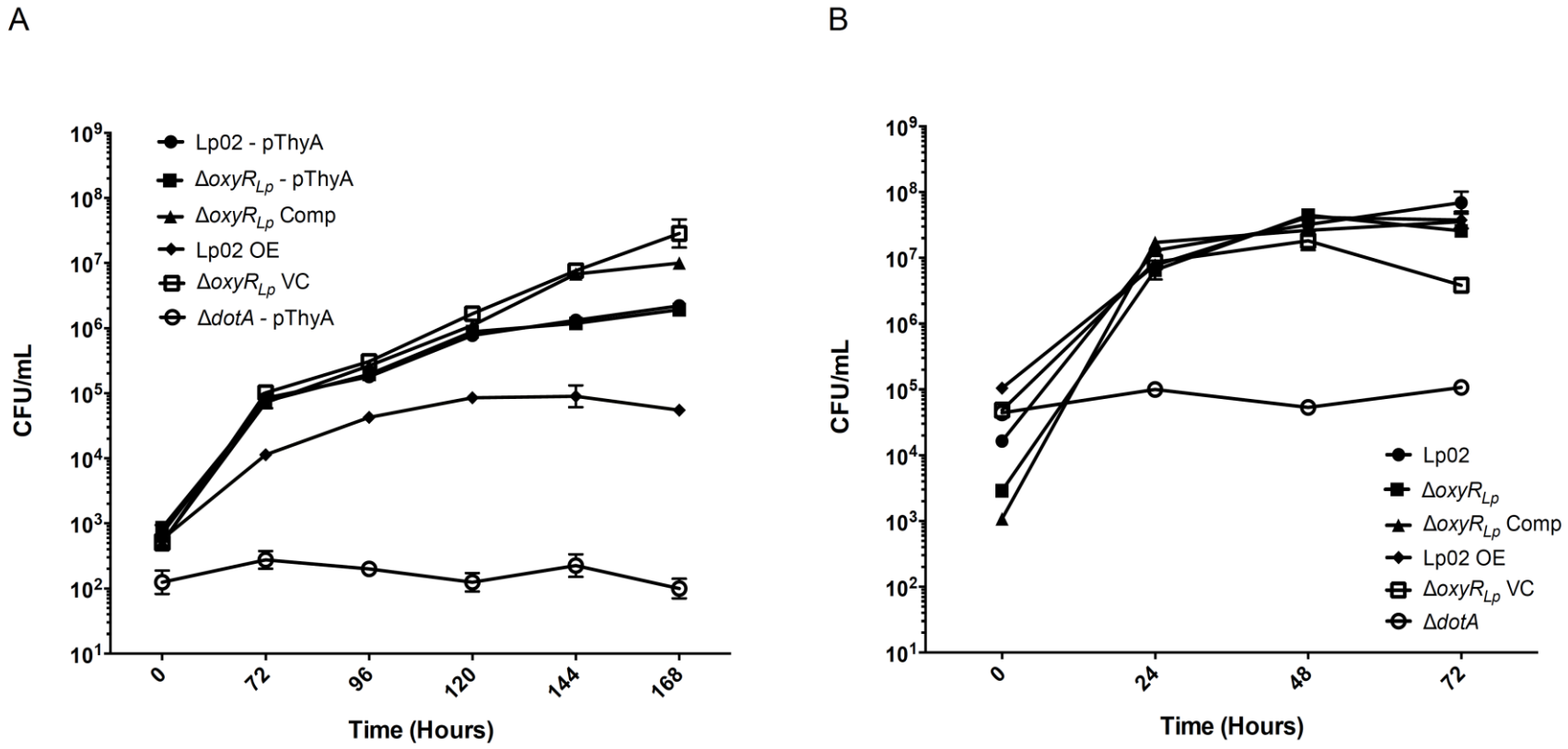

Figure 4.2 OxyR$_{Lp}$ is not required for intracellular growth. Intracellular growth kinetics of *L. pneumophila* Lp02 (solid circles), Δ*oxyR$_{Lp}$* (solid square), Δ*oxyR$_{Lp}$* harboring *oxyR$_{Lp}$* complementation plasmid pJT396 (Δ*oxyR$_{Lp}$* Comp*)* (solid triangle), Lp02 harboring *oxyR$_{Lp}$* complementation plasmid pJT396 (overexpressing OxyR$_{Lp}$, Lp02 OE) (solid diamond), Δ*oxyR$_{Lp}$* containing pJB908 (Vector control, Δ*oxyR$_{Lp}$* VC) (open square), and Δ*dotA* (open circle) in *Acanthamoeba castellanii* A) or U937-derived macrophages B). In

panel A) Lp02 - pThyA, Δ*oxyR*$_{Lp}$ - pThyA, and *ΔdotA* -pThyA strains harbor pBH6119 (pThyA). Infections were conducted at 25°C and 37°C within *A. castellanii* and U937 cells, respectively. Data in panels A) and B) are means of duplicate infections plated in triplicate and represent one of three independent experiments. Errors bars represent ± standard errors of the means (SEM).

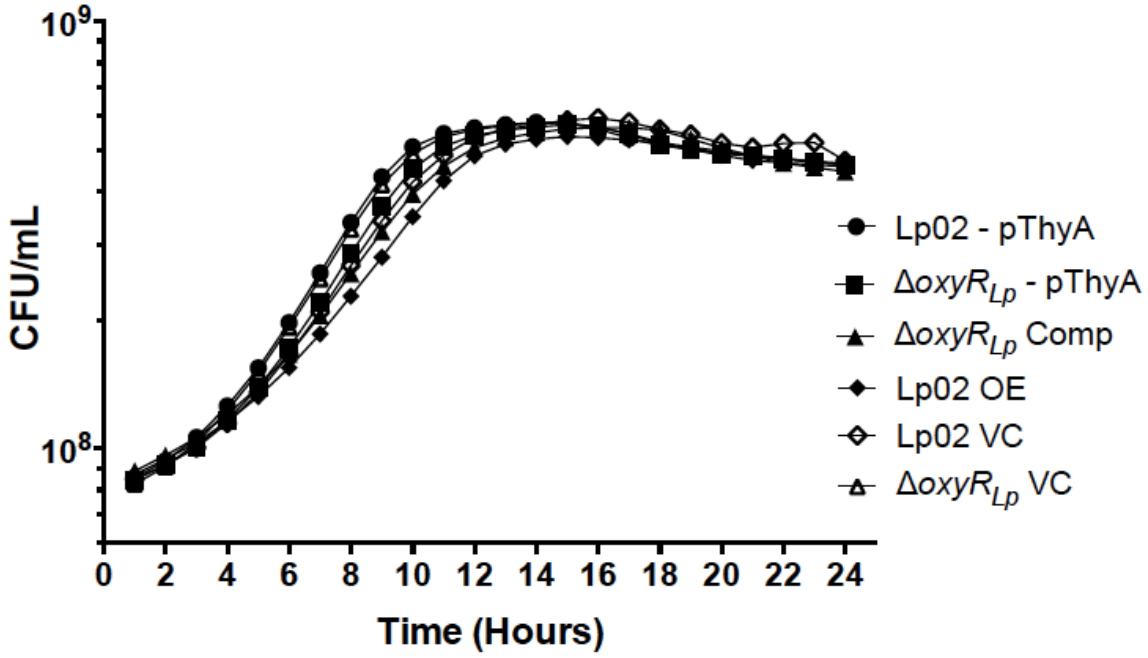

Figure 4.3 Growth profiles of *L. pneumophila* strains in BYE broth is not affected when OxyR$_{Lp}$ is deleted, complemented or overexpressed. Examined were *L. pneumophila* Lp02 (partental) (Lp02 - pThyA), Δ*oxyR*$_{Lp}$ (Δ*oxyR*$_{Lp}$ - pThyA), Δ*oxyR*$_{Lp}$ harboring *oxyR*$_{Lp}$ complementation construct pJT396 (Δ*oxyR*$_{Lp}$ Comp), Lp02 harboring *oxyR*$_{Lp}$ complementation construct pJT396 (Lp02 OE), and Lp02 as well as Δ*oxyR*$_{Lp}$ harboring empty vector pJB908 (Lp02 VC and Δ*oxyR*$_{Lp}$ VC, respectively). Lp02 – pThyA and Δ*oxyR*$_{Lp}$ – pThyA strains harbor pBH6119 (pThyA). Data represents one of three independent experiments conducted in triplicate with error bars representing ± standard errors of the means (SEM) of three technical replicates.

4.3.3 *In vitro* expression of $oxyR_{Lp}$ is not regulated by $OxyR_{Lp}$ and/or the CpxRA two-component system.

Expression of $OxyR_{Ec}$ is negatively autoregulated by direct binding of $OxyR_{Ec}$ to its promoter region (Christman *et al.*, 1989). Conversely, expression of $OxyR_{Lp}$ does not appear to be autoregulated as binding of the $oxyR_{Lp}$ promoter region by $OxyR_{Lp}$ was not observed in EMSA studies conducted by LeBlanc *et al.* (2008). To corroborate the absence of $OxyR_{Lp}$ autoregulation in *L. pneumophila*, GFP reporter assays were employed to determine the activity levels of the $oxyR_{Lp}$ promoter (P_{oxyR}) over time. To accomplish this, a 291 bp fragment of P_{oxyR} was cloned into pBH6119 generating the P_{oxyR}-GFP reporter construct pJT277 and electroporated into parental Lp02 (JT294) and the Δ$oxyR_{Lp}$ (JT549) mutant strain (Table 4.1). In parental Lp02 background, P_{oxyR} activity increases until it reaches ~220 RFU/OD_{600} at seven hours and remains at this level until ~ 11 hours, then begins increasing once again reaching a maximum of ~440 RFU/OD_{600} units at 20 hours (Figure 4.4A). In contrast, P_{oxyR} activity in Δ$oxyR_{Lp}$ strain background does not exhibit an increase and plateau like that observed in Lp02 during the first 11 hours, but rather has minute increases in activity until ~10 hours, reaching ~170 RFU/OD600, at which point the rate of activity increases to meet similar activity levels seen in Lp02 (Figure 4.4A). Even though differences in P_{oxyR} activity profile occur within the first 10 hours between Lp02 and Δ$oxyR_{Lp}$ backgrounds, the differences are not statistically significant when examined by student's t-test and therefore likely not substantial enough to be considered biologically relevant. Thus, these results indicate $oxyR_{Lp}$ expression is not autoregulated, agreeing with the findings of LeBlanc *et al.* (2008).

Sequence analysis of the P_{oxyR} region was conducted in an attempt to identify potential regulatory element(s) that may contribute to the regulation of $oxyR_{Lp}$ expression. One putative

CpxR binding site was identified based on comparison to the GTAAA-N_6-GWAAA consensus sequence identified by Altman and Segal (2008). This site, containing two mismatches to the consensus sequence, is located 156 bp upstream of the OxyR translational start site (Figure 4.4B). CpxR, the response regulator of the CpxRA two-component system, regulates virulence-associated genes as well as those involved in other cellular processes in *L. pneumophila*; however, not all of the regulon members under the direct control of the CpxRA system have been identified (Gal-Mor and Segal, 2003a; Altman and Segal, 2008; Tanner *et al.*, 2016). To ascertain if $oxyR_{Lp}$ is a member of the CpxRA regulon, the P_{oxyR}-GFP reporter construct (pJT277) was electroporated into Δ*cpxR* (JT387), Δ*cpxA* (JT530), and Δ*cpxRA* (JT546) mutant strains to determine if P_{oxyR} activity was impacted by lack of CpxR and/or CpxA (Table 4.1). Interestingly, in each of the Δ*cpxR*, Δ*cpxA*, and Δ*cpxRA* mutant strain backgrounds, P_{oxyR} activity exhibits a delay within the first 9 hours and then increases to reach maximums of ~440, 425, and 470 RFU/OD_{600} units, respectively, at 20 hours; a P_{oxyR} profile almost identical to the profile observed in the Δ$oxyR_{Lp}$ mutant strain background that is also not statistically significantly different when compared to the Lp02 profile (Figure 4.4C and 4.4A). These results suggest the CpxRA system does not regulate $oxyR_{Lp}$ expression; however, with the P_{oxyR} profile being very similar in the Δ$oxyR_{Lp}$ and Δ*cpx* mutant strains it became plausible that perhaps $OxyR_{Lp}$ and CpxR co-regulate $oxyR_{Lp}$ expression.

To assess potential co-regulation of $oxyR_{Lp}$ expression by $OxyR_{Lp}$ and CpxR, an in-frame deletion of $oxyR_{Lp}$ was generated in Δ*cpxR*, Δ*cpxA*, and Δ*cpxRA* mutant strain backgrounds, generating Δ*cpxR* Δ$oxyR_{Lp}$ (JT709), Δ*cpxA* Δ$oxyR_{Lp}$ (JT710), and Δ*cpxRA* Δ$oxyR_{Lp}$ (JT711) combinatorial mutant strains (Table 4.1). The P_{oxyR} activity profiles remained unchanged in the combinatorial mutant strain backgrounds closely resembling the profiles observed in the Δ$oxyR_{Lp}$

and Δ*cpx* mutant strain backgrounds (Figure 4.4D, 4.4B, and 4.4A). Taken together, these results indicate *oxyR*$_{Lp}$ expression is not regulated by OxyR$_{Lp}$ and/or the CpxRA system under the conditions examined.

A

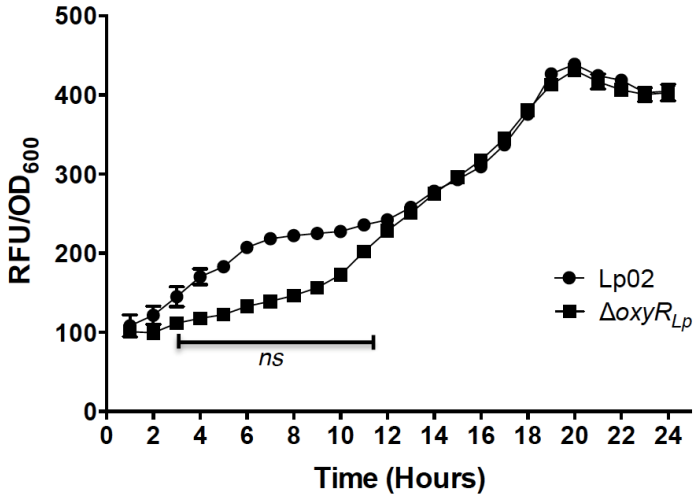
RFU/OD600
Time (Hours)
Lp02
ΔoxyRLp
ns

B

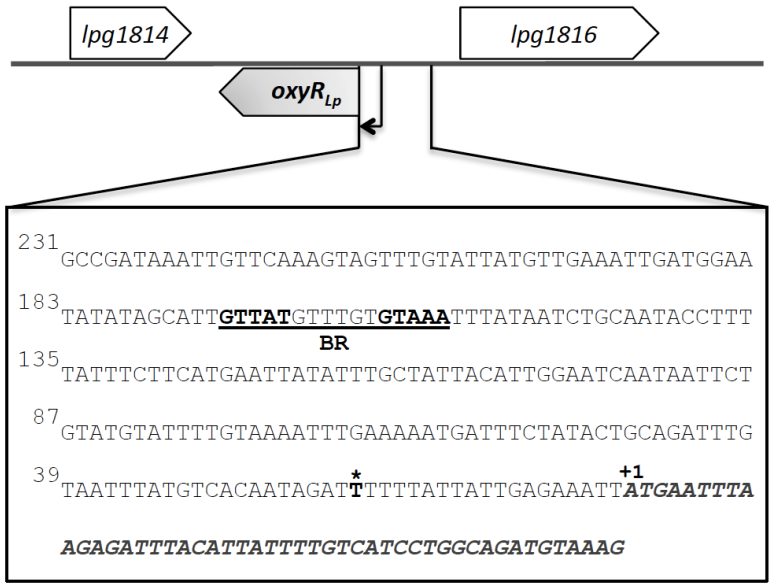
lpg1814
lpg1816
oxyRLp
231 GCCGATAAATTGTTCAAAGTAGTTTGTATTATGTTGAAATTGATGGAA
183 TATATAGCATTGTTATGTTTGTGTAAATTTATAATCTGCAATACCTTT
BR
135 TATTTCTTCATGAATTATATTTGCTATTACATTGGAATCAATAATTCT
87 GTATGTATTTTGTAAAATTTGAAAAATGATTTCTATACTGCAGATTTG
39 TAATTTATGTCACAATAGATTTTTTTATTATTGAGAAATTATGAATTTA
+1
AGAGATTTACATTATTTTGTCATCCTGGCAGATGTAAAG

C

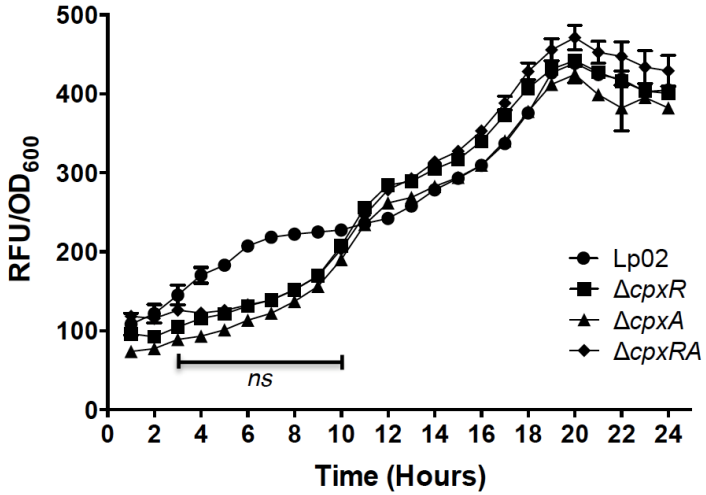
RFU/OD600
Time (Hours)
Lp02
ΔcpxR
ΔcpxA
ΔcpxRA
ns

D

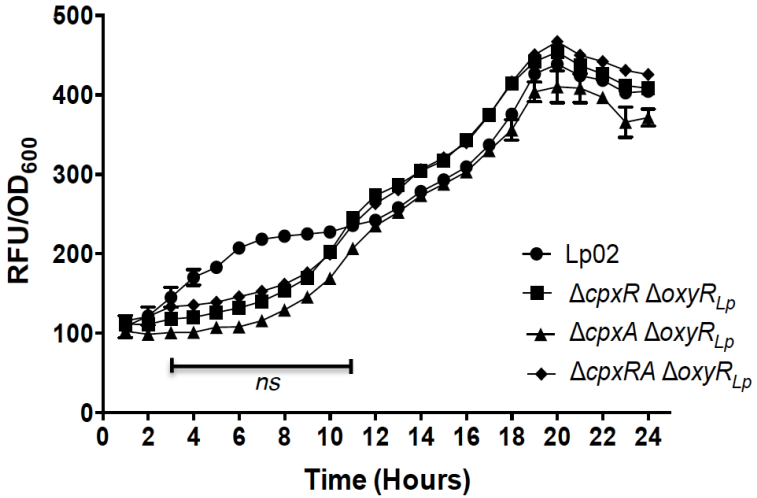
RFU/OD600
Time (Hours)
Lp02
ΔcpxR ΔoxyRLp
ΔcpxA ΔoxyRLp
ΔcpxRA ΔoxyRLp
ns

Figure 4.4 *In vitro* expression of $oxyR_{Lp}$ is not regulated by $OxyR_{Lp}$ and/or the CpxRA two-component system. Each strain in panels A), C), and D) are harboring the pJT277 reporter construct in which the P_{oxyR} region drives the expression of GFP. All data is presented as normalized fluorescence values (RFU/OD_{600}). A) P_{oxyR} activity was assessed in *L. pneumophila* Lp02 (solid circle) and Δ$oxyR_{Lp}$ (solid square). B) Schematic diagram of P_{oxyR} region annotated with a potential CpxR binding site (BR), with the boldface font indicating the sequence likely recognized by CpxR and non-boldface font indicating the nucleotide spacer region. Transcriptional start site determined by Sahr *et al.* (2012) is in boldface font and marked with an asterisk. $oxyR_{Lp}$ coding sequence is in italicized boldface font with the first nucleotide of the start codon designated as +1. Numbering for the promoter region begins at the first nucleotide upstream the $oxyR_{Lp}$ start codon. P_{oxyR} activity assessed in C) *L. pneumophila* Lp02 (solid circle), Δ*cpxR* (solid square), Δ*cpxA* (solid triangle), and Δ*cpxRA* (solid diamond)**,** as well as D) *L. pneumophila* Lp02 (solid circle), Δ*cpxR*Δ$oxyR_{Lp}$ (solid square), Δ*cpxA*Δ$oxyR_{Lp}$ (solid triangle), and Δ*cpxRA*Δ$oxyR_{Lp}$ (solid triangle). Results in panels A), C), and D) represent one of three independent experiments, with error bars representing ± standard errors of the means (SEM) of three technical replicates and *ns* indicating no significant differences in P_{oxyR} activity between the strains examined for the time period within the line segment as determined by Student's *t*-test with Welch's correction.

4.3.4 CpxR directly binds the *oxyR*$_{Lp}$ promoter region

Although GFP reporter assays demonstrated that lack of CpxR and/or CpxA did not significantly affect *oxyR*$_{Lp}$ expression levels *in vitro* it must still be determined if CpxR can bind the putatively identified CpxR binding site in the P_{oxyR} region. The rationale for this approach is that in the event that CpxR does bind, this would indicate that the biological importance of the binding event may occur under specific conditions. In consideration of this, recombinant His_{10}-CpxR was purified and verified for identity and functionality. For identification, purified His_{10}-CpxR was trypsin digested and subjected to MALDI mass spectrometry. Peptides with identities within the spectrum covered 73.8% of the His_{10}-CpxR amino acid sequence and 49.2% of the peptide sequences confirmed by tandem mass spectrometry, validating the purified product as *L. pneumophila* CpxR (Figure 4.5A and 4.5B).

A

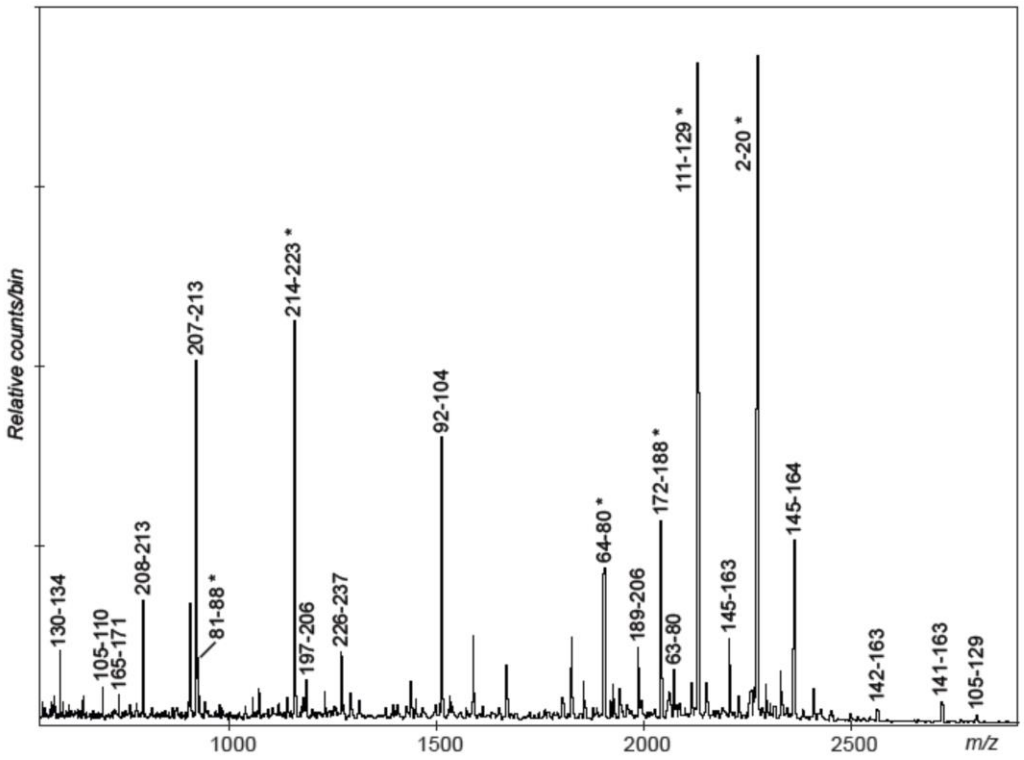

B

*MGHHHHHHHHHHSSGHIEGRHM***MSSSILIIDDDTELTDLLTQYLEPEG**
FNVVCVHDGENGVKRALNQVFDAIILDVMLPKLNGFEVLKAIREHLET
PVLMLTARGDDIDRIVGLEIGADDYLPKPCNPRELVARLRAILRRTQK
IPTPKPIIEQHNIIVDCSKRHVTMGGKFLELTNAEFNILEMLIKSPGQ
AFSKEELTEYALGRKYTAYDRSIDVHISNLRNKLGDNPQGEPLVKTVR
GFGYMFNA

Figure 4.5 Identity of purified *L. pneumophila* His$_{10}$-CpxR is confirmed by MALDI mass spectrometry. A) Part of a MALDI mass spectrum of the His$_{10}$-CpxR protein after digestion with trypsin. The labeled ions have the same $[M+H]^+$ as those expected from peptides of the cloned gene. B) CpxR amino acid sequence (Boldface font) obtained from the Legiolist database (http://genolist.pasteur.fr/LegioList) with the addition of the polyhistidine-tag (italicized font). Peptides with identities within the spectrum are underlined and those confirmed by tandem mass spectrometry are in grey.

For functional analysis, EMSA studies were carried out with purified His_{10}-CpxR and radiolabeled *icmR* promoter (P_{icmR}) fragment (Figure 4.6A); a gene identified elsewhere to be directly regulated by CpxR in *L. pneumophila* (Gal-Mor and Segal, 2003a). An initial shift of the *icmR* probe was observed with 13 μM recombinant CpxR and reaches a maximum shift with 24.6 μM (Figure 4.6A). Specificity of this binding was confirmed by competition with unlabeled probe, which reduced the band shift, whereas an unlabeled fragment corresponding to the internal region of an unrelated gene, *magA*, did not affect band migration (Figure 4.7A). To further substantiate binding specificity, DNase I protection analysis was performed with the radiolabeled sense strand of the P_{icmR} fragment which identified a single protected region (Figure 4.6B). Alignment of the sequence corresponding to the protected region with the known sequence of the P_{icmR} fragment revealed the His_{10}-CpxR bound region to include the motif, GTAAA-N_6-GAAAG, which is identical to the motif determined by Gal-Mor and Segal (2003a) to be bound by CpxR within the P_{icmR} (Figure 4.6C). Therefore, the identity of purified recombinant CpxR is confirmed and the purified protein is deemed functional as it elicits binding with specificity.

With the identity and binding specificity confirmed, His_{10}-CpxR was then employed in EMSA studies with radiolabeled P_{oxyR} fragment to determine if CpxR directly binds the P_{oxyR} region (Figure 4.8A). Gradual migration of the *oxyR* probe was observed with the degree of migration correlating with increasing concentrations of His_{10}-CpxR and achieving a maximum shift with 24.6 μM (Figure 4.8A). Competition with unlabeled probe reduced the band shift while an unlabeled *magA* internal fragment did not affect band migration, verifying the binding of CpxR to the P_{oxyR} region is specific (Figure 4.7B).

To precisely determine the sequence of the site that bound His_{10}-CpxR within the P_{oxyR} region, DNase I protection assays were performed with the radiolabeled sense strand of the P_{oxyR} fragment (Figure 4.8B). A single protected region was observed of which a partial sequence could be determined from the accompanying DNA sequence ladder. Determination of the complete sequence was not possible as the protected region extended beyond the resolution of the aligned DNA sequence ladder. However, the partial sequence of the protected region provided enough information to verify that the inclusion of the motif GTTAT-N_6-GTAAA. Thus, these results indicate that CpxR directly binds the P_{oxyR} region with specificity to a single binding motif that matches the consensus CpxR binding site sequence (Figure 4.4B).

A

Lane	1	2	3	4	5	6	7
His_{10}-CpxR (μM)	0	2.7	5.5	8.2	13.6	19.1	24.6

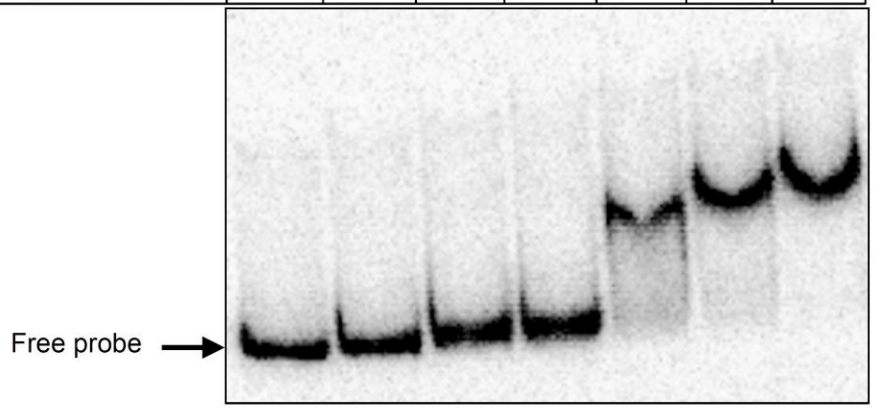

B

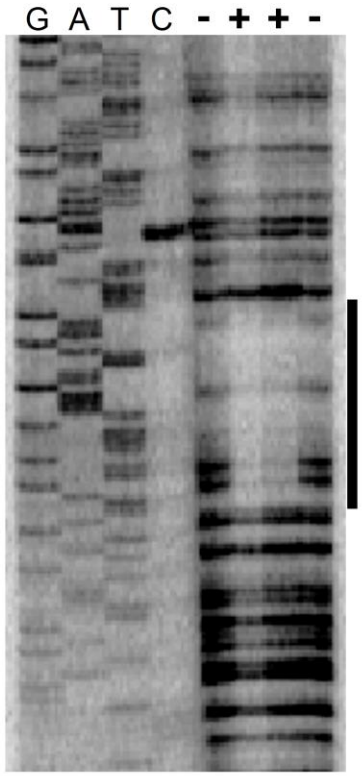

C

PF icmRprom_DP

TATGACGGATGTTATGAATGAGCTTATTCAAGGGGGCCCAAGCCGTGATTATACTCCCCTGGATGAGTTAATGTATGA

-103 -78 -10 *

TTAGTTGTTT**GTAAA**GAATTA**GAAAG**TTTTATTGGACCAAGATATATTGAAAGATATATTTTGA**TATATGT**AAAGT**A**A

GAGATTTAGCTCAGGAGTGGTAATA***ATGGGTAATAATACTGATGACAGTGCACGAAATCCATTTGGTTTTTATACGCC***

ACCTCGTGTTAAAGAGATAGGTGAACCTGATGTAACT

PR icmRprom_DP

Figure 4.6 Purified recombinant CpxR is functional as it binds to the *icmR* promoter region (P_{icmR}). A) Mobility shift assay performed with purified His_{10}-CpxR and P^{32} radiolabelled P_{icmR} region. Amount of His_{10}-CpxR used in each binding reaction is indicated above each lane. B) DNase I protection assay with footprint denoted by the shaded bar. P^{32} radiolabelled P_{icmR} region was incubated with (+) or without (-) His_{10}-CpxR prior to treatment with DNase I. Sanger sequencing ladder of the P_{icmR} region is indicated by G, A, T, C. C) Schematic of the P_{icmR} region. CpxR binding region deduced by DNaseI protection assay is within the open box, with the sequence recognized by CpxR in boldface font and dashed underlined. Nucleotide numbering for the bound region corresponds to the distance from the translational start site. The -10 RNA polymerase binding site and transcriptional start site determined by Gal-Mor *et al.* (2002) are designated by boldface font with underline and bold face font with an asterisk, respectively. Arrows indicate primers used in promoter fragment generation with *icmR* coding sequence in boldface font and italicized.

A

P_{icmR}

Lane	1	2	3	4	5
His_{10}-CpxR (μM)	0	13.6	13.6	13.6	0
Specific Comp. DNA	-	-	+	-	-
Non-specific DNA	-	-	-	+	-
BSA (μM)	0	0	0	0	13.6

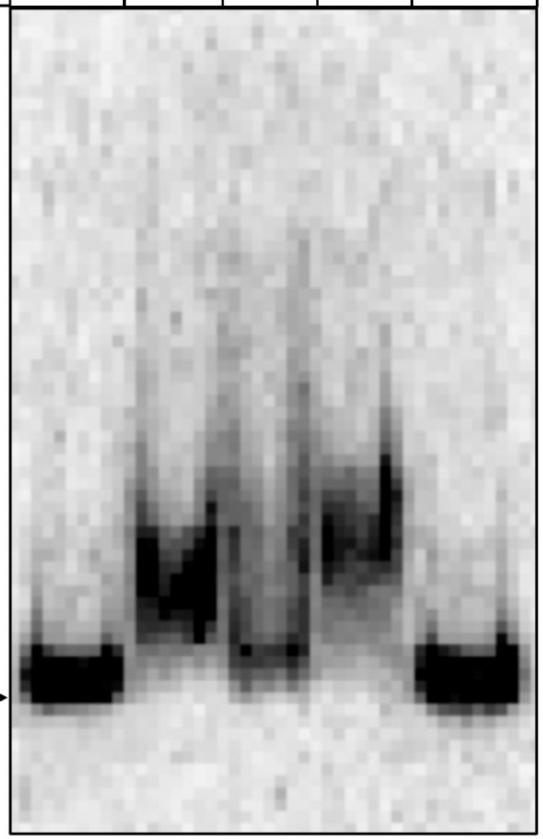

Free probe

B

P_{oxyR}

1	2	3	4	5
0	13.6	13.6	13.6	0
-	-	+	-	-
-	-	-	+	-
0	0	0	0	13.6

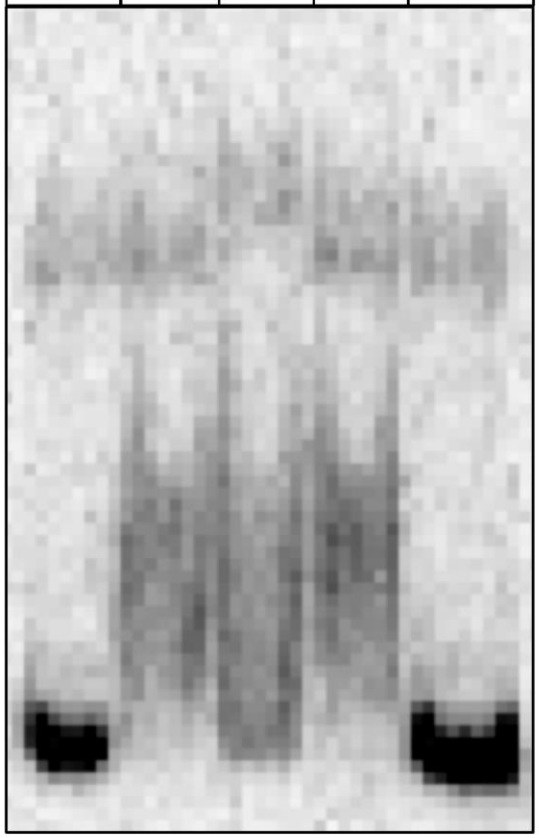

Figure 4.7 CpxR binding of *icmR* and *oxyR*$_{Lp}$ promoter regions is specific. Mobility shift assays conducted with purified His$_{10}$-CpxR and A) *icmR* (P_{icmr}) or B) *oxyR* (P_{oxyR}) promoter regions in the presence (+) or absence (-) of non-radiolabelled P_{icmR} or P_{oxyR} regions (Specific Comp. DNA) or non-radiolabelled *magA* internal gene region (Non-specific DNA). Also included was bovine serum albumin (BSA) as a protein binding control. Protein amounts included in binding reactions is indicated above each lane.

A

Lane	1	2	3	4	5	6	7
His_{10}-CpxR (μM)	0	2.7	5.5	8.2	13.6	19.1	24.6

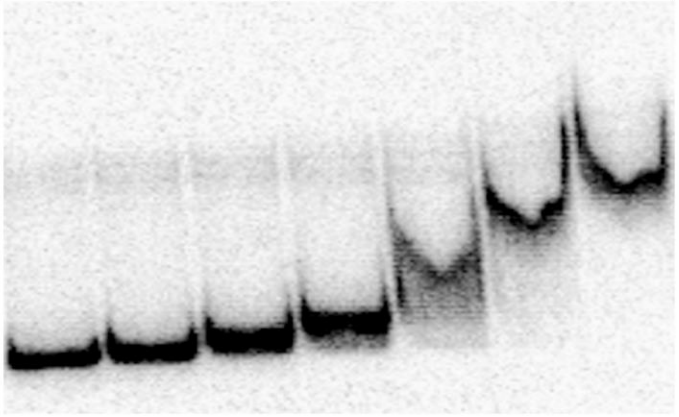

B

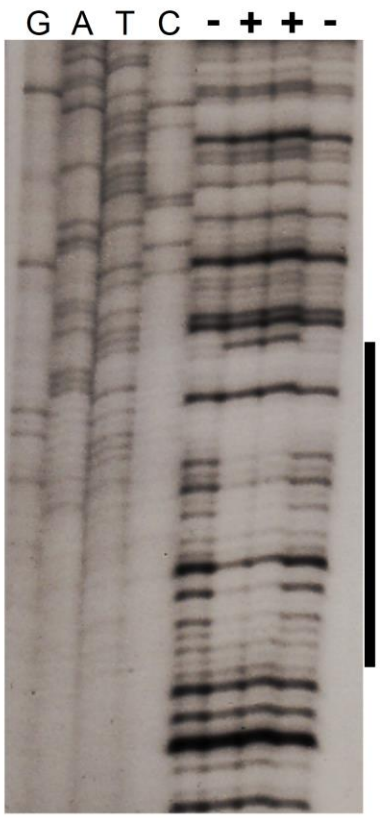

C

PF oxyRprom

-156

GCCGATAAATTGTTCAAAGTAGTTTGTATTATGTTGAAATTGATGGAATATATAGCATT**GTTAT**GTTTGT**GTAAA**TTT

ATAATCTGCAATACCTTTTATTTCTTCATGAATTATATTTGCTATTACATTGGAATCAATAATTCTGTATGTATTTTG

TAAAATTTGAAAAATGATTTCTATACTGCAGATTTGTAATTTATGTCACAATAGAT**T**TTTTATTATTGAGAAATT***ATG***

AATTTAAGAGATTTACATTATTTTGTCATCCTGGCAGATGTAAAG

PR oxyRprom_gfp

Figure 4.8 CpxR binds to the *oxyR*$_{Lp}$ promoter region (P_{oxyR}). A) Mobility shift assay performed with purified His$_{10}$-CpxR and P^{32} radiolabelled P_{oxyR} region. Amount of His$_{10}$-CpxR used in each binding reaction is indicated above each lane. B) DNase I protection assay with footprint denoted by the shaded bar. P^{32} radiolabelled P_{oxyR} region was incubated with (+) or without (-) His$_{10}$-CpxR prior to treatment with DNase I. Sanger sequencing ladder of the P_{oxyR} region is indicated by G, A, T, C. C) Schematic of the P_{oxyR} region. CpxR binding region deduced by DNaseI protection assay is within the open box, with the sequence recognized by CpxR in boldface font and dashed underlined. Solid line of box indicates readable sequence associated with sequencing ladder, dashed line indicates continued footprint without corresponding readable sequencing ladder. Nucleotide numbering for the bound region corresponds to the distance from the translational start site. Transcriptional start site determined by Sahr *et al.* (2012) is in boldface font and marked with an asterisk. Arrows indicate primers used in promoter fragment generation with *oxyR*$_{Lp}$ coding sequence in boldface font and italicized.

4.3.5 OxyR$_{Lp}$ regulates expression of *icmR* and *cpxRA*

The discrepancy between verification of a CpxR binding site in the P_{oxyR} region and unaltered $oxyR_{Lp}$ expression levels in single and combinatorial *cpxRA* mutant strains led us to revalidate our experimental approaches of employing GFP reporter assays to determine promoter activity profiles. The P_{icmR} GFP reporter construct, pJT502, was generated and P_{icmR} activity monitored in parental Lp02 as well as Δ*cpxR*, Δ*cpxA*, Δ*cpxRA*, and Δ$oxyR_{Lp}$ mutant strain backgrounds (Table 4.1). In parental Lp02, P_{icmR} activity began at ~600 RFU/OD$_{600}$ units and exhibited minor gradual increases until 12 hours at which point the rate of activity increased and reached a maximum level of approximately 1645 RFU/OD$_{600}$ units by 24 hours (Figure 4.9A). In comparison to Lp02 levels, P_{icmR} activity overall is diminished in Δ*cpxR* and Δ*cpxRA* backgrounds with initial values of ~165 RFU/OD$_{600}$ units and demonstrated only gradual increases in activity to maximums of 509 and 385 RFU/OD$_{600}$ units, respectively (Figure 4.9A). Whereas in Δ*cpxA*, P_{icmR} activity began at a similar level observed in Lp02 then displayed a slight decrease in activity levels until eight hours, wherein the rate of activity significantly increased and reached an elevated maximum of approximately 2500 RFU/OD$_{600}$ units by 22 hours (Figure 4.8A). These changes in P_{icmR} profile that occur in the *cpx* mutant strain backgrounds correlate with the previous findings of Gal-Mor and Segal (2003a) that CpxR activates *icmR* expression, as P_{icmR} activity is significantly diminished in the absence of CpxR and elevated in the absence of CpxA. Lack of CpxA is expected to increase activity as studies elsewhere have found removal of the sensor kinase to result in the presence of constitutively phosphorylated CpxR, its active state, due to the absence of phosphatase activity normally elicited by the sensor kinase (Danese *et al.*, 1995; Raivio and Silhavy, 1997; Spinola *et al.*, 2010;

Wolfe *et al.*, 2008). Thus the *cpx* mutant strains function in the expected manner, yielding anticipated changes in P_{icmR} activity.

The Δ$oxyR_{Lp}$ mutant strain was included in the P_{icmR} GFP reporter assays as an intended control as no effects on P_{icmR} activity were anticipated. Surprisingly, a significant change in P_{icmR} profile was observed in the Δ$oxyR_{Lp}$ background in comparison to Lp02 (Figure 4.9A). Initially, the P_{icmR} profile remains unchanged between the Δ$oxyR_{Lp}$ and the Lp02 backgrounds however, after eight hours P_{icmR} activity increases at an accelerated rate, reaching a maximum of ~2420 RFU/OD_{600} units in the Δ$oxyR_{Lp}$ mutant strain (Figure 4.9A). This elevated level of activity implies that $OxyR_{Lp}$ negatively regulates *icmR* expression; however, this interaction maybe direct or indirect. Interestingly, the changes in the P_{icmR} profile in the Δ$oxyR_{Lp}$ mutant strain resemble the changes that occur in the Δ*cpxA* mutant strain, where CpxR is likely constitutively active. Therefore, it is plausible that $OxyR_{Lp}$ is indirectly altering P_{icmR} activity through regulation of *cpxR* expression. To investigate this potential interaction, the reporter construct pJT730 containing the promoter region that drives the expression of the *cpxRA* two-component system ($P_{lpg1441\text{-}cpxA}$), was electroporated into the Δ$oxyR_{Lp}$ mutant strain and the promoter activity compared to the activities in parental Lp02 and the Δ*cpxA* mutant strain; where in the Δ*cpxA* mutant strain $P_{lpg1441\text{-}cpxA}$ activity is elevated due to the positive autoregulation exhibited by CpxR (Table 4.1) (Tanner *et al.*, 2016). Similarly to what is observed in Δ*cpxA*, $P_{lpg1441\text{-}cpxA}$ activity is initially slightly elevated in the Δ$oxyR_{Lp}$ mutant strain but decreases with time to levels that are similar to those observed in Lp02 and then after 10 hours increases at an accelerated rate in comparison to Lp02 (Figure 4.9B). The maximum level of activity of ~1600 RFU/OD_{600} units reached in Δ$oxyR_{Lp}$ is elevated in comparison to Lp02 but slightly lower than the maximum of ~1800 RFU/OD600 achieved in the Δ*cpxA* background (Figure 4.9B). Taken together, the

absence of *oxyR*$_{Lp}$ results in elevated *cpxR* expression, which has the downstream effect of increased *icmR* expression; indicating OxyR$_{Lp}$ negatively regulates *cpxR* expression.

A

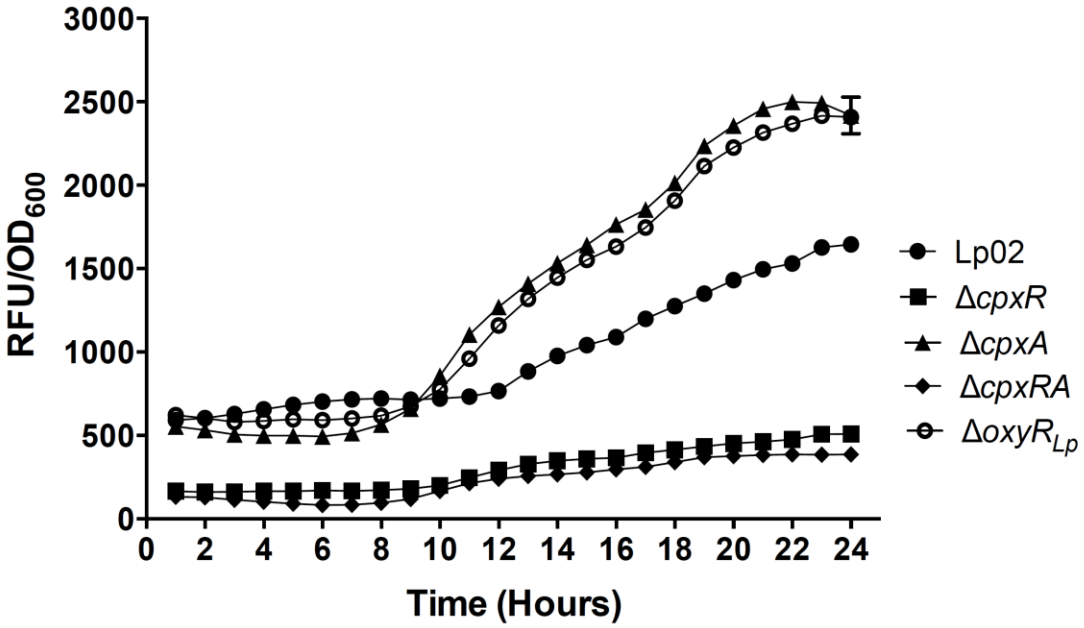
3000
2500
2000
1500
1000
500
0
RFU/OD600
0 2 4 6 8 10 12 14 16 18 20 22 24
Time (Hours)
Lp02
ΔcpxR
ΔcpxA
ΔcpxRA
ΔoxyRLp

B

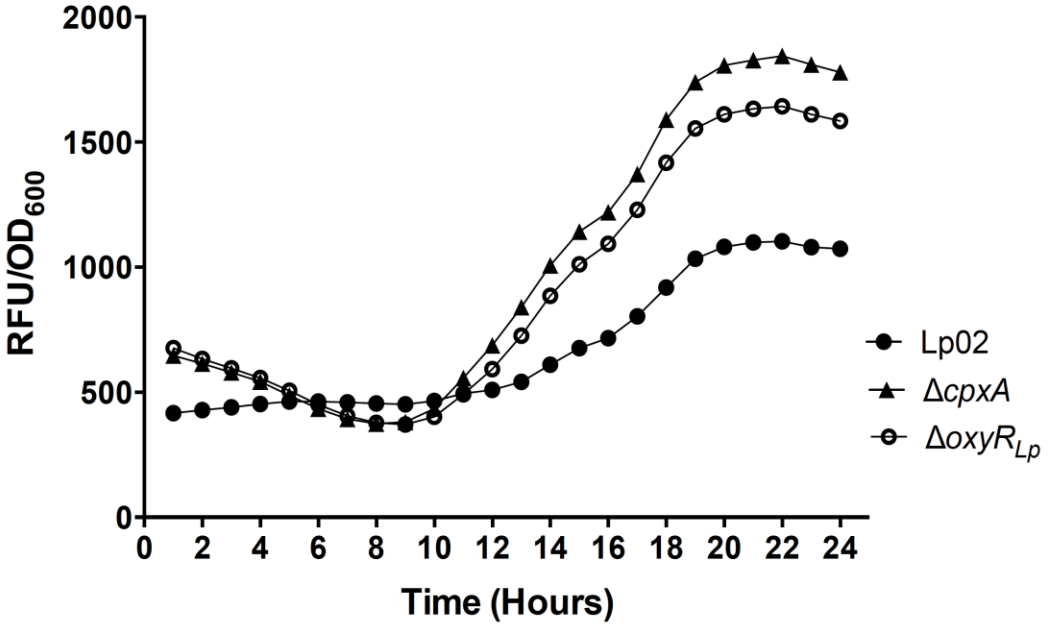
2000
1500
1000
500
0
RFU/OD600
0 2 4 6 8 10 12 14 16 18 20 22 24
Time (Hours)
Lp02
ΔcpxA
ΔoxyRLp

Figure 4.9 $OxyR_{Lp}$ negatively regulates the expression of the *cpxRA* two-component system. GFP reporter constructs were expressed in *L. pneumophila* Lp02 strains and normalized fluorescence values (RFU/OD_{600}) determined. A) *L. pneumophila* Lp02 (solid circle), Δ*cpxR* (solid square), Δ*cpxA* (solid triangle), and Δ*cpxRA* (solid diamond) strains harboring pJT502 reporter construct in which the P_{icmR} region drives the expression of GFP. B) *L. pneumophila* Lp02 (solid circle), Δ*cpxA* (solid triangle) and Δ$oxyR_{Lp}$ (open circle) harboring pJT730 reporter construct in which the $P_{lpg1441\text{-}cpxA}$ region drives the expression of GFP. Results represent of one of three independent experiments conducted in triplicate. Error bars represent ± standard errors of the means (SEM) of three technical replicates.

4.4 DISCUSSION

The lifestyle of *L. pneumophila* involves navigating a variety of extra- and intracellular environments. To evoke the necessary changes in gene expression needed to endure the challenges of these vastly different niches, *L. pneumophila* possesses regulatory factors that include two-component systems, alternative sigma factors as well as an array of transcription factors (Chien *et al.*, 2004). The transcription factor, $OxyR_{Lp}$, has been identified to regulate the expression of genes associated with alleviating oxidative stress but no longer capable of responding to oxidative changes in *L. pneumophila* (LeBlanc *et al.*, 2006; LeBlanc *et al.*, 2008). However, genetic deletion of $oxyR_{Lp}$ from the *L. pneumophila* chromosome was unable to be achieved by LeBlanc *et al.* (2008) suggesting that the functional role of $OxyR_{Lp}$, while undefined, was essential to the viability of *L. pneumophila*.

By adopting an alternative mutational strategy we were able to generate an $oxyR_{Lp}$ in-frame null mutant in *L. pneumophila,* confirmed at the DNA level via sequencing and at the protein level via immunoblot analysis (Figure 4.1A). Interestingly, the recovery of a Δ*oxyR L. pneumophila* mutant on laboratory media did not require the addition of factors that alleviate the presence of reactive oxygen species (ROS) such as the catalase enzyme, to achieve isolated single colonies. Elsewhere, genetic deletion of *oxyR* in the Gram-negative bacteria *Pseudomonas aeruginosa*, *Haemophilus influenzae*, *Shigella flexneri,* and *Vibrio cholerae* resulted in a lack of isolated colonies when grown on rich laboratory medium that could only be rescued by addition or expression of factors that alleviate oxidative stress (Maciver and Hansen, 1996; Hassett *et al.*, 2000; Daugherty *et al.*, 2012; Wang *et al.*, 2012). Because the *L. pneumophila* Δ*oxyR* mutant strain does not seem to elicit similar sensitivities observed in other organisms with OxyR

homologues, the findings of LeBlanc *et al.* (2008) that suggest $OxyR_{Lp}$ does not respond to oxidative stress are further corroborated.

Until now *oxyR*$_{Lp}$ was considered essential leaving only a few avenues of investigation, one being *oxyR*$_{Lp}$ expression levels. Three separate laboratories have observed growth phase dependent changes in *oxyR*$_{Lp}$ expression under *in vitro* growth conditions, where *oxyR*$_{Lp}$ expression is up regulated during the post-exponential growth phase (Bruggemann *et al.*, 2006; LeBlanc *et al.*, 2008; Weissenmayer *et al.*, 2011). This is important as changes specific to the post-exponential growth phase implies a potential role in regulating cell cycle changes and/or virulence factor expression in *L. pneumophila*. However, transcriptional changes do not always equate to changes in protein level due to factors such as mRNA turnover as well as post-transcriptional regulation [reviewed in (Zhang *et al.*, 2010)]. Our findings agree with the latter as densitometric analysis of parental Lp02 growth phase samples immunoblotted for $OxyR_{Lp}$ did not reveal a significant change in $OxyR_{Lp}$ protein levels during the post-exponential phase that would correlate with the ~3-fold changes observed by Bruggemann *et al.* (2006) and Weissenmayer *et al.* (2011) (Figure 4.1A and 4.1B).

Lack of $OxyR_{Lp}$ did not appear to alter intracellular growth phenotypes as no differences in growth profiles were observed between parental Lp02 and the Δ*oxyR*$_{Lp}$ mutant strains in either *A. castellanii* or U937 cells (Figure 4.2A and 4.2B). This finding implies that $OxyR_{Lp}$ does not have an essential role in responding to intracellular stresses, virulence factor expression or cell cycle changes. However, the *L. pneumophila* Philadelphia genome, available on the Legiolist database (http://genolist.pasteur.fr/LegioList), contains a second OxyR homologue designated *oxyR1* (*lpg0173*). The only other organisms to our knowledge that contain two OxyR homologues is the Gram-positive bacterium, *Deinococcus radiodurans* (Yin *et al.*, 2010) and the

Gram-negative pathogen, *Vibrio vulnificus*. Studies of these two homologues within *D. radiodurans* has revealed each individually to be necessary for resistance to oxidative stress but also function synergistically in this regard, as a mutant lacking both *oxyR* homologues exhibits increased sensitivity to oxidative stress (Chen *et al.*, 2008; Yin *et al.*, 2010). In *V. vulnificus*, it was found that each homologue of OxyR functioned in sensing changes in oxidation; however, each had distinct gene targets as well as different sensing thresholds with one homologue responding to very low levels of H_2O_2 in comparison to its counterpart (Kim *et al.*, 2014). Perhaps in *L. pneumophila*, *oxyR1* is the dominant sensor and regulator of stress and therefore able to compensate for the absence of $oxyR_{Lp}$, resulting in minimal to no phenotypes in the Δ$oxyR_{Lp}$ mutant strain. Analysis of an *L. pneumophila oxyR1* mutant as well as an *oxyR1*$oxyR_{Lp}$ combinatorial mutant strain is an essential first step toward investigating this hypothesis, and is currently underway in our laboratory.

Interestingly, overexpression of OxyRLp in the parental Lp02 background resulted in reduced bacterial counts in comparison to bacterial counts achieved with Lp02 and the Δ$oxyR_{Lp}$ mutant strains in *A. castellanii* (Figure 4.2A). The overexpression reflects a ~10 fold increase in cellular levels of $OxyR_{Lp}$ that could be effecting the inherent growth of *L. pneumophila* through toxic accumulation and thereby decreasing its viability in *A. castellanii* protozoa; however, the overexpressing strain exhibits growth profiles similar to parental Lp02 in U937 cells (Figure 4.2B) and in BYE broth (Figure 4.3), making toxicity an unlikely factor. It is more probable that the regulatory impacts of $OxyR_{Lp}$ have become unbalanced, whereby a product(s) regulated by $OxyR_{Lp}$ is either over or under produced that is affecting *L. pneumophila* growth specifically in the *A. castellanii* host cell (see below).

Efforts to determine the manner of regulation of $oxyR_{Lp}$ expression resulted in convoluted findings. A CpxR binding site was identified within the P_{oxyR} region (Figure 4.4B); however, P_{oxyR} activity levels in the Δ*cpxR*, Δ*cpxA* or Δ*cpxRA* mutant strain backgrounds were similar indicating that lack of CpxR did not affect $oxyR_{Lp}$ expression (Figure 4.4C). Yet, *in vitro* binding assays demonstrated that CpxR could specifically bind the motif identified within the P_{oxyR} region (Figure 4.8A, 4.8B, and 4.8C). The discrepancy of whether CpxR regulates $oxyR_{Lp}$ expression is likely conditionally based. Here, we have utilized a single condition, the rich laboratory medium BYE, when CpxR regulation of $oxyR_{Lp}$ is perhaps required under less ideal conditions that may include nutrient limitation, pH changes or exposure to elevated levels of metal ions (Nakayama and Watanabe, 1995; Danese and Silhavy, 1998; Yamamoto and Ishihama, 2005; Acosta *et al.*, 2015). Alternatively, or in combination with environmental conditions, the P_{oxyR} region may contain an alternative transcriptional start site (TSS), which has been identified to occur in several genes by RNA-seq within the *L. pneumophila* Paris genome (Sahr *et al.*, 2012). Under this scenario, CpxR could be key to initiating or repressing transcription at this site under specific conditions yet to be determined. Several avenues of further investigation will need to be taken in order to resolve the potential regulatory role CpxR has in $oxyR_{Lp}$ expression.

Surprisingly, during our investigations of *oxyR* expression we uncovered an unexpected regulatory interaction. We identified what appears to be a regulatory hierarchy where $OxyR_{Lp}$ negatively regulates the expression of the *cpxRA* system (Figure 4.9B), which then affects the expression of downstream CpxRA regulon members such as *icmR* (Figure 4.9A). The aforementioned hierarchy is quite interesting as it draws connections to different aspects and observations in this study as detailed in the following: i) Negative regulation of the CpxRA

system may in part explain the limited growth phenotype of the $OxyR_{Lp}$ overexpression strain, Lp02 OE (Figure 4.2A), as we recently identified the CpxRA system to be absolutely required by *L. pneumophila* for intracellular replication in *A. castellanii* (Tanner *et al.*, 2016); ii) Transcriptomic analyses has determined that the CpxRA system regulates a significant number of genes including $oxyR_{Lp}$ in *L. pneumophila* (Tanner *et al.*, 2016), implicating a wider regulatory influence for $oxyR_{Lp}$ expression and a rationale for limiting $OxyR_{Lp}$ levels at a threshold throughout the progressive growth phases as observed (Figure 4.1A and 4.1B), potentially avoiding perturbations to multiple regulatory networks; and iii) With $OxyR_{Lp}$ regulating *cpxRA* expression (Figure 4.9B) and CpxR likely regulating $oxyR_{Lp}$ expression conditionally (Figure 4.8A and 4.9B), a unique regulatory loop may exist that would allow CpxR to either enhance or suppress its own expression via the regulatory role of $OxyR_{Lp}$.

In light of these results, the role of $OxyR_{Lp}$ in *L. pneumophila* as a transcriptional regulator is clear, thus far exhibiting negative regulation of its targets, *cpxRA* (this study) and *ahpC2D* (LeBlanc *et al.*, 2008). However, deletion of $oxyR_{Lp}$ did not impact growth of *L. pneumophila* under *in vitro* and *in vivo* conditions in this study. Additionally, the presence of an *oxyR* paralog *oxyR1* implies, but not yet determined, a synergistic functional role. Taken together, we propose that the regulatory role of $OxyR_{Lp}$ is functionally redundant in *L. pneumophila*.

Chapter 5. CONCLUSIONS AND FUTURE DIRECTIONS

L. pneumophila is a highly adapted pathogen. It has the ability to persist in extracellular environments as well as readily resist the killing elicited by predatory protozoa present in the diverse aquatic environments in which this bacterium resides (Hilbi *et al.*, 2011). *L. pneumophila* has utilized these eukaryotic encounters to evolve as an intracellular pathogen, acquiring hundreds of genes that encode effector proteins and tailoring these effectors for translocation to the host cytosol via the Dot/Icm type IVB secretion system (Gomez-Valero *et al.*, 2011; Ensminger, 2016). The deployed effectors aid *L. pneumophila* in the establishment of a protective replicative niche by disrupting key host cellular pathways including the evasion of phagosome-lysosome fusion and diversion of vesicular trafficking (Finsel and Hilbi, 2015). These survival strategies cultivated in protozoa has enabled *L. pneumophila* to also infect human alveolar macrophages as similar cellular processes are targeted within these host cells to achieve intracellular replication (Escoll *et al.*, 2013). The resulting Legionnaires' disease that follows macrophage infection is a severe complication to individuals with compromised immunity and often results in fatalities (Fraser *et al.*, 1977; Fields *et al.*, 2002; Marrie, 2008).

Prevention of these disease outcomes can only improve with a better understanding of the factors that contribute to the pathogenicity of *L. pneumophila* within its environmental and human hosts. The CpxRA TCS has been identified as part of the regulatory repertoire employed by *L. pneumophila* to coordinate virulence gene expression; however, the number of genes determined as CpxRA regulon members has remained rather limited and no intracellular growth phenotypes that correlate to the virulence gene regulation have been recognized (Gal-Mor and Segal, 2003a; Altman and Segal, 2008). Thus, the studies of this thesis were undertaken to better define the regulatory role of the CpxRA TCS in *L. pneumophila*, with a focus on genes related to

virulence as well as to re-examine this systems influence on the host-pathogen interactions of *L. pneumophila*. During my investigations of CpxR as a potential regulator of $oxyR_{Lp}$ gene expression, interesting results were produced that prompted further examination into the transcriptional regulator $OxyR_{Lp}$ itself.

Bioinformatic searches of regulatory regions within an organism's genome for elements putatively recognized by a transcription factor of interest, using prior knowledge of that factors defined consensus binding sequence as input, is a valid and commonly used method for identifying potential regulatory targets (Stormo, 2000). Application of this method in *L. pneumophila* has successfully identified regulatory targets of CpxR, with a total of 15 genes determined as being directly impacted by CpxR until the most recent search conducted by Feldheim *et al.* (2015) expanded it to 38 genes (Altman and Segal, 2008). However, this method of promoter mining may miss important targets depending on the stringency applied to the consensus sequence used and the types of restrictions set in regards to the proximity these sequences can occur to coding sequences (Stormo, 2000). We therefore chose to acquire a global overview of the CpxRA TCS regulatory interactions via microarray analysis, as this approach would provide genome-wide direct and indirect regulatory targets and thus more effectively expand the CpxRA TCS regulon in *L. pneumophila*.

Comparative analysis of the *L. pneumophila* Lp02 (parental) and Δ*cpxRA* mutant strain transcriptomes, identified hundreds of genes to be differentially expressed in the absence of the CpxRA system when examined in the exponential and post-exponential growth phases. Focusing the analysis on virulence-associated genes revealed additional Dot/Icm effector proteins to be activated or repressed by CpxR, as well as a significant number of Type II secreted substrates to be activated by CpxR. The latter is a considerable finding as Type II secreted substrates are also

required by *L. pneumophila* to achieve intracellular replication in amoeba and somewhat required in murine macrophages; thus, further establishing the CpxRA TCS as a key virulence regulator in *L. pneumophila* (DebRoy *et al.*, 2006; Rossier *et al.*, 2009; Tyson *et al.*, 2013).

With these novel CpxRA targets revealed the next logical step would be to identify which of these target genes CpxR directly influences in *L. pneumophila*. Here, bioinformatic analysis of each targets promoter region for the presence of CpxR binding sites would be beneficial and subsequent EMSA analysis required to confirm CpxR interaction with these regulatory elements. In conjunction to this more pointed approach, a global means of identifying direct CpxR targets could also be undertaken by employing ChIP-seq. Granted this is a more costly as well as labour intensive process, it would provide a data set that can be correlated to the acquired transcriptome data, which together will present a more complete picture of the CpxRA regulon in *L. pneumophila*.

The identification of additional CpxRA regulated genes that are tied to virulence in *L. pneumophila* prompted us to re-examine the role of this system in intracellular replication. When the Δ*cpxR*, Δ*cpxA*, and Δ*cpxRA* mutant strains were subjected to intracellular growth kinetic assays within the *A. castellanii* and U937-derived macrophages host models, definitive phenotypes were observed. The Δ*cpxR* and Δ*cpxRA* mutant strains were unable to replicate in the amoeba host where as all *cpx* mutant strains elicited similar replication to that of the parental Lp02 strain in U937 cells. These phenotypes observed in the amoeba host were supported through complementation, whereby the supplementation of the respective strains with *cpxR* or *cpxRA in trans* restored intracellular growth. Furthermore, the Δ*cpxR* and Δ*cpxRA* mutant strains also exhibited marked sodium resistance when grown to the post-exponential phase in broth, a phenotype often associated with avirulent *L. pneumophila* (Sadosky *et al.*, 1993; Vogel *et al.*,

1996; Byrne and Swanson, 1998). Together, these phenotypes highlight for the first time the essentiality of the CpxRA virulence regulation to *L. pneumophila* intracellular survival, albeit the requirement of the CpxRA system is specific to the amoeba host.

With the affirmation of an intracellular growth phenotype, it would be of value to investigate the infection process that occurs with the Δ*cpxR* and Δ*cpxRA* mutant strains in more detail, in order to identify the reason(s) behind the abrogated growth observed in the amoeba host. Points of the infection process that should be assessed are entry and vacuole establishment, which can be achieved by fixing infected samples at appropriate times after *L. pneumophila* strains have been applied and monitoring the progression via immunofluorescence microscopy. Results from these experiments would reveal whether the Dot/Icm system is perhaps non-functional in the Δ*cpxR* and Δ*cpxRA* mutant strains as these two processes have been shown to be dependent upon a functional Dot/Icm system (Segal and Shuman, 1999a; Hilbi *et al.*, 2001). Translocations assays could also be carried out to investigate whether the Dot/Icm system of these *cpx* mutant strains retains the ability to transfer well characterized effector proteins, in order to more definitively define a dysfunctional Dot/Icm system as the basis for the impaired intracellular growth of Δ*cpxR* and Δ*cpxRA* mutant strains. Depending on the outcomes of these experiments, correlations to the regulatory data could be made as the Dot/Icm system components *dotA, icmV, icmW, icmR,* and *lvgA* all require CpxR for activation of their expression.

When evaluating the now affirmed role of the CpxRA TCS in enhancing the virulence of *L. pneumophila* to the effects this system has on virulence in other Gram-negative bacteria, *L. pneumophila* can be regarded as somewhat of the exception. Many of the bacterial species containing a CpxRA system have been found to utilize this system to inhibit the expression of

virulence factors and/or major virulence regulators (Vogt and Raivio, 2012). *L. pneumophila* on the other hand, utilizes the CpxRA TCS for the most part to induce the expression of Dot/Icm system components and effectors as well as Type II secreted substrates, albeit CpxR negatively regulates some Dot/Icm effectors. Although, this negative regulation is likely to achieve the timely expression of factors necessary during specific points of the infection process and perhaps if left unregulated would be detrimental the survival *of L. pneumophila*. The question then arises as to why a divergence in functionality would occur in *L. pneumophila*? One likely explanation lies in the fact that *L. pneumophila* has acquired and retained the largest collection of effector proteins in comparison to any other pathogen studied thus far (Ensminger, 2016). Each of these acquired factors would then require coordination at the genetic level to achieve both appropriate timing and levels of expression. Modifying the regulatory regions of these acquired genes to contain the binding motifs of regulatory proteins already being utilized for other regulatory purposes would be an efficient means of accomplishing this. Thus, adopting the regulatory abilities of this TCS as well as others has likely occurred to fulfill a large regulatory void.

Another diversion that is evident within the *L. pneumophila* CpxRA TCS is the absence of accessory proteins commonly associated with this system in other bacterial species. Thus far a homologue of the negative regulatory protein, CpxP, has not been identified within the *L. pneumophila* genome, and consequently the regulatory sRNA, CpxQ, is also likely absent. This leaves the questions of how the down regulation of the CpxRA system is achieved, and what sRNAs make up the post-transcriptional regulatory arm of this system in *L. pneumophila*? A plausible answer to one of these questions is provided through the results I obtained when investigating the regulatory interactions between the CpxRA TCS and the transcriptional regulator $OxyR_{Lp}$.

When conducting GFP transcriptional reporter assays with several mutant strains, it was found that the $P_{lpg1441\text{-}cpxA}$ promoter region had significantly elevated activity in the Δ*oxyR*$_{Lp}$ mutant strain in comparison to the activity observed in the parental Lp02 strain. This indicates OxyR as a negative regulator of CpxRA expression, as I defined this promoter region to drive the expression of the *cpxRA* genes during the studies conducted in Chapter 3 and published in Tanner *et al.* (2016). Therefore, this result provides the first evidence that *L. pneumophila* has employed an alternative regulatory factor to execute the negative regulation of the CpxRA TCS, perhaps replacing the absence of the CpxP protein with $OxyR_{Lp}$. EMSA analysis should be conducted to identify whether this regulatory impact is achieved through direct or indirect mechanisms.

As for determining the post-transcriptional regulatory arm of the *L. pneumophila* CpxRA TCS, an RNA-seq experiment would be need to be conducted with the parental Lp02 strain and the Δ*cpxRA* mutant strain. This highly sensitive method of transcriptome analysis would provide an accurate depiction of the sRNAs under the control of the CpxRA system and provide a starting point for further investigations.

I feel another avenue of the *L. pneumophila* CpxRA TCS that should be explored and is currently lacking in the literature, is the environmental signals that activate this system. Having this insight in combination with the regulatory impacts of the CpxRA TCS system would supply a more detailed picture of how this system functions and is utilized in *L. pneumophila*. Starting points for this investigation could be the input signals identified to activate the CpxRA TCS of *E. coli*, and choosing those that are likely to be encountered during the *L. pneumophila* life cycle including pH changes, exposure to copper, and surface adhesion (Danese and Silhavy, 1998; Otto and Silhavy, 2002; Yamamoto and Ishihama, 2005). This knowledge base could then be

applied to the development of improved control methods, with this system serving as a novel target for controlling *L. pneumophila* levels in our water systems and ultimately limiting the incidence of disease.

Chapter 6. REFERENCES

Abdel-Nour, M., Duncan, C., Low, D.E. and Guyard, C., (2013) Biofilms: the stronghold of *Legionella pneumophila*. *Int J Mol Sci* **14**: 21660-21675.

Abdelhady, H. and Garduno, R.A., (2013) The progeny of *Legionella pneumophila* in human macrophages shows unique developmental traits. *FEMS Microbiol Lett* **349**: 99-107.

Abu Kwaik, Y., (1996) The phagosome containing *Legionella pneumophila* within the protozoan *Hartmannella vermiformis* is surrounded by the rough endoplasmic reticulum. *Appl Environ Microbiol* **62**: 2022-2028.

Abu Kwaik, Y., Gao, L.Y., Harb, O.S. and Stone, B.J., (1997) Transcriptional regulation of the macrophage-induced gene (*gspA*) of *Legionella pneumophila* and phenotypic characterization of a null mutant. *Mol Microbiol* **24**: 629-642.

Abu-Zant, A., Asare, R., Graham, J.E. and Abu Kwaik, Y., (2006) Role for RpoS but not RelA of *Legionella pneumophila* in modulation of phagosome biogenesis and adaptation to the phagosomal microenvironment. *Infect Immun* **74**: 3021-3026.

Acosta, N., Pukatzki, S. and Raivio, T.L., (2015) The *Vibrio cholerae* Cpx envelope stress response senses and mediates adaptation to low iron. *J Bacteriol* **197**: 262-276.

Agirrezabala, X., Fernandez, I.S., Kelley, A.C., Carton, D.G., Ramakrishnan, V. and Valle, M., (2013) The ribosome triggers the stringent response by RelA via a highly distorted tRNA. *EMBO Rep* **14**: 811-816.

Al-Khodor, S., Kalachikov, S., Morozova, I., Price, C.T. and Abu Kwaik, Y., (2009) The PmrA/PmrB two-component system of *Legionella pneumophila* is a global regulator

required for intracellular replication within macrophages and protozoa. *Infect Immun* **77**: 374-386.

Altman, E. and Segal, G., (2008) The response regulator CpxR directly regulates expression of several *Legionella pneumophila icm/dot* components as well as new translocated substrates. *J Bacteriol* **190**: 1985-1996.

Angelini, S., My, L. and Bouveret, E., (2012) Disrupting the Acyl Carrier Protein/SpoT interaction in vivo: identification of ACP residues involved in the interaction and consequence on growth. *PLoS One* **7**: e36111.

Appleman, J.A., Chen, L.L. and Stewart, V., (2003) Probing conservation of HAMP linker structure and signal transduction mechanism through analysis of hybrid sensor kinases. *J Bacteriol* **185**: 4872-4882.

Bachman, M.A. and Swanson, M.S., (2001) RpoS co-operates with other factors to induce *Legionella pneumophila* virulence in the stationary phase. *Mol Microbiol* **40**: 1201-1214.

Bachman, M.A. and Swanson, M.S., (2004) Genetic evidence that *Legionella pneumophila* RpoS modulates expression of the transmission phenotype in both the exponential phase and the stationary phase. *Infect Immun* **72**: 2468-2476.

Bairoch, A., Boeckmann, B., Ferro, S. and Gasteiger, E., (2004) Swiss-Prot: juggling between evolution and stability. *Brief Bioinfor* **5**: 39-55.

Bardill, J.P., Miller, J.L. and Vogel, J.P., (2005) IcmS-dependent translocation of SdeA into macrophages by the *Legionella pneumophila* type IV secretion system. *Mol Microbiol* **56**: 90-103.

Battesti, A. and Bouveret, E., (2006) Acyl carrier protein/SpoT interaction, the switch linking SpoT-dependent stress response to fatty acid metabolism. *Mol Microbiol* **62**: 1048-1063.

Berger, K.H. and Isberg, R.R., (1993) Two distinct defects in intracellular growth complemented by a single genetic locus in *Legionella pneumophila*. *Mol Microbiol* **7**: 7-19.

Berger, K.H., Merriam, J.J. and Isberg, R.R., (1994) Altered intracellular targeting properties associated with mutations in the *Legionella pneumophila dotA* gene. *Mol Microbiol* **14**: 809-822.

Berk, S.G., Ting, R.S., Turner, G.W. and Ashburn, R.J., (1998) Production of respirable vesicles containing live *Legionella pneumophila* cells by two *Acanthamoeba* spp. *Appl Environ Microbiol* **64**: 279-286.

Bouyer, S., Imbert, C., Rodier, M.H. and Hechard, Y., (2007) Long-term survival of *Legionella pneumophila* associated with *Acanthamoeba castellanii* vesicles. *Environ Microbiol* **9**: 1341-1344.

Bozue, J.A. and Johnson, W., (1996) Interaction of *Legionella pneumophila* with *Acanthamoeba castellanii*: uptake by coiling phagocytosis and inhibition of phagosome-lysosome fusion. *Infect Immun* **64**: 668-673.

Brand, B.C., Sadosky, A.B. and Shuman, H.A., (1994) The *Legionella pneumophila icm* locus: a set of genes required for intracellular multiplication in human macrophages. *Mol Microbiol* **14**: 797-808.

Brencic, A., McFarland, K.A., McManus, H.R., Castang, S., Mogno, I., Dove, S.L. and Lory, S., (2009) The GacS/GacA signal transduction system of *Pseudomonas aeruginosa* acts exclusively through its control over the transcription of the RsmY and RsmZ regulatory small RNAs. *Mol Microbiol* **73**: 434-445.

Brenner, D.J., Steigerwalt, A.G. and McDade, J.E., (1979) Classification of the Legionnaires' disease bacterium: *Legionella pneumophila,* genus novum, species nova, of the family *Legionellaceae,* familia nova. *Ann Intern Med* **90**: 656-658.

Brenner, D.J., Steigerwalt, A.G., Weaver, R.E., McDade, J.E., Feeley, J.C. and Mandel, M., (1978) Classification of the Legionnaires' disease bacterium: An interim report. *Curr Microbiol* **1**: 71-75.

Brombacher, E., Urwyler, S., Ragaz, C., Weber, S.S., Kami, K., Overduin, M. and Hilbi, H., (2009) Rab1 guanine nucleotide exchange factor SidM is a major phosphatidylinositol 4-phosphate-binding effector protein of *Legionella pneumophila*. *J biol chem* **284**: 4846-4856.

Bruggemann, H., Hagman, A., Jules, M., Sismeiro, O., Dillies, M.A., Gouyette, C., Kunst, F., Steinert, M., Heuner, K., Coppee, J.Y. and Buchrieser, C., (2006) Virulence strategies for infecting phagocytes deduced from the *in vivo* transcriptional program of *Legionella pneumophila*. *Cell Microbiol* **8**: 1228-1240.

Bryan, A., Abbott, Z.D. and Swanson, M.S., (2013) Constructing unmarked gene deletions in *Legionella pneumophila*. *Methods Mol Biol* **954**: 197-212.

Buelow, D.R. and Raivio, T.L., (2005) Cpx signal transduction is influenced by a conserved N-terminal domain in the novel inhibitor CpxP and the periplasmic protease DegP. *J Bacteriol* **187**: 6622-6630.

Buelow, D.R. and Raivio, T.L., (2010) Three (and more) component regulatory systems - auxiliary regulators of bacterial histidine kinases. *Mol Microbiol* **75**: 547-566.

Burstein, D., Zusman, T., Degtyar, E., Viner, R., Segal, G. and Pupko, T., (2009) Genome-scale identification of *Legionella pneumophila* effectors using a machine learning approach. *PLoS Pathog* **5**: e1000508.

Buscher, B.A., Conover, G.M., Miller, J.L., Vogel, S.A., Meyers, S.N., Isberg, R.R. and Vogel, J.P., (2005) The DotL protein, a member of the TraG-coupling protein family, is essential for Viability of *Legionella pneumophila* strain Lp02. *J Bacteriol* **187**: 2927-2938.

Butland, G., Peregrin-Alvarez, J.M., Li, J., Yang, W., Yang, X., Canadien, V., Starostine, A., Richards, D., Beattie, B., Krogan, N., Davey, M., Parkinson, J., Greenblatt, J. and Emili, A., (2005) Interaction network containing conserved and essential protein complexes in *Escherichia coli*. *Nature* **433**: 531-537.

Byrne, B. and Swanson, M.S., (1998) Expression of *Legionella pneumophila* virulence traits in response to growth conditions. *Infect Immun* **66**: 3029-3034.

Cambronne, E.D. and Roy, C.R., (2007) The *Legionella pneumophila* IcmSW complex interacts with multiple Dot/Icm effectors to facilitate type IV translocation. *PLoS Pathog* **3**: e188.

Campodonico, E.M., Chesnel, L. and Roy, C.R., (2005) A yeast genetic system for the identification and characterization of substrate proteins transferred into host cells by the *Legionella pneumophila* Dot/Icm system. *Mol Microbiol* **56**: 918-933.

Carlsson, K.E., Liu, J., Edqvist, P.J. and Francis, M.S., (2007) Influence of the Cpx extracytoplasmic-stress-responsive pathway on *Yersinia* sp.-eukaryotic cell contact. *Infect Immun* **75**: 4386-4399.

Carvalho, F.R., Nastasi, F.R., Gamba, R.C., Foronda, A.S. and Pellizari, V.H., (2008) Occurrence and diversity of *Legionellaceae* in polar lakes of the Antarctic peninsula. *Curr Microbiol* **57**: 294-300.

Cazalet, C., Rusniok, C., Bruggemann, H., Zidane, N., Magnier, A., Ma, L., Tichit, M., Jarraud, S., Bouchier, C., Vandenesch, F., Kunst, F., Etienne, J., Glaser, P. and Buchrieser, C., (2004) Evidence in the *Legionella pneumophila* genome for exploitation of host cell functions and high genome plasticity. *Nat Genet* **36**: 1165-1173.

Chandran Darbari, V. and Waksman, G., (2015) Structural Biology of Bacterial Type IV Secretion Systems. *Annu Rev Biochem* **84**: 603-629.

Chao, Y., Papenfort, K., Reinhardt, R., Sharma, C.M. and Vogel, J., (2012) An atlas of Hfq-bound transcripts reveals 3' UTRs as a genomic reservoir of regulatory small RNAs. *EMBO J* **31**: 4005-4019.

Chao, Y. and Vogel, J., (2016) A 3' UTR-Derived Small RNA Provides the Regulatory Noncoding Arm of the Inner Membrane Stress Response. *Mol Cell* **61**: 352-363.

Chen, H., Xu, G., Zhao, Y., Tian, B., Lu, H., Yu, X., Xu, Z., Ying, N., Hu, S. and Hua, Y., (2008) A novel OxyR sensor and regulator of hydrogen peroxide stress with one cysteine residue in *Deinococcus radiodurans*. *PLoS One* **3**: e1602.

Chen, J., de Felipe, K.S., Clarke, M., Lu, H., Anderson, O.R., Segal, G. and Shuman, H.A., (2004) *Legionella* effectors that promote nonlytic release from protozoa. *Science* **303**: 1358-1361.

Chiang, S.M. and Schellhorn, H.E., (2012) Regulators of oxidative stress response genes in *Escherichia coli* and their functional conservation in bacteria. *Arch Biochem Biophys* **525**: 161-169.

Chien, M., Morozova, I., Shi, S., Sheng, H., Chen, J., Gomez, S.M., Asamani, G., Hill, K., Nuara, J., Feder, M., Rineer, J., Greenberg, J.J., Steshenko, V., Park, S.H., Zhao, B., Teplitskaya, E., Edwards, J.R., Pampou, S., Georghiou, A., Chou, I.C., Iannuccilli, W.,

Ulz, M.E., Kim, D.H., Geringer-Sameth, A., Goldsberry, C., Morozov, P., Fischer, S.G., Segal, G., Qu, X., Rzhetsky, A., Zhang, P., Cayanis, E., De Jong, P.J., Ju, J., Kalachikov, S., Shuman, H.A. and Russo, J.J., (2004) The genomic sequence of the accidental pathogen *Legionella pneumophila*. *Science* **305**: 1966-1968.

Choi, H., Kim, S., Mukhopadhyay, P., Cho, S., Woo, J., Storz, G. and Ryu, S.E., (2001) Structural basis of the redox switch in the OxyR transcription factor. *Cell* **105**: 103-113.

Christie, P.J. and Vogel, J.P., (2000) Bacterial type IV secretion: conjugation systems adapted to deliver effector molecules to host cells. *Trends Microbiol* **8**: 354-360.

Christman, M.F., Storz, G. and Ames, B.N., (1989) OxyR, a positive regulator of hydrogen peroxide-inducible genes in *Escherichia coli* and *Salmonella typhimurium*, is homologous to a family of bacterial regulatory proteins. *Proc Natl Acad Sci U S A* **86**: 3484-3488.

Cianciotto, N.P., (2013) Type II secretion and *Legionella* virulence. *Curr Top Microbiol Immunol* **376**: 81-102.

Cirillo, J.D., Falkow, S. and Tompkins, L.S., (1994) Growth of *Legionella pneumophila* in *Acanthamoeba castellanii* enhances invasion. *Infect Immun* **62**: 3254-3261.

Coers, J., Kagan, J.C., Matthews, M., Nagai, H., Zuckman, D.M. and Roy, C.R., (2000) Identification of Icm protein complexes that play distinct roles in the biogenesis of an organelle permissive for *Legionella pneumophila* intracellular growth. *Mol Microbiol* **38**: 719-736.

Conover, G.M., Derre, I., Vogel, J.P. and Isberg, R.R., (2003) The *Legionella pneumophila* LidA protein: a translocated substrate of the Dot/Icm system associated with maintenance of bacterial integrity. *Mol Microbiol* **48**: 305-321.

Coordinators, N.R., (2015) Database resources of the National Center for Biotechnology Information. *Nucleic Acids Res* **43**: D6-17.

Critchley, M. and Bentham, R., (2009) The efficacy of biocides and other chemical additives in cooling water systems in the control of amoebae. *J Appl Microbiol* **106**: 784-789.

Dalebroux, Z.D., Edwards, R.L. and Swanson, M.S., (2009) SpoT governs *Legionella pneumophila* differentiation in host macrophages. *Mol Microbiol* **71**: 640-658.

Dalebroux, Z.D., Yagi, B.F., Sahr, T., Buchrieser, C. and Swanson, M.S., (2010) Distinct roles of ppGpp and DksA in *Legionella pneumophila* differentiation. *Mol Microbiol* **76**: 200-219.

Danese, P.N. and Silhavy, T.J., (1998) CpxP, a stress-combative member of the Cpx regulon. *J Bacteriol* **180**: 831-839.

Danese, P.N., Snyder, W.B., Cosma, C.L., Davis, L.J. and Silhavy, T.J., (1995) The Cpx two-component signal transduction pathway of *Escherichia coli* regulates transcription of the gene specifying the stress-inducible periplasmic protease, DegP. *Genes Dev* **9**: 387-398.

Daugherty, A., Suvarnapunya, A.E. and Runyen-Janecky, L., (2012) The role of *oxyR* and *soxRS* in oxidative stress survival in *Shigella flexneri*. *Microbiol Res* **167**: 238-245.

de Felipe, K.S., Glover, R.T., Charpentier, X., Anderson, O.R., Reyes, M., Pericone, C.D. and Shuman, H.A., (2008) *Legionella* eukaryotic-like type IV substrates interfere with organelle trafficking. *PLoS Pathog* **4**: e1000117.

de Felipe, K.S., Pampou, S., Jovanovic, O.S., Pericone, C.D., Ye, S.F., Kalachikov, S. and Shuman, H.A., (2005) Evidence for acquisition of *Legionella* type IV secretion substrates via interdomain horizontal gene transfer. *J Bacteriol* **187**: 7716-7726.

De Wulf, P., Akerley, B.J. and Lin, E.C., (2000) Presence of the Cpx system in bacteria. *Microbiology* **146 (Pt 2)**: 247-248.

De Wulf, P., Kwon, O. and Lin, E.C., (1999) The CpxRA signal transduction system of *Escherichia coli*: growth-related autoactivation and control of unanticipated target operons. *J Bacteriol* **181**: 6772-6778.

De Wulf, P., McGuire, A.M., Liu, X. and Lin, E.C., (2002) Genome-wide profiling of promoter recognition by the two-component response regulator CpxR-P in *Escherichia coli*. *J Biol Chem* **277**: 26652-26661.

DebRoy, S., Dao, J., Soderberg, M., Rossier, O. and Cianciotto, N.P., (2006) *Legionella pneumophila* type II secretome reveals unique exoproteins and a chitinase that promotes bacterial persistence in the lung. *Proc Natl Acad Sci U S A* **103**: 19146-19151.

Declerck, P., Behets, J., Margineanu, A., van Hoef, V., De Keersmaecker, B. and Ollevier, F., (2009) Replication of *Legionella pneumophila* in biofilms of water distribution pipes. *Microbiol Res* **164**: 593-603.

Declerck, P., Behets, J., van Hoef, V. and Ollevier, F., (2007) Detection of *Legionella* spp. and some of their amoeba hosts in floating biofilms from anthropogenic and natural aquatic environments. *Water Res* **41**: 3159-3167.

Derre, I. and Isberg, R.R., (2004) *Legionella pneumophila* replication vacuole formation involves rapid recruitment of proteins of the early secretory system. *Infect Immun* **72**: 3048-3053.

Di Paolo, G. and De Camilli, P., (2006) Phosphoinositides in cell regulation and membrane dynamics. *Nature* **443**: 651-657.

Dong, J., Iuchi, S., Kwan, H.S., Lu, Z. and Lin, E.C., (1993) The deduced amino-acid sequence of the cloned *cpxR* gene suggests the protein is the cognate regulator for the membrane sensor, CpxA, in a two-component signal transduction system of *Escherichia coli*. *Gene* **136**: 227-230.

Dumenil, G. and Isberg, R.R., (2001) The *Legionella pneumophila* IcmR protein exhibits chaperone activity for IcmQ by preventing its participation in high-molecular-weight complexes. *Mol Microbiol* **40**: 1113-1127.

Dumenil, G., Montminy, T.P., Tang, M. and Isberg, R.R., (2004) IcmR-regulated membrane insertion and efflux by the *Legionella pneumophila* IcmQ protein. *J Biol Chem* **279**: 4686-4695.

Dutta, R., Qin, L. and Inouye, M., (1999) Histidine kinases: diversity of domain organization. *Mol Microbiol* **34**: 633-640.

Dutta, R., Yoshida, T. and Inouye, M., (2000) The critical role of the conserved Thr247 residue in the functioning of the osmosensor EnvZ, a histidine Kinase/Phosphatase, in *Escherichia coli*. *J Biol Chem* **275**: 38645-38653.

Edelstein, P.H., Hu, B., Higa, F. and Edelstein, M.A., (2003) lvgA, a novel *Legionella pneumophila* virulence factor. *Infect Immun* **71**: 2394-2403.

Edwards, R.L., Jules, M., Sahr, T., Buchrieser, C. and Swanson, M.S., (2010) The *Legionella pneumophila* LetA/LetS two-component system exhibits rheostat-like behavior. *Infect Immun* **78**: 2571-2583.

Ensminger, A.W., (2016) *Legionella pneumophila*, armed to the hilt: justifying the largest arsenal of effectors in the bacterial world. *Curr Opin Microbiol* **29**: 74-80.

Ensminger, A.W., Yassin, Y., Miron, A. and Isberg, R.R., (2012) Experimental evolution of *Legionella pneumophila* in mouse macrophages leads to strains with altered determinants of environmental survival. *PLoS Pathog* **8**: e1002731.

Erental, A., Kalderon, Z., Saada, A., Smith, Y. and Engelberg-Kulka, H., (2014) Apoptosis-like death, an extreme SOS response in *Escherichia coli*. *mBio* **5**: e01426-01414.

Escoll, P., Rolando, M., Gomez-Valero, L. and Buchrieser, C., (2013) From amoeba to macrophages: exploring the molecular mechanisms of *Legionella pneumophila* infection in both hosts. *Curr Top Microbiol Immunol* **376**: 1-34.

Faucher, S.P., Friedlander, G., Livny, J., Margalit, H. and Shuman, H.A., (2010) *Legionella pneumophila* 6S RNA optimizes intracellular multiplication. *Proc Natl Acad Sci U S A* **107**: 7533-7538.

Faucher, S.P., Mueller, C.A. and Shuman, H.A., (2011) *Legionella pneumophila* Transcriptome during Intracellular Multiplication in Human Macrophages. *Front Microbiol* **2**: 60.

Faucher, S.P. and Shuman, H.A., (2013) Methods to study *Legionella* transcriptome in vitro and in vivo. *Methods Mol Biol* **954**: 567-582.

Faulkner, G., Berk, S.G., Garduno, E., Ortiz-Jimenez, M.A. and Garduno, R.A., (2008) Passage through *Tetrahymena tropicalis* triggers a rapid morphological differentiation in *Legionella pneumophila*. *J Bacteriol* **190**: 7728-7738.

Faulkner, G. and Garduno, R.A., (2002) Ultrastructural analysis of differentiation in *Legionella pneumophila*. *J Bacteriol* **184**: 7025-7041.

Feldheim, Y.S., Zusman, T., Speiser, Y. and Segal, G., (2015) The *Legionella pneumophila* CpxRA two-component regulatory system - New insights into CpxR's function as a dual

regulator and its connection to the effectors regulatory network. *Mol Microbiol* 10.1111/mmi.13290.

Fettes, P.S., Forsbach-Birk, V., Lynch, D. and Marre, R., (2001) Overexpresssion of a *Legionella pneumophila* homologue of the *E. coli* regulator *csrA* affects cell size, flagellation, and pigmentation. *Int J Med Microbiol : IJMM* **291**: 353-360.

Fields, B.S., (1996) The molecular ecology of *legionellae*. *Trends Microbiol* **4**: 286-290.

Fields, B.S., Benson, R.F. and Besser, R.E., (2002) *Legionella* and Legionnaires' disease: 25 years of investigation. *Clin Microbiol Rev* **15**: 506-526.

Finsel, I. and Hilbi, H., (2015) Formation of a pathogen vacuole according to *Legionella pneumophila*: how to kill one bird with many stones. *Cell Microbiol* **17**: 935-950.

Finsel, I., Ragaz, C., Hoffmann, C., Harrison, C.F., Weber, S., van Rahden, V.A., Johannes, L. and Hilbi, H., (2013) The *Legionella* effector RidL inhibits retrograde trafficking to promote intracellular replication. *Cell Host Microbe* **14**: 38-50.

Fleischer, R., Heermann, R., Jung, K. and Hunke, S., (2007) Purification, reconstitution, and characterization of the CpxRAP envelope stress system of *Escherichia coli*. *J Biol Chem* **282**: 8583-8593.

Fliermans, C.B., Cherry, W.B., Orrison, L.H., Smith, S.J., Tison, D.L. and Pope, D.H., (1981) Ecological distribution of Legionella pneumophila. *Appl Environ Microbiol* **41**: 9-16.

Fliermans, C.B., Cherry, W.B., Orrison, L.H. and Thacker, L., (1979) Isolation of *Legionella pneumophila* from nonepidemic-related aquatic habitats. *Appl Environ Microbiol* **37**: 1239-1242.

Fonseca, M.V., Sauer, J.D., Crepin, S., Byrne, B. and Swanson, M.S., (2014) The *phtC-phtD* locus equips *Legionella pneumophila* for thymidine salvage and replication in macrophages. *Infect Immun* **82**: 720-730.

Fraser, D.W. and McDade, J.E., (1979) Legionellosis. *Sci Am* **241**: 82-99.

Fraser, D.W., Tsai, T.R., Orenstein, W., Parkin, W.E., Beecham, H.J., Sharrar, R.G., Harris, J., Mallison, G.F., Martin, S.M., McDade, J.E., Shepard, C.C. and Brachman, P.S., (1977) Legionnaires' disease: description of an epidemic of pneumonia. *N Engl J Med* **297**: 1189-1197.

Gal-Mor, O. and Segal, G., (2003a) Identification of CpxR as a positive regulator of *icm* and *dot* virulence genes of *Legionella pneumophila*. *J Bacteriol* **185**: 4908-4919.

Gal-Mor, O. and Segal, G., (2003b) The Legionella pneumophila GacA homolog (LetA) is involved in the regulation of *icm* virulence genes and is required for intracellular multiplication in *Acanthamoeba castellanii*. *Microb Pathog* **34**: 187-194.

Gal-Mor, O., Zusman, T. and Segal, G., (2002) Analysis of DNA regulatory elements required for expression of the *Legionella pneumophila icm* and *dot* virulence genes. *J Bacteriol* **184**: 3823-3833.

Gao, R. and Stock, A.M., (2009) Biological insights from structures of two-component proteins. *Annu Rev Microbiol* **63**: 133-154.

Gao, R. and Stock, A.M., (2010) Molecular strategies for phosphorylation-mediated regulation of response regulator activity. *Curr Opin Microbiol* **13**: 160-167.

Garduño, R.A., (2008) Life Cycle, Growth Cycles and Developmental Cycle of *Legionella pneumophila*. In: *Legionella pneumophila:* Pathogenesis and Immunity. P.S. Hoffman (ed). New York, New York, USA: Springer US, pp. 65-84.

Garduno, R.A., Garduno, E., Hiltz, M. and Hoffman, P.S., (2002) Intracellular growth of *Legionella pneumophila* gives rise to a differentiated form dissimilar to stationary-phase forms. *Infect Immun* **70**: 6273-6283.

Garduno, R.A., Quinn, F.D. and Hoffman, P.S., (1998) HeLa cells as a model to study the invasiveness and biology of *Legionella pneumophila*. *Can J Microbiol* **44**: 430-440.

Gaspar, A.H. and Machner, M.P., (2014) VipD is a Rab5-activated phospholipase A1 that protects *Legionella pneumophila* from endosomal fusion. *Proc Natl Acad Sci U S A* **111**: 4560-4565.

Ghrairi, T., Chaftar, N., Jarraud, S., Berjeaud, J.M., Hani, K. and Frere, J., (2013) Diversity of *legionellae* strains from Tunisian hot spring water. *Res Microbiol* **164**: 342-350.

Gibson, M.M., Bagga, D.A., Miller, C.G. and Maguire, M.E., (1991) Magnesium transport in *Salmonella typhimurium*: the influence of new mutations conferring Co2+ resistance on the CorA Mg2+ transport system. *Mol Microbiol* **5**: 2753-2762.

Glick, T.H., Gregg, M.B., Berman, B., Mallison, G., Rhodes, W.W., Jr. and Kassanoff, I., (1978) Pontiac fever. An epidemic of unknown etiology in a health department: I. Clinical and epidemiologic aspects. *Am J Epidemiology* **107**: 149-160.

Gomez-Valero, L. and Buchrieser, C., (2013) Genome dynamics in *Legionella*: the basis of versatility and adaptation to intracellular replication. *Cold Spring Harb Perspect in Med* **3**.

Gomez-Valero, L., Rusniok, C., Cazalet, C. and Buchrieser, C., (2011) Comparative and functional genomics of *legionella* identified eukaryotic like proteins as key players in host-pathogen interactions. *Front Microbiol* **2**: 208.

Gordon, J.E. and Christie, P.J., (2014) The *Agrobacterium* Ti Plasmids. *Microbiol Spectr* **2**.

Grabowicz, M., Koren, D. and Silhavy, T.J., (2016) The CpxQ sRNA Negatively Regulates Skp To Prevent Mistargeting of beta-Barrel Outer Membrane Proteins into the Cytoplasmic Membrane. *mBio* **7**.

Hales, L.M. and Shuman, H.A., (1999) The *Legionella pneumophila rpoS* gene is required for growth within *Acanthamoeba castellanii*. *J Bacteriol* **181**: 4879-4889.

Hammer, B.K. and Swanson, M.S., (1999) Co-ordination of *Legionella pneumophila* virulence with entry into stationary phase by ppGpp. *Mol Microbiol* **33**: 721-731.

Hammer, B.K., Tateda, E.S. and Swanson, M.S., (2002) A two-component regulator induces the transmission phenotype of stationary-phase *Legionella pneumophila*. *Mol Microbiol* **44**: 107-118.

Hardiman, C.A. and Roy, C.R., (2014) AMPylation is critical for Rab1 localization to vacuoles containing *Legionella pneumophila*. *mBio* **5**: e01035-01013.

Harding, C.R., Mattheis, C., Mousnier, A., Oates, C.V., Hartland, E.L., Frankel, G. and Schroeder, G.N., (2013) LtpD is a novel *Legionella pneumophila* effector that binds phosphatidylinositol 3-phosphate and inositol monophosphatase IMPA1. *Infect Immun* **81**: 4261-4270.

Hassett, D.J., Alsabbagh, E., Parvatiyar, K., Howell, M.L., Wilmott, R.W. and Ochsner, U.A., (2000) A protease-resistant catalase, KatA, released upon cell lysis during stationary phase is essential for aerobic survival of a *Pseudomonas aeruginosa oxyR* mutant at low cell densities. *J Bacteriol* **182**: 4557-4563.

Hauryliuk, V., Atkinson, G.C., Murakami, K.S., Tenson, T. and Gerdes, K., (2015) Recent functional insights into the role of (p)ppGpp in bacterial physiology. *Nature Rev Microbiol* **13**: 298-309.

Heeb, S., Blumer, C. and Haas, D., (2002) Regulatory RNA as mediator in GacA/RsmA-dependent global control of exoproduct formation in *Pseudomonas fluorescens* CHA0. *J Bacteriol* **184**: 1046-1056.

Herbert, E.E., Cowles, K.N. and Goodrich-Blair, H., (2007) CpxRA regulates mutualism and pathogenesis in *Xenorhabdus nematophila*. *Appl Environ Microbiol* **73**: 7826-7836.

Heusipp, G., Nelson, K.M., Schmidt, M.A. and Miller, V.L., (2004) Regulation of *htrA* expression in *Yersinia enterocolitica*. *FEMS Microbiol Lett* **231**: 227-235.

Hicks, L.A., Garrison, L.E., Nelson, G.E. and Hampton, L.M., (2011) Legionellosis --- United States, 2000-2009. *MMWR. Morb Mortal Wkly Rep* **60**: 1083-1086.

Hilbi, H., Hoffmann, C. and Harrison, C.F., (2011) *Legionella* spp. outdoors: colonization, communication and persistence. *Environ Microbiol Rep* **3**: 286-296.

Hilbi, H., Segal, G. and Shuman, H.A., (2001) Icm/dot-dependent upregulation of phagocytosis by *Legionella pneumophila*. *Mol Microbiol* **42**: 603-617.

Hindre, T., Bruggemann, H., Buchrieser, C. and Hechard, Y., (2008) Transcriptional profiling of *Legionella pneumophila* biofilm cells and the influence of iron on biofilm formation. *Microbiology* **154**: 30-41.

Hirano, Y., Hossain, M.M., Takeda, K., Tokuda, H. and Miki, K., (2007) Structural studies of the Cpx pathway activator NlpE on the outer membrane of *Escherichia coli*. *Structure (London, England : 1993)* **15**: 963-976.

Hoffmann, C., Finsel, I., Otto, A., Pfaffinger, G., Rothmeier, E., Hecker, M., Becher, D. and Hilbi, H., (2014) Functional analysis of novel Rab GTPases identified in the proteome of purified *Legionella*-containing vacuoles from macrophages. *Cell Microbiol* **16**: 1034-1052.

Holden, E.P., Winkler, H.H., Wood, D.O. and Leinbach, E.D., (1984) Intracellular growth of *Legionella pneumophila* within *Acanthamoeba castellanii* Neff. *Infect Immun* **45**: 18-24.

Horwitz, M.A., (1983) Formation of a novel phagosome by the Legionnaires' disease bacterium (*Legionella pneumophila*) in human monocytes. *J Exp Med* **158**: 1319-1331.

Horwitz, M.A., (1984) Phagocytosis of the Legionnaires' disease bacterium (*Legionella pneumophila*) occurs by a novel mechanism: engulfment within a pseudopod coil. *Cell* **36**: 27-33.

Horwitz, M.A. and Silverstein, S.C., (1980) Legionnaires' disease bacterium (*Legionella pneumophila*) multiples intracellularly in human monocytes. *J Clin Invest* **66**: 441-450.

Hovel-Miner, G., Pampou, S., Faucher, S.P., Clarke, M., Morozova, I., Morozov, P., Russo, J.J., Shuman, H.A. and Kalachikov, S., (2009) SigmaS controls multiple pathways associated with intracellular multiplication of *Legionella pneumophila*. *J Bacteriol* **191**: 2461-2473.

Hubber, A. and Roy, C.R., (2010) Modulation of host cell function by *Legionella pneumophila* type IV effectors. *Annu Rev Cell Dev Biol* **26**: 261-283.

Humair, B., Wackwitz, B. and Haas, D., (2010) GacA-controlled activation of promoters for small RNA genes in *Pseudomonas fluorescens*. *Appl Environ Microbiol* **76**: 1497-1506.

Hunke, S., Keller, R. and Muller, V.S., (2012) Signal integration by the Cpx-envelope stress system. *FEMS Microbiol Lett* **326**: 12-22.

Huynh, T.N., Noriega, C.E. and Stewart, V., (2010) Conserved mechanism for sensor phosphatase control of two-component signaling revealed in the nitrate sensor NarX. *Proc Natl Acad Sci U S A* **107**: 21140-21145.

Ingmundson, A., Delprato, A., Lambright, D.G. and Roy, C.R., (2007) *Legionella pneumophila* proteins that regulate Rab1 membrane cycling. *Nature* **450**: 365-369.

Isaac, D.D., Pinkner, J.S., Hultgren, S.J. and Silhavy, T.J., (2005) The extracytoplasmic adaptor protein CpxP is degraded with substrate by DegP. *Proc Natl Acad Sci U S A* **102**: 17775-17779.

Isberg, R.R., O'Connor, T.J. and Heidtman, M., (2009) The *Legionella pneumophila* replication vacuole: making a cosy niche inside host cells. *Nature Rev Microbiol* **7**: 13-24.

Itou, H. and Tanaka, I., (2001) The OmpR-family of proteins: insight into the tertiary structure and functions of two-component regulator proteins. *J Biochem* **129**: 343-350.

Jacob, A.I., Kohrer, C., Davies, B.W., RajBhandary, U.L. and Walker, G.C., (2013) Conserved bacterial RNase YbeY plays key roles in 70S ribosome quality control and 16S rRNA maturation. *Mol Cell* **49**: 427-438.

Jank, T., Bohmer, K.E., Tzivelekidis, T., Schwan, C., Belyi, Y. and Aktories, K., (2012) Domain organization of *Legionella* effector SetA. *Cell Microbiol* **14**: 852-868.

Jean, S. and Kiger, A.A., (2012) Coordination between RAB GTPase and phosphoinositide regulation and functions. *Nature Rev Mol Cell Biol* **13**: 463-470.

Jeong, K.C., Sexton, J.A. and Vogel, J.P., (2015) Spatiotemporal regulation of a *Legionella pneumophila* T4SS substrate by the metaeffector SidJ. *PLoS Pathog* **11**: e1004695.

Joshi, A.D., Sturgill-Koszycki, S. and Swanson, M.S., (2001) Evidence that Dot-dependent and -independent factors isolate the *Legionella pneumophila* phagosome from the endocytic network in mouse macrophages. *Cell Microbiol* **3**: 99-114.

Jubelin, G., Vianney, A., Beloin, C., Ghigo, J.M., Lazzaroni, J.C., Lejeune, P. and Dorel, C., (2005) CpxR/OmpR interplay regulates curli gene expression in response to osmolarity in *Escherichia coli*. *J Bacteriol* **187**: 2038-2049.

Kagan, J.C. and Roy, C.R., (2002) *Legionella* phagosomes intercept vesicular traffic from endoplasmic reticulum exit sites. *Nat Cell Biol* **4**: 945-954.

Kagan, J.C., Stein, M.P., Pypaert, M. and Roy, C.R., (2004) *Legionella* subvert the functions of Rab1 and Sec22b to create a replicative organelle. *J Exp Med* **199**: 1201-1211.

Kazakov, A.E., Vassieva, O., Gelfand, M.S., Osterman, A. and Overbeek, R., (2003) Bioinformatics classification and functional analysis of PhoH homologs. *In Silico Biol* **3**: 3-15.

Kenney, L.J., (2002) Structure/function relationships in OmpR and other winged-helix transcription factors. *Curr Opin Microbiol* **5**: 135-141.

Kessler, A., Schell, U., Sahr, T., Tiaden, A., Harrison, C., Buchrieser, C. and Hilbi, H., (2013) The *Legionella pneumophila* orphan sensor kinase LqsT regulates competence and pathogen-host interactions as a component of the LAI-1 circuit. *Environ Microbiol* **15**: 646-662.

Kim, S., Bang, Y.J., Kim, D., Lim, J.G., Oh, M.H. and Choi, S.H., (2014) Distinct characteristics of OxyR2, a new OxyR-type regulator, ensuring expression of Peroxiredoxin 2 detoxifying low levels of hydrogen peroxide in *Vibrio vulnificus*. *Mol Microbiol* **93**: 992-1009.

Komano, T., Yoshida, T., Narahara, K. and Furuya, N., (2000) The transfer region of IncI1 plasmid R64: similarities between R64 tra and *Legionella icm/dot* genes. *Mol Microbiol* **35**: 1348-1359.

Koonin, E.V. and Rudd, K.E., (1996) Two domains of superfamily I helicases may exist as separate proteins. *Prot Sci : a publication of the Protein Society* **5**: 178-180.

Ku, B., Lee, K.H., Park, W.S., Yang, C.S., Ge, J., Lee, S.G., Cha, S.S., Shao, F., Heo, W.D., Jung, J.U. and Oh, B.H., (2012) VipD of *Legionella pneumophila* targets activated Rab5 and Rab22 to interfere with endosomal trafficking in macrophages. *PLoS Pathog* **8**: e1003082.

Kubori, T., Hyakutake, A. and Nagai, H., (2008) *Legionella* translocates an E3 ubiquitin ligase that has multiple U-boxes with distinct functions. *Mol Microbiol* **67**: 1307-1319.

Kubori, T., Koike, M., Bui, X.T., Higaki, S., Aizawa, S. and Nagai, H., (2014) Native structure of a type IV secretion system core complex essential for *Legionella* pathogenesis. *Proc Natl Acad Sci U S A* **111**: 11804-11809.

Kuiper, M.W., Wullings, B.A., Akkermans, A.D., Beumer, R.R. and van der Kooij, D., (2004) Intracellular proliferation of *Legionella pneumophila* in *Hartmannella vermiformis* in aquatic biofilms grown on plasticized polyvinyl chloride. *Appl Enviro Microbiol* **70**: 6826-6833.

Kulkarni, P.R., Cui, X., Williams, J.W., Stevens, A.M. and Kulkarni, R.V., (2006) Prediction of CsrA-regulating small RNAs in bacteria and their experimental verification in *Vibrio fischeri*. *Nucleic Acids Res* **34**: 3361-3369.

Kuroda, T., Kubori, T., Thanh Bui, X., Hyakutake, A., Uchida, Y., Imada, K. and Nagai, H., (2015) Molecular and structural analysis of *Legionella* DotI gives insights into an inner membrane complex essential for type IV secretion. *Sci Rep* **5**: 10912.

Kwon, E., Kim, D.Y., Ngo, T.D., Gross, C.A., Gross, J.D. and Kim, K.K., (2012) The crystal structure of the periplasmic domain of *Vibrio parahaemolyticus* CpxA. *Prot Sci : a publication of the Protein Society* **21**: 1334-1343.

Labandeira-Rey, M., Dodd, D., Fortney, K.R., Zwickl, B., Katz, B.P., Janowicz, D.M., Spinola, S.M. and Hansen, E.J., (2011) A *Haemophilus ducreyi* CpxR deletion mutant is virulent in human volunteers. *J Infect Dis* **203**: 1859-1865.

Labandeira-Rey, M., Mock, J.R. and Hansen, E.J., (2009) Regulation of expression of the *Haemophilus ducreyi* LspB and LspA2 proteins by CpxR. *Infect Immun* **77**: 3402-3411.

LeBlanc, J.J., Brassinga, A.K., Ewann, F., Davidson, R.J. and Hoffman, P.S., (2008) An ortholog of OxyR in *Legionella pneumophila* is expressed postexponentially and negatively regulates the alkyl hydroperoxide reductase (*ahpC2D*) operon. *J Bacteriol* **190**: 3444-3455.

LeBlanc, J.J., Davidson, R.J. and Hoffman, P.S., (2006) Compensatory functions of two alkyl hydroperoxide reductases in the oxidative defense system of *Legionella pneumophila*. *J Bacteriol* **188**: 6235-6244.

Lee, C., Lee, S.M., Mukhopadhyay, P., Kim, S.J., Lee, S.C., Ahn, W.S., Yu, M.H., Storz, G. and Ryu, S.E., (2004) Redox regulation of OxyR requires specific disulfide bond formation involving a rapid kinetic reaction path. *Nat Struc Mol Biol* **11**: 1179-1185.

European Centre for Disease Prevention and Control, (2015) Legionnaires' disease in Europe, 2013. Stockholm: ECDC. 10.2900/203078. http://ecdc.europa.eu/en/publications/Publications/legionnaires-disease-2015.pdf

Leskinen, K., Varjosalo, M. and Skurnik, M., (2015) Absence of YbeY RNase compromises the growth and enhances the virulence plasmid gene expression of *Yersinia enterocolitica* O:3. *Microbiology* **161**: 285-299.

Levesque, S., Plante, P.L., Mendis, N., Cantin, P., Marchand, G., Charest, H., Raymond, F., Huot, C., Goupil-Sormany, I., Desbiens, F., Faucher, S.P., Corbeil, J. and Tremblay, C.,

(2014) Genomic characterization of a large outbreak of *Legionella pneumophila* serogroup 1 strains in Quebec City, 2012. *PLoS One* **9**: e103852.

Li, G. and Marlin, M.C., (2015) Rab family of GTPases. In: Rab GTPases. G. Li (ed). Springer New York, pp. 1-15.

Li, L., Mendis, N., Trigui, H. and Faucher, S.P., (2015) Transcriptomic changes of *Legionella pneumophila* in water. *BMC Genomics* **16**: 637.

Liu, J., Obi, I.R., Thanikkal, E.J., Kieselbach, T. and Francis, M.S., (2011) Phosphorylated CpxR restricts production of the RovA global regulator in *Yersinia pseudotuberculosis*. *PLoS One* **6**: e23314.

Liu, J., Thanikkal, E.J., Obi, I.R. and Francis, M.S., (2012) Elevated CpxR~P levels repress the Ysc-Yop type III secretion system of *Yersinia pseudotuberculosis*. *Res Microbiol* **163**: 518-530.

Loboda, A.V., Krutchinsky, A.N., Bromirski, M., Ens, W. and Standing, K.G., (2000) A tandem quadrupole/time-of-flight mass spectrometer with a matrix-assisted laser desorption/ionization source: design and performance. *Rapid Commun Mass Spectrom : RCM* **14**: 1047-1057.

Lucas, M., Gaspar, A.H., Pallara, C., Rojas, A.L., Fernandez-Recio, J., Machner, M.P. and Hierro, A., (2014) Structural basis for the recruitment and activation of the *Legionella phospholipase* VipD by the host GTPase Rab5. *Proc Natl Acad Sci U S A* **111**: E3514-3523.

Luo, Z.Q. and Isberg, R.R., (2004) Multiple substrates of the *Legionella pneumophila* Dot/Icm system identified by interbacterial protein transfer. *Proc Natl Acad Sci U S A* **101**: 841-846.

Lynch, D., Fieser, N., Gloggler, K., Forsbach-Birk, V. and Marre, R., (2003) The response regulator LetA regulates the stationary-phase stress response in *Legionella pneumophila* and is required for efficient infection of *Acanthamoeba castellanii*. *FEMS Microbiol Lett* **219**: 241-248.

Machner, M.P. and Isberg, R.R., (2006) Targeting of host Rab GTPase function by the intravacuolar pathogen *Legionella pneumophila*. *Dev Cell* **11**: 47-56.

Machner, M.P. and Isberg, R.R., (2007) A bifunctional bacterial protein links GDI displacement to Rab1 activation. *Science* **318**: 974-977.

Maciver, I. and Hansen, E.J., (1996) Lack of expression of the global regulator OxyR in *Haemophilus influenzae* has a profound effect on growth phenotype. *Infect Immun* **64**: 4618-4629.

Magnusson, L.U., Farewell, A. and Nystrom, T., (2005) ppGpp: a global regulator in *Escherichia coli*. *Trends Microbiol* **13**: 236-242.

Mampel, J., Spirig, T., Weber, S.S., Haagensen, J.A., Molin, S. and Hilbi, H., (2006) Planktonic replication is essential for biofilm formation by *Legionella pneumophila* in a complex medium under static and dynamic flow conditions. *Appl Environ Microbiol* **72**: 2885-2895.

Marra, A., Blander, S.J., Horwitz, M.A. and Shuman, H.A., (1992) Identification of a *Legionella pneumophila* locus required for intracellular multiplication in human macrophages. *Proc Natl Acad Sci U S A* **89**: 9607-9611.

Marrie, T., (2008) Legionnaires' Disease—Clinical Picture. In: *Legionella pneumophila*: Pathogenesis and Immunity. P. Hoffman, H. Friedman & M. Bendinelli (eds). New York, NY, USA: Springer US, pp. 133-150.

Marston, B.J., Lipman, H.B. and Breiman, R.F., (1994) Surveillance for Legionnaires' disease. Risk factors for morbidity and mortality. *Arch Intern Med* **154**: 2417-2422.

Martinelli, F., Carasi, S., Scarcella, C. and Speziani, F., (2001) Detection of *Legionella pneumophila* at thermal spas. *New Microbiol* **24**: 259-264.

Martinez-Hackert, E. and Stock, A.M., (1997) Structural relationships in the OmpR family of winged-helix transcription factors. *J Mol Biol* **269**: 301-312.

Mascher, T., Helmann, J.D. and Unden, G., (2006) Stimulus perception in bacterial signal-transducing histidine kinases. *Microbiol Mol Biol Rev : MMBR* **70**: 910-938.

Matthews, M. and Roy, C.R., (2000) Identification and subcellular localization of the *Legionella* pneumophila IcmX protein: a factor essential for establishment of a replicative organelle in eukaryotic host cells. *Infect Immun* **68**: 3971-3982.

McCoy-Simandle, K., Stewart, C.R., Dao, J., DebRoy, S., Rossier, O., Bryce, P.J. and Cianciotto, N.P., (2011) *Legionella pneumophila* type II secretion dampens the cytokine response of infected macrophages and epithelia. *Infect Immun* **79**: 1984-1997.

McDade, J.E., Shepard, C.C., Fraser, D.W., Tsai, T.R., Redus, M.A. and Dowdle, W.R., (1977) Legionnaires' disease: isolation of a bacterium and demonstration of its role in other respiratory disease. *New Engl J Med* **297**: 1197-1203.

McEwen, J. and Silverman, P., (1980) Chromosomal mutations of *Escherichia coli* that alter expression of conjugative plasmid functions. *Proc Natl Acad Sci U S A* **77**: 513-517.

Merriam, J.J., Mathur, R., Maxfield-Boumil, R. and Isberg, R.R., (1997) Analysis of the *Legionella pneumophila fliI* gene: intracellular growth of a defined mutant defective for flagellum biosynthesis. *Infect Immun* **65**: 2497-2501.

Moffat, J.F. and Tompkins, L.S., (1992) A quantitative model of intracellular growth of *Legionella pneumophila* in *Acanthamoeba castellanii*. *Infect Immun* **60**: 296-301.

Molmeret, M., Alli, O.A., Zink, S., Flieger, A., Cianciotto, N.P. and Kwaik, Y.A., (2002) *icmT* is essential for pore formation-mediated egress of *Legionella pneumophila* from mammalian and protozoan cells. *Infect Immun* **70**: 69-78.

Molmeret, M., Horn, M., Wagner, M., Santic, M. and Abu Kwaik, Y., (2005) Amoebae as training grounds for intracellular bacterial pathogens. *Appl Environ Microbiol* **71**: 20-28.

Molofsky, A.B. and Swanson, M.S., (2003) *Legionella pneumophila* CsrA is a pivotal repressor of transmission traits and activator of replication. *Mol Microbiol* **50**: 445-461.

Molofsky, A.B. and Swanson, M.S., (2004) Differentiate to thrive: lessons from the *Legionella pneumophila* life cycle. *Mol Microbiol* **53**: 29-40.

Morash, M.G., Brassinga, A.K., Warthan, M., Gourabathini, P., Garduno, R.A., Goodman, S.D. and Hoffman, P.S., (2009) Reciprocal expression of integration host factor and HU in the developmental cycle and infectivity of *Legionella pneumophila*. *Appl Environ Microbiol* **75**: 1826-1837.

Morozova, I., Qu, X., Shi, S., Asamani, G., Greenberg, J.E., Shuman, H.A. and Russo, J.J., (2004) Comparative sequence analysis of the *icm/dot* genes in *Legionella*. *Plasmid* **51**: 127-147.

Moskowitz, S.M., Brannon, M.K., Dasgupta, N., Pier, M., Sgambati, N., Miller, A.K., Selgrade, S.E., Miller, S.I., Denton, M., Conway, S.P., Johansen, H.K. and Hoiby, N., (2012) PmrB mutations promote polymyxin resistance of *Pseudomonas aeruginosa* isolated from colistin-treated cystic fibrosis patients. *Antimicrob Agents Chemother* **56**: 1019-1030.

Mousnier, A., Schroeder, G.N., Stoneham, C.A., So, E.C., Garnett, J.A., Yu, L., Matthews, S.J., Choudhary, J.S., Hartland, E.L. and Frankel, G., (2014) A new method to determine in vivo interactomes reveals binding of the *Legionella pneumophila* effector PieE to multiple rab GTPases. *mBio* **5**.

Mukherjee, S., Liu, X., Arasaki, K., McDonough, J., Galan, J.E. and Roy, C.R., (2011) Modulation of Rab GTPase function by a protein phosphocholine transferase. *Nature* **477**: 103-106.

Muller, M.P., Peters, H., Blumer, J., Blankenfeldt, W., Goody, R.S. and Itzen, A., (2010) The *Legionella* effector protein DrrA AMPylates the membrane traffic regulator Rab1b. *Science* **329**: 946-949.

Murata, T., Delprato, A., Ingmundson, A., Toomre, D.K., Lambright, D.G. and Roy, C.R., (2006) The *Legionella pneumophila* effector protein DrrA is a Rab1 guanine nucleotide-exchange factor. *Nat Cell Biol* **8**: 971-977.

Murga, R., Forster, T.S., Brown, E., Pruckler, J.M., Fields, B.S. and Donlan, R.M., (2001) Role of biofilms in the survival of *Legionella pneumophila* in a model potable-water system. *Microbiology* **147**: 3121-3126.

Nagai, H., Kagan, J.C., Zhu, X., Kahn, R.A. and Roy, C.R., (2002) A bacterial guanine nucleotide exchange factor activates ARF on *Legionella* phagosomes. *Science* **295**: 679-682.

Nagai, H. and Kubori, T., (2011) Type IVB Secretion Systems of *Legionella* and Other Gram-Negative Bacteria. *Front Microbiol* **2**: 136.

Nagai, H. and Roy, C.R., (2001) The DotA protein from *Legionella pneumophila* is secreted by a novel process that requires the Dot/Icm transporter. *EMBO J* **20**: 5962-5970.

Nakayama, S., Kushiro, A., Asahara, T., Tanaka, R., Hu, L., Kopecko, D.J. and Watanabe, H., (2003) Activation of *hilA* expression at low pH requires the signal sensor CpxA, but not the cognate response regulator CpxR, in *Salmonella enterica* serovar Typhimurium. *Microbiology* **149**: 2809-2817.

Nakayama, S. and Watanabe, H., (1995) Involvement of *cpxA*, a sensor of a two-component regulatory system, in the pH-dependent regulation of expression of *Shigella sonnei virF* gene. *J Bacteriol* **177**: 5062-5069.

Nakayama, S. and Watanabe, H., (1998) Identification of *cpxR* as a positive regulator essential for expression of the *Shigella sonnei virF* gene. *J Bacteriol* **180**: 3522-3528.

Neunuebel, M.R., Chen, Y., Gaspar, A.H., Backlund, P.S., Jr., Yergey, A. and Machner, M.P., (2011) De-AMPylation of the small GTPase Rab1 by the pathogen *Legionella pneumophila*. *Science* **333**: 453-456.

Neunuebel, M.R., Mohammadi, S., Jarnik, M. and Machner, M.P., (2012) *Legionella pneumophila* LidA affects nucleotide binding and activity of the host GTPase Rab1. *J Bacteriol* **194**: 1389-1400.

Nevo, O., Zusman, T., Rasis, M., Lifshitz, Z. and Segal, G., (2014) Identification of *Legionella pneumophila* effectors regulated by the LetAS-RsmYZ-CsrA regulatory cascade, many of which modulate vesicular trafficking. *J Bacteriol* **196**: 681-692.

Ninio, S., Celli, J. and Roy, C.R., (2009) A *Legionella pneumophila* effector protein encoded in a region of genomic plasticity binds to Dot/Icm-modified vacuoles. *PLoS Pathog* **5**: e1000278.

Ninio, S., Zuckman-Cholon, D.M., Cambronne, E.D. and Roy, C.R., (2005) The *Legionella* IcmS-IcmW protein complex is important for Dot/Icm-mediated protein translocation. *Mol Microbiol* **55**: 912-926.

O'Brien, K.M., Lindsay, E.L. and Starai, V.J., (2015) The *Legionella pneumophila effector protein*, LegC7, alters yeast endosomal trafficking. *PLoS One* **10**: e0116824.

O'Connor, T.J., Adepoju, Y., Boyd, D. and Isberg, R.R., (2011) Minimization of the *Legionella pneumophila* genome reveals chromosomal regions involved in host range expansion. *Proc Natl Acad Sci U S A* **108**: 14733-14740.

Ogasawara, H., Yamada, K., Kori, A., Yamamoto, K. and Ishihama, A., (2010) Regulation of the *Escherichia coli csgD* promoter: interplay between five transcription factors. *Microbiology* **156**: 2470-2483.

Orr, A., Ivanova, V.S. and Bonner, W.M., (1995) "Waterbug" dialysis. *BioTechniques* **19**: 204-206.

Otto, K. and Silhavy, T.J., (2002) Surface sensing and adhesion of *Escherichia coli* controlled by the Cpx-signaling pathway. *Proc Natl Acad Sci U S A* **99**: 2287-2292.

Parsot, C., Hamiaux, C. and Page, A.L., (2003) The various and varying roles of specific chaperones in type III secretion systems. *Curr Opin Microbiol* **6**: 7-14.

Perkins, D.N., Pappin, D.J., Creasy, D.M. and Cottrell, J.S., (1999) Probability-based protein identification by searching sequence databases using mass spectrometry data. *Electrophoresis* **20**: 3551-3567.

Pessi, G., Williams, F., Hindle, Z., Heurlier, K., Holden, M.T., Camara, M., Haas, D. and Williams, P., (2001) The global posttranscriptional regulator RsmA modulates production

of virulence determinants and N-acylhomoserine lactones in *Pseudomonas aeruginosa*. *J Bacteriol* **183**: 6676-6683.

Pitre, C.A., Tanner, J.R., Patel, P. and Brassinga, A.K., (2013) Regulatory control of temporally expressed integration host factor (IHF) in *Legionella pneumophila*. *Microbiology* **159**: 475-492.

Pogliano, J., Lynch, A.S., Belin, D., Lin, E.C. and Beckwith, J., (1997) Regulation of *Escherichia coli* cell envelope proteins involved in protein folding and degradation by the Cpx two-component system. *Genes Dev* **11**: 1169-1182.

Potrykus, K. and Cashel, M., (2008) (p)ppGpp: still magical? *Ann Rev Microbiol* **62**: 35-51.

Pruckler, J.M., Benson, R.F., Moyenuddin, M., Martin, W.T. and Fields, B.S., (1995) Association of flagellum expression and intracellular growth of *Legionella pneumophila*. *Infect Immun* **63**: 4928-4932.

Purcell, M. and Shuman, H.A., (1998) The *Legionella pneumophila icmGCDJBF* genes are required for killing of human macrophages. *Infect Immun* **66**: 2245-2255.

Raivio, T.L., (2014) Everything old is new again: an update on current research on the Cpx envelope stress response. *Biochim Biophys Acta* **1843**: 1529-1541.

Raivio, T.L., Leblanc, S.K. and Price, N.L., (2013) The *Escherichia coli* Cpx envelope stress response regulates genes of diverse function that impact antibiotic resistance and membrane integrity. *J Bacteriol* **195**: 2755-2767.

Raivio, T.L., Popkin, D.L. and Silhavy, T.J., (1999) The Cpx envelope stress response is controlled by amplification and feedback inhibition. *J Bacteriol* **181**: 5263-5272.

Raivio, T.L. and Silhavy, T.J., (1997) Transduction of envelope stress in *Escherichia coli* by the Cpx two-component system. *J Bacteriol* **179**: 7724-7733.

Rao, C., Benhabib, H. and Ensminger, A.W., (2013) Phylogenetic reconstruction of the *Legionella pneumophila* Philadelphia-1 laboratory strains through comparative genomics. *PLoS One* **8**: e64129.

Rasis, M. and Segal, G., (2009) The LetA-RsmYZ-CsrA regulatory cascade, together with RpoS and PmrA, post-transcriptionally regulates stationary phase activation of *Legionella pneumophila* Icm/Dot effectors. *Mol Microbiol* **72**: 995-1010.

Rasouly, A., Schonbrun, M., Shenhar, Y. and Ron, E.Z., (2009) YbeY, a heat shock protein involved in translation in *Escherichia coli*. *J Bacteriol* **191**: 2649-2655.

Raychaudhury, S., Farelli, J.D., Montminy, T.P., Matthews, M., Menetret, J.F., Dumenil, G., Roy, C.R., Head, J.F., Isberg, R.R. and Akey, C.W., (2009) Structure and function of interacting IcmR-IcmQ domains from a type IVb secretion system in *Legionella pneumophila*. *Structure (London, England : 1993)* **17**: 590-601.

Richards, A.M., Von Dwingelo, J.E., Price, C.T. and Abu Kwaik, Y., (2013) Cellular microbiology and molecular ecology of *Legionella*-amoeba interaction. *Virulence* **4**: 307-314.

Robertson, P., Abdelhady, H. and Garduno, R.A., (2014) The many forms of a pleomorphic bacterial pathogen-the developmental network of *Legionella pneumophila*. *Front Microbiol* **5**: 670.

Rolando, M. and Buchrieser, C., (2014) *Legionella pneumophila* type IV effectors hijack the transcription and translation machinery of the host cell. *Trends Cell Biol* **24**: 771-778.

Rossier, O., Dao, J. and Cianciotto, N.P., (2009) A type II secreted RNase of *Legionella pneumophila* facilitates optimal intracellular infection of *Hartmannella vermiformis*. *Microbiology* **155**: 882-890.

Rossier, O., Starkenburg, S.R. and Cianciotto, N.P., (2004) *Legionella pneumophila* type II protein secretion promotes virulence in the A/J mouse model of Legionnaires' disease pneumonia. *Infect Immun* **72**: 310-321.

Rowbotham, T.J., (1980) Preliminary report on the pathogenicity of *Legionella pneumophila* for freshwater and soil amoebae. *J Clin Pathol* **33**: 1179-1183.

Rowbotham, T.J., (1986) Current views on the relationships between amoebae, *legionellae* and man. *Isr J Med Sci* **22**: 678-689.

Sadosky, A.B., Wiater, L.A. and Shuman, H.A., (1993) Identification of *Legionella pneumophila* genes required for growth within and killing of human macrophages. *Infect Immun* **61**: 5361-5373.

Sahr, T., Bruggemann, H., Jules, M., Lomma, M., Albert-Weissenberger, C., Cazalet, C. and Buchrieser, C., (2009) Two small ncRNAs jointly govern virulence and transmission in *Legionella pneumophila*. *Mol Microbiol* **72**: 741-762.

Sahr, T., Rusniok, C., Dervins-Ravault, D., Sismeiro, O., Coppee, J.Y. and Buchrieser, C., (2012) Deep sequencing defines the transcriptional map of *L. pneumophila* and identifies growth phase-dependent regulated ncRNAs implicated in virulence. *RNA Biol* **9**: 503-519.

Schell, U., Simon, S., Sahr, T., Hager, D., Albers, M.F., Kessler, A., Fahrnbauer, F., Trauner, D., Hedberg, C., Buchrieser, C. and Hilbi, H., (2015) The alpha-hydroxyketone LAI-1 regulates motility, Lqs-dependent phosphorylation signaling and gene expression of *Legionella pneumophila*. *Mol Microbiol* **99**: 778-793.

Schoebel, S., Cichy, A.L., Goody, R.S. and Itzen, A., (2011) Protein LidA from *Legionella* is a Rab GTPase supereffector. *Proc Natl Acad Sci U S A* **108**: 17945-17950.

Schoebel, S., Oesterlin, L.K., Blankenfeldt, W., Goody, R.S. and Itzen, A., (2009) RabGDI displacement by DrrA from *Legionella* is a consequence of its guanine nucleotide exchange activity. *Mol Cell* **36**: 1060-1072.

Segal, G., (2013) The *Legionella pneumophila* two-component regulatory systems that participate in the regulation of Icm/Dot effectors. *Curr Top Microbiol Immunol* **376**: 35-52.

Segal, G., Purcell, M. and Shuman, H.A., (1998) Host cell killing and bacterial conjugation require overlapping sets of genes within a 22-kb region of the *Legionella pneumophila* genome. *Proc Natl Acad Sci U S A* **95**: 1669-1674.

Segal, G. and Shuman, H.A., (1997) Characterization of a new region required for macrophage killing by *Legionella pneumophila*. *Infect Immun* **65**: 5057-5066.

Segal, G. and Shuman, H.A., (1998) How is the intracellular fate of the *Legionella pneumophila* phagosome determined? *Trends Microbiol* **6**: 253-255.

Segal, G. and Shuman, H.A., (1999a) *Legionella pneumophila* utilizes the same genes to multiply within *Acanthamoeba castellanii* and human macrophages. *Infect Immun* **67**: 2117-2124.

Segal, G. and Shuman, H.A., (1999b) Possible origin of the *Legionella pneumophila* virulence genes and their relation to *Coxiella burnetii*. *Mol Microbiol* **33**: 669-670.

Sexton, J.A., Miller, J.L., Yoneda, A., Kehl-Fie, T.E. and Vogel, J.P., (2004a) *Legionella pneumophila* DotU and IcmF are required for stability of the Dot/Icm complex. *Infect Immun* **72**: 5983-5992.

Sexton, J.A., Pinkner, J.S., Roth, R., Heuser, J.E., Hultgren, S.J. and Vogel, J.P., (2004b) The *Legionella pneumophila* PilT homologue DotB exhibits ATPase activity that is critical for intracellular growth. *J Bacteriol* **186**: 1658-1666.

Seyfzadeh, M., Keener, J. and Nomura, M., (1993) *spoT*-dependent accumulation of guanosine tetraphosphate in response to fatty acid starvation in *Escherichia coli*. *Proc Natl Acad Sci U S A* **90**: 11004-11008.

Sharma, U.K. and Chatterji, D., (2010) Transcriptional switching in *Escherichia coli* during stress and starvation by modulation of sigma activity. *FEMS Microbiol Rev* **34**: 646-657.

Shevchenko, A., Wilm, M., Vorm, O. and Mann, M., (1996) Mass spectrometric sequencing of proteins silver-stained polyacrylamide gels. *Anal Chem* **68**: 850-858.

Shivaji, T., Sousa Pinto, C., San-Bento, A., Oliveira Serra, L.A., Valente, J., Machado, J., Marques, T., Carvalho, L., Nogueira, P.J., Nunes, B. and Vasconcelos, P., (2014) A large community outbreak of Legionnaires disease in Vila Franca de Xira, Portugal, October to November 2014. *Euro surveillance : bulletin Europeen sur les maladies transmissibles = European communicable disease bulletin* **19**: 20991.

Shohdy, N., Efe, J.A., Emr, S.D. and Shuman, H.A., (2005) Pathogen effector protein screening in yeast identifies *Legionella* factors that interfere with membrane trafficking. *Proc Natl Acad Sci U S A* **102**: 4866-4871.

Skaliy, P. and McEachern, H.V., (1979) Survival of the Legionnaires' disease bacterium in water. *Ann of Intern Med* **90**: 662-663.

Slamti, L. and Waldor, M.K., (2009) Genetic analysis of activation of the *Vibrio cholerae* Cpx pathway. *J Bacteriol* **191**: 5044-5056.

Snyder, W.B., Davis, L.J., Danese, P.N., Cosma, C.L. and Silhavy, T.J., (1995) Overproduction of NlpE, a new outer membrane lipoprotein, suppresses the toxicity of periplasmic LacZ by activation of the Cpx signal transduction pathway. *J Bacteriol* **177**: 4216-4223.

Soderberg, M.A., Dao, J., Starkenburg, S.R. and Cianciotto, N.P., (2008) Importance of type II secretion for survival of *Legionella pneumophila* in tap water and in amoebae at low temperatures. *Appl Environ Microbiol* **74**: 5583-5588.

Soderberg, M.A., Rossier, O. and Cianciotto, N.P., (2004) The type II protein secretion system of *Legionella pneumophila* promotes growth at low temperatures. *J Bacteriol* **186**: 3712-3720.

Spinola, S.M., Fortney, K.R., Baker, B., Janowicz, D.M., Zwickl, B., Katz, B.P., Blick, R.J. and Munson, R.S., Jr., (2010) Activation of the CpxRA system by deletion of *cpxA* impairs the ability of *Haemophilus ducreyi* to infect humans. *Infect Immun* **78**: 3898-3904.

Srikanth, S. and Berk, S.G., (1993) Stimulatory effect of cooling tower biocides on amoebae. *Appl Environ Microbiol* **59**: 3245-3249.

Srikanth, S. and Berk, S.G., (1994) Adaptation of amoebae to cooling tower biocides. *Microb Ecol* **27**: 293-301.

Steele, T.W., Moore, C.V. and Sangster, N., (1990) Distribution of *Legionella longbeachae* serogroup 1 and other legionellae in potting soils in Australia. *Appl Environ Microbiol* **56**: 2984-2988.

Stenmark, H., (2009) Rab GTPases as coordinators of vesicle traffic. *Nat Rev Mol Cell Biol* **10**: 513-525.

Stewart, C.R., Muthye, V. and Cianciotto, N.P., (2012) *Legionella pneumophil*a persists within biofilms formed by *Klebsiella pneumoniae*, *Flavobacterium* sp., and *Pseudomonas fluorescens* under dynamic flow conditions. *PLoS One* **7**: e50560.

Stormo, G.D., (2000) DNA binding sites: representation and discovery. *Bioinformatics (Oxford, England)* **16**: 16-23.

Suh, H.Y., Lee, D.W., Lee, K.H., Ku, B., Choi, S.J., Woo, J.S., Kim, Y.G. and Oh, B.H., (2010) Structural insights into the dual nucleotide exchange and GDI displacement activity of SidM/DrrA. *EMBO J* **29**: 496-504.

Sutherland, M.C., Nguyen, T.L., Tseng, V. and Vogel, J.P., (2012) The *Legionella* IcmSW complex directly interacts with DotL to mediate translocation of adaptor-dependent substrates. *PLoS Path* **8**: e1002910.

Suzuki, K., Wang, X., Weilbacher, T., Pernestig, A.K., Melefors, O., Georgellis, D., Babitzke, P. and Romeo, T., (2002) Regulatory circuitry of the CsrA/CsrB and BarA/UvrY systems of *Escherichia coli*. *J Bacteriol* **184**: 5130-5140.

Swanson, M.S. and Hammer, B.K., (2000) *Legionella pneumophila* pathogesesis: a fateful journey from amoebae to macrophages. *Ann Rev Microbiol* **54**: 567-613.

Swanson, M.S. and Isberg, R.R., (1995) Association of *Legionella pneumophila* with the macrophage endoplasmic reticulum. *Infect Immun* **63**: 3609-3620.

Szurmant, H., White, R.A. and Hoch, J.A., (2007) Sensor complexes regulating two-component signal transduction. *Curr Opin Struct Biol* **17**: 706-715.

Tan, Y., Arnold, R.J. and Luo, Z.Q., (2011) *Legionella pneumophila* regulates the small GTPase Rab1 activity by reversible phosphorylcholination. *Proc Natl Acad Sci U S A* **108**: 21212-21217.

Tan, Y. and Luo, Z.Q., (2011) *Legionella pneumophila* SidD is a deAMPylase that modifies Rab1. *Nature* **475**: 506-509.

Tanner, J.R., Li, L., Faucher, S.P. and Brassinga, A.K., (2016) The CpxRA Two-Component System Contributes to *Legionella pneumophila* Virulence. *Mol Microbiol* **100**: 1017-1038.

Thomas, V., Bouchez, T., Nicolas, V., Robert, S., Loret, J.F. and Levi, Y., (2004) Amoebae in domestic water systems: resistance to disinfection treatments and implication in *Legionella* persistence. *J Appl Microbiol* **97**: 950-963.

Tiaden, A., Spirig, T., Carranza, P., Bruggemann, H., Riedel, K., Eberl, L., Buchrieser, C. and Hilbi, H., (2008) Synergistic contribution of the *Legionella pneumophila lqs* genes to pathogen-host interactions. *J Bacteriol* **190**: 7532-7547.

Tiaden, A., Spirig, T., Sahr, T., Walti, M.A., Boucke, K., Buchrieser, C. and Hilbi, H., (2010) The autoinducer synthase LqsA and putative sensor kinase LqsS regulate phagocyte interactions, extracellular filaments and a genomic island of *Legionella pneumophila*. *Environ Microbiol* **12**: 1243-1259.

Tiaden, A., Spirig, T., Weber, S.S., Bruggemann, H., Bosshard, R., Buchrieser, C. and Hilbi, H., (2007) The *Legionella pneumophila* response regulator LqsR promotes host cell interactions as an element of the virulence regulatory network controlled by RpoS and LetA. *Cell Microbiol* **9**: 2903-2920.

Tilney, L.G., Harb, O.S., Connelly, P.S., Robinson, C.G. and Roy, C.R., (2001) How the parasitic bacterium *Legionella pneumophila* modifies its phagosome and transforms it into rough ER: implications for conversion of plasma membrane to the ER membrane. *J Cell Sci* **114**: 4637-4650.

Toledano, M.B., Kullik, I., Trinh, F., Baird, P.T., Schneider, T.D. and Storz, G., (1994) Redox-dependent shift of OxyR-DNA contacts along an extended DNA-binding site: a mechanism for differential promoter selection. *Cell* **78**: 897-909.

Toulabi, L., Wu, X., Cheng, Y. and Mao, Y., (2013) Identification and structural characterization of a *Legionella* phosphoinositide phosphatase. *J Biol Chem* **288**: 24518-24527.

Tschauner, K., Hornschemeyer, P., Muller, V.S. and Hunke, S., (2014) Dynamic interaction between the CpxA sensor kinase and the periplasmic accessory protein CpxP mediates signal recognition in *E. coli*. *PLoS One* **9**: e107383.

Tyson, J.Y., Pearce, M.M., Vargas, P., Bagchi, S., Mulhern, B.J. and Cianciotto, N.P., (2013) Multiple *Legionella pneumophila* Type II secretion substrates, including a novel protein, contribute to differential infection of the amoebae *Acanthamoeba castellanii*, *Hartmannella vermiformis*, and *Naegleria lovaniensis*. *Infect Immun* **81**: 1399-1410.

Tyson, J.Y., Vargas, P. and Cianciotto, N.P., (2014) The novel *Legionella pneumophila* type II secretion substrate NttC contributes to infection of amoebae *Hartmannella vermiformis* and *Willaertia magna*. *Microbiology* **160**: 2732-2744.

Urwyler, S., Nyfeler, Y., Ragaz, C., Lee, H., Mueller, L.N., Aebersold, R. and Hilbi, H., (2009) Proteome analysis of *Legionella* vacuoles purified by magnetic immunoseparation reveals secretory and endosomal GTPases. *Traffic (Copenhagen, Denmark)* **10**: 76-87.

Vakevainen, M., Greenberg, S. and Hansen, E.J., (2003) Inhibition of phagocytosis by *Haemophilus ducreyi* requires expression of the LspA1 and LspA2 proteins. *Infect Immun* **71**: 5994-6003.

Vakulskas, C.A., Potts, A.H., Babitzke, P., Ahmer, B.M. and Romeo, T., (2015) Regulation of bacterial virulence by Csr (Rsm) systems. *Microbiol Mol Biol Rev : MMBR* **79**: 193-224.

van Heijnsbergen, E., Schalk, J.A., Euser, S.M., Brandsema, P.S., den Boer, J.W. and de Roda Husman, A.M., (2015) Confirmed and potential sources of *legionella* reviewed. *Environ Sci Technol* **49**: 4797-4815.

VanRheenen, S.M., Dumenil, G. and Isberg, R.R., (2004) IcmF and DotU are required for optimal effector translocation and trafficking of the *Legionella pneumophila* vacuole. *Infect Immun* **72**: 5972-5982.

Vercruysse, M., Kohrer, C., Davies, B.W., Arnold, M.F., Mekalanos, J.J., RajBhandary, U.L. and Walker, G.C., (2014) The highly conserved bacterial RNase YbeY is essential in *Vibrio cholerae*, playing a critical role in virulence, stress regulation, and RNA processing. *PLoS Pathog* **10**: e1004175.

Vincent, C.D., Buscher, B.A., Friedman, J.R., Williams, L.A., Bardill, P. and Vogel, J.P., (2006a) Identification of non-*dot/icm* suppressors of the *Legionella pneumophila* DeltadotL lethality phenotype. *J Bacteriol* **188**: 8231-8243.

Vincent, C.D., Friedman, J.R., Jeong, K.C., Buford, E.C., Miller, J.L. and Vogel, J.P., (2006b) Identification of the core transmembrane complex of the *Legionella* Dot/Icm type IV secretion system. *Mol Microbiol* **62**: 1278-1291.

Vincent, C.D., Friedman, J.R., Jeong, K.C., Sutherland, M.C. and Vogel, J.P., (2012) Identification of the DotL coupling protein subcomplex of the *Legionella* Dot/Icm type IV secretion system. *Mol Microbiol* **85**: 378-391.

Vincent, C.D. and Vogel, J.P., (2006) The *Legionella pneumophila* IcmS-LvgA protein complex is important for Dot/Icm-dependent intracellular growth. *Mol Microbiol* **61**: 596-613.

Vinella, D., Albrecht, C., Cashel, M. and D'Ari, R., (2005) Iron limitation induces SpoT-dependent accumulation of ppGpp in *Escherichia coli*. *Mol Microbiol* **56**: 958-970.

Vogel, J.P., Andrews, H.L., Wong, S.K. and Isberg, R.R., (1998) Conjugative transfer by the virulence system of *Legionella pneumophila*. *Science* **279**: 873-876.

Vogel, J.P., Roy, C. and Isberg, R.R., (1996) Use of salt to isolate *Legionella pneumophila* mutants unable to replicate in macrophages. *Ann N Y Acad Sci* **797**: 271-272.

Vogt, S.L. and Raivio, T.L., (2012) Just scratching the surface: an expanding view of the Cpx envelope stress response. *FEMS Microbiol Lett* **326**: 2-11.

Vogt, S.L. and Raivio, T.L., (2014) Hfq reduces envelope stress by controlling expression of envelope-localized proteins and protein complexes in enteropathogenic *Escherichia coli*. *Mol Microbiol* **92**: 681-697.

Wang, H., Chen, S., Zhang, J., Rothenbacher, F.P., Jiang, T., Kan, B., Zhong, Z. and Zhu, J., (2012) Catalases promote resistance of oxidative stress in *Vibrio cholerae*. *PLoS One* **7**: e53383.

Weber, R.F. and Silverman, P.M., (1988) The Cpx proteins of *Escherichia coli* K12. Structure of the CpxA polypeptide as an inner membrane component. *J Mol Biol* **203**: 467-478.

Weber, S., Wagner, M. and Hilbi, H., (2014) Live-cell imaging of phosphoinositide dynamics and membrane architecture during *Legionella* infection. *mBio* **5**: e00839-00813.

Weissenmayer, B.A., Prendergast, J.G., Lohan, A.J. and Loftus, B.J., (2011) Sequencing illustrates the transcriptional response of *Legionella pneumophila* during infection and identifies seventy novel small non-coding RNAs. *PLoS One* **6**: e17570.

Wendrich, T.M., Blaha, G., Wilson, D.N., Marahiel, M.A. and Nierhaus, K.H., (2002) Dissection of the mechanism for the stringent factor RelA. *Molecular cell* **10**: 779-788.

Whiley, H. and Bentham, R., (2011) *Legionella longbeachae* and legionellosis. *Emerg Infect Diseases* **17**: 579-583.

Willett, J.W. and Kirby, J.R., (2012) Genetic and biochemical dissection of a HisKA domain identifies residues required exclusively for kinase and phosphatase activities. *PLoS Genet* **8**: e1003084.

Wolfe, A.J., Parikh, N., Lima, B.P. and Zemaitaitis, B., (2008) Signal integration by the two-component signal transduction response regulator CpxR. *J Bacteriol* **190**: 2314-2322.

Xiao, H., Kalman, M., Ikehara, K., Zemel, S., Glaser, G. and Cashel, M., (1991) Residual guanosine 3',5'-bispyrophosphate synthetic activity of *relA* null mutants can be eliminated by *spoT* null mutations. *J Biol Chem* **266**: 5980-5990.

Yamamoto, K. and Ishihama, A., (2005) Transcriptional response of *Escherichia coli* to external copper. *Mol Microbiol* **56**: 215-227.

Yin, L., Wang, L., Lu, H., Xu, G., Chen, H., Zhan, H., Tian, B. and Hua, Y., (2010) DRA0336, another OxyR homolog, involved in the antioxidation mechanisms in *Deinococcus radiodurans*. *J Microbiol (Seoul, Korea)* **48**: 473-479.

Yu, V.L., Plouffe, J.F., Pastoris, M.C., Stout, J.E., Schousboe, M., Widmer, A., Summersgill, J., File, T., Heath, C.M., Paterson, D.L. and Chereshsky, A., (2002) Distribution of *Legionella* species and serogroups isolated by culture in patients with sporadic community-acquired legionellosis: an international collaborative survey. *J Infect Dis* **186**: 127-128.

Zhang, W., Li, F. and Nie, L., (2010) Integrating multiple 'omics' analysis for microbial biology: application and methodologies. *Microbiology* **156**: 287-301.

Zhou, X., Keller, R., Volkmer, R., Krauss, N., Scheerer, P. and Hunke, S., (2011) Structural basis for two-component system inhibition and pilus sensing by the auxiliary CpxP protein. *J Biol Chem* **286**: 9805-9814.

Zhu, Y., Hu, L., Zhou, Y., Yao, Q., Liu, L. and Shao, F., (2010) Structural mechanism of host Rab1 activation by the bifunctional *Legionella* type IV effector SidM/DrrA. *Proc Natl Acad Sci U S A* **107**: 4699-4704.

Zusman, T., Aloni, G., Halperin, E., Kotzer, H., Degtyar, E., Feldman, M. and Segal, G., (2007) The response regulator PmrA is a major regulator of the *icm/dot* type IV secretion system in *Legionella pneumophila* and *Coxiella burnetii*. *Mol Microbiol* **63**: 1508-1523.

Zusman, T., Degtyar, E. and Segal, G., (2008) Identification of a hypervariable region containing new *Legionella pneumophila* Icm/Dot translocated substrates by using the conserved *icmQ* regulatory signature. *Infect Immun* **76**: 4581-4591.

Zusman, T., Gal-Mor, O. and Segal, G., (2002) Characterization of a *Legionella pneumophila relA* insertion mutant and toles of RelA and RpoS in virulence gene expression. *J Bacteriol* **184**: 67-75.

APPENDIX

APPENDIX 1. qPCR analysis of specific gene targets in strains of interest

Purpose: Was conducted to support GFP assay data, at request of reviewers. Work was published in: Microbiology, 2013: Chantalle A.J. Pitre, Jennifer R. Tanner, Palak Patel, and Ann Karen C. Brassinga. (2013). Regulatory control of temporally expressed integration host factor (IHF) in *Legionella pneumophila.* 159(Pt3):475-92. doi: 10.1099/mic.0.062117-0. I was responsible for conducting the RNA extractions, cDNA synthesis, qRT-PCR, evaluating and interpreting qPCR data, generating the below figure, supplying written methodology, as well as editing of the manuscript.

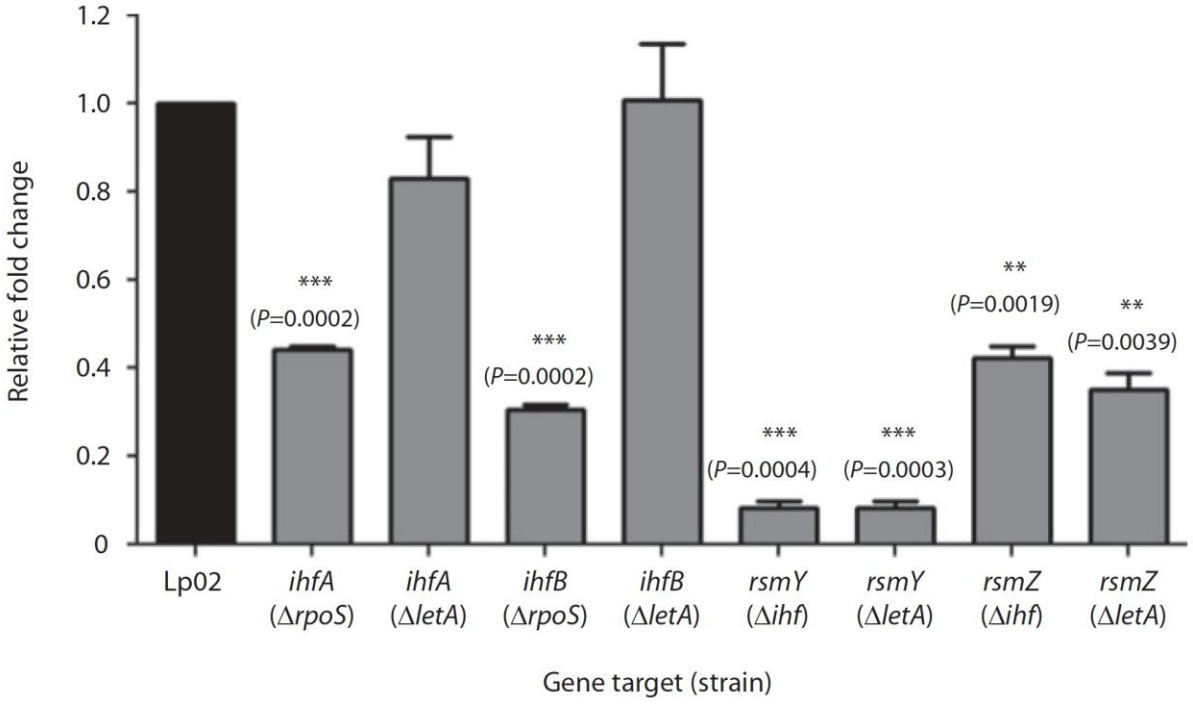

Figure A1. Gene expression in Δ *rpoS*, Δ *ihf* and Δ *letA* mutant strains. Relative fold change in expression of *ihfA* and *ihfB* in Lp02Δ *rpoS* and Δ *letA* strains as well as *rsmY* and *rsmZ* in Lp02Δ *ihf and* Δ *letA* strains. Transcript levels in Lp02 wild-type strains were normalized to 1.0, and compared with transcript levels in Lp02Δ *rpoS*, Lp02Δ *ihf* and *Lp02*Δ *letA* strains. Data are

representative of three biological replicates conducted in triplicate with error bars representing SEM, and *P* values were determined by the two-tailed Student's test of the normalized data.

APPENDIX 2. Infection of *Acanthamoeba castellanii* with *Legionella pneumophila* Lp02

Purpose: Was conducted to supply example of *Legionella* containing vacuole within the well-established host, *Acanthamoeba castellanii*, for readers to refer to as well as to satisfy reviewers request. Work was published in: Microbiologyopen, 2015: Jacqueline R. Hellinga, Rafael A. Garduño, Jay D. Kormish, Jennifer R. Tanner, Deirdre Khan, Kristyn Buchko, Celine Jimenez, Mathieu M. Pinette, and Ann Karen C. Brassinga. (2015). Identification of vacuoles containing extraintestinal differentiated forms of *Legionella pneumophila* in colonized *Caenorhabditis elegans* soil nematodes. 4(4):660-81. doi: 10.1002/mbo3.271. I was responsible for maintaining the *A. castellanii* cultures, conducting the infections, supplying written methodology, as well as editing of the manuscript.

Link to Video S3:

http://onlinelibrary.wiley.com.uml.idm.oclc.org/store/10.1002/mbo3.271/asset/supinfo/mbo3271-sup-0006-VideoS3a.wmv?v=1&s=0bf1896b1db7b62a83a4ee69259371e7f149f0ad